2009

IDENTIFICATION OF CLINICAL, LABORATORY AND GENETIC COVARIATES FOR PHARMACOKINETICS, EFFICACY AND TOXICITY OF SORAFENIB IN PATIENTS WITH SOLID TUMORS

LOKESH JAIN
Virginia Commonwealth University

IDENTIFICATION OF CLINICAL, LABORATORY AND GENETIC COVARIATES FOR PHARMACOKINETICS, EFFICACY AND TOXICITY OF SORAFENIB IN PATIENTS WITH SOLID TUMORS

A dissertation submitted in partial fulfillment of the requirements for the degree of Doctor in Philosophy at Virginia Commonwealth University.

by

LOKESH JAIN
M. Pharm., Birla Institute of Technology and Science (BITS), Pilani, India, 2005

Co-Director: Jürgen Venitz, M.D., Ph.D.
Associate Professor, Department of Pharmaceutics

&

Co-Director: William D. Figg, Pharm.D., MBA
Head, Molecular Pharmacology Section and Clinical Pharmacology Research Core
National Cancer Institute, National Institutes of Health

Virginia Commonwealth University
Richmond, Virginia
August 2009

Acknowledgements

First and foremost, I would like to sincerely thank my advisors, Drs. Jürgen Venitz and William D. Figg, for giving me the opportunity to pursue graduate studies under their guidance.

Dr. Jürgen Venitz for his continuous professional support, guidance, encouragement and patience throughout my graduate program. He was always delighted in sharing his vast knowledge and kind warmth.

Dr. William D. Figg for providing me the wonderful opportunity of pursuing my research work at National Cancer Institute (NCI), NIH and for keeping patience during these years. The clinical research experience he provided will be useful for my future career.

Many thanks to my graduate committee members, Drs. Patricia W. Slattum, Howard T. Karnes and John D. Roberts for their advice and time for serving on my committee.

Principle investigators and medical fellows at NCI, Drs. Elise C. Kohn, Giuseppe Giaccone, Robert Yarchoan, William L. Dahut, Heidi H. Kong, Shivaani Kummar, Nilofar Azad and Jeanny Aragon-Ching for sharing the clinical knowledge and data from their clinical trials.

Drs. Peter Byron, Wu-Pong, Phillip Gerk and all other faculty members in VCU School of Pharmacy for their professional guidance and support during these years.

Erin R. Gardner, Tristan Sissung and Sukyung Woo at NCI for teaching me the details of bioanalysis by mass spectrometry, genotyping studies and population pharmacokinetic modeling. Their scientific advice was vital for successful completion of my Ph.D. work. They always welcomed my questions and answered them timely with friendly gestures.

Pravin Jadhav, a great friend and a mentor, who was always there for professional as well as general queries. Scientific interaction with him was influential in keeping me aligned with my goals.

Kathy Compton and all other members in Dr. Figg's lab for providing a supporting environment during the time I spent at NCI.

The staff in Department of Pharmaceutics and Office of International Education at VCU, Laura, Keyetta and Ingrid for ensuring that I keep up with everything needed to maintain my bona-fide student status. Their friendly reminders were always helpful.

Satjit Brar, Pankaj Gupta, David Lee, Prajakta Badri, Taghreed Obeid, Soniya Vaidya, Abhishek Gulati, Kumar Shah, Priya Nadkarni, Swati Agarwal, Amit Somani, Kshitij Jain and Vivek Kaushik for their valued friendship and support.

My parents, Kailash Chand Jain and Hemlata Jain, my brother Jinendra Jain, my in-laws, Manju Kothari, and other family members for their unconditional love and support.

Last, but not least, my wife, Rati, for her understanding and love during these years. Her unwavering patience and encouragement was crucial for completion of this dissertation.

Table of Contents

List of Tables

Page

List of Figures

Page

List of Abbreviations

ACN	Acetonitrile
ALT	Alanine transaminase
ANOVA	Analysis of variance
AST	Aspartate transaminase
AUC	Area under the curve
$AUC_{\tau,sd}$	Area under the curve for a dosing duration (τ) after single-dose
$AUC_{\tau,ss}$	Area under the curve for a dosing duration (τ) at steady-state
BID	Twice-a-day
BRIP	Between-run imprecision
BSA	Body surface area
BSV	Between-subject variability
BW	Body weight
CCK	Cell counting kit
CL	Clearance
CL_{Cr}	Creatinine clearance
CL_{int}	Clearance intrinsic
CM	Compartmental model
C_{max}	Maximum plasma concentration
CR	Complete response
CRC	Colorectal cancer

CV	Coefficient of variation
DDI	Drug-drug interaction
DEV	Deviation from the nominal
EGF	Endothelial growth factor
EHR	Entero-hepatic recirculation
ELISA	Enzyme linked immuno sorbent assay
FDA	Food and Drug Administration
FO	First-order estimation
FOCE	First-order conditional estimation
FTS	Fernesyl thiosalicylic acid
fu	Fraction unbound
GI	Gastro-intestinal
GLM	General linear modeling
GM	Geometric mean
HCC	Hepato-cellular carcinoma
HFSR	Hand-foot skin reaction
HHV	Human herpesvirus 8
HPLC	High performance liquid chromatography
INTER	Interaction
IOV	Inter-occasion variability
IS	Internal standard
KS	Kaposi's sarcoma
LC	Liquid chromatography

LDL	Low density lipoproteins
LOD	Lower limit of detection
LOQ	Lower limit of quantitation
LQ	Lower quartile
MAb	Monoclonal antibody
MAPK	Mitogen activated protein kinase
Mcl-1	Myeloid cell leukemia 1
mCRPC	Metastatic castrate resistant prostate cancer
MS	Mass spectrometry
MVD	Microvessel density
NCI	National cancer institute
NIH	National Institutes of Health
NONMEM	Non-linear mixed effect modeling
NSCLC	Non-small cell lung cancer
OFV	Objective function value
OS	Overall survival
PCR	Polymerase chain reaction
PD	Progressive disease
PDGF	Platelet derived growth factor
Peqv	Probability of equivalence
PFS	Progression free survival
PG	Pharmacogenetics
PK	Pharmacokinetics

Pp	Prediction p-value
PPB	Plasma protein binding
PR	Partial response
PSA	Prostate specific antigen
Q	Inter-compartmental clearance
QC	Quality control
QD	Once-a-day
Raf	Raf protein
Ras	Ras protein
RCC	Renal-cell carcinoma
rhuMAb	Recombinant humanized monoclonal antibody
RSD	Relative standard deviation
RSE	Relative standard error
RTK	Receptor tyrosine kinases
S/N	Signal to noise ratio
SCr	Serum creatinine
SD	Stable disease
SNP	Single nucleotide polymorphism
ST	Solid tumors
$t_{1/2}$	Half-life
TKI	Tyrosine kinase inhibitor
T_{max}	Time to maximum plasma concentration (Cmax)
TPMT	Thio-purine methyl transferase

TS	Thymidylate synthase
TVCL	Typical value of clearance
ULN	Upper-limit of normal
UQ	Upper quartile
Vc	Volume of central compartment
Vd	Volume of distribution
VEGF	Vascular endothelial growth factor
VEGFR	Vascular endothelial growth factor receptor
Vp	Volume of peripheral compartment
WRIP	Within-run imprecision

Abstract

IDENTIFICATION OF CLINICAL, LABORATORY AND GENETIC COVARIATES FOR PHARMACOKINETICS, EFFICACY AND TOXICITY OF SORAFENIB IN PATIENTS WITH SOLID TUMORS

By Lokesh Jain, M. Pharm.

A dissertation submitted in partial fulfillment of the requirements for the degree of Doctor in Philosophy at Virginia Commonwealth University

Virginia Commonwealth University, 2009

Major-Director: Jürgen Venitz, M.D., Ph.D.
Associate Professor, Department of Pharmaceutics

&

Major-Director: William D. Figg, Pharm.D., MBA
Head, Molecular Pharmacology Section and Clinical Pharmacology Research Core
National Cancer Institute, National Institutes of Health

The goal of this research work was to understand the clinical-pharmacology based treatment approaches for sorafenib. Treatment with sorafenib is associated with high inter-patient variability in pharmacokinetic exposures, efficacy and toxicity.
We explored the demographic, laboratory, clinical and pharmacogenetic factors to elucidate the sources of variability. In addition, we examined the impact of pharmacogenetic variation in VEGFR2, an important mediator of the VEGF pathway, on risk of prostate cancer.

To support these investigations, (mainly single-dose) pharmacokinetic, pharmacogenetic, efficacy and toxicity information were collected from patients with solid tumors, enrolled in five phase I / II clinical trials at National Cancer Institute. Non-compartmental analysis-general linear modeling (NCA-GLM), population pharmacokinetic analysis and several correlative studies were performed to characterize the sources of variability in pharmacokinetics and response. The role of prostate specific antigen (PSA) and *ex-vivo* anti-angiogenic activity as efficacy markers was evaluated, respectively, for patients with prostate cancer treated with sorafenib and patients with solid tumors treated with combination of sorafenib and bevacizumab. Sweat concentrations of sorafenib were measured to study its association with development of hand-foot skin reaction (HFSR). Only body weight was a significant covariate for volume of distribution by population pharmacokinetic analysis, while BSA, albumin and UGT1A9*3 appeared to be significant by NCA-GLM. However, the contribution of these covariates in overall exposure variability was very small; hence, these were considered clinically irrelevant. The association of sorafenib exposure with efficacy in patients with prostate cancer, colorectal cancer and combined solid tumors were not significant; exposure-efficacy relationship for lung cancer patients requires further evaluation. Sorafenib exposures appeared to be associated with incidences of rash in single agent trials and with HFSR in trials involving treatment with sorafenib and bevacizumab combination. *In-vitro* cell-line experiments determined that prostate specific antigen (PSA) is not a suitable marker of efficacy in patients with prostate cancer treated with sorafenib. The e*x-vivo* anti-angiogenic activity, measured by rat-aortic ring assay using patient serum samples,

appeared to be not associated with clinical response. Sorafenib concentration in sweat, upto ≥5 ng/mL, apparently was not associated with HFSR. The VEGFR2 H472Q polymorphism was associated with progression-free survival (PFS) (with an apparent heterozygous advantage for survival) and toxicities in patients treated with drugs against the VEGF pathway. Patients who developed hypertension and HFSR on bevacizumab and sorafenib therapy, respectively, appeared to have longer PFS. Therefore, these side effects should be effectively managed to avoid/delay the treatment discontinuation. The VEGFR2 H472Q and V297I genotype were not predictive of risk of prostate cancer in Caucasian subjects.

CHAPTER ONE

INTRODUCTION AND BACKGROUND

1-1 Introduction

Advances in our understanding of molecular mechanism underlying malignant transformation of cell growth has shifted the focus of cancer drug discovery from development of conventional non-specific cytotoxic drugs towards rationally designed, targeted therapies with activity against cancer-specific pathways. In the last century, the only treatment modalities available to a patient with cancer were surgery, radiation and (mostly) cytotoxic chemotherapies. While surgery is not curative in advanced metastatic diseases, the use of radiation and cytotoxic chemotherapies is limited by severe, dose-limiting toxicities and inability to discriminate between normal and malignant growing cells (1).

In the 1980s, the scientists started deciphering the key elements involved in cancer cell regulation or relay in of signals in cellular signal transduction pathways. The discovery of cancer oncogenes and tumor suppressor genes, which keep check on tumor development and growth, and identification of epigenetic events such as promoter hyper-methylation, which describes the impact of environmental factors on genes governing the cancer cell growth (2, 3) were few of the pioneering milestones. In the following years, key signal

transduction pathways were identified, further studies on oncogene functions and oncoproteins were conducted, and pathological consequences of their dysregulation were studied. It was established that malfunctioning or over-expression of oncogenes/oncoproteins transforms healthy cells into malignant ones. Consequently, these biomolecules were explored as targets for new cancer therapies, later to be called 'molecularly targeted anticancer therapies'. In subsequent years, several new targeted therapies were approved in the U.S.A. for clinical use, as summarized in **Table 1-1**. Toxicity profiles for these treatments differ from traditional cytotoxic therapies with negligible haemotological toxicities (e.g., bone-marrow suppression). Majority of these drugs are better tolerated with predictable and manageable side effect profiles.

Table 1-1 U.S. FDA-approved, molecularly targeted anticancer therapies

Generic name	Category	Biological Target	Oncological Indication
Trastuzumab	MAb	HER2 protein	Breast cancer
Bevacizumab	MAb	VEGF protein	Breast cancer, Colorectal cancer, NSCLC
Cetuximab	MAb	EGF Receptor	Colorectal cancer, Head and neck cancer
Panitumumab	MAb	EGF protein	Colorectal cancer
Imatinib	TKI	bcr-abl fusion protein	Chronic myeloid leukemia, Gastrointestinal stromal tumor
Erlotinib	TKI	EGF Receptor	NSCLC
Gefitinib[†]	TKI	EGF Receptor	NSCLC
Sunitinib	TKI	PDGF Receptor, VEGF Receptor 2, RET, CSF-1R and flt3	Renal cell carcinoma, Gastrointestinal stromal tumor
Sorafenib	TKI	VEGF Receptor 2, Ras and Raf kinases	Renal cell carcinoma, Hepatocellular carcinoma
Lapatnib	TKI	EGFR and HER2/neu proteins	Breast cancer

[†]Only used for patients who were benefiting with the drug before FDA relabeling.
HER2: Human epidermal growth factor receptor 2, VEGF: Vascular endothelial growth factor, EGF: Endothelial growth factor, PDGF: Platelet derived growth factor, RET: Rearranged during transfection proto-oncogene, CSF-1R: Colony stimulating factor-1 receptor, flt3: FMS-like tyrosine kinase 3, MAb: Monoclonal antibodies, NSCLC: Non-small cell lung cancer, TKI: Tyrosine kinase inhibitor

1-2 Background

1-2.1 The Ras/ Raf/MEK/ERK pathway

The Ras/Raf/MEK/ERK pathway (**Fig 1-1**) is at the heart of the signaling networks for cell growth; ubiquitously present, it governs cell proliferation, differentiation and survival. The steps involved in relaying of signals through this pathway are as follows:

Binding of ligands, such as endothelial growth factor (EGF), vascular endothelial growth factor (VEGF) and platelet derived growth factor (PDGFβ), to respective cell surface receptors or receptor tyrosine kinases (RTKs) (e.g., EGFR, VEGFR and PDGFR) initiates receptor dimerization and autophosphorylation on tyrosine residues. Ligand stimulated RTKs relay signals to MAPK cascade (composed of three sequential kinases Raf/MEK/ERK) via activation of Ras, a small G-protein. Activated Ras recruits Raf from cytosol to cell membrane and causes its activation, which in turn activates several downstream effectors including MEK, ERK, various substrates in cytoplasm (membrane proteins, phospholipase A_2, RTKs) and nucleus (transcription factors), and regulates cell proliferation, differentiation, survival and apoptosis (4).

Over-expression of ligands for RTKs (e.g., EGF, VEGF, and PDGF) that relay signals through the MAPK pathway or constitutive activation of components of Ras/Raf/MEK/ERK cascade (e.g., Ras oncogenes, K-ras, H-ras and N-ras; and mutant B-raf^{V599E}) results in uncontrolled cell growth, leading to tumor formation. Approximately 30% of human tumors contain mutations in one of the three Ras genes; K-ras, H-ras and N-ras (5). Mutations in K-ras protein are most common with frequencies of 70-90% in

pancreatic adenocarcinomas, approximately 50% in colon carcinomas and 20-50% in lung adenocarcinomas (5, 6). Mutations in B-raf gene are also very common with frequencies of approximately 70% in human malignant melanomas and 15% in colon cancers. Most frequent among B-raf mutations is the V599E amino acid change within the kinase activation domain, which makes it constitutively active (5, 7). Several anti-cancer drugs have been designed against these targets in the Ras/Raf pathway; **Table 1-1** lists drugs that are currently approved or under clinical development.

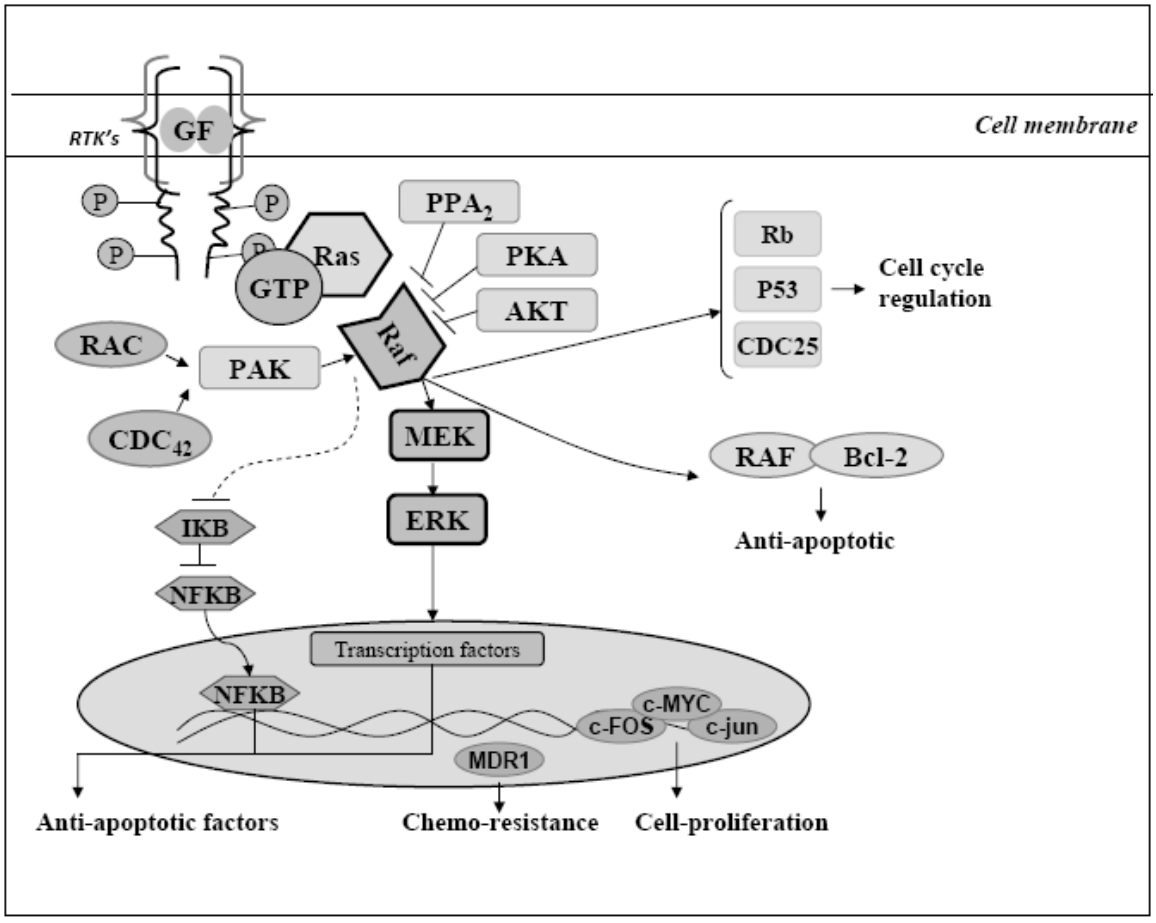

Fig 1-1. Schematic representation of the multiple pathways activated by Raf-kinases. (Adapted from Caraglia M et al, (8))

1-2.2 Sorafenib

Sorafenib (BAY 43-9006; 4-[4-[[4-chloro-3-(trifluoromethyl)phenyl]carbamoylamino] phenoxy]-*N*-methyl-pyridine-2-carboxamide; **Fig 1-2**), a novel bis-aryl urea, is approved in more than 70 countries for the treatment of patients with advanced kidney cancer, and in more than 60 countries for treatment of patients with advanced liver cancer (9). It is currently under clinical evaluation for a number of solid tumors, including the non-small cell lung cancer (NSCLC) and breast cancer.

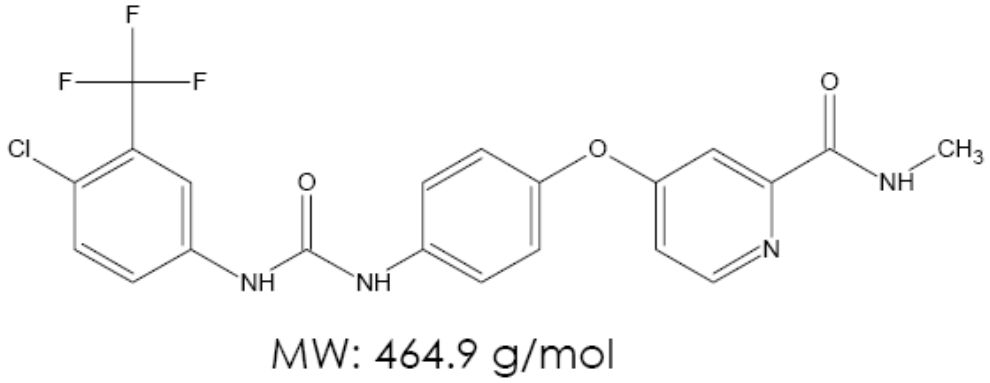

Fig 1-2 Molecular structure of sorafenib (IUPAC name: 4-[4-[[4-chloro-3 (trifluoromethyl) phenyl] carbamoylamino] phenoxy]-*N*-methyl-pyridine-2-carboxamide)

1-2.2.1 Mechanism of Action

Sorafenib targets both the tumor cells as well as tumor vasculature, and inhibits tumor cell proliferation and angiogenesis. Key targets for sorafenib are outlined in **Fig 1-3**. In tumor cells, sorafenib inhibits the intracellular B-raf (wild type, IC_{50} = 22 nM; and mutant, IC_{50} = 38 nM) and C-raf (wild type, IC_{50} = 6 nM) serine/threonine kinases in Ras/Raf pathway (10). Raf protein acts as an intermediate signaling molecule for multiple pathways (**Fig 1-1**) (8). Thus, inhibition of Raf proteins by sorafenib effectively blocks

the external or constitutive activation of the Ras/Raf pathway, which helps in restricting the aberrant cell proliferation.

Sorafenib also blocks the cell surface receptors (i.e., RTKs) on endothelial cell surfaces of tumor vasculature, which directly inhibits their autophosphorylation following binding of extra-cellular ligands. Specifically, sorafenib blocks the activation of VEGFR2 by VEGF (IC_{50}=90 nM) and PDGFR by PDGFβ (IC_{50} = 38 nM) (10). While VEGF is a key molecular modulator of angiogenesis, PDGFβ plays an important role in maturation of newly formed tubular structures by recruitment of mural cells like pericytes. Inhibition of VEGFR, PDGFR along with c-Kit, c-Ret, Flt-3 slows down the process of angiogenesis.

Additionally, Yu and colleagues (11) demonstrated *in-vitro* pro-apoptotic activity for sorafenib, mediated by reduction in levels of anti-apoptotic protein Mcl-1 (Myeloid cell leukemia 1) by destabilization and down-regulation in a time- and dose- dependent manner without affecting the other Bcl-2 family members.

As a tumor grows, the lack of sufficient blood supply creates an hypoxic environment, stimulating the release of factors like HIF-1α, which induces angiogenesis by activating the transcription of VEGF (12). **Fig 1-3** shows that these growth factors act in an autocrine manner on tumor cells or by the paracrine pathway on surrounding endothelial cells. Autocrine action on tumor cells increases their sensitivity towards growth factors, and paracrine action on endothelial cells stimulates the process of angiogenesis, which helps in increasing the blood supply to tumor from existing host blood vessels to relieve

tumor hypoxia. Sorafenib blocks both of these processes by its action on downstream targets, as shown in **Fig 1-3**.

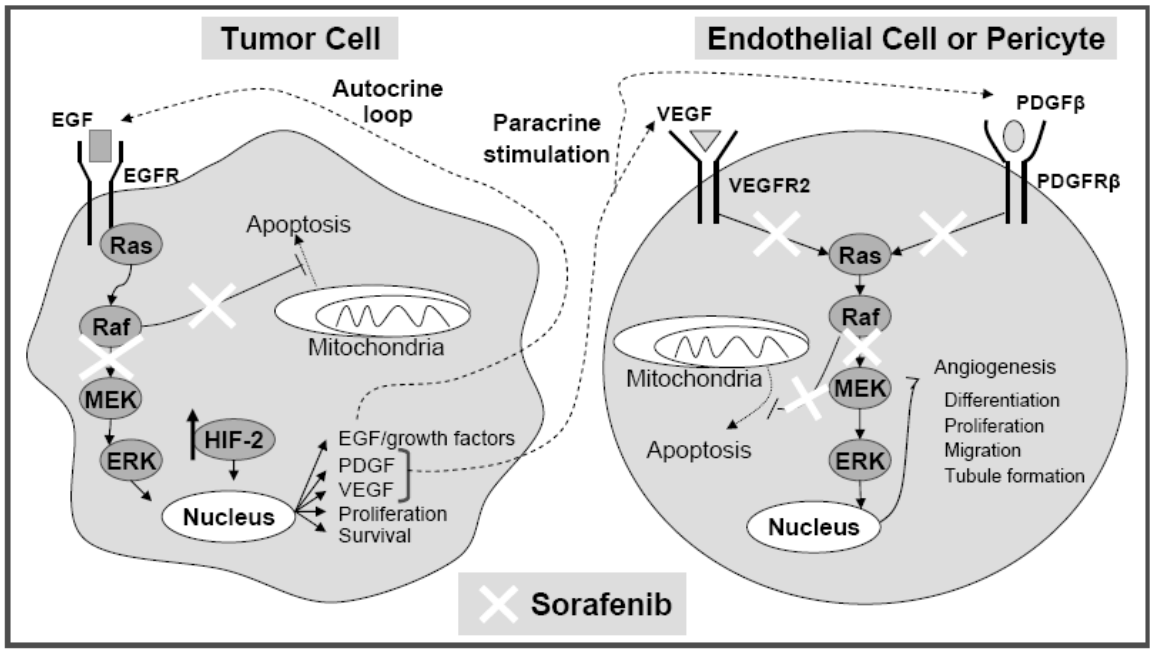

Fig 1-3 Key targets of sorafenib

1-2.2.2 Preclinical studies

In molecular biology assays, sorafenib inhibited various components of the Ras/Raf/MEK/ERK pathway. In cellular assays, sorafenib inhibited the MAPK pathway in colon (HCT-116, HT 29), pancreatic (Mia PaCa 2) and breast (MDA-MB-231) cancer cell lines expressing mutant K-ras or wild type or mutant B-raf, but did not show similar inhibitory effects in non small cell lung cancer cell lines (NCI-H460, A549) also expressing mutant K-ras (10). *In-vivo*, sorafenib demonstrated dose-dependent inhibition of tumor growth in mice tumor xenograft models of human colon (HT-29, Colo-205, both are B-raf$_{V599E}$ positive; DLD-1, K-ras positive), lung (NCI-H460, A549), breast (MDA-

MB-231, containing G463V b-raf and K-ras oncogenes), ovarian (SK-OV-3, over-expresses EGFR and HER2/neu), pancreatic (Mia PaCa 2, K-ras positive), melanoma (LOX, UACC 903 and 1205 Lu containing B-raf$_{V599E}$) and thyroid (containing oncogenic RET) cancer cell lines (1, 10). No toxicity was observed in these models when measured as weight loss relative to control animals or drug-related lethality. Additionally, sorafenib reduced microvessel area and microvessel density in these models, confirming its anti-angiogenic activity (10).

1-2.2.3 Clinical studies

Sorafenib has undergone or is undergoing multiple clinical trials both as a single agent and in combination with other chemotherapeutic agents. Results from phase I, phase II, phase III clinical trials along with clinical drug-drug interaction studies are summarized in **appendix 1-1 to 1-4**.

Five phase I/II clinical trials at NCI are currently evaluating the effectiveness or safe dose of sorafenib, as a single agent or in combination therapy, in metastatic castrate resistant prostate cancer (mCRPC), NSCLC, colorectal cancer (CRC), Kaposi's sarcoma (KS) and other solid tumors (ST). The rationales for use of sorafenib in these cancers are discussed below:

Rationale: Sorafenib in metastatic castrate resistant prostate cancer (mCRPC)

Prostate cancer is the leading non-cutaneous cancer among American men. A total of 192,280 cases are expected in the U.S. in year 2009, and 27360 will succumb to this

disease (13). Both androgen-independent or androgen-dependent prostate cancer cells require Ras protein for growth and survival (14). Inhibition of Ras by S-trans, trans fernesyl thiosalicylic acid (FTS) resulted in growth arrest and cell death of LNCaP and PC-3 prostate cancer cell lines (14). The Ras/Raf/MEK/ERK pathway is at the convergence of various signaling inputs, which could mediate the progression of prostate cancer from being androgen-dependent to becoming androgen-independent, hence inhibition of this pathway by sorafenib can be viewed as a potentially useful target for therapeutic intervention (15).

Levels of angiogenesis factors VEGF, PDGF and bFGF were found to be higher in prostate cancer tissue relative to normal tissue (16). Siegel et al (17) demonstrated that microvessel density (MVD) was higher in prostate cancer tissue than the adjacent hypoplastic or benign tissue, which increased the chances of metastasis. In pre-clinical settings, anti-angiogenic drugs have been shown to inhibit the growth of prostate cancer (18), and, clinically, improvement in the overall survival and progression free survival was seen following inclusion of anti-angiogenic drugs in clinical trials for patients with mCRPC (19). Sorafenib is thought to be effective in patients with prostate cancer because of its activity on Ras/Raf and VEGF pathway.

Rationale: Sorafenib in solid tumors (ST) in combination with bevacizumab

As mentioned in 1-3.1, sorafenib acts by a dual mechanism, namely inhibition of Raf kinase in the Ras/Raf/MEK/ERK pathway and inhibition of RTKs including VEGFR2 and PDGFβ. Bevacizumab, a recombinant humanized anti-VEGF monoclonal antibody

(rhuMAb), blocks the binding of human VEGF to its receptors (i.e. VEGFR1, 2 and 3) (20). It is composed of human IgG1 framework regions and antigen-binding complementarity-determining regions from a murine monoclonal antibody (muMAb VEGF A.4.6.1). While both agents are effective as single agents, in selected tumors, simultaneous attenuation of the Ras/Raf and VEGF pathways by sorafenib and bevacizumab combinations is thought to provide synergistic antitumor activity. However, this combined effect might also result in increased toxicity compared to each agent alone.

Rationale: Sorafenib in non-small cell lung cancer (NSCLC)

The underlying cause for 20-40% of NSCLC is inappropriate activation of Ras/Raf pathway by a point mutation in K-ras (21). Somatic activation of K-ras by spontaneous recombination in mice has shown to predispose these animals to cancer, predominantly lung cancer (22). A causal relationship between smoking, K-ras mutation and occurrence of lung cancer has been reported earlier (23, 24). Sorafenib is a potent inhibitor of both wild type and mutant B-raf ($B\text{-}raf^{V599E}$) and C-raf, which are downstream to the Ras protein in the Ras/Raf pathway; therefore, it inhibits the downstream signaling. Sorafenib has shown activity against NSCLC cell lines NCI-H460 and A549 with tumor growth inhibition of 27% to 68%, and has also shown regression of tumor growth in NCI-H460 NSCLC tumor xenograft model (25). Based on these mechanistic and pre-clinical evidences, sorafenib was thought to be effective in the treatment of human NSCLC.

Rationale: Sorafenib in metastatic colorectal cancer (CRC) in combination with Cetuximab

Cetuximab is approved by FDA for treatment of EGFR expressing CRC. It is a recombinant monoclonal antibody which binds specifically to the extracellular domain of epidermal growth factor receptor (EGFR, also known as HER1 or c-ErbB) in normal and tumor cells and competitively inhibits the binding of EGF and other ligands such as TGF-α to these receptor sites (26). Cetuximab binding to EGFR limits the downstream signaling by inhibiting the phosphorylation and activation of RTKs. However, the clinical response rate for cetuximab is only 10% (27), possibly because of drug resistance caused by mutations in the downstream Ras protein. The frequency of mutation in the K-ras protein in patients with CRC was reported to be approximately 50% (5, 6).

Sorafenib acts on B-raf and C-raf proteins which are further downstream to the Ras protein; hence, its combination with cetuximab may help in improving the overall response rate. Additionally, both VEGF and EGFR are validated targets for treatment in CRC. Clinically, the response rate for combination of bevacizumab (anti-VEGF agent) and cetuximab was 23%, and the median time to progression of disease was 4 months in patients with CRC (28, 29). Hence, simultaneous inhibition of EGFR, VEGFR2 and Ras/Raf pathway by combination of sorafenib and cetuximab is thought to provide better efficacy in patients with CRC than either agent alone.

Rationale: Sorafenib in patients with Kaposi's sarcoma (KS)

KS is a tumor caused by human herpesvirus 8 (HHV), which is associated with HIV infection, i.e., AIDS in some cases. Typically, it spreads on the skin but may also involve the mouth, GI tract and respiratory tract. Changes in skin lesions for patients with KS

may accompany with changes in the amount of blood vessels and/or blood flow to the lesions. The VEGFR2, VEGFR3, PDGF and c-kit are known to play a role in pathogenesis of KS (30, 31). Sorafenib is shown to inhibit the functioning of these molecules; thus, it may help in restricting the tumor growth/progression in patients with KS. Patients with HIV associated KS also receive ritonavir, the HIV protease inhibitor commonly used to treat patients with AIDS. Ritonavir is known to be a potent inhibitor of CYP3A4 (32), an important metabolic enzyme for sorafenib. Therefore, co-administration of ritonavir with sorafenib may affect sorafenib's plasma exposures; hence, in this dose escalation trial, the first cohort of patients on ritonavir was to be administered a lower than approved doses of sorafenib (i.e., 200 mg QD rather than clinically approved dose of 400 mg BID). The objectives of this trial were to investigate the pharmacokinetic interactions of sorafenib and ritonavir, and safety and efficacy of sorafenib, when administered with or without ritonavir, in patients with KS.

1-2.2.4 Biopharmaceutics and pharmacokinetics of sorafenib

Sorafenib is poorly soluble in water and has high lipophilicity, with solubility values for the tosylate salt ranging from 0.034 mg/100 mL at pH 1.0 to 0.013 mg/100 mL at pH 4.5 (33) and experimental hydrophobicity (log P) value of approximate 3.8 (34). Its calculated pKa values, 1.6 and 12.9[1], are outside the physiological pH range; hence, it largely remains neutral under physiological conditions.

1-2.2.4.1 Absorption and Bioavailability

[1] pKa predictions are based on ACD/labs software

In preclinical studies, sorafenib was almost completely absorbed in bile-duct cannulated female CD-1 mice (oral bioavailability (F_{oral}), 78.6%) and male Wistar rats (F_{oral}, 79.2%), and moderately absorbed in dogs (F_{oral}, 67.6%) following oral administration with time to maximum plasma concentrations (T_{max}) ranging between 1.5-2 hr (33).

In humans, sorafenib has never been administered intravenously; therefore its F_{oral} is unknown. Mean relative bioavailability (F_{rel}) of orally administered sorafenib tablet against polysorbate-80 based oral solution ranged from 38 to 49% (35), reflecting the importance of GI dissolution. Oral administration with a moderate fat-content meal did not affect the F_{rel}, but administration with high-fat meal reduced F_{rel} by 29%, compared to fasting state (35). T_{max} in patients ranged between 0-24 hr (approximate median 3 hr), with secondary peaks observed at 8-12 hr and 24 hr post-dose, indicating entero-hepatic recirculation (EHR), which was also seen pre-clinically with biliary-excretion of sorafenib in bile-duct cannulated rats. In Caco-2 cell line experiments, sorafenib was found to be highly permeable based on a comparison with 22 reference compounds. However, *in vivo* preclinical data indicated that the extent of absorption in bile cannulated rats was approximately 80%, and the absolute oral bioavailability in dogs was ~59.9%. In an *in vivo* mass balance study in humans it was determined that approximate 77% of the administered dose was excreted in feces (51% as parent drug) (33). The unchanged drug excreted in feces could have come from unabsorbed parent drug in GI tract and EHR. Their exact contribution is not known, but approximately 10% of the dose (5-8% as unchanged drug) was recovered in the first fecal sample (0-48 h) (33), suggesting that the fraction of unabsorbed drug in GI would be only approximately 10%. The extent of

absorption and gastrointestinal solubility could also vary between subjects. Based on the definition of solubility and permeability in BCS classification (36), sorafenib may be classified as a BCS class II or IV drug because of its low gastrointestinal solubility and medium to high gastrointestinal permeability. In P-gp-expressing L-MDR1 cell line experiments, sorafenib was found to be a weak to moderate substrate of the P-gp efflux transporters (33), consistent with medium to high gastrointestinal permeability; however, the actual contribution of P-gp-mediated efflux, if any, in therapeutically relevant gastrointestinal concentrations is unknown.

1-2.2.4.2 Distribution

Sorafenib is highly plasma protein bound (PPB) with 99.5% of sorafenib bound primarily to serum albumin, and to a lesser extent to α- and β- globulins and low density lipoproteins (LDLs). The plasma-to-blood ratio for sorafenib was 1.33, suggesting no significant accumulation in RBC's or platelets (33).

In preclinical quantitative organ and tissue distribution studies with radio-labeled drug, sorafenib and its metabolites were found to be homogenously distributed throughout the body, with the exception of the brain, seminal vesicles and solid bones. The highest exposure of sorafenib was found to be in the liver. Sorafenib was rapidly eliminated from all organs and tissues (with $t_{1/2}$~20-36 hr) with exception of skin for which $t_{1/2}$ was 72.8 hr (33). In a mass balance study in healthy male volunteers, with administration of 100 mg sorafenib as a solution formulation, 96% of the dose was recovered within 14 days, 77% of which was excreted in feces (51% as unchanged drug and 19% as N-

demethylated metabolite, M6) and 19% was excreted in urine as the glucuronide metabolites (37). About 5-8% of unchanged drug was recovered in the first fecal sample (0-48 hr), and larger fractions of 19-25% were found in the second (48-72 hr) and third (72-96 hr) samples (33). Neither the N-oxide metabolite nor the glucuronide metabolite was detected in feces, and no unchanged drug was found in urine (37). The excretion of a large proportion of unchanged drug in feces may be caused by, 1) unabsorbed drug because of low GI solubility and/or 2) EHR of sorafenib (see **section 1-3.4.1**). The EHR for sorafenib may be described by two processes, 1) biliary excretion of unchanged drug , 2) glucurodination of drug, biliary excretion of glucuronide metabolite into the gut, deconjugation and subsequent reabsorption into the systemic circulation and/or fecal elimination, 3) oxidation of drug to N-oxide metabolite, biliary excretion of N-oxide metabolite into the gut, reduction by colonic bacteria to the parent drug and subsequent reabsorption in systemic circulation and/or fecal elimination (33). Following oral administration, sorafenib (parent drug) accounts for 70-85% of circulating moieties in human plasma while approximately 17% remain in the form of N-oxide metabolite (33).

1-2.2.4.3 Metabolism

Sorafenib is metabolized by two parallel pathways, namely phase I oxidative metabolism by CYP3A4 enzymes and glucuronidation by UGT1A9 enzymes (37). A total of eight metabolites have been identified in humans (**Fig 1-4**), of which five were present in plasma (35). The metabolites M2, M4 and M5 were active against similar targets as sorafenib in *in-vitro* pharmacological assays, but their plasma levels were much lower

than sorafenib (33). The most predominant human metabolite, M2, was both less potent and less active than sorafenib (33).

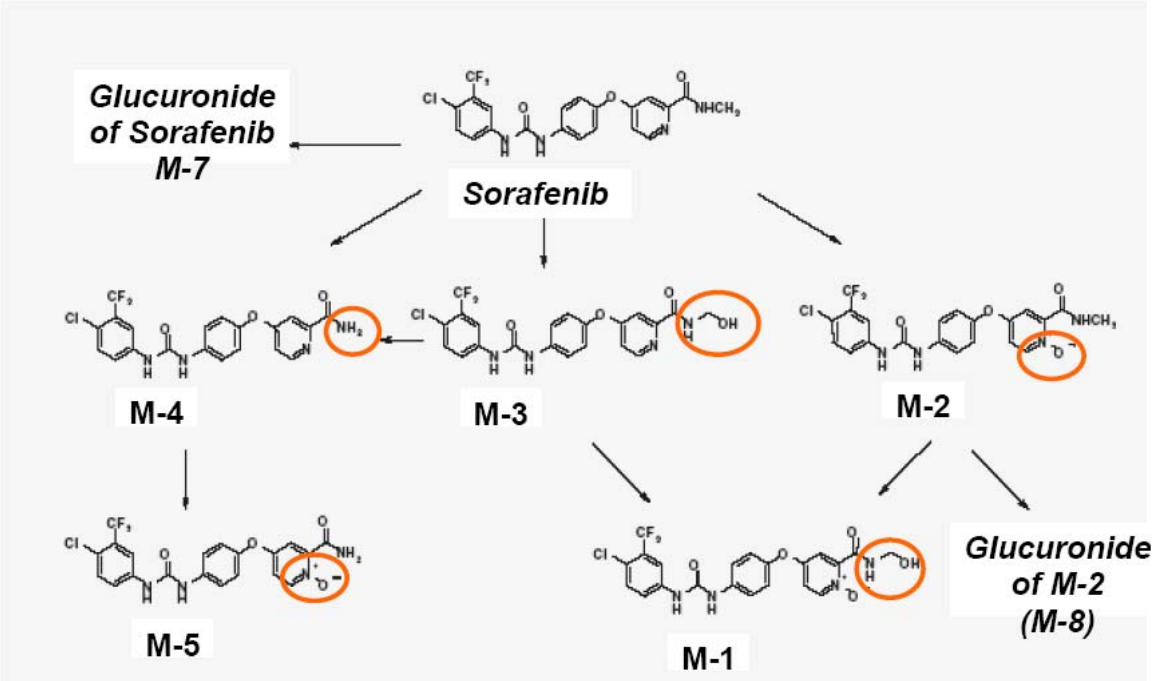

Fig 1-4 Metabolic profile for sorafenib

1-2.2.4.4 Elimination

In cancer patients, the mean terminal plasma half-life for sorafenib ranged between 25-48 hr. As mentioned in **1-3.4.2**, sorafenib is primarily excreted unchanged in feces and only a small proportion is eliminated in urine as metabolites.

1-2.2.5 Dose proportionality studies

In phase I clinical studies with sorafenib, the main exposure parameters estimated were $AUC_{0\text{-}12 \text{ or } 0\text{-}24,}$ C_{max}, t_{max}, $t_{1/2}$ and steady-state accumulation ratio (i.e., $AUC_{\tau}^{SS}/AUC_{\tau}^{SD}$). Considerable inter-patient variability was observed for sorafenib pharmacokinetics in

these trials, as shown in **Table 1-2**. Variability in pharmacokinetic parameters after administration of multiple doses was greater than the variability on day 1 (**Table 1-2**). In these studies, a less-than-proportional increase in AUC and C_{max} was observed with escalating doses of sorafenib, and plateau in AUC and C_{max} was reached at doses of 600 mg BID (35), most likely due to its limited GI solubility (solubility-limited absorption). Steady-state for sorafenib was reached after approximately seven days, with little additional drug accumulation thereafter (38). This indicates that sorafenib follows time-independent pharmacokinetics; suggesting that drug levels after multiple doses can be predicted from first/single dose pharmacokinetics. Throughout the dose range of 50 to 800 mg BID, the ratio of AUC and C_{max} of N-oxide metabolite to sorafenib were similar, suggesting constant (first-order, non-saturable) CYP3A4 metabolism at or above therapeutic doses (37).

Table 1-2. Summary of exposure parameters from phase I clinical trials

Dosing schedule (reference)	Dose (BID)	AUC_{0-12} (mg.h/L)						C_{max} (mg/L)						$t_{1/2}$ (hr)		
		Day 1			Last day			Day 1			Last day			Last day		
		N	GM	%CV	N	GM	%CV	N	GM	%CV	N	GM	%CV	N	GM	%CV
7 on/7off (39)	100	1	6.8	NC	3	24.4	76	3	1.0	32	3	3.5	74	3	38.1	48
	200	1	6.1	NC	3	19.1	17	3	0.8	86	3	2.6	9	3	20.1	13
	400	2	18.0	5	4	56.6	91	4	2.3	37	4	6.2	107	3	20.0	22
	600	3	21.0	81	6	64.8	77	6	2.7	61	6	6.6	71	6	24.3	21
21 on/7 off (38)	100	4	4.8	105	4	30.2	37	4	0.7	100	4	4.4	11	4	25.2	40
	200	3	24.9	34	3	50.5	13	3	3.6	24	3	6.3	50	2	29.8	13
	400	9	24.0	43	5	76.5	25	10	3.0	71	6	10.0	24	3	23.8	39
	600	12	30.4	56	6	77.0	46	12	4.6	56	8	9.2	45	6	38.6	38
28 on/7 off (40)	100	3	10.1	97	5	38.1	37	7	2.0	72	5	4.7	29	4	26.3	27
	200	4	10.9	38	5	34.7	44	6	1.3	34	5	4.0	52	4	31.8	10
	400	4	21.8	59	3	47.8	24	4	2.9	68	3	5.4	41	3	27.4	24
	600	3	10.1	97	5	38.1	37	7	2.0	72	5	4.7	29	4	26.3	27
Continuous (35)	100	3	23.8	43	NC	NC	NC	4	2.3	54	NC	NC	NC	NC	NC	NC
	200	3	16.1	83	NC	NC	NC	4	2.8	88	NC	NC	NC	NC	NC	NC
	400	5	71.7	43	NC	NC	NC	5	9.4	44	NC	NC	NC	NC	NC	NC
	600	8	79.0	52	NC	NC	NC	12	9.8	51	NC	NC	NC	NC	NC	NC

GM, Geometric mean, CV, Coefficient of variation, NC, Not calculated

1-2.2.6 Clinical drug-drug / drug-disease interaction studies

Results from different drug-drug interaction (DDI) studies for sorafenib are summarized in appendix 1-4, and the important findings are summarized below:

a) When a single 50 mg dose of sorafenib was co-administered with a potent CYP3A4 inhibitor ketoconazole (400 mg QD, started three days prior to co-administration with sorafenib) no significant change in sorafenib plasma exposures was observed; however, the plasma concentrations of the nN-oxide metabolite were significantly decreased (37). This may be explained by compensatory elimination of sorafenib by parallel glucuronidation pathways, assumed to be not substantially affected by ketoconazole. Glucuronidation may be a high capacity pathway under normal physiological conditions, i.e., not saturated. However, in *in-vitro* studies with human liver microsomes and c-DNA expressed UGT1A isoforms, ketoconazole has also been shown to inhibit UGT1A9 enzyme with K_i value of 31.9±3.3 μmol/L (41). It is possible that the ketoconazole dose was not sufficient to inhibit both the CYP3A4 and UGT1A9 pathways; therefore, we do not observe any significant changes in sorafenib exposures.

b) In a probe substrate clinical trial studying the effect of sorafenib on CYP3A4, co-administration of sorafenib with CYP3A4 substrate midazolam showed no significant changes in midazolam exposure, which suggests that sorafenib is neither an inhibitor nor an inducer of CYP3A4 (35).

c) Following co-administration with another CYP3A4 substrate, gefitinib, in patients with NSCLC, no changes in systemic exposures of sorafenib was observed, but AUC for gefitinib decreased by 38%. The exact mechanisms for this reduction in gefitinib

exposure is not known but is thought to be mediated by mechanisms other than enzyme induction, e.g., PPB displacement (42).

d) Sorafenib inhibited the glucuronidation of irinotecan, which is known to be metabolized by UGT1A1 and UGT1A9 pathways. When sorafenib (400 mg BID) was administered in continuous dosing cycle with irinotecan 125 mg/m^2 (administered on days 1, 8, 15 and 22 of each cycle), mean AUC_{0-10} and C_{max} of sorafenib increased by 68% and 78%, respectively, but the reduced 140 mg fixed dose of irinotecan had no effect on exposures of sorafenib (43). *In-vitro* experiments demonstrated that the inhibitory rate constants (Ki) for inhibition of glucuronidation by UGT1A1 and UGT1A9 pathways by sorafenib were 1 μM and 2 μM (35), consistent with the *in-vivo* effect of sorafenib on irinotecan.

e) To assess the effects of chronic hepatic impairment on the pharmacokinetics of sorafenib, sorafenib systemic exposures were compared between patients with Child-Pugh A and B hepatocellular carcinoma (44). Patients with Child-Pugh B had higher mean values for both AUC_{0-8} hr and C_{max}, although these differences were not statistically significant (44). Plasma exposures of metabolite M5 (see **Fig 1-4**) were slightly lower in Child-Pugh B patients, while levels of M2 and M4 were not different between two groups (44).

Overall, these results indicate that alterations in sorafenib metabolism via the UGT1A9 pathway may be more important than the CYP3A4 pathway. However, there are no clinical studies showing that the inhibition of CYP3A4 has no effect on sorafenib exposures when it is administered in a clinically relevant dosing regimen, i.e., 400 mg

BID. This suggests the need for further exploration of both the CYP3A4 and UGT1A9 metabolic pathways.

Except P-gp, for which sorafenib is a weak to moderate substrate, no other transporters systems are known to be involved in the GI absorption of sorafenib. However, based on its known disposition profile, i.e., hepatobiliary elimination, it may interfere with disposition of (drug) substrates of MRP2 and BCRP transporters. Co-administration of sorafenib with docetaxel and doxorubicin, both of which are partly excreted by hepatobiliary elimination and are substrates for P-gp and MRP2 transporters (45-48), increased their respective systemic exposures by 21-80% (Appendix 1-4) (49, 50).

1-2.3 Population pharmacokinetic analysis

At the annual meeting of the American Association of Pharmaceutical Sciences (AAPS) in 2007, Rajagopalan et al (51) from Bayer Health Care presented the population pharmacokinetic analysis for sorafenib in cancer patients (n=229) with additional single dose pharmacokinetic data in healthy subjects (n=69). Population pharmacokinetic analysis was performed with NONMEM using the first-order conditional estimation (FOCE) method with η-ε interaction. The base pharmacokinetic model was a two-compartmental model with first order absorption (k_a), absorption lag time and relative oral bioavailability modeled as a function of dose to incorporate the observed infra-proportional increase in sorafenib exposure with increasing single doses. Covariates examined included, age, body weight, creatinine clearance, gender, ethnicity (Japanese vs. non-Japanese), disease (cancer patient vs. healthy subject), and baseline laboratory

markers (both as continuous variables and categorical variables i.e., less than upper normal limits (ULN) vs. greater than ULN). Laboratory values for SGOT, SGPT, total bilirubin, alkaline phosphatase, and total protein were examined.

The absorption rate constant and the relative bioavailability were found to be influenced by ethnicity. The final model population (mean) values were: clearance (CL/F) =3.31 L/hr (inter-patient variability, 25%), volume of distribution for central compartment (Vc/F) =85.2 L (inter-patient variability, 10%), volume of distribution for peripheral compartment (Vp/F) =24.6 L (inter-patient variability, 45%), inter-compartmental clearance (Q)=1.29 L/hr, first-order absorption rate constant (ka)=0.229 hr^{-1} (inter-patient variability, 104%), and t_{lag}=0.214 hr. The CL/F of 3.31 L/hr suggests a low hepatic extraction ratio when compared with hepatic blood flow of 90 L/hr, even though true *in-vivo* CL_{total} is not known. The population mean of ka for Japanese patients was 0.106 hr^{-1}, and relative oral bioavailability was 28.9%, lower compared to non-Japanese patients (51).

1-2.4 Efficacy of sorafenib in various solid tumors

Sorafenib has been investigated in several solid tumors as a single agent or in combination therapy, including the renal cell carcinoma, hepatocellular carcinoma, melanoma, head and neck carcinoma, nasopharyngeal carcinoma, breast cancer and NSCLC etc. Its response rate varies widely among patients with different tumors (see **Table 1-3**), which may be attributed to differences in underlying tumor biology, variation in sorafenib exposures among patients and physiological or genetic differences. The

tumor response in these trials was measured by RECIST (response evaluation criteria in solid tumors). RECIST is a set of published guidelines which evaluate the changes in measurable lesions from their baseline size in order to classify drug response in following categories: complete response (CR), disappearance of all target lesions; partial response (PR), 30% decrease in the sum of the longest diameter (LD) of target lesions; stable disease (SD), < 30% decrease and < 20% increase in sum of LD of target lesions; and progressive disease (PD), ≥ 20% increase in sum of LD of target lesions (52).

Table 1-3 Summary of treatment outcomes with sorafenib in selected Phase II/III trials

Trial	**CR**[†] **(%)**	**PR**[†] **(%)**	**SD**[†] **(%)**	**PD**[†] **(%)**	**Not evaluable (%)**	**PFS (months)**	**OS (months)**	**Current status for tumor type**
Phase III, RCC (53)	<1	10	74	12	4	5.5	NR	Approved
Phase III, HCC (54)	0	2	71	NR	NR	4.1	10.7	Approved
Phase II, HCC (44)	0	2	34	35	23	4.2	9.2	Approved
Phase II, Melanoma (55)	0	3	16	73	NR	2.5	NR	Not Approved
Phase II, mCRPC (56)	0	20	14	66	NR	3.9	14.6	Not Approved
Phase II, Head and Neck Cancer (57)	0	4	37	37	4	1.8	4.2	Not Approved

CR, Complete response, PR, Partial response, SD, Stable disease, PD, Progressive disease, PFS, Duration of progression free survival, OS, Duration of overall survival, RCC, Renal cell carcinoma, HCC, Heaptocellular carcinoma, mCRPC, Metastatic castrate resistant prostate cancer, NR, Not reported

[†] Response evaluation was based on RECIST criteria

1-2.5 Toxicities and their plausible mechanisms

Sorafenib treatment-related adverse events observed in selected phase I/II/III clinical trials are summarized in **Table 1-4**. The most common treatment-related toxicities for sorafenib are hand-foot reaction syndrome (HFSR), diarrhea, skin rash / desquamation, hypertension and fatigue (58). Clinically, sorafenib is administered in continuous dosing cycles, and, being a cytostatic agent, long-term administration is required to achieve/maintain therapeutic benefit; hence, even lower incidences/grades of toxicities may have an adverse impact on patients' quality of life. As described in **Table 1-5,** several patients had to reduce doses or to discontinue sorafenib treatment because of these treatment-related toxicities. The possible mechanistic causes for these toxicities are discussed below:

(A) Dermatological toxicities

The dermatological toxicities may be caused by slow removal of sorafenib from the skin, compared to other organs as observed in preclinical animal studies ($t_{1/2}^{skin}$~72.8 hr versus $t_{1/2}^{other\ organs}$~20-36 hr) (49). Other hypotheses regarding sorafenib-induced dermatological toxicities are, (a) accumulation of potentially toxic concentrations in eccrine sweat glands that are present in greatest density in the palms and soles, (b) inhibitory effects of sorafenib on MAP-kinase pathway in keratinocytes (59) and (c) damaged vascular integrity due to the dual VEGFR2 and PDGFR inhibition by sorafenib (60).

(B) Cardiovascular toxicities

Hypertension is a common side effect of most anti-angiogenic therapies. It may be caused by vascular stiffness resulting from inhibition of replication of endothelial cells or by reduction in number of arterioles and capillaries, leading to reduction in vascular surface area and an increase in peripheral vascular resistance (59). Sorafenib may also alter the angiotensin-II regulated control of blood pressure in renin-angiotensin system, which is mediated by protein kinases such as EGFR, PDGFR etc (59). Veronese et al (61) conducted a pharmacodynamic study on 20 patients to help understand the mechanism of sorafenib-associated hypertension. Factors considered for the analysis were known mediators of vascular tone and hypertension (i.e., aldosterone, catecholamines, endothelin, urotensin II, serum VEGF and von Willebrand factor), which were measured at baseline and after three weeks of therapy. Results indicated that sorafenib-induced hypertension may be associated with changes in catecholamines and indices of vascular stiffness.

(C) GI toxicities

One possible cause for diarrhea may be the persistent contact of sorafenib and/or metabolites with GI lumen because of its low solubility, which may cause irritation of GI lumen. Both VEGF and MAP-kinase pathways are involved in mucosal defense and repair; inhibition of these pathways by sorafenib may increase the sensitivity of GI lumen to these drugs (59). Sorafenib is also recycled via EHR, which may further worsen the diarrhea by re-circulating the drug to GI lumen.

(D) Constitutional toxicities

The exact reason for treatment-associated fatigue is not known, but it may be caused by natural progression of disease, independent of administered treatment. Other possible reasons are decrease in ATP (62) with cytostatic treatments or hypothyroidism associated with anticancer treatments.

Table 1-4 Summary of the most frequent sorafenib-related adverse events from selected phase I/III trials.

Toxicities	Combined phase I trials, ref[†] (63), % (n)		Phase III RCC, ref (53), % (n)		Phase III HCC, ref (54), % (n)		Phase II Melanoma, ref (55), % (n)
	All grades	gr ≥ 3	All grades	gr ≥ 3	All grades	gr ≥ 3	gr ≥ 3
Fatigue	40 (70)	6 (11)	37 (165)	5 (22)	22	4	16 (21)
Anorexia	35 (60)	1 (2)	16 (73)	<1 (3)	14	<1	NR
Diarrhea	34 (59)	4 (7)	43 (195)	2 (11)	39	8	8 (11)
Rash:desquamation	27 (46)	2 (4)	40 (180)	1 (4)	16	1	7 (10)
HFSR	25 (44)	8 (13)	30 (134)	6 (25)	21	8	7 (9)
Hypertension	NR	NR	17 (76)	4 (16)	5	2	NR
Nausea	11 (2)	0 (0)	23 (102)	<1 (3)	11	<1	NR

[†]ref = reference number

RCC, Renal cell carcinoma, HCC, Hepatocellular carcinoma, NR, Not reported, HFSR, Hand-foot skin reaction

Table 1-5 Summary of treatment discontinuations/interruptions/dose reductions due to treatment associated side effects from selected sorafenib trials

Trial	Dose reductions (%)	Dose interruptions (%)	Treatment discontinuation (%)
Phase III, RCC (53)	13	21	10
Phase III, HCC (54)	26	44	38
Phase II, HCC (44)	NR	NR	20
Phase II, Melanoma (55)	16	27	0
Phase II, mCRPC (56)	NR	NR	6
Phase II, Head and Neck Cancer (57)	57	50	4

RCC, Renal cell carcinoma, HCC, Hepatocellular carcinoma,
mCRPC, Metastatic castrate resistant prostate cancer, NR, Not reported

1-3 Relevance of pharmacogenetic evaluation

Considerable inter-patient variability in sorafenib exposures (**Table 1-2**), possible ethnicity-dependent differences in oral absorption rate and bioavailability observed in the population pharmacokinetic analysis, and large inter-patient variability in response rates and incidences/grades of toxicities (**Tables 1-3 and 1-4**) are characteristic for sorafenib. Several factors may contribute to this variability: intrinsic patient factors (e.g., age, gender, race, extent of EHR, PPB and genetics), extrinsic factors (e.g., concomitant medications or concomitant illnesses) or factors limiting the performance of dosage form (e.g., poor solubility and high lipophilicity). These factors may also include genetic differences in pharmacokinetics or pharmacodynamics. Identification of genetic markers and their subsequent inclusion in FDA approved labels, such as dihydropyrimidine dehydrogenase (DPD) for **capecitabine**, G6PD for **primaquine**, Her2/neu for **trastuzumab**, UGT1A1 for **irinotecan**, TPMT variants for **azathioprine**, Philadelphia (Ph1) chromosome deficiency for **busulfan**, is a result of pharmacogenomic explorations, and suggests that a significant portion of inter-individual variability in tumor response, in incidence and severity of adverse effects and in drug and/or metabolite exposures may be explained by differences in the genetic makeup of patients (7). FDA has identified pharmacogenomics as a key opportunity in their "Critical Path" recommendations for the development of new medicinal compounds (40). The observed ethnic differences in bioavailability and absorption rate for sorafenib, reported in population pharmacokinetic analysis, also suggest possible underlying genetic differences in expression of drug metabolizing enzymes or transporters.

The process of identifying these genetic variations and understanding the clinical significance are still evolving; however, several methods have been suggested: The traditional method has been the *candidate gene approach*, in which a single gene or a small number of genes (pre-identified based on existing knowledge) are evaluated in their ability to explain the differences in the pharmacokinetics/pharmacodynamics of the drug. The pathways-based (polygenic) approach, involving the evaluation of multiple single nucleotide polymorphisms (SNP) in components of a 'biological' or 'pharmacological' pathway, is thought to be a better predictor of therapeutic responses compared to the single gene variant approach (64, 65). Another evolving method is the *whole-genome analysis,* in which the entire genome is taken into consideration without bias towards a particular gene or pathway, using techniques like the SNP chip and gene expression platforms. A major advantage of this approach is identification of previously unknown genetic variants, but the disadvantages are enormous amount of information, high rate of false positive findings and huge expenses.

For the current exploratory studies using sorafenib, the polygenic pathway approach has been used to investigate the effect of known genetic polymorphism in drug metabolizing enzyme and drug targets on drug exposure (pharmacokinetics) and drug responses (pharmacodynamics, tumor response and incidences and severity of adverse events).

Genetic variants

The underlying hypothesis behind genotype-phenotype-exposure-response associations is that drug exposures, drug responses and toxic effects can be predicted by the

identification of patients' genotype or phenotype before the start of chronic treatment (66). The functional consequences of genetic variations range from no effect to altered expression of the encoded protein to changes in cellular function/location (66). The genetic variations in metabolic enzymes and drug targets that were studied for sorafenib are described below:

1-3.1 Metabolic Enzymes

1-3.1.1 CYP3A4 and CYP3A5

Cytochrome P450 enzymes are primarily expressed in the liver and intestine; they are responsible for the oxidative metabolism of endogenous steroids, hormones as well as many drugs (67). CYP3A5 is expressed in similar levels at all developmental stages, but CYP3A4 is an enzyme specific for adults (68); expression levels for both of these enzymes vary based on ethnicity. Considerable inter-individual variability has been observed in the expression and metabolic activity of CYP3A enzymes, of which 70-90% is thought to be attributable to genetic control (69). It is important to consider these genetic differences to avoid possible DDIs.

Until today, 20 CYP3A4 alleles, consisting of 38 SNPs have been reported (66). Most occur at low frequency or are prevalent in specific populations. For example, the frequency of CYP3A4*1B (-392 A>G) SNP located in 5'-regulatory region is 3.6-9.6% in Caucasians and 53-67% in African-Americans (70). This SNP is reported to be epidemiologically associated with a number of disease states, including prostate cancer, leukemias caused by treatment with epipodophyllotoxins, and early puberty (69). So far

no association has been reported between the CYP3A4*1B genotype and the pharmacokinetics of its known substrates (70). Shimanda et al (71) compared the expression and activity of various cytochrome P-450 enzymes in liver microsomes from Japanese and Caucasians patients (N=30 each group). They reported no race-related differences in CYP3A4 expressions, but observed differences in activity, where metabolic activation by CYP3A4 was found to be higher in Caucasians than in Japanese patients. The CYP3A4*1B SNP was absent in the Japanese population (72). However, this SNP appears to not explain the lower relative bioavailability for patients' with Japanese ethnicity compared to Caucasians, as observed in population pharmacokinetic analysis (51).

CYP3A5 is polymorphically expressed in adults with detectable expression of 10-20% in Caucasians, 33% in Japanese and 55% in African-Americans (70, 72). CYP3A5*3 SNP is associated with low expression of CYP3A5 protein (70). CYP3A5*3 SNP causes splice site defect, which results in incorporation of intronic sequences in mature mRNA, leading to premature truncation of translation and production of truncated protein. The frequency of this polymorphic variant varies from approximately 90% in Caucasians, 75% in Japanese to 50% in African-Americans. CYP3A4 and CYP3A5 are considered to have overlapping substrate specificity. No SNP in the CYP3A5 gene has been described which can explain the variability in metabolism of its substrates.

1-3.1.2 UGT1A9

The UGT enzyme system is divided into two superfamilies, UGT1 and UGT2, which are further subdivided into three subfamilies, i.e., UGT1A, UGT2A and UGT2B. Several genetic polymorphisms are described in the UGT1A gene which includes UGT1A1, UGT1A6, UGT1A7, UGT1A9, UGT1A10 etc.

UGT1A9 is expressed in the liver as well as in a number of extra-hepatic tissues, including the GI tract, kidney, ovary, prostate and breast (73). Due to its large substrate spectrum and abundance in these tissues, UGT1A9 plays a central role in the detoxification of a substantial number of molecules. Girard et al. identified a number of polymorphisms within the promoter region and exon 1 of the gene, which were related to protein expression and the glucuronidation activity (74). Expression of UGT1A9 in human liver samples were higher for patients with promoter region variations at positions -275 ($p=0.006$), -331/-440 ($p=0.046$), -665 ($p=0.042$) and -2152 ($p=0.0004$). UGT1A9*2 ($C^{3}Y$), UGT1A9*3 ($M^{33}T$), UGT1A9*4 ($Y^{242}X$) and UGT1A9*5 ($D^{256}N$) SNPs in the coding region have shown to result in complete or partial inactivation of glucuronidation activity for substrates such as SN-38, the active metabolite of irinotecan (74). UGT1A9*3 dramatically reduced the SN-38 glucuronide formation, with only 3.8% activity compared to UGT1A9*1 allele (75). The UGT1A9*1/*3 genotype was present in about 4% of Caucasians but was absent in African-Americans (75). The UGT1A9*5 SNP was identified in Japanese subjects and the variants were found to have less than 5% catalytic activity towards SN38 glucuronidation when compared to wild type carriers (76). Recently, Girard et. al. reported a novel I399 C>T SNP in the intronic region of UGT1A9 gene, which resulted in increased glucuronidation of UGT1A1 and UGT1A9 substrates in

in- vitro human liver microsomes studies (77); the frequency of this SNP was 44% in Caucasians liver samples. The homozygous UGT1A9 I399TT genotype was associated with 1.7-fold higher expression of UGT1A1 protein and 2.5- and 1.8-fold higher capacity to glucuronidate SN-38 and bilirubin respectively, in the liver microsomal samples that harbored the reference UGT1A1 -53$(TA)_{6/6}$ repeats. Sandanaraj et al (78) tested the findings of Girard et al (77) in Asian cancer patients, and confirmed 2.3 fold higher expression of UGT1A9 mRNA in liver tissues of subjects restricted to harboring only the $(TA)_{6/6}$ polymorphic repeats in the TATA box region of the UGT1A1 gene; they also showed the SNP to be associated with increased glucuronidation activity and significantly low systemic exposure to SN-38 (78).

1-3.2 Drug targets

Sorafenib targets the VEGFR-2 and Ras/Raf pathways. Functional polymorphisms in these targets may alter receptor-sensitivity and/or drug-activity. Characterization of such polymorphism is important to understand the inter-individual differences in drug effect or toxicities.

1-3.2.1 Kinase Domain Receptor (KDR) or Vascular Endothelial Growth Factor Receptor2 (VEGFR2)

VEGF is important for initiation and regulation of angiogenesis. Although the biological effects of VEGF are mediated by two receptors (VEGF receptor1 or Flt1 and VEGF receptor 2 or Flk1/KDR). The interaction between VEGF and VEGFR2 is believed to be more important for angiogenesis during tumor development. Försti et al. reported 8 SNPs

in VEGFR2 gene region (79). Two of them, rs2305948 (Val297Ile) and rs1870377 (Gln472His) have a higher incidence and result in more important functional effects. They are located within the immunoglobulin-like (Ig like) domains 3 and 5, respectively. Ig-like domain 3 has been shown to be critical for VEGF binding. Ig-like domains 4–7, on the other hand, have been shown to contain structural features that inhibit receptor signaling in the absence of VEGF (79). The frequencies of variant allele for these SNPs in Swedish and Polish patients with breast cancer were 27% and 50%, respectively (79). Exploration of these polymorphisms is important to understand the differences in efficacy or toxicity of sorafenib.

CHAPTER TWO

RESEARCH HYPOTHESES

Overview

This research project is designed to explore the clinical pharmacology-based treatment approaches for sorafenib in patients with mCRPC, CRC, NSCLC, KS and other solid refractory tumors, following administration as single agent or in combination therapy. Sorafenib is associated with high inter-individual variability in plasma exposures (pharmacokinetics), clinical efficacy and incidences of treatment-related toxicities (**Tables 1-2**, **1-3 and 1-4**): For example, the coefficient of variation (%CV) on AUC_{τ}^{SD} for 400 mg BID dose is reported to vary between 24-91%, the rate of partial response and stable disease (from selected phase II/III clinical trials) varied between 2-20% and 14-74%, respectively. Several patients refused further treatment or were administered reduced, possibly sub-therapeutic, doses of sorafenib because of treatment-related toxicities (**Table 1-5**). Markers for prediction of sorafenib-associated variability in exposure, effect and toxicity are not known, but need to be elucidated to maximize the treatment effectiveness and to minimize the treatment-related side effects and treatment discontinuations.

This project specifically aims to identify possible demographic, clinical or pharmacogenetic covariates that may influence the plasma exposures (pharmacokinetic profiles) of sorafenib, and to evaluate the impact of variable exposures on treatment efficacy and incidences of treatment-associated toxicities. In addition, a few other laboratory and pharmacogenetic markers for clinical efficacy and toxicity, and pharmacogenetic markers for prostate cancer risk are to be explored.

The research hypotheses that will be tested are as follows (**Fig 2-1**):

1. Demographic variables such as body weight, body surface area (BSA), age, gender and ethnicity have quantifiable effects on sorafenib exposures.
2. Abnormal liver function, characterized by lower than normal levels of albumin and total protein, and above normal levels of ALT, AST, alkaline phosphatase and total bilirubin, have quantifiable effects on sorafenib exposures.
3. Pharmacogenetic variations in metabolic enzymes for sorafenib, i.e., CYP3A4*1B, CYP3A5*3C, UGT1A9*3 and UGT1A9*5, have quantifiable effects on sorafenib exposures.
4. Variability in exposures of sorafenib among patients is associated with variable clinical efficacy of sorafenib in patients with various solid tumors, after adjusting for differences in tumor types.
5. Pharmacogenetic variations in VEGFR2, a drug target for sorafenib is associated with differences in clinical efficacy among patients with solid tumors.
6. Variability in sorafenib exposures among patients is associated with variable incidences and severity of treatment-associated toxicities.

7. Pharmacogenetic variations in VEGFR2, a drug target for sorafenib are associated with incidences of hypertension, a treatment-associated side effect.
8. Sorafenib induces the production of prostate specific antigen (PSA) by the prostate gland; therefore, PSA is not a suitable surrogate marker for clinical efficacy in patients with prostate cancer treated with sorafenib.
9. Clinical responses for patients with solid tumor treated with sorafenib in combination with bevacizumab are predicted by the extent of *ex-vivo* anti-anti-angiogenic activity in steady-state serum samples from these patients.
10. The occurrence of sorafenib-induced hand-foot skin reaction (HFSR), a cutaneous side effect involving the palms and soles of hand and foot, is related to excretion of sorafenib in sweat by eccrine glands.
11. Subjects with genetic variations in VEGFR2, an important mediator for VEGF angiogenesis pathway, are at increased risk of prostate cancer relative to patients with wild-type genotype.
12. Toxicities induced by anti-VEGF (i.e., bevacizumab)/ VEGFR2 inhibitor (i.e., sorafenib) therapies serve as phenotypic markers for efficacy of these agents in patients with solid tumors.

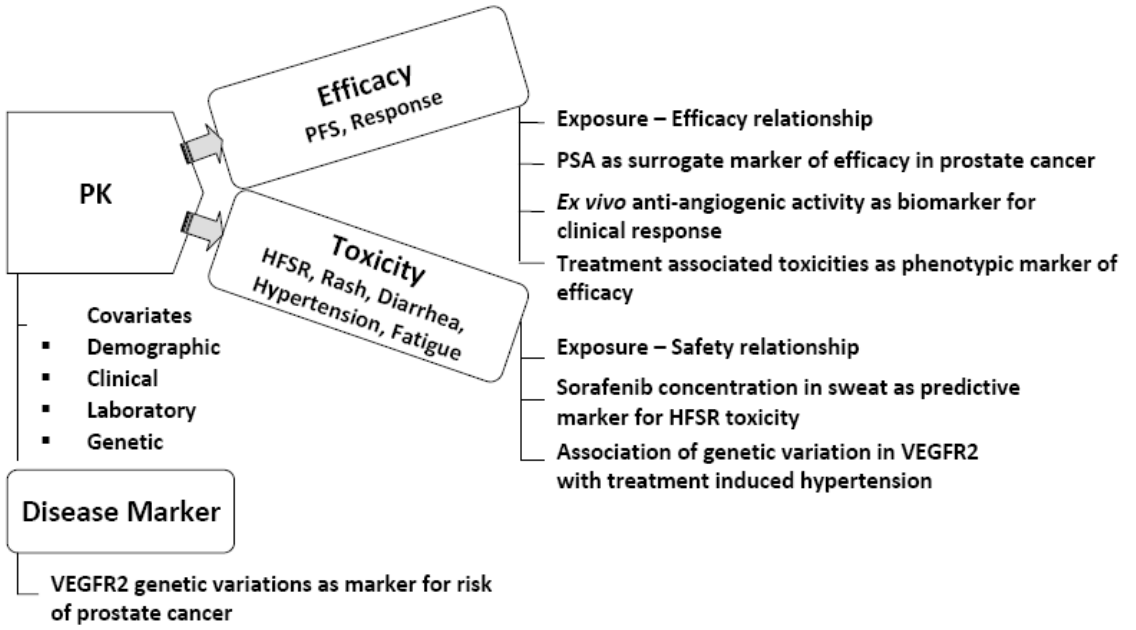

Fig 2-1 Schematic illustration of various components for exploration of clinical and pharmacogenetic markers for exposure, efficacy and toxicity of sorafenib treatments in cancer patients with solid tumors

To test these hypotheses, 24-hr sorafenib plasma concentration-time profiles on day 1 and at steady-state (for selected patients) were measured from five phase I/II clinical trials at the National Cancer Institute (NCI), evaluating the efficacy or safe dose of sorafenib in patients with mCRPC, CRC, NSCLC, KS and ST. In addition, patients were genotyped for CYP3A4*1B, CYP3A5*3C, UGT1A9*3, UGT1A9*5, VEGFR2 H472Q and VEGFR2 V297I SNPs, and demographic and clinical covariates information were collected at baseline. Information such as clinical response, progression-free survival (PFS) as well as toxicities (nature and grades) was collected over the course of sorafenib treatment in these studies. Characterization of pharmacokinetics and covariate analysis for sorafenib exposures were performed by non-compartmental analysis (NCA)-general

linear modeling (GLM) and population pharmacokinetics approach. Correlative studies by one-way ANOVA, Chi-square tests and Kaplan Meier survival analysis were used to evaluate other pharmacokinetic/pharmacodynamic/pharmacogenetic associations.

In-vitro cell line experiments were performed to study the impact of sorafenib treatment on release of PSA (measured using ELISA) from prostate cancer LNCaP cells. Excretion of sorafenib in sweat was measured by liquid chromatography-mass spectrometry to investigate its association with development of HFSR.

CHAPTER THREE

BIOANALYTICAL METHOD FOR QUANTITATION OF SORAFENIB IN HUMAN PLASMA

3-1 Introduction

Only few bioanalytical methods have been described for quantification of sorafenib in human plasma. An HPLC-UV method was described to quantify sorafenib in mouse serum matrix, but was limited by poor sensitivity (lower limits of quantification (LOQ), 80 ng/mL) and long run time of 35 min(80). Recently another HPLC-UV method was reported for human plasma as biological matrix with shorter run time of 14 min but poorer quantification limits of 500 ng/mL (81). Two LC/MS/MS methods were also described (37, 82). One of them was based on a complex liquid-liquid extraction with quantifiability upto 10 ng/mL, while the other method was based on a simple protein precipitation with LOQ of 7.3 ng/mL and run time of 6 min. Both of these methods required plasma volumes of 100 μL or higher.

Published analytical methods were limited by complex extraction procedure, long run-time, poor sensitivity and requirement of large plasma volume; hence, it was considered essential to improve the currently available procedures. Therefore, a simple, selective, rapid and sensitive LC-MS/MS method was developed which also used a less volume of

plasma (83) compared to other published methods (37, 82). The procedures used in development and validation of this novel bioanalytical method for quantification of sorafenib in human plasma, using liquid chromatography with electrospray ionization-tandem mass spectrometric detection, are described in this chapter.

3-2 Physicochemical characteristics of sorafenib

Sorafenib (**Fig 3-1**) is a bis-aryl urea which remains unionized at physiological pH. The pK_a values for sorafenib predicted using ACD/labs (software from Advanced Chemistry Development, Inc) were 1.6±0.3 and 12.9±0.7, respectively for Pyridine Nitrogen and terminal Caboxamide Nitrogen (**Fig 3-1**). The prediction of pKa for pyridine nitrogen is lower than its normal value, i.e. 5.14, possibly because of resonance between the pyridine and carboxamide group resulting in transfer of proton from Caboxamide Nitrogen to Pyridine Nirogen. Sorafenib is highly lipophilic and has very low solubility in aqueous solvents.

3-3 Experimental procedures

3-3.1 Materials and reagents

Sorafenib and the internal standard ([$^{2}H_{3}$, ^{15}N] sorafenib) were provided by Bayer Health Care (New Haven, CT, USA). Acetonitrile (Optima grade) and formic acid (purity ≥ 98 %) were purchased from Fisher Scientific and Sigma-Aldrich, respectively. Deionized water was generated with a Hydro-Reverse osmosis system (Durham, NC, USA) connected to a Milli-Q UV Plus purifying system (Millipore, Billerica, MA, USA). Drug-free heparinized human plasma was obtained from the National Institutes of Health (NIH)

Clinical Center Blood Bank (Bethesda, MD, USA). Initially these experiments were performed in eppendroff tubes, but most recently all the experiments were being performed in Kimbel® glass tubes purchased from VWR Scientific (Westchester, PA).

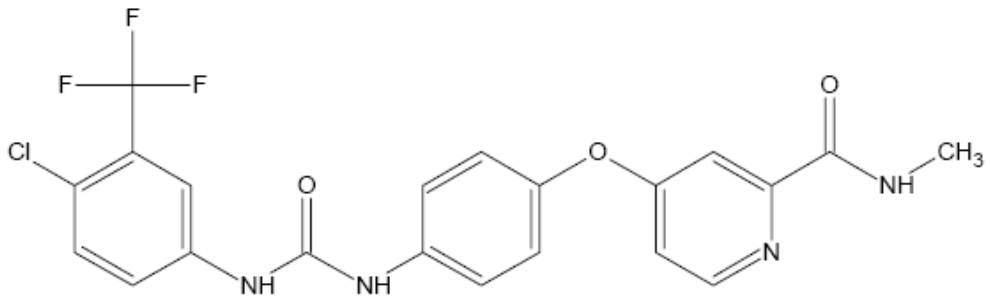

MW: 464.9 g/mol

Molecular weight: 637 g/mol (tosylate salt), 464.9 g/mol (free base)

Solubility (tosylate salt): 0.034 mg/100mL at pH 1.0, to 0.013 mg/100mL at pH 4.5

Predicted* pKa: 1.6±0.3, 12.9±0.7

Lipophilicity (experimental logP) (34): 3.8

Fig 3-1 Structure and physicochemical properties of sorafenib. *pKa predictions are based on ACD/labs software (version 9.0, Advanced Chemistry Development, Inc., used in April 2006) (84).

3-3.2 Stock solutions and standards

3-3.2.1 Preparation of sorafenib standard dilutions

Stock solutions of sorafenib were prepared by dissolving the drug in acetonitrile/water: 90/10 (v/v) mixture at a concentration of 1 mg/mL, which was stored in glass tubes at -20 ºC. Serial (working) dilutions were prepared from this stock solution for the preparation of calibration and quality control (QC) samples, as shown in **Table 3-1**.

Table 3-1 Calculations for preparation of serial dilutions using sorafenib master stock of 1 mg/mL concentration.

Stock	Secondary stock Concentration (ng/ml)	Add (µL)	of stock	+ µL of ACN:water - 90:10 (v/v)
A	20000	20	Master (1 mg / mL)	980
B	10000	500	A	500
C	5000	500	B	500
D	1000	200	C	800
E	250	250	D	750
F	100	400	E	600
G	50	500	F	500

3-3.2.2 Preparation of dilutions for internal standard ([$^{2}H_3$, ^{15}N] sorafenib)

The internal standard (IS) master stock and working stock were prepared respectively at concentrations of 1 mg/mL and 50 µg/mL in acetonitrile/water: 90/10 (v/v) mixture. Both the master and working internal standard stocks were stored at -20 ºC. Working stock was directly added to the precipitation solvent (100 µL of 50 µg/mL stock in 200 mL of ACN) to get the dilution of approximately 2000 times resulting in final concentration of 25 ng/mL.

3-3.2.3 Preparation of Quality Control (QC) samples

QC samples were prepared in batch, by addition of standard solutions to plasma in volumetric flasks as shown in **Table 3-2**, to obtain three different final concentrations of 8 ng/mL, 160 ng/mL and 1600 ng/mL. These were divided into 300 µL aliquots, which were stored in glass tubes at -20 ºC.

Table 3-2 Calculations for preparation of QC samples

QC concentration	Volume/concentration of master stock	Volume of plasma
8 ng/ml	8 µL of 5000 ng/ml	q.s. 5 ml
160 ng/ml	8 µL of 100,000 ng/ml	q.s. 5 ml
1600 ng/ml	8 µL of 1000,000 ng/ml	q.s. 5 ml

3-3.3 Sample preparation

3-3.3.1 Preparation of standards

Two sets of standard curves were prepared everyday by adding 5 µL of specific stock to 45 µL of blank human plasma as shown in **Table 3-3** in clean, labeled glass tubes. These samples were processed using the optimized extraction procedure as mentioned in **section 3-3.4** below.

Table 3-3 Calculations for preparation of standard calibrators

Sample name for HPLC	Plasma volume (µL)	Stock from Table 3-1	Amount of stock solution (µL)	Final concentration (ng/mL)
Blank	50	-	-	Blank
IS only	50	-	-	IS only
5 ng/ml	45	G	5	5
10 ng/ml	45	F	5	10
25 ng/ml	45	E	5	25
100 ng/ml	45	D	5	100
500 ng/ml	45	C	5	500
1000 ng/ml	45	B	5	1000
2000 ng/ml	45	A	5	2000

3-3.3.2 Preparation of QC samples

On the day of the assay runs, for each QC strength, one 300 µL aliquot was defrosted and divided into 5 aliquotes of 50 µL volume each, in glass tubes. These samples were treated in the same way as standard calibrators using the extraction procedure mentioned in **section 3-3.4** below.

3-3.3.3 Preparation of patient samples

Similar to QCs, patient samples were thawed and 50 µL aliquot was transferred to clean glass tubes, which was extracted by procedure mentioned in **section 3-3.4** below.

3-3.4 Extraction procedure

Total 100 µL of 50 µg/mL internal standard stock was added to 200 mL of ACN, which was then used as a precipitation solvent. The scheme for the extraction procedure is shown in **Fig 3-2**. Fifty microliters (50 µL) of standard calibrator / QC sample / patient plasma sample was subjected to protein precipitation with 500 µL of ACN containing internal standard. This mixture was vortex mixed and centrifuged at 3700 g for 10 min. Supernatant was transferred to Waters® clear glass microvials, of which 25 µL was injected onto the column.

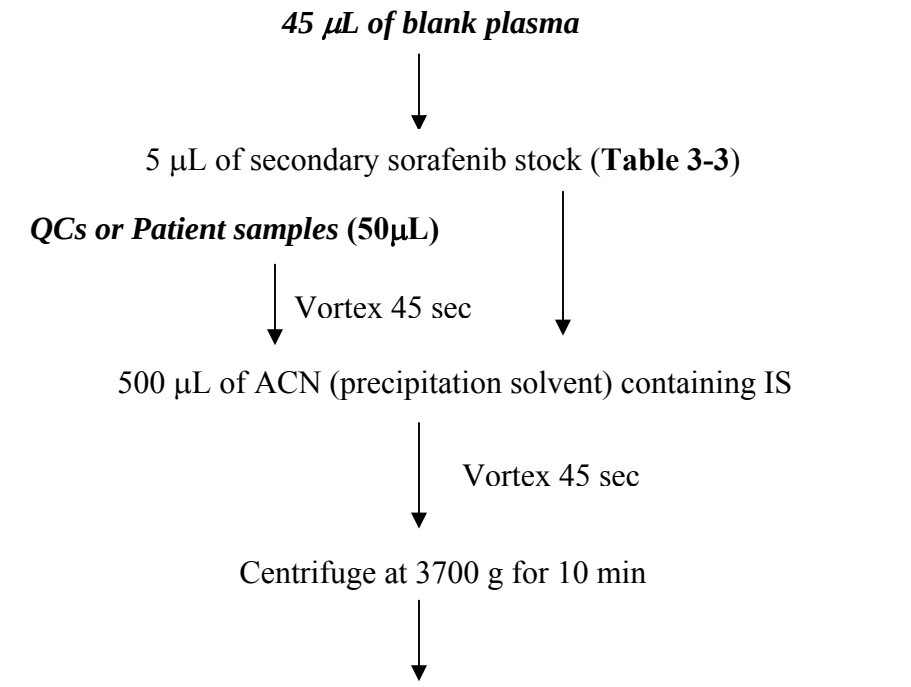

Fig 3-2 Extraction procedure for sorafenib

3-4 Equipment and chromatographic conditions

Optimized experimental conditions for HPLC and MS system are listed below:

3-4.1 HPLC: Waters® 2695 Alliance separation module

3-4.1.1 Pump

Mobile phase A: Acetonitrile

Mobile phase B: 0.1 % formic acid

Isocratic method: A/B - 65/35 (v/v)

Total run time: 4 minutes

Retention time: Approx. 1.5 minutes both for sorafenib and sorafenib internal standard

3-4.1.2 Injector

Injection volume: 25 μL

3-4.1.3 Column

Waters SymmetryShield RP8 (2.1×50 mm, 3.5 μm)

Column compartment temperature: 35 ˚C

3-4.1.4. Wash solutions

Needle wash: Acetonitrile with 0.1% formic acid

Seal wash: Acetonitrile: Water- 20: 80 (v/v)

3-4.2 Mass spectrometer: Micromass Quattro micro API mass spectrometer

3-4.2.1. Ionization: Electrospray Positive

Multiple Reaction Monitoring (MRM) mode:

Sorafenib; parent ion ($M+H^+$): 464.9 (*m/z*)

product ion ($M+H^+$): 252.0 (*m/z*)

Sorafenib internal standard; parent ion ($M+H^+$): 469.0 (*m/z*)

product ion ($M+H^+$): 256.0 (*m/z*)

3-4.2.2 Source Conditions

Cone voltage: 45 V

Collision energy: 33 eV

Capillary voltage: 3.50 kV

Desolvation temperature: 410 °C

Desolvation gas flow: 610 L/h

Source temperature: 130º C

IE1: 1.0; IE2: 1.0

Exit: 10

3-5 Data evaluation

QuanLynx, a component of MassLynx, was used for generation of each calibration curve. The output was based on a least-squares linear regression analysis, with the appropriate weighting factor, of the peak area ratio of sorafenib and the internal standard against the nominal drug concentration. The least-squares regression line was not forced through the origin (0, 0), and blank (zero concentration) samples were not included in the calibration curve. The concentrations of the QC and unknown samples were determined by back-calculation (interpolation) using the standard calibration curve.

3-6 Validation procedures

Validation was carried out on six different days, following the lab standard operating procedure (SOP), which was written based on guidelines for Bioanalytical Method Validation published by FDA. On each day of analysis, calibration standards were prepared in duplicate at 5, 10, 25, 100, 500, 1000 and 2000 ng/mL (concentration range 5-2000 ng/mL). Five QC samples at each concentration were also thawed and analyzed with standard calibrators. Each validation run included two blank (zero concentration) samples and one sample containing only internal standard, along with the calibrators and

QC samples. The validation parameters were calculated by using the methods described below.

3-6.1 Selectivity

The intent of the selectivity study is to ensure that there is no interference or matrix effect by endogenous matrix constituents in elution of sorafenib and internal standard. To examine the interference, blank plasma samples from six different sources were analyzed using the LC-MS/MS method. The obtained chromatograms were then visually examined for interfering peaks across the retention window for sorafenib and internal standard. The peak area of blank sample should be less than 5% of the area for the lower limit of quantification (LOQ) to be considered as non-interfering (i.e., not statistically different from zero). The method used to evaluate the matrix effect is described in section 3-6.2.

3-6.2 Recovery, Matrix Effect and Process Efficiency

Recovery, matrix effect and process efficiency were estimated at a low (10 ng/mL) and a high concentration (2000 ng/mL). Sorafenib stock solution aliquots were added either pre-extraction or post-extraction, and the internal standard was added post-extraction in all the samples. Recovery was calculated as the response ratio (sorafenib peak area/ internal standard peak area) measured in pre-extraction sorafenib spiked samples (n=5), as a percentage of that measured from post-extraction sorafenib spiked samples (n=5). The matrix effect was determined by comparison of the absolute sorafenib response area in post-extraction sorafenib spiked samples (n=5) with that of response ratio observed in mobile phase, i.e., acetonitrile/water:90/10 mixture (n=3). The response ratios for the

post-extraction spiked samples and mobile phase were compared to calculate the internal standard adjusted matrix effect. The process efficiency, defined as the overall extractability (i.e., recovery in presence of any matrix effect) of the assay method, was estimated as the sorafenib response ratio observed after extraction relative to the sorafenib response ratio observed in pure solvent. The calculation of these parameters is further shown in **Table 3-7**.

3-6.3 Limits of Detection and Quantification (LOD and LOQ)

The LOD is defined as the smallest concentration that can be distinguished from the blank. It is also the concentration having a signal of three times the noise in blank plasma samples across the retention window of sorafenib. It was determined by calculating the S/N ratio for a low concentration i.e. 1 ng/mL.

The lower limit of quantitation (LLOQ) was determined as the lowest concentration for which sorafenib spiked in six different sources of plasma resulted in reliable and reproducible measurements with acceptable accuracy and precision (<20% bias and imprecision). It is also the concentration for which signal to noise (S/N) ratio is at least 6:1.

3-6.4 Accuracy and Precision

The calibrator predicted concentration values for QC samples, run in quintuplicate at each concentration level on six different days, were used to assess the accuracy and precision of the assay.

Inaccuracy / bias / percent deviation from actual value was defined as the percent difference between the mean calibrator predicted concentration and nominal concentrations for each QC.

$$\%\,\mathrm{DEV} = \left(\frac{[\text{nominal}] - [\text{observed}]}{[\text{nominal}]} \right) \times 100\%$$

The imprecision was calculated by performing the one way analysis of variance (ANOVA) on calibrator predicted concentrations for each QC using run day as a factor. The between-runs mean square variance (MS_{bet}), the within-run mean square variance (MS_{wit}), and the grand mean of observed concentrations across all the runs were obtained from ANOVA and were used in formulas below to calculate the between and within run imprecisions (BRIP and WRIP).

$$\mathrm{BRIP} = \frac{\sqrt{(MS_{bet} - MS_{wit})/n}}{\mathrm{GM}} \times 100\%$$

$$\mathrm{WRIP} = \frac{\sqrt{MS_{wit}}}{\mathrm{GM}} \times 100\%$$

where n = number of replicates within each validation run, GM = grand mean

3-6.5 Stability

3-6.5.1 Freeze-thaw stability

QC samples at nominal concentrations of 8, 160 and 1600 ng/mL were subjected to three freeze-and-thaw cycles, in quintuplicate for each cycle, with each freeze cycle lasting for at least 12 h. All these samples were analyzed using LC-MS/MS method on the same day and the results were compared with the mean calibrator predicted concentrations (which were also used for calculation of accuracy in **section 3-6.3**).

3-6.5.2 Auto-sampler stability

An entire set of samples (two calibration curves and QC samples in quintuplicate) were left in the auto-sampler at 4 °C after the initial run. Analysis was repeated after 7 h and then again after 24 h. Predicted concentrations for 7^{th} and 24^{th} h were then compared with those obtained for 0^{th} h samples.

3-6.5.3 Short term (bench-top) stability

A set of sorafenib working stocks prepared in ACN/water: 90/10 solvent mixture at concentrations of 10 and 2000 ng/mL were left at work bench (room temperature) for 6 h. Another set of identical samples were stored at -20 °C. After 6 h these samples were analyzed together and concentrations were compared.

3-6.5.4 Dilution Analysis

Sample dilution was validated for samples for which plasma concentrations were found to be above the upper limit of quantification (ULOQ) in initial analysis. QC samples of concentration 10,000 ng/mL were prepared and a 5µL volume was diluted ten-fold with 45 µL of human blank plasma; these samples were then processed as normal samples. Predicted concentrations from these samples were used to calculate the accuracy and precision of dilution analysis.

3-7 Results and Discussion

3-7.1 Selectivity

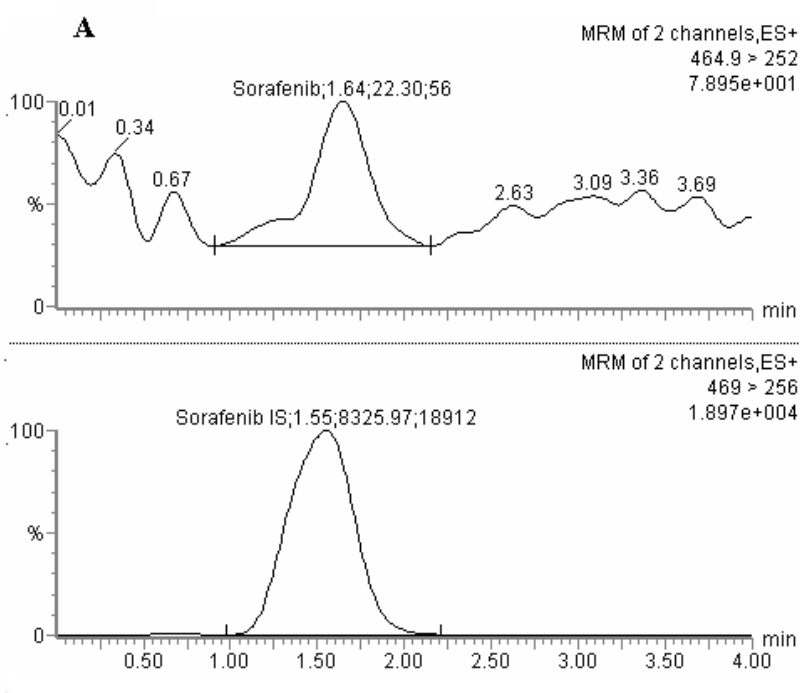
A
MRM of 2 channels,ES+
464.9 > 252
7.895e+001
Sorafenib;1.64;22.30;56
100
%
0
0.01
0.34
0.67
2.63
3.09
3.36
3.69
min
MRM of 2 channels,ES+
469 > 256
1.897e+004
Sorafenib IS;1.55;8325.97;18912
100
%
0
min
0.50
1.00
1.50
2.00
2.50
3.00
3.50
4.00

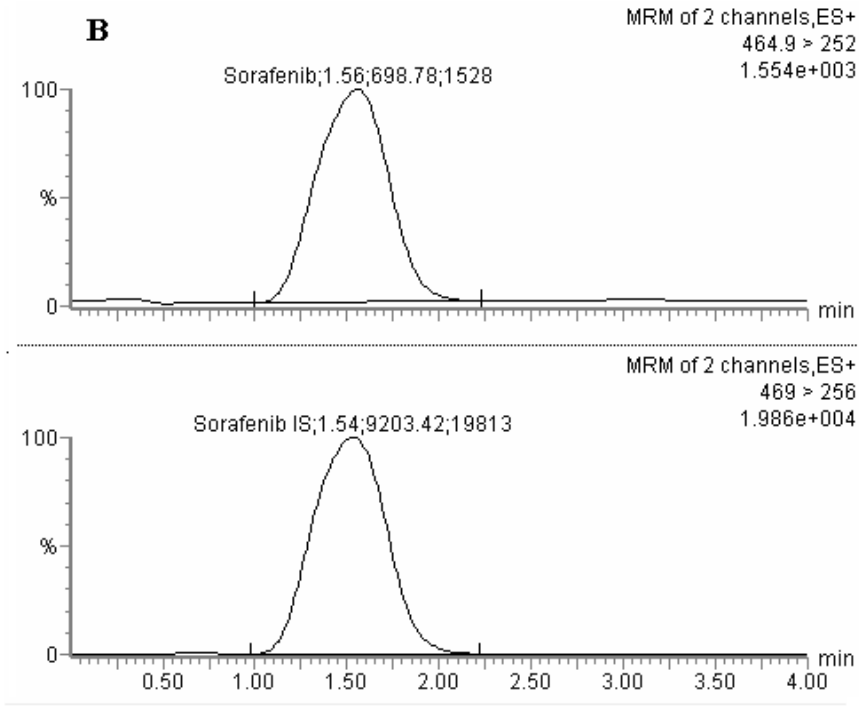
B
MRM of 2 channels,ES+
464.9 > 252
1.554e+003
Sorafenib;1.56;698.78;1528
100
%
0
min
MRM of 2 channels,ES+
469 > 256
1.986e+004
Sorafenib IS;1.54;9203.42;19813
100
%
0
min
0.50
1.00
1.50
2.00
2.50
3.00
3.50
4.00

Fig 3-3 Typical chromatogram showing 464.9 →252.0 m/z (sorafenib) and 469.0 →269.0 m/z (internal standard) transitions for; (a) blank human plasma with internal standard; (b) a calibrator sample spiked with 5 ng/mL sorafenib (LLOQ) with internal standard.

The peak area of the blank sample, observed across the retention window of sorafenib and internal standard for six blank samples, was less than 5% of the peak area for LOQ, suggesting that the method can distinguish the peak for analyte of interest from all other chemical peaks. Typical chromatograms for blank plasma and plasma spiked with 5 ng/mL of sorafenib are shown in **Fig 3-3**.

3-7.2 Calibration Curve

The lowest bias over the concentration range of 5-2000 ng/mL was obtained following regression analysis of the data to a quadratic fit with a weighting factor of 1/x (x being the nominal concentration) for the ratio of the peak area of sorafenib and the internal standard against the nominal concentration. The mean correlation coefficient for regression equations, generated for six different days, was 0.9995 (SD, ± 0.0005; range 0.9988-0.9998).

The percentage deviations from nominal (% DEV) were calculated for each calibrator concentration using the calibration curve predicted concentrations (**Tables 3-4 (a) and (b)**). The %DEV ranged from -4.33 to 3.08, which suggested a good fit of the data to the weighted quadratic regression.

3-7.3 Limits of Detection and Quantification

Plasma samples with a final concentration of sorafenib of 1 ng/mL were analyzed to determine the lower limit of detection (LOD) for sorafenib. The LOD was determined by estimating the signal to noise ratio using Quanlynx software, and was estimated to be 0.2 ng/mL. The lower limit of quantitation (LLOQ) was determined to be 5 ng/mL with percent relative standard deviation (% RSD) of 7.45% and % DEV of -4.33 %, using calibration curve predictions (**Table 3-4(b)**). Five different lots of human plasma were spiked with sorafenib to the final concentration of 5 ng/mL and were analyzed. The % RSD and % DEV were found to be 4.80 % and 2.00 % respectively. This further confirmed that the analytical method was able to quantify the LLOQ in an accurate and reproducible manner.

3-7.4 Accuracy and Precision

The assay was adequately accurate with bias of less than 15% for all the individual measurements, on each validation day at all three concentrations. The between-run and within-run imprecision values were less than 5%, well within the acceptable limits. The results for accuracy, precision and dilution analysis are reported in **Table 3-5**. The bias and imprecision for dilution analysis samples were 3.82 % and 3.92 %, respectively. This established that the samples of concentrations above the calibration range can be diluted ten-fold with blank human plasma to reduce its concentration to the level that would be within the estimation range for analysis.

3-7.5 Recovery, Matrix Effect and Process Efficiency

The results for recovery, matrix effect and process efficiency are shown in **Tables 3-6 (a), 3-6 (b) and 3-7**. The recovery and process efficiency were 80-100% at both low (10 ng/mL) and high (2000 ng/mL) concentrations, and the matrix effect was approximately 20%. The observed variability (% RSD) for a set of observations at any concentration level was less than 8%, which was within the acceptable limits.

Table 3-4 (a) Calibrator predicted concentrations from six days of validation runs

Nominal Concentration	Day 1 r^2=0.9988		Day 2 r^2=0.9996		Day 3 r^2=0.9998		Day 4 r^2=0.9990		Day 5 r^2=0.9998		Day 6 r^2=0.9998	
	Rep 1	Rep 2	Rep 1	Rep 2	Rep 1	Rep 2	Rep 1	Rep 2	Rep 1	Rep 2	Rep 1	Rep 2
5	4.8	5.3	4.6	5.4	4.4	4.8	4.5	4.8	4.2	4.9	4.6	5.1
10	10.4	9.5	9.8	10.2	11.1	10	10.3	10.5	10	11.2	9.7	11
25	24.6	25	24.7	24.6	23.9	28.3	26.1	24.6	24.5	25.7	24.5	25.2
100	100	104.6	100.4	103.2	96.1	99.5	98.3	105.4	108	99.6	103.8	100.1
500	451.7	501.5	509.5	500.9	507.4	496	507.1	510.4	488.8	502.7	487.3	488.2
1000	1023.4	1036	1011.1	969.4	981.9	1016.3	1000.1	968.8	1002.1	996.4	1010.3	1016.2
2000	1958.2	2024.5	2039.1	1967.2	2014.4	1985.8	2063.9	1945.1	1998.3	2003.8	2013.9	1979.5

Table 3-4 (b) Summary of calibrator predicted concentrations from Table 3-4 (a)

Nominal Concentration	Mean	SD	RSD(%)	DEV (%)	N
5	4.78	0.36	7.45	-4.33	12
10	10.31	0.56	5.42	3.08	12
25	25.14	1.15	4.59	0.57	12
100	101.58	3.41	3.35	1.58	12
500	495.96	16.22	3.27	-0.81	12
1000	1002.67	20.82	2.08	0.27	12
2000	1999.48	34.49	1.72	-0.03	12

Table 3-5 Intra-run and inter-run quality control accuracy and precision

	Nominal sorafenib concentration (ng/mL)			
	8	**160**	**1600**	**10000 (dilution 10x)**
N	30	30	30	20
Grand mean (ng/mL)	7.99	159.46	1485.79	9618.00
SD (ng/mL)	0.47	7.60	86.38	41.88
RSD (%)	5.93	4.77	5.81	4.35
DEV (%)	-0.12	-0.34	-7.14	-3.82
Deviation Range (%)	(-10 to 15)	(-7.44 to 13.75)	(-14.99 to 3.90)	(-13.13 to 1.83)
Imprecision				
Within-run (%)	4.53	2.64	1.19	3.98
Between-run (%)	1.68	1.75	2.50	*

*No additional variability

SD: standard deviation, % relative standard deviation (RSD) = (SD/Grand mean)*100

% Deviation (DEV) = (([nominal] – [observed])/[nominal])*100

Deviation range: range of deviations for QC samples with same nominal concentrations

Table 3-6 (a) Response ratios for samples with pre- and post-extraction addition of sorafenib, and pure drug solutions for low concentrations

Nominal Concentration (ng/mL)	**Response for Pre-Extraction**	**Response for Post-Extraction**	**Response for Pure drug**
10	0.254	0.247	0.264
10	0.267	0.259	0.267
10	0.276	0.252	0.257
10	0.257	0.264	
10	NA	0.273	
Mean	0.26	0.26	0.26
SD	0.01	0.01	0.01
%CV	3.80	3.93	1.95

Table 3-6 (b) Response ratios for samples with pre- and post-extraction addition of sorafenib, and pure drug solutions for high concentrations

Nominal Concentration (ng/mL)	Response for Pre-Extraction	Response for Post-Extraction	Response for Pure drug
2000	54.425	51.413	52.442
2000	54.840	51.791	51.198
2000	54.763	52.472	51.948
2000	55.876	52.765	
2000	55.759	51.163	
Mean	55.13	51.92	51.86
SD	0.65	0.68	0.63
%CV	1.17	1.32	1.21

Table 3-6 (c) Absolute response for samples with pre- and post-extraction addition of sorafenib, and pure drug solutions for low concentrations

Nominal Concentration (ng/mL)	Response for Pre-Extraction	Response for Post-Extraction	Response for Pure drug
10	1274.20	1198.67	1663.05
10	1426.61	1287.96	1687.25
10	1519.74	1315.42	1593.29
10	1418.18	1369.95	
10		1450.91	
Mean	1409.68	1324.58	1647.86
SD	101.37	93.93	48.79
%CV	7.19	7.09	2.96

Table 3-6 (d) Absolute response for samples with pre- and post-extraction addition of sorafenib, and pure drug solutions for high concentrations

Nominal Concentration (ng/mL)	Response for Pre-Extraction	Response for Post-Extraction	Response for Pure drug
2000	246338.73	208855.33	304687.41
2000	232021.20	232372.84	296021.41
2000	230365.72	239895.36	298377.06
2000	204823.20	240550.92	
2000	237468.59	234026.25	
Mean	230203.49	231140.14	299695.29
SD	15496.91	12958.38	4480.87
%CV	6.73	5.61	1.50

Table 3-7 Recovery, matrix effect and process efficiency

		Based on absolute response		**Based on response ratio**[†]	
		Sorafenib concentration (ng/mL)		**Sorafenib concentration (ng/mL)**	
		10	**2000**	**10**	**2000**
A	Mean extracted response (n = 5)	1409.68	230203.49	0.2635	55.13
	RSD (%)	7.19	6.73	3.80	1.17
B	Mean unextracted response (n = 5)	1324.58	231140.14	0.2590	51.92
	RSD (%)	7.09	5.61	3.93	1.32
C	Mean response in pure solvent (n = 3)	1647.86	299695.29	0.2627	51.86
	RSD (%)	2.96	1.50	1.95	1.21
	Recovery, A/B*100, (%)	106.42	99.59	101.74	106.18
	Matrix effect, (1-B/C)*100, (%)	19.62	22.87	1.41	-0.12
	Process efficiency, A/C*100, (%)	85.55	76.81	100.30	106.31

[†]Response ratio = peak area for sorafenib/ peak area for internal standard

3-7.6 Stability

3-7.6.1 Freeze-thaw Stability

The results for freeze-thaw stability are shown in **Table 3-8**. After three freeze-thaw cycles, mean observed concentrations deviated less than 6% for each QC concentration. This indicates that repeated freeze-thaw cycles do not considerably affect the sample integrity of sorafenib in human plasma.

Table 3-8 Freeze-thaw stability for sorafenib in plasma samples

Sorafenib concentration (ng/mL)	**Back predicted mean concentration (%RSD) & Percentage of corresponding mean concentrations at Cycle 0***			
	Cycle 0	**Cycle 1**	**Cycle 2**	**Cycle 3**
8	7.99	7.74 (7.34%)	7.7 (7.40%)	7.58 (7.57%)
		96.87%	96.37%	94.87%
160	159.46	153 (4.55%)	153.82 (1.80%)	151.54 (2.88%)
		95.95%	96.46%	95.03%
1600	1485.79	1463.12 (1.21%)	1479.46 (0.71%)	1438.94 (1.17%)
		98.47%	99.57%	96.85%

*Cycle 0 indicates the mean back-calculated concentrations reported in **Table 3-5**

3-7.6.2 Autosampler Stability

The results for autosampler stability study are presented in **Table 3-9**. The percent change from the initial analysis was less than 1% at all three QC concentrations. This indicated that the processed sorafenib samples were stable at 4°C after placing in the autosampler tray for at least 24 h.

Table 3-9 Autosampler or re-injection stability for sorafenib

Sorafenib QC concentration (ng/mL)	**Mean response (% RSD) & Percent change from mean response at zero hour**		
	0^{th} h	**7^{th} h**	**24^{th} h**
8	8.44 (0.02%)	8.36 (0.02%)	8.36 (0.03%)
		-0.95%	-0.95%
160	172.36 (0.03%)	171.80 (0.03%)	171.88 (0.03%)
		-0.32%	-0.28%
1600	1650.46 (0.01%)	1652.90 (0.01%)	1645.06 (0.01%)
		0.15%	-0.33%

3-7.6.3 Short-term (bench-top) Stability

The percent concentration change for samples, which were left outside at room temperature for 6 h versus the samples stored at -20 ˚C was -8.82 % and -1.79 %, respectively for 10 and 2000 ng/mL solutions. These changes were within the acceptable limits; hence sorafenib was considered stable in ACN/water:90/10 mixture for at least 6 h at room temperature.

3-7.6.4 Long-term Stability

The long-term stability study was not performed with this newly developed LC-MS/MS method. However, the previously published LC-MS/MS method reported less than 10% change in sorafenib concentration following storage at -70 °C for at least 179 days (82).

3-8 Conclusions

In conclusion, a rapid and sensitive method for determination of sorafenib in human plasma was developed and validated. This method requires only a small volume of

plasma (50 µL) and has a short run time of 4 minutes. This method was found to meet or exceed all FDA guidelines for bioanalytical method validation. The quadratic calibration curve fit was found to be appropriate, and the results for selectivity, accuracy and precision, freeze-thaw cycle stability and short-term stability were within the acceptable limits. The method was later used for analysis of plasma samples from patients treated with sorafenib at 400 mg/Q12h and at 200 mg/Q12h as single agent or in combination with other chemotherapeutic agent.

CHAPTER FOUR

CHARACTERIZATION OF PHARMACOKINETICS AND EXPLORATION OF POTENTIAL COVARIATES BY NON-COMPARTMENTAL ANALYSIS – GENERAL LINEAR MODELING AND POPULATION PHARMACOKINETIC MODELING APPROACH FOR PATIENTS WITH SOLID TUMORS

4-1 Introduction

Sorafenib is approved in more than 60 countries for treatment of advanced renal cell carcinoma and/or advanced hepatocellular carcinoma, and is being extensively used clinically. Several clinical trials have studied pharmacokinetics, efficacy, toxicity and pharmacodynamic biomarkers for sorafenib. These clinical trials are summarized in appendix 1-1, 1-2 and 1-3. The clinically approved dose for sorafenib is 400 mg BID (49); however, both 200 and 400 mg BID doses have been studied in combination with other chemotherapies.

High inter-patient variability has been reported for sorafenib pharmacokinetics based on both non-compartmental and population pharmacokinetic analysis. Results of non-compartmental analysis from selected clinical studies are summarized in **Table 4-1 (a)**

and (b). The %CV on sorafenib exposures (area under the curve, AUC) and peak plasma concentrations (C_{max}) ranged from 5-83% and 33-88% for 200 or 400 mg BID doses. The median time to peak plasma concentration (t_{max}) varied between 2-9.5 h. The heterogeneity in studied patient population, with respect to type of cancer, disease stage, patient demographics, co-morbidities, and physiological differences are few possible reasons for variability between studies (single dose pharmacokinetics and patient characteristics for selected sorafenib trials are described in **Table 4-1 (a) and (b)**).

The variability in exposure (pharmacokinetics) for anticancer drugs may explain the variability in treatment associated toxicities or efficacy. Calvert and Egorin demonstrated that thrombocytopenia caused by carboplatin was directly related to its systemic exposure (AUC), which in turn was dependent on the renal clearance of the parent drug. They devised a formula for the estimation of desired AUC, based on creatinine clearance of individual patients, and advocated its use for estimation of optimal, likely non-toxic doses for cisplatin (85). Relling and colleagues demonstrated that therapeutic success with methotrexate in pediatric acute lymphoblastic leukemia (ALL) was related to achieving desired concentrations in plasma. They showed that monitoring of steady-state concentrations for methotrexate and dose adjustments based on that, helped in improving the treatment outcome (86). Stewart and colleagues demonstrated that hematologic toxicities due to topotecan were related to its systemic exposure in children with different types of refractory tumors (87).

Similarly, the variability in sorafenib exposures may also predict the differences in its efficacy and toxicities among patients. Our group had found that the incidence rate of hand-foot skin reaction (HFSR) increases with increased cumulative sorafenib doses, following the co-administration with bevacizumab, an anti-VEGF monoclonal antibody (60). However, to best of our knowledge, there is no published evidence of a significant exposure-toxicity or exposure-response relationship for sorafenib. Treatment-associated toxicities for some drugs in the same tyrosine kinase inhibitor category as sorafenib have shown to be associated with drug plasma levels, such as association of severity of rash with erlotinib steady-state systemic exposures (i.e., AUC_{τ}^{ss}) (88).

Several studies explored the markers to explain the variability in exposure/efficacy/toxicity in order to identify patients who are likely to benefit from treatment and those at higher risk of toxicities. Population pharmacokinetic-pharmacodynamic analysis, a powerful approach to identify such pharmacokinetic and pharmacodynamic markers, has increasingly been used in various stages of drug development and is expected by the FDA for most new submissions for drug approval. One example of its use is the dosing recommendation for a widely used anticancer drug, docetaxel: it is recommended that patients with liver function markers values of greater than 1.5-times of ULN, should not be administered docetaxel (US FDA label) or doses should be reduced (European summary of product characteristics) (89, 90). These recommendations were based on population pharmacokinetic analysis which showed that abnormal liver function predicted low clearance for docetaxel, which in turn was related with higher incidences of febrile neutropenia (90). Dose adjustment for anticancer drugs

based on body size metrics such as BSA and BW has been in use for a long time. Increasingly, pharmacogenetic and molecular markers are also being employed to select the right treatment and right dose. For example, polymorphisms in metabolic enzymes have been established as a determinant of plasma levels for anticancer drugs such as DHFR for methotrexate, UGT1A1 for irinotecan, and TMPT for 6-mercaptopurine; and genetic variation in drug targets have shown to describe the differences in response or toxicity, such as influence of polymorphism in TS on response and toxicity for 5-fluorouracil. Similarly, molecular markers such as EGFR expression for erlotinib and cetuximab, and c-kit expression for imatinib are currently being clinically used for selection of right treatment.

Identification of markers for efficacy and toxicity are not only important to increase the clinical utility of new drug regimens, but also to avoid the false-negative conclusions about inefficacy of these drugs in certain tumor types. The latter is critical to facilitate the availability of drugs with activity in a selected patient population.

We performed an exploratory analysis to identify the sources of variability in sorafenib's systemic exposures (pharmacokinetics), efficacy and toxicity profiles. The heterogeneity in the patient population under study, with respect to type of cancer, demographics, (patho-) physiological and pharmacogenetic differences was evaluated as potential contributing covariates. Sorafenib pharmacokinetics was characterized for patients with mCRPC, NSCLC, CRC, ST and KS, by both non-compartmental and population pharmacokinetic modeling approaches, and covariates for pharmacokinetics parameters

were screened by general linear modeling (GLM) and population pharmacokinetics covariate analysis. The advantages and limitations of these approaches are discussed in sections 4-2 and 4-3. The methodologies used for these analyses along with results are described in this chapter.

Table 4-1 (a) Summary of patient characteristics and results of single-dose pharmacokinetics for selected sorafenib trials with a 400 mg BID dose

Study†	N	Age(mean/range) (years)	Male/ Female (%)	PK Sampling Schedule (h)	C_{max} (mg/L)		AUC_{0-12} (h*mg/L)		T_{max} (h)	
					GM	%CV	GM	%CV	Median	Range
Clark (39)	2	53.7	58:42	0,0.5,1,2,6,10,12,24	2.3	37	18.0	5	9.2	2.0-12.0
Moore (40)	4	33-70	41:59	NR	2.9	68	21.8	59	2.9	1.0-12.3
Strumberg (91)	5	18-75	64:36	NR	9.4	44	71.7	43	3.0	0.0-12.0
Awada (38)	9	42-79	57:43	0,2,3,4,6,12,24	3.0	NR	24	NR	NR	0.0-12.0

NR: Not reported

Table 4-1 (b) Summary of single-dose pharmacokinetics for a 200 mg BID dose of sorafenib from literature. Age range, gender proportion, cancer type and pharmacokinetic sampling for these patients were same as mentioned in **Table 4-1 (a)**

Study†	N	C_{max} (mg/L)		AUC_{0-12} (h*mg/L)		T_{max} (h)	
		GM	%CV	GM	%CV	Median	Range
Clark (39)	4	0.8	86	6.1	NR	6.0	2.0-6.0
Moore (40)	4	1.3	34	10.9	38	5.0	2.0-12.0
Strumberg (91)	3	2.8	88	16.1	83	2.0	0.0-4.0
Awada (38)	10	3.6	NR	24.9	NR	NR	0.0-12.0

† Patients with different solid tumors were enrolled on these trials. PK: pharmacokinetics, C_{max}: peak plasma concentration, AUC: area under the curve, T_{max}: time to peak plasma concentration, GM: geometric mean, CV: coefficient of variation, NR: Not reported.

4-2 Non-compartmental pharmacokinetic analysis

Non-compartmental pharmacokinetic analysis describes the plasma concentration-time profiles in terms of exposure metrics such as area under the curve (AUC), peak plasma concentration (C_{max}) and time to peak plasma concentration (t_{max}) etc. The key parameter for non-compartmental analysis is the total systemic drug exposure or AUC, which is calculated by trapezoidal rule without assuming any specific compartmental model; however, estimates can be highly dependent on the blood sampling schedule.

In non-compartmental analysis, estimation of pharmacokinetic parameters are based on a two-stage approach, where (i) exposure metrics are calculated separately for each individual (or each plasma concentration – time profile), and (ii) those are then pooled together to calculate the central tendency (e.g., mean) and dispersion (e.g., %CV) from their distributions. These parameters are calculated independently for each dose level on every occasion, after giving equal weight to each individual. Separate analysis for each dose level or occasion may result in smaller subgroup sample sizes, which may lead to poor precision in estimated mean parameters.

The estimated individual pharmacokinetic parameters are then used to screen the covariates by general linear modeling approach, which is described later in this chapter. Advantages and limitations of non-compartmental analysis in context of data collected for sorafenib clinical trials are described below:

4-2.1 Advantages of non-compartmental analysis

1. Non-compartmental analysis is computationally very simple.

2. Estimation of pharmacokinetic parameters using non-compartmental analysis is generally based on observed plasma concentration-time profiles after a single dose, which is usually less variable than plasma concentration-time profiles after multiple doses. If we draw a parallel between non-compartmental analysis and probe substrate study, in non-compartmental analysis a single dose of sorafenib (probe substrate) is administered to understand the behavior or response of the system. Such responses (in this case pharmacokinetics of sorafenib) can then be compared among subjects to answer the questions of our interest, which are: how differently people behave to single dose of sorafenib and what patient specific factors can help in explaining that variability. However, more reliable estimates of AUCs are required to get the dependable answers to these questions.

3. Non-compartmental analysis does not involve any compartmental pharmacokinetic assumptions.

4-2.2 Limitations of non-compartmental analysis

1. With sparse data, non-compartmental analysis is not possible.

2. Data from multiple occasions collected for same patient cannot be used together to calculate the overall pharmacokinetic parameters.

3. For reliable estimation of AUCs, samples should be collected upto at least 2-3 half-lives, which was not possible with current administered dosing schedule of sorafenib. Sorafenib's half-life ranges between 25-48 h, and it was administered twice a day at 200/400 mg dose level. Although, population pharmacokinetic analysis can be used with sparse samples, but we would need pharmacokinetic samples upto 2-3 half-lives to obtain the unbiased individual estimates of pharmacokinetic parameters.

4. It is not possible to test various 'what-if' scenarios, because we can not perform simulations with non-compartmental analysis approach.

5. In non-compartmental analysis, mean pharmacokinetic parameters are calculated by giving equal weight to data from all the individuals. It does not account for differences in uncertainty at each individual level and at each observation level.

4-3 Population pharmacokinetic analysis

This approach is suitable for both rich and sparse data, which can be combined together even if they represent different dose levels or different routes of administration. Population pharmacokinetic analysis uses a mixed effect modeling approach and requires an explicitly specified pharmacokinetic model prior to analysis. It is a one-stage analysis approach, in which complete study population, rather than individuals, are considered as a unit of analysis for estimation of pharmacokinetic parameters, their distributions and their relationship with covariates within the population. Mixed effect modeling refers to evaluation of variability in two forms, fixed effect (measurable or attributable variability)

and random effect (unobservable or non-attributable variability), examples of which are shown in **Fig. 4-1**.

Most of the limitations of non-compartmental analysis can be overcome by population pharmacokinetic analysis. Specific advantages and limitations of this approach, in context of sorafenib data, are as below:

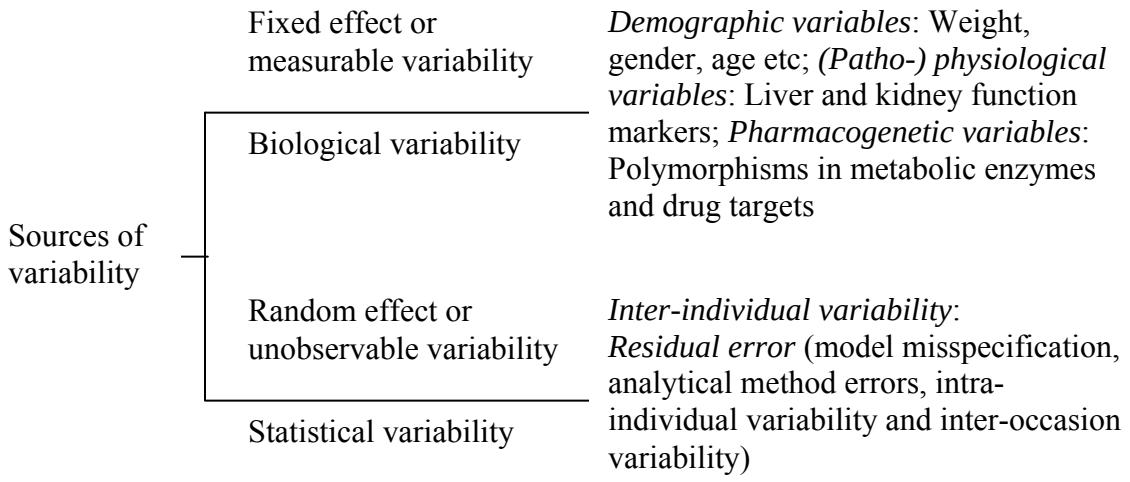

Fig 4-1 Examples of sources of variability in population pharmacokinetic analysis

4-3.1 Advantages

1. This approach combines the data from different occasions (plasma concentration –time profiles after single dose and at steady-state), and from different dose levels (200 or 400 mg BID) simultaneously, for the estimation of population and individual pharmacokinetic parameters. Contrary to non-compartmental analysis, the estimated variability and precision on population pharmacokinetic parameter estimates are not biased by small sample size in population subgroups assuming

random sampling. Also, the results are more generalized than the non-compartmental analysis, because a larger number of subjects are evaluated.

2. Population pharmacokinetics allows estimation of physiologically relevant parameters such as clearance (CL) and volume of distribution (V_d) for each subject, even if only a few samples are collected (i.e. sparse sampling). With current sorafenib data, even though terminal phase samples were not collected, parameters like CL and V_d could still be calculated because rich steady-state data were available for approx. 30% of patients. However, these estimates may be biased towards patients with steady-state observations.

3. Population pharmacokinetic modeling gives us the flexibility to perform simulations, which helps in testing various 'what-if' scenarios. This property not only helps in clinical decision making but may also in optimizing the clinical trial design.

4. Differences in uncertainty at each individual level (by estimation of inter-individual variability) and at each observation level (by estimation of residual varability) are explicitly accounted for during population pharmacokinetic analysis. This technique gives more weight to subjects with rich (more precise) data than the subjects with sparse sampling (or data with poor precision).

5. It is a powerful approach to identify the individual-specific characteristics that influence the disposition of the drug. Both individual specific and population pharmacokinetics parameters are calculated.

4-3.2 Limitations

1. Population pharmacokinetic analysis is computationally intensive and performer requires specific training in technique and use of software.

2. It is based on compartmental assumptions, and usually one model is used for all individuals within the study population. However, that may not always be true. Differences may exist in drug disposition between subjects, for example, one person can have a distinct entero-hepatic recycling phenomenon while others may have a limited or no entero-hepatic disposition for the same drug. Results may also be biased by non-random sampling or sampling at pre-specified time-points.

4-4 Characterization of pharmacokinetics by non-compartmental analysis

There were four objectives of non-compartmental analysis:

1). Characterization of sorafenib exposures in mCRPC, NSCLC, CRC, ST and KS.

2). Evaluation of impact of bevacizumab co-administration on sorafenib pharmacokinetics

3). Evaluation of impact of ritonavir co-administration on sorafenib pharmacokinetics

4). Screening of potential covariates for exposure parameters of sorafenib by general linear modeling

4-4.1 Methods

4-4.1.1 Patients and study design

Samples collected from 106 patients with solid tumors enrolled in 5 phase I/II sorafenib clinical trials at NCI were used for non-compartmental analysis. These trials evaluated the efficacy or safe dose of sorafenib, as a single agent or in combination therapy, for mCRPC, NSCLC, CRC, KS and other ST. These were single-arm, single-center, open-label trials. The clinical protocols were approved by the Institutional Review Board, and all the patients provided informed consent before participation in these trials. Enrollment was restricted to patients with normal organ function and age 18 years and older. Patients with prostate caner and lung cancer received clinically approved dose of sorafenib, i.e., 400 mg BID as single agent, and patients with CRC were treated with 400 mg BID sorafenib and cetuximab (400 mg/m^2 loading dose in week 1, followed by 250 mg/m^2 IV weekly) combination. Patients with solid tumors were treated with a combination of 200 mg BID sorafenib and 5 mg/kg bevacizumab IV biweekly. The design of trial enrolling patients with solid tumor allowed the evaluation of impact of bevacizumab co-administration on sorafenib pharmacokinetics, which is also described in results section 4-4.2. Patients with KS were enrolled into a dose escalation trial where they received sorafenib as either single agent (at a starting dose of 200 mg BID) or in combination with ritonavir (starting dose for sorafenib was 200 mg QD). Because pharmacokinetics was drawn for patients receiving sorafenib with and without ritonavir, impact of ritonavir co-

administration on sorafenib pharmacokinetics was also evaluated. Day 1 pharmacokinetics for KS trial was not drawn; hence it was not included in covariate screening by non-compartmental analysis.

4-4.1.2 Sample collection

Samples for pharmacokinetic analysis for these patients were collected after initial doses and at steady –state. The dosing and sampling schedules for trials under consideration are shown in **Table 4-2**. Serial samples were drawn upto 12 hr after first dose and one sample was drawn 12 hr post-second dose. Blood samples were collected in heparinized tubes and were centrifuged at 2400 rpm for 5 minutes. Following that plasma was aliquoted and stored at -80 °C until the time of bio-analysis for sorafenib.

4-4.1.3 Sample bio-analysis

Samples were analyzed using a validated method based on liquid chromatography with tandem mass spectrometric detection, as described in chapter 3.

4-4.1.4 Genotyping analysis

Details of methods used for genotyping analysis are described in chapter 7. In brief, genomic DNA was extracted from serum or plasma or whole blood samples using QiaBlood extraction kit (Qiagen, Valencia, CA) and stored at 4 °C. Genotyping was performed via direct sequencing for CYP3A4*1B, CYP3A5*3, UGT1A9*3, UGT1A9*5, VEGFR2 H472Q and VEGFR2 V297I single nucleotide polymorphisms (SNPs). Single or nested PCR reactions were performed, which were followed by sequencing PCR using

Big Dye Terminator Cycle Sequencing kit. The PCR primers used for sequencing are shown in **Table 4-3** Sequencing was performed on ABI Prism 3130 xl Genetic Analyzer (Applied BioSystems).

4-4.1.5 Pharmacokinetic analysis

Non-compartmental analysis was performed separately for plasma concentration – time profiles from day 1 and for steady-state. Plasma concentration – time profiles for only a single dosing duration (upto 12 h) can be used for estimation of exposure metrics by non-compartmental analysis; therefore, concentrations at 12^{th} h post-second-dose were not considered. The samples for which estimated concentrations were below the limits of quantification (5 ng/mL) were assigned half-of-the LOQ values (2.5 ng/mL). The time-points for which samples were missing were not included in the analysis.

Pharmacokinetic parameters, including area under the curve (AUC_{0-12}), peak plasma concentration (C_{max}) and time to peak plasma concentration (t_{max}) for day 1 and at steady state (if applicable) were calculated by using the WinNonlin professional software version 5.0 (Pharsight Corporation, Mountain View, CA, USA). Accumulation ratios, if applicable, were calculated by comparison of the exposures for a dosing interval at steady-state ($AUC_{0-12}{}^{\tau}{}_{SS}$) with exposures after first dose ($AUC_{0-12}{}^{\tau}{}_{SD}$).

4-4.1.6 Statistical analysis

Distribution of these parameters across trials was compared by assessing the central tendency (mean, median) and dispersion (standard deviation and 95% confidence interval). The distribution of pharmacokinetic parameters was skewed; hence, log-

transformation was performed to stabilize the variance and to make the distribution more normal. The calculated summary statistics were back-transformed to normal scale for description; the final reported parameters were geometric mean (GM), %CV and 95% CI. The statistical analyses were performed using JMP 8.0 (SAS Institute Inc., Cary, NC, USA) statistical software.

4-4.2 Results and Discussion

The plasma concentration – time profile after administration of initial doses and at steady-state are shown in **Fig 4-2 (a), (b) and (c)**, and pharmacokinetic parameters and their distributions after administration of first dose and at steady-state are summarized in **Table 4-4 (a) and (b)**.

The geometric mean for C_{max} for 400 mg BID sorafenib dose ranged from 1.8 to 2.7 mg/L with %CV ranging from 46-87%, and the geometric mean for AUC_{0-12} varied between 13.9 to 19.6 mg/L*h with %CV of 45-79%. For the 200 mg BID dose, geometric means for C_{max} and AUC_{0-12} were 1.3 mg/L and 10.2 mg/L*h, respectively with % CV of ~65%. The T_{max} ranged between 2-12 h, with median of 6 to 8 h. The high inter-subject variability in these pharmacokinetic parameters was in accordance with previously reported results (**Table 4-1**). Accumulation ratios for 200 and 400 mg doses were 4.14 (range 1.09 – 27.97; **Table 4-5 (a)**) and 3.23 (range 0.74-16.83; **Table 4-5 (b)**), respectively, which was expected based on sorafenib's half-life of 25-48 hr (49). The potential sources of variability in these pharmacokinetic parameters are explored in section 4-5, and effect of this variability on efficacy and toxicity are evaluated in chapters 5 and 6.

Table 4-2. The dosing and pharmacokinetic sampling schedule for sorafenib trials

Trial Name	Tumor type	Stage of clinical trial	Sorafenib dosing schedule (Dose in mg)	Sampling schedule
Bay-mCRPC	mCRPC	Phase II	400 BID , 28 days CC*	**C1D1**: 0, 0.25, 0.5, 1, 2, 4, 6, 8, 12, 24 h
Bay-Bev	various solid tumors	Phase I	200 BID, 28 days CC*	***Arm A*, C1D1, C2D1; *Arm B*, C2D1**: 0, 0.25, 0.5, 1, 2, 4, 6, 8, 12, 24 h
Bay-NSCLC	NSCLC	Phase II	400 BID , 28 days CC*	**C1D1, C1D15**: 0, 0.25, 0.5, 1, 2, 4, 6, 8, 12, 24 h
Bay-KS	KS	Phase I	200 QD/200 BID/400 BID , 28 days CC*	**C1D7**: 0, 1, 2, 4, 6, 8, 12, 16, 24 h
Bay-CRC	CRC	Phase II	400 BID , 28 days CC*	**C1D1**: 0, 0.25, 0.5, 1, 2, 4, 6, 8, 12, 24 h

*CC: Continuous cycle
mCRPC, metastatic castrate resistant prostate cancer, NSCLC, non-small cell lung cancer, KS, Kaposi's sarcoma, CRC, colorectal carcinoma, C1D1, cycle 1 day 1, C2D1, cycle 2 day 1, C1D15, cycle 1 day 15. One cycle was of four week duration.

Schematic presentation of sampling schedule shown in Table 4-2

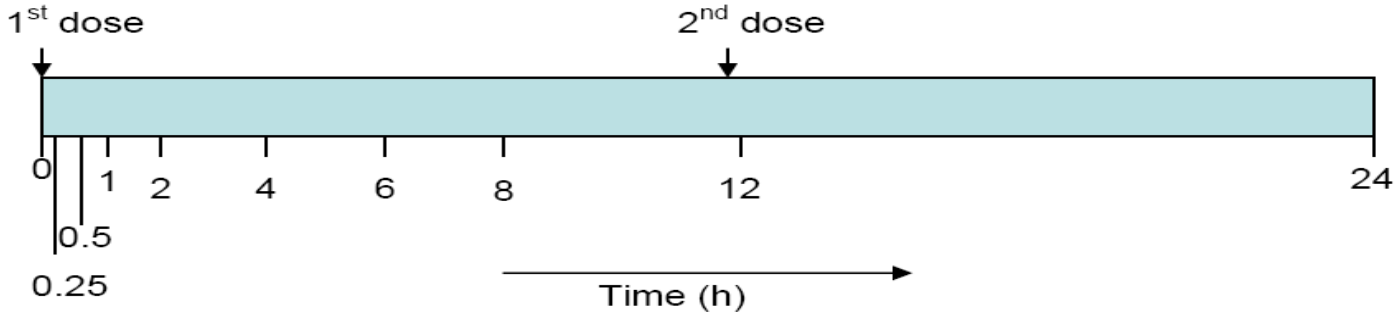

Table 4-3 List of PCR primers for CYP3A4*1B, CYP3A5*3C, UGT1A9*3, UGT1A9*5, VEGFR2 H472Q and VEGFR V297I SNPs

Variant	PCR Type	Forward (F) Primer (5′-3′)	Reverse (R) Primer (5′-3′)	Annealing temperature
CYP3A4*1B	Single	F1:CTGTGTGAGGAGTTTGGTGAG	R1:TGGAAGAGGCTTCTCCACCTTG	64º C
		F2:GTTCTGTCTGTCTGGGTTTGG	R2:CACACCACTCACTGACCTCCT	
CYP3A5*3C	Nested	F1:TCCTCAGAATCCACAGCTG	R1:TAAACTTCACTAGCCCGATTCT	64º C
		F2:AGCACTTGATGATTTACCTGCC	R2:CCAGGAAGCCAGACTTTGATC	
		F3:AGTGGCATAGGAGATACCCAC	R3:AGGTTCTAGTTCATTAGGGTG	
UGT1A9*3	Nested	F1:TTGATAACTGTGGCTTAATTGTTGCC	R1:CCAAAGGTGAAGTATTCTTAAGG	64º C
		F2: ATTTCTCCCTCCCCTCCGTG	R2:GTGCTAAAGGAGAGATAACTTAC	
		F3: AGAAATAGCCTCTGAAATTCTCC	R3:TCCCTGATGGCAGTTGATACCA	
UGT1A9*5	Nested	F1: TCCCTGATGGCAGTTGATACCA	R1:AGTGGCAAAGTATTCCCCTGG	64º C
		F2: TGATGGCTTGCACAGGGTGG	R2:CAAAAATGTCATTGTATGAACCCA	
		F3: ACCAGCCCCCTTCCTCTATG	R3:GCATGACTACAACCACCTCATG	
VEGFR2 Val297Ile (rs2305948)	Single/ Nested	F1: GGTTTGAACCCAAGTTCCTG	R1: CACTTTCACCACGTGAGGTTT	60º C
		F2: TGGCCTCCCTAACAAGAAAA	R2: TGGTGTCCCTGTTTTTAGCA	
		F3: CCCTGACAAATGTGCTGTTC	R3: TGCTGTGCTTTGGAAGTTCA	
VEGFR2 Gln472His (rs1870377)	Single/ Nested	F1: CAGAATCACCCTACACAGATGC	R1: TTCCCAGAATAGCTGCTTCC	60º C
		F2: TGGTACTGCTAAAAGTCAATGG	R2: GGCTGCGTTGGAAGTTATTT	
		F3: CCTGGAAGTCCTCCACACTT	R3: AACCAAAGTCTGAATCTTTTCCTT	

Table 4-4 (a) Summary of non-compartmental pharmacokinetic parameters after single dose of sorafenib

Study	Dose	N	C_{max} (ng/mL)			AUC_{0-12} (ng/mL*h)			T_{max} (h)	
			GM ($x10^3$)	%CV	95%CI ($x10^3$)	GM ($x10^3$)	%CV	95%CI ($x10^3$)	Median	Range
Bay-mCRPC	400 mg BID	46	1.8	87	1.4-2.4	13.9	79	10.7-18.1	6.4	2-12.2
Bay-Bev	200 mg BID	24	1.3	64	1-1.8	10.2	69	7.3-14.4	8.2	2-12.8
Bay-NSCLC	400 mg BID	18	2.7	67	2-3.8	19.6	79	13.8-27.8	6	2-12.2
Bay-KS	200 mg BID	NC	NC	NC	NC	NC	NC	NC	NC	NC
Bay-CRC	400 mg BID	18	2.1	46	1.6-2.7	14.4	45	10.9-19	8	2-12.2

Table 4-4 (b) Summary of non-compartmental pharmacokinetic parameters at steady-state for sorafenib

Study	Dose	Cycle (C), Day (D)	N	C_{max} (ng/mL)			AUC_{0-12} (ng/mL*h)			T_{max} (h)	
				GM($x10^3$)	%CV	95%CI ($x10^3$)	GM($x10^3$)	%CV	95%CI ($x10^3$)	Median	Range
Bay-mCRPC	400 mg BID	NC	NC	NC	NC	NC	NC	NC	NC	NC	NC
Bay-Bev	200 mg BID	C2, D1	9	4.1	64	2.6-6.3	35.1	59	22.6-54.5	4	0.4-8.1
Bay-NSCLC	400 mg BID	C1, D15	17	8.4	54	6-11.8	67.2	50	49.6-91	4	0.3-12
Bay-KS	200 mg BID	C1, D7	2	7.4	47	NC	64.2	38	NC	NC	1, 12.0
Bay-CRC	400 mg BID	NC	NC	NC	NC	NC	NC	NC	NC	NC	NC

Bay-mCRPC: Phase II trial of sorafenib in metastatic castrate resistant prostate cancer, **Bay-Bev**: Phase I trial of sorafenib and bevacizumab combination in patients with solid tumors, **Bay-NSCLC**: Phase II trial of sorafenib in non-small cell lung cancer, **Bay-KS**: Phase I trial of sorafenib in patients with Kaposi's sarcoma, **Bay-CRC**: Phase II trial of sorafenib and cetuximab combination in patients with colorectal cancer, **C_{max}**: Peak plasma concentration, **AUC_{0-12}**: Area under the curve for 0 to 12 h duration, **T_{max}**: Time to peak plasma concentration, **GM**: Geometric mean, **CV**: Coefficient of variation, **CI**: Confidence interval, **NC**: Not calculated

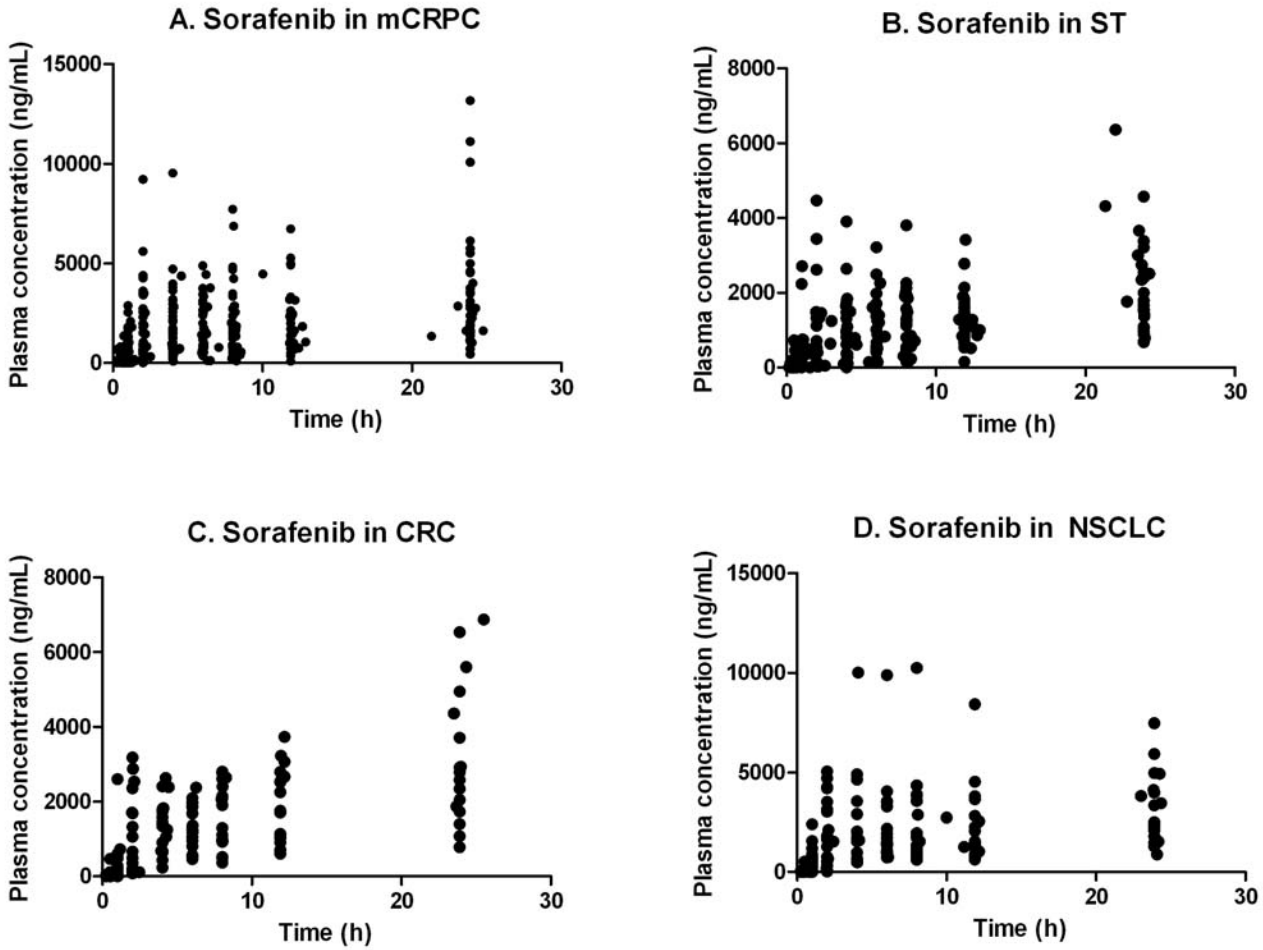

Fig 4-2 (a) Measured plasma concentration – time profiles (normal scale) for sorafenib after administration of initial doses in patients with (A) metastatic castrate resistant prostate cancer (mCRPC), (B) solid tumors (ST), (C) colorectal cancer (CRC) and (D) non-small cell lung cancer (NSCLC)

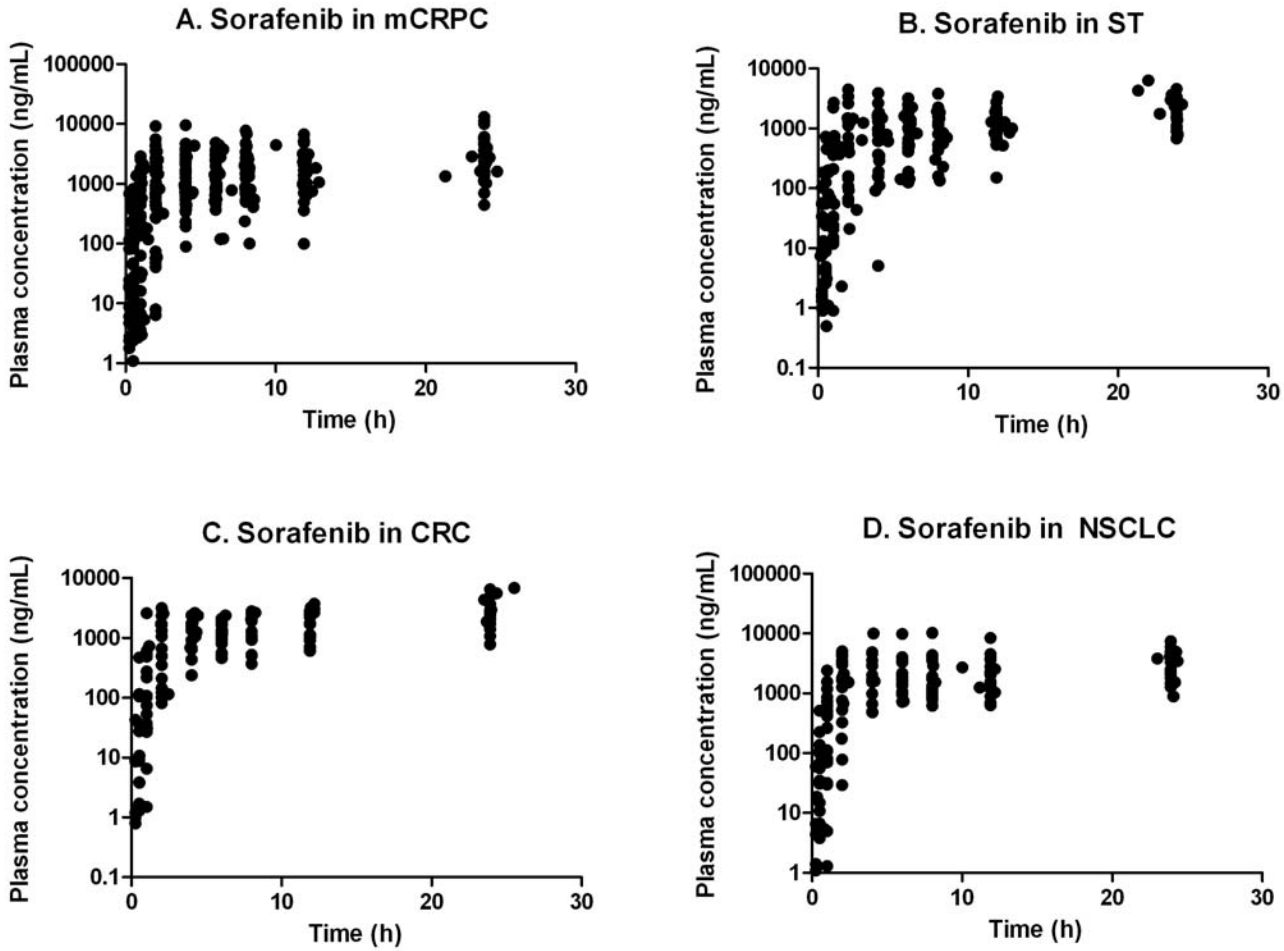

Fig 4-2 (b) Measured plasma concentration – time profiles (log scale) for sorafenib after administration of initial doses in patients with (A) metastatic castrate resistant prostate cancer (mCRPC), (B) solid tumors (ST), (C) colorectal cancer (CRC) and (D) non-small cell lung cancer (NSCLC)

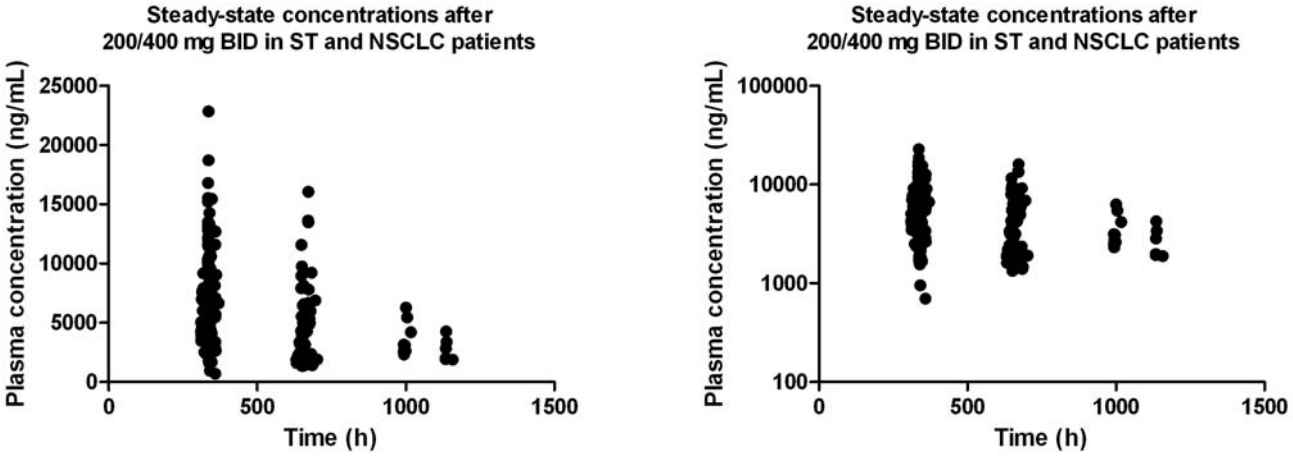

Fig 4-2 (c) Measured plasma concentration – time profiles for sorafenib after administration of multiple doses in patients with solid tumors (ST) and non-small cell lung cancer (NSCLC) (A) in normal scale, (B) in log scale

Table 4-5 (a) Accumulation ratios for patients with solid tumors treated with sorafenib and bevacizumab combination

Pt ID	**$AUC_{0-12}^{SS\sim day\ 30}$ (ng/mL*hr)**	**AUC_{0-12}^{SD} (ng/mL*hr)**	**$AUC_{0-12}^{SS}/AUC_{0-12}^{SD}$ Ratio**
1	88856.4	17431.7	5.1
2	48308.9	17177.4	2.8
3	24314.2	4491.8	5.4
4	22788.3	21154.0	1.1
6	24161.6	8208.9	2.9
7	20249.3	7760.0	2.6
8	35140.0	1256.9	28.0
		Median	2.9
		Range	(1.1 – 28.0)

Table 4-5 (b) Accumulation ratios for patients with non-small cell lung cancer treated with sorafenib

Pt ID	$AUC_{0-12}^{SS\sim day\ 15}$ (ng/mL*hr)	AUC_{0-12}^{SD} (ng/mL*hr)	$AUC_{0-12}^{ss}/AUC_{0-12}^{SD}$
1	92989.9	27989.1	3.3
2	68471.9	15018.9	4.6
3	70208.8	37238.8	1.9
4	75951.9	17063.7	4.5
5	103173.6	91943.2	1.1
6	110654.2	41098.0	2.7
7	81383.9	9633.6	8.4
8	25165.9	30578.2	0.8
9	118102.0	7016.6	16.8
10	27549.4	37039.9	0.7
11	105102.4	6468.6	16.2
12	74349.5	35595.6	2.1
13	175654.6	12531.3	14.0
14	36481.0	15375.4	2.4
15	31176.5	12440.3	2.5
16	96662.3	24411.4	4.0
17	29702.2	9199.1	3.2
		Median	3.2
		Range	0.7 – 16.8

4-4.2.1 Effect of bevacizumab co-administration on sorafenib pharmacokinetics

The design of this phase I trial conducted to establish the safe dose of sorafenib and bevacizumab combination in patients with solid tumors is shown in **Fig 4-3**. Patients were recruited in either arm A or arm B. Patients on arm A received sorafenib alone for 4 weeks followed by treatment with sorafenib and bevacizumab combination, while

patients on arm B first received bevacizumab for 4 weeks followed by combination therapy. Thus, the effect of bevacizumab co-administration can be studied by comparing the sorafenib exposure parameters between arm A, cycle 1, day 1 and arm B, cycle 2, day 1.

The plasma concentration – time profiles for sorafenib from patients enrolled in these two arms are shown in **Fig 4-4**, with a mean plasma concentration (± SD) and time designated respectively on the ordinate and abscissa. The mean plasma concentrations (point estimates) were higher for patients on arm B than arm A; however, the differences were not statistically significant. The AUC_{0-12} and C_{max} were also not statistically different between these two arms (p values 0.2391 and 0.3058, respectively). These results indicate that co-administration of bevacizumab may not influence sorafenib exposures.

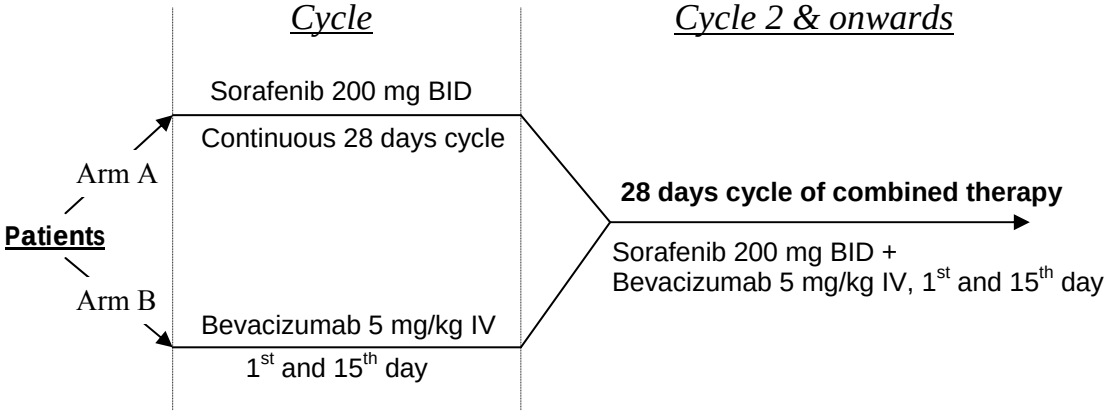

Fig 4-3 Schematic representation of phase I trial evaluating the maximum tolerable dose of sorafenib and bevacizumab combination in patients with solid tumors

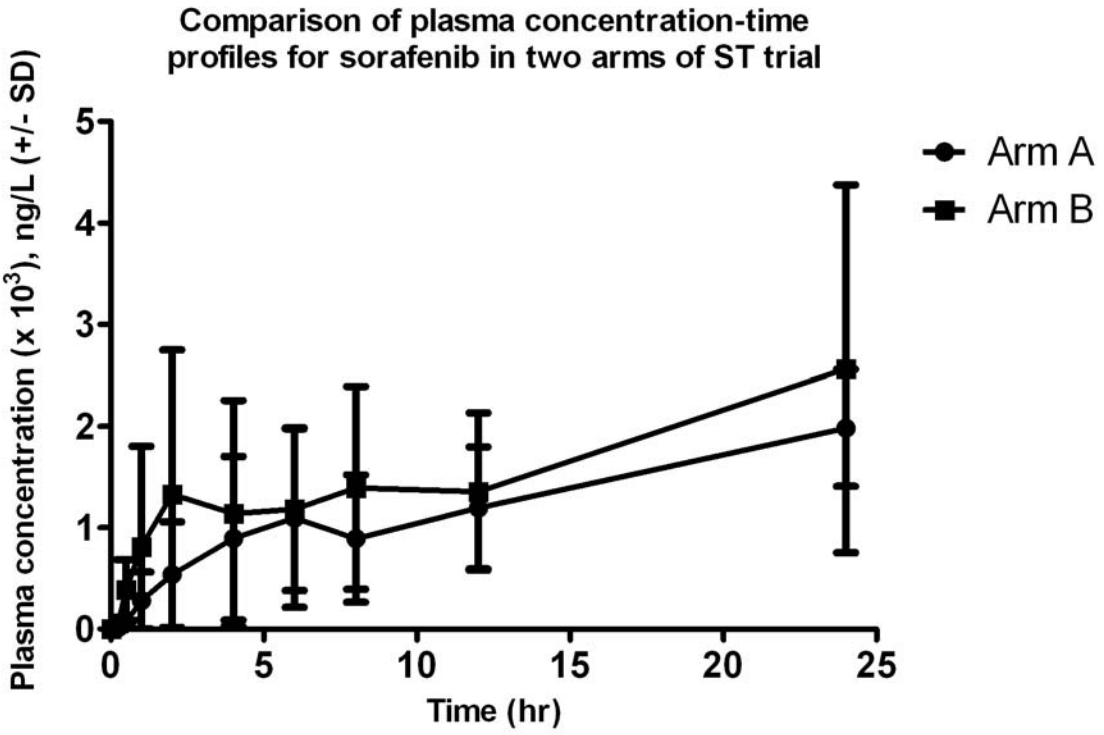

Fig 4-4 Comparison of plasma concentration – time profiles for sorafenib administered as single agent (Arm A) and in combination with bevacizumab (following prior administration of bevacizumab for 4 weeks) (Arm B).

4-4.2.2 Effect of ritonavir co-administration on sorafenib exposures

Another phase I trial included in current analysis evaluated the safe dose of sorafenib in patients with KS, when administered with or without ritonavir. The design of this is shown in **Fig 4-5** below. Patients with AIDS-related KS received sorafenib in combination with ritonavir. Ritonavir is known to be a strong inhibitor of CYP3A4 enzyme, which is also one of the metabolic enzymes for sorafenib. Because of the potential for drug interaction these patients were started at a lower dose of sorafenib, i.e., 200 mg QD. Patients not receiving ritonavir started at 200 mg BID doses, half-of-the

clinically approved 400 mg BID dose. Sorafenib pharmacokinetics between these two groups was compared to evaluate the impact of ritonavir co-administration on disposition of sorafenib. Assuming that steady-state for sorafenib is reached by day 7 based on its half-life of 25-48 h; sorafenib exposures for a dosing interval at steady-state ($AUC_{0\text{-}\tau,\,SS}$) would be comparable in these two groups. In absence of any interaction, $AUC_{0\text{-}12,\,SS}$ for sorafenib 200 mg BID without ritonavir should not be significantly different from $AUC_{0\text{-}24,\,SS}$ for sorafenib 200 mg QD with ritnovair. However, the limitation of this comparison was small sample size; so far only 8 subjects have been recruited in this trial.

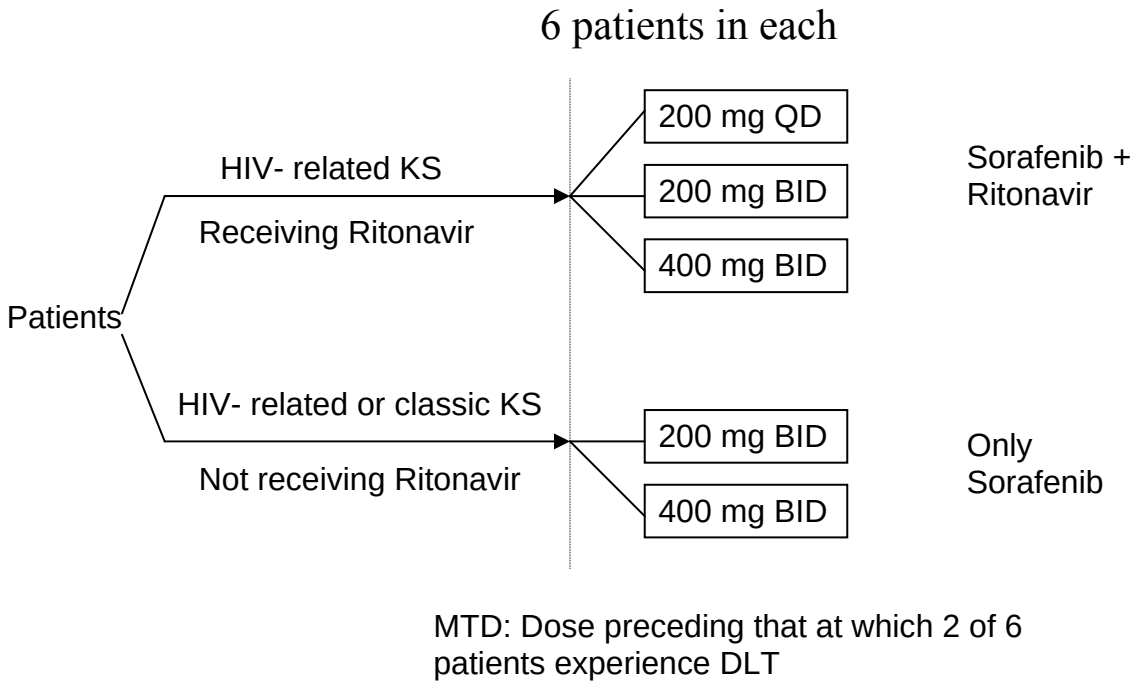

Fig 4-5 Schematic representation of phase I trial evaluating the maximum tolerable dose of sorafenib in patients with Kaposi's sarcoma

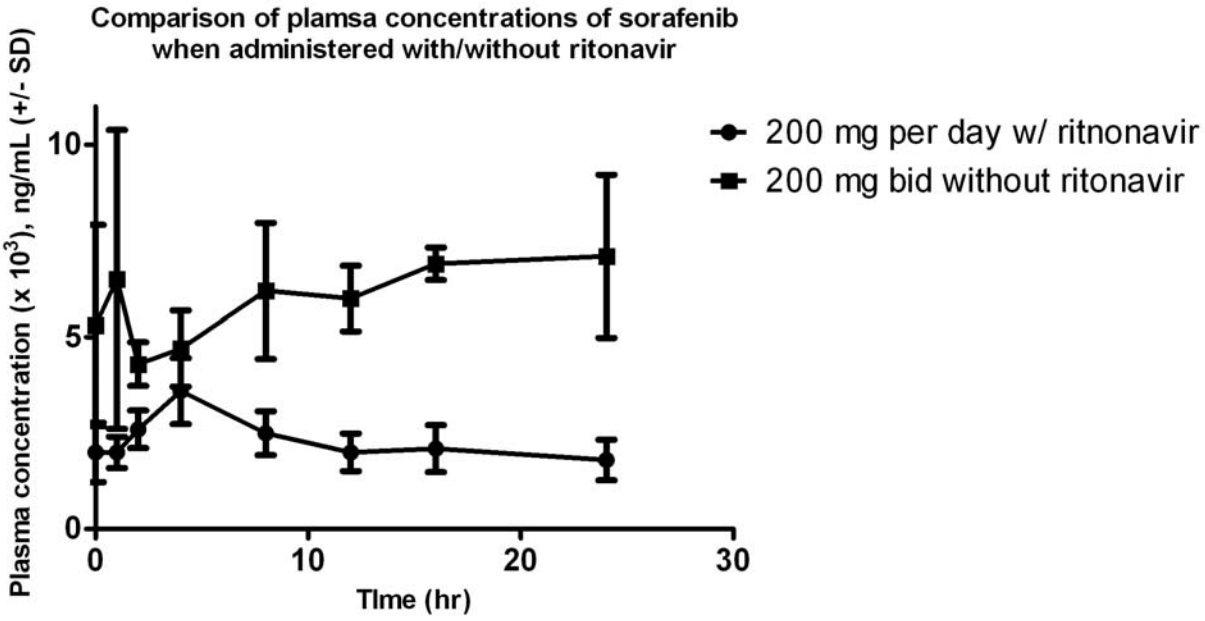

Fig 4-6 (A) Comparison of plasma concentration-time profiles for sorafenib 200 mg BID administered as single agent versus sorafenib 200 mg QD administered with ritonavir.

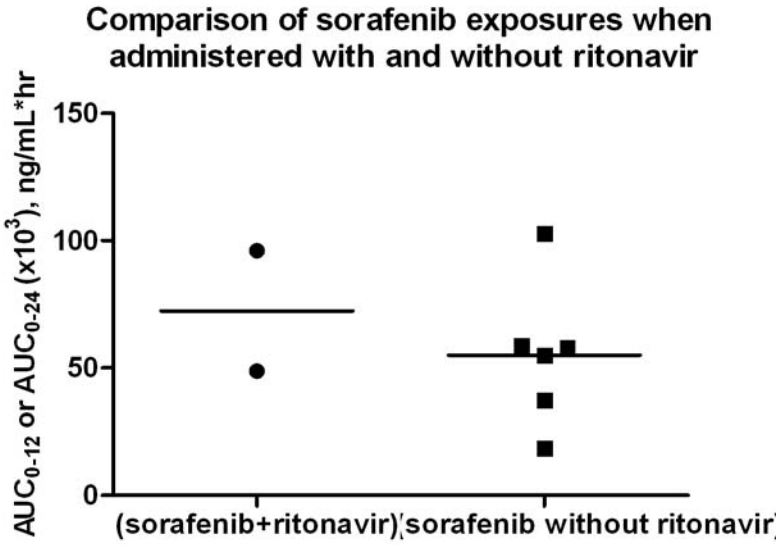

Fig 4-6 (B) Comparison of sorafenib exposures, $AUC_{0\text{-}12,\,SS}$ for sorafenib 200 mg BID administered as single agent versus $AUC_{0\text{-}24,\,SS}$ for sorafenib 200 mg QD administered with ritonavir.

Comparison of plasma concentration-time profiles for patients who received sorafenib with or without ritonavir demonstrated that concentrations for 200 mg BID dosing regimen are higher than 200 mg QD administration (**Fig 4-6 (A)**), which is as expected. Comparison of exposure metrics in these groups revealed that exposures after co-administration with ritonavir ($AUC_{0\text{-}24,\ SS}$) were not significantly different from exposures after administration as single agent ($AUC_{0\text{-}12,\ SS}$) (**Fig 4-6 (B)**). Ritonavir co-administration appeared to have no significant effect on sorafenib exposures. These results were consistent with findings from another prospective DDI clinical trial, which demonstrated that sorafenib exposures were not significantly affected by co-administration with ketoconazole, also a potent CYP3A4 inhibitor (37).

4-5 Exploratory covariate screening by non-compartmental analysis-general linear modeling approach

As shown in **Table 4-1 (a) and (b),** and **Table 4-4**, the pharmacokinetics for orally administered sorafenib was highly variable among patients with various types of solid tumors. An exploratory analysis was conducted to identify the clinically important covariates that may explain the inter-patient differences in systemic exposures and peak plasma-concentrations for sorafenib. The subsets of patients with full pharmacokinetic profiles from prostate cancer, colorectal cancer, lung cancer and solid tumor trials were used for this analysis. Patients from KS trial were not included in this analysis, because no samples were collected after administration of initial doses (only day 7 samples were collected) and also sorafenib was co-administered with ritonavir, which has a potential of drug-interaction with sorafenib. Although no interaction was observed with current small

sample size (**section 4-4.2.1**); but that needs to be confirmed with larger sample size. We used demographic (age, gender, weight, BSA and ethnicity), clinical or laboratory (AST, ALT, albumin, alkaline phosphatase, total protein, total bilirubin, serum creatinine and creatinine clearance) and pharmacogenetic (genetic variation in CYP3A4, CYP3A4, UGT1A9 and VEGFR2) variables as covariates in this exploratory analysis. The results of this non-compartmental covariate analysis were used as guidance for selection of covariates for population pharmacokinetic analysis.

4-5.1 Methods

4-5.1.1 Pharmacokinetic metrics

Covariate analysis was performed for the pharmacokinetic metrics, $AUC_{0\text{-}12}$ and C_{max}, which are summarized in **Table 4-4**. Patients on these trials were administered either 200 or 400 mg BID sorafenib doses. In order to correct for the different dose levels, the calculated pharmacokinetic metrics were normalized by the amount of administered dose, assuming linear pharmacokinetics as previously shown for dosage range of 50 to 400 mg BID (35). Both dose-normalized $AUC_{0\text{-}12}$ (AUC/D) and C_{max} (Cmax/D) distributions were skewed to the right, as shown in **Fig 4-7**. Hence, these metrics were ln-transformed to obtain a reasonably symmetric distribution, which also satisfied the assumptions for parametric statistical tests. Further analysis was performed with ln-transformed values.

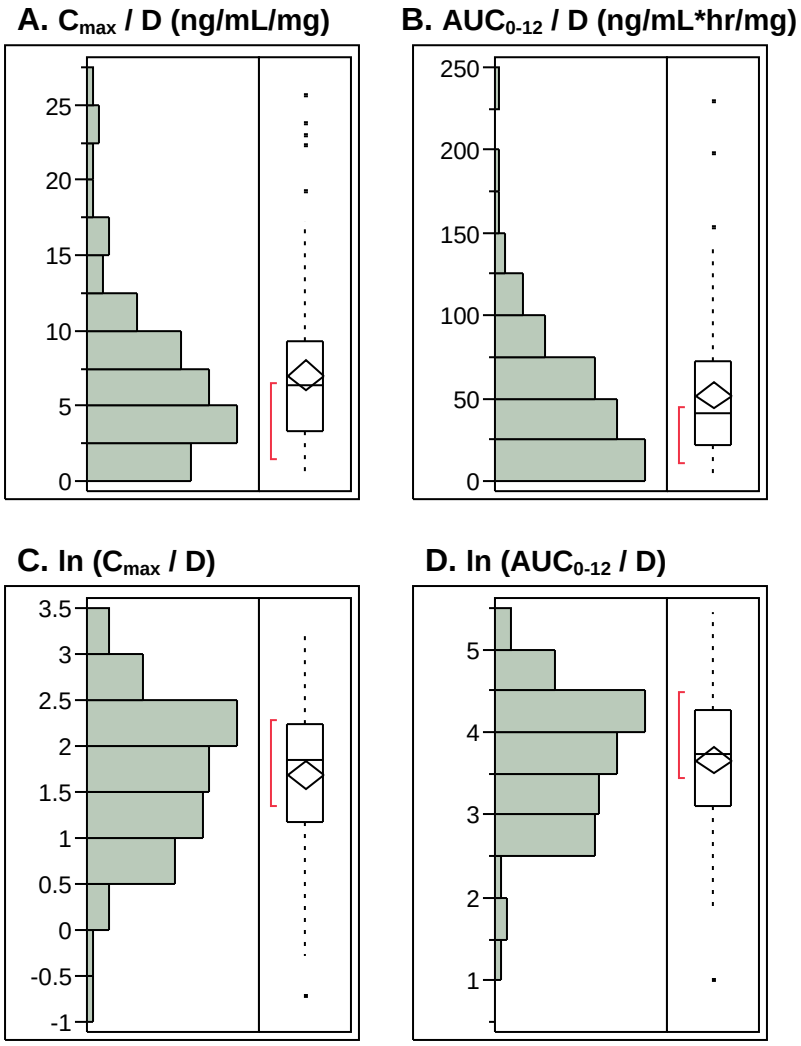

Fig. 4-7 Distribution of dose normalized C_{max} and $AUC_{0\text{-}12}$. (A) and (B) – normal scale values, (C) and (D) – ln-transformed values. In right margins, box and whisker plots are shown, where center of the diamond represents mean, the solid horizontal line in the box represents median, edges of the box depict inter-quartile range and the flanking whiskers represents the data within the 1.5 times inter-quartile range. The points outside the whiskers are considered outliers.

4-5.1.2 Assessment of covariates

The possible (expected) mechanistic impact of candidate covariates (which were screened to explain the inter-individual variability) on sorafenib pharmacokinetics are summarized in **Table 4-6**. The administered dose and trial were included as covariates to assess pharmacokinetic linearity and differences in pharmacokinetic parameters across clinical trials. Other covariates included in this analysis represented standard demographic information, hepatic and renal function markers, and genetic marker variations in studied population.

BSA was calculated using the DuBois and DuBois formula:

$$BSA = 0.20247 * height(m)^{0.725} * weight(kg)^{0.425}$$

where height and weight were measured in meter and kilogram units.

Renal function was estimated as creatinine clearance (CL_{Cr}), which was calculated using the Cockroft-Gault equation:

$$CL_{Cr} = \frac{Gender * ((140 - Age) * Weight)}{72 * SCr}$$

where weight was measured in kilogram units, age in years and SCr in g/dL.

The gender variable took value of 1 for males and 0.85 for females. CL_{Cr} values above 150 mL/min were right truncated, because values above 150 mL/min are physiologically unlikely.

Hepatic and renal function markers were evaluated both as continuous (actual lab values) and nominal variables (High (H), Normal (N) and Low (L)). The classification as nominal variables was performed to differentiate the patients with ‘normal’ and ‘abnormal’ organ function, and was considered to be more helpful in clinical decision making.

Genetic variation in the metabolic enzymes for sorafenib, namely CYP3A4, CYP3A5 and UGT1A9, were also evaluated as covariates. Genetic variability in the drug target for sorafenib, namely VEGFR2, was also evaluated as covariate for exposure metrics, although, no mechanistically plausible relationship was expected.

Distributions of these covariates were assessed for any imbalances, skewness or collinearity. For nominal covariates, frequency distributions of subgroups were compared for imbalances. For continuous covariates, measures of central tendency (mean, median) and dispersion (standard deviations and range) were evaluated for skewness, uni-modality and fold range. Collinearity was assessed by multivariate correlation (between continuous variables) or one-way ANOVA (between nominal and continuous variables). The statistical analysis was performed using JMP 8.0 (SAS Institute Inc., Cary, NC, USA) statistical software.

Table 4-6 List of covariates and their expected (possible) effects on sorafenib pharmacokinetics/exposures.

S.N.	Category	Covariate Name	Expected effect on sorafenib exposures
1	**Demographic**	**Body weight (BW)**	Increase in BW may decrease AUC and C_{max}, because of increase in metabolic clearance (CL) and volume of distribution (V_d).
2		**Body surface area (BSA)**	It is a composite matrix of BW and height. Effects on pharmacokinetics are expected to be similar to BW, i.e., decrease in AUC and C_{max} with increase in BSA.
3		**Age**	Aging may cause reduction in liver mass, liver blood flow, plasma protein binding and activity of liver metabolic enzymes, which would affect the CL and/or V_d (66), and may increase the AUC and C_{max}.
4		**Height**	Height does not change after reaching the adulthood. Variation in height among adult individuals would not have any additional effect in addition to what are expected based on changes in BW and BSA.
5		**Gender**	Generally, females have lower BW, lower V_d and were also found to have higher expression of CYP3A4 mRNA and CYP3A4 enzymes (66). These differences

			may affect the metabolic CL and V_d of sorafenib, resulting in higher AUC and C_{max} for females compared to males.
6		**Ethnicity**	Expression and activity of drug metabolic enzymes and drug transporters may vary among patients with different ethnicities, which may alter the AUC and/or Cmax.
7	**Liver function markers**	**Albumin**	It is a marker of liver synthetic function. Lower than normal levels may suggest dysfunction in synthesis or elimination organs for albumin, such as liver or kidney. These dysfunctions may reduce the sorafenib CL, resulting in increased AUC. However, poor nutritional states leading to protein catabolism may also lower albumin levels. Sorafenib's pharmacokinetics may also get affected because of its high affinity towards albumin, where increase in fraction of free drug (because of lower albumin levels) may increase its plasma clearance or distribution to peripheral tissues, resulting in decrease in AUC and C_{max}.
8		**Total protein**	Total protein comprises of albumin (major proportion) and globulins (α,β,γ); hence change in its level may alter the proportion of free drug available for drug

		effect or undergoing metabolism. Effects on AUC and C_{max} will be similar to that described for albumin.
9	**ALT and AST**	These are leak enzymes which tell us about the integrity of liver cells. Higher than normal levels suggest damage in liver cells (92) may result in reduced metabolism of sorafenib by liver enzymes resulting in increased AUC and C_{max}.
10	**Alkaline phosphatase**	It is an enzyme present in the cells lining the biliary ducts of the liver. Higher than normal levels suggest obstruction of bile duct. Sorafenib is predominantly cleared by hepato-biliary elimination; hence, obstruction of bile duct would affect its clearance and extent of recirculation, which may increase its systemic exposures. However, this effect should be interpreted with caution because levels of this enzyme also increases in bone metastasis associated with cancer.
11	**Total bilirubin**	Decrease in levels of total bilirubin may suggest prehepatic (i.e., RBC hemolysis), hepatic (i.e., deficiencies in bilirubin metabolism and biliary excretion) or post-hepatic (i.e., obstruction in bilirubin excretion) changes in bilirubin pathway. Specifically, its levels would reflect not only the normal hepatic function but also

			the hepatic UGT1A1 enzyme activity as well as canalicular transport function (e.g., mediated by MRP2); which may affect sorafenib's disposition to liver and its metabolism influencing AUC and C_{max}.
12	**Kidney function markers**	**Serum creatinine and creatinine clearance**	These markers reflect the state of renal function. Values of CL_{Cr} in range of 40-59 (both inclusive) suggest mild renal dysfunction, range 20-39 suggest moderate dysfunction and below 20 suggests severe dysfunction. Only sorafenib glucuronide metabolites equivalent to 19% of administered dose are eliminated by renal route; hence, effect of kidney function on sorafenib AUC and C_{max} would be minimal.
13	**Pharmacogenetic markers**	**CYP3A4*1B**	This polymorphism is located in the promoter region of CYP3A4 gene, and is usually reported to result in a gain of function (i.e., increased metabolic activity); however, there is a lack of consensus about functional impact of this polymorphism. This polymorphism may increase the metabolic clearance of sorafenib, resulting in decrease in AUC and C_{max}.
14		**CYP3A5*3C**	This polymorphism is located in intron 3, and results in splicing defect in mRNA

		for CYP3A5 protein, leading to reduced translation and lower protein (enzyme) expression. The CYP3A5*3 variant allele commonly exists in linkage with CYP3A4*1B wild type allele; in addition, these enzymes exhibit significant overlap in substrate specificity (93). This polymorphism may result in reduced metabolic clearance and increased AUC and C_{max} of sorafenib
15	**UGT1A9*3**	This polymorphism is located in the coding region (exon 1) of UGT1A9 gene. Carries of variant allele had significantly reduced glucuronidation activity (3.8% glucuronidation activity for SN-38 in comparison to wild type carriers) (75). This effect on glucuronidation activity may result in reduced metabolic clearance of sorafenib, resulting in increase in AUC and C_{max}.
16	**UGT1A9*5**	This polymorphism is also located in the coding region (exon 1) of UGT1A9 gene; and carriers of variant allele had significant reduction in glucuronidation activity (less than 5% catalytic activity for SN-38 glucuronidation in comparison to wild type allele carriers) (75). This polymorphism may also result in reduced metabolic clearance of sorafenib, resulting in increase in AUC and C_{max}.

17	**VEGFR2 H472Q**	This polymorphism exists in exon 11 of VEGFR2 gene, and is located in immunoglobulin-like (Ig-like) domain 5. Ig-like domains 4-7 have been shown to contain structural features that inhibit receptor signaling in absence of VEGF (79). Mechanistically, this polymorphism is not expected to affect the sorafenib pharmacokinetics, but because we had data available for variations in this genotype, we included it as a covariate.
18	**VEGFR2 V297I**	This polymorphism exists in exon 7 of VEGFR2 gene, and is located in Ig-like domain 3, which is shown to be critical for VEGF binding (79). Mechanistically, this polymorphism is also not expected to affect the sorafenib pharmacokinetics, but it was screened as covariate because data were available for variations in this genotype.

4-5.1.3 Covariate Screening

To identify the important covariates, both ln-transformed exposure metrics were individually fit to each nominal and continuous covariate using a linear model (i.e., one-way ANOVA or linear regression). The contribution of these covariates to the overall variability in the respective pharmacokinetic metrics and their statistical significance were respectively assessed by coefficient of determination (r^2) and p-value. *A priori* cut-off for r^2 and p-value were set to 0.1 and <0.05, respectively; covariates which met either of the two criteria were further evaluated for mechanistic plausibility. In addition, intercept and effect size estimates (relative to intercept) or intercept and slope estimates were reported for ANOVA and linear regression, respectively. Because the exposure metrics were ln-transformed prior to analysis, the effect size and slope were multiplied with 100 to be interpreted as percent (%) change on normal scale. The statistical analysis was performed using JMP 8.0 (SAS Institute Inc., Cary, NC, USA) statistical software.

4-5.1.4 Final Model

A stepwise regression with forward selection and backward elimination was used for development of final model, individually for both exposure metrics. All candidate covariates were eligible for inclusion in the final model. The cut-off p-value of 0.25 was used for entering the covariates (forward selection) in the development of full model, followed by removal (backward elimination) of covariates from full model with a p-value of 0.10. These liberal p-values were chosen considering the exploratory nature of this analysis.

The statistical analysis was performed using JMP 8.0 (SAS Institute Inc., Cary, NC, USA) statistical software.

4-5.2 Results and Discussion

4-5.2.1 Pharmacokinetic metrics

The distribution of each pharmacokinetic metrics and their ln-transformed values are shown in **Table 4-7**. As shown in **Table 4-7** and **Fig 4-7** , both dose-normalized AUC_{0-12} and C_{max} were right skewed, hence they were ln transformed which followed normal symmetric distribution. Both C_{max}/D and AUC_{0-12}/D were highly variable with %CV greater than 70%, and their values varied by more than 50 folds. Ln-transformation reduced the variance in these parameters to 20-50%, which although statistically reduced the chances of finding correlations with covariates, but was considered important to meet the assumptions of normality for statistical tests.

Table 4-7. Summary of pharmacokinetic parameters for sorafenib trials

Dose normalized PK metrics	N	Mean	Median	Min	LQ	UQ	Max	%CV	Fold range
Cmax/D [ng/mL/mg]	106	7.1	6.4	0.5	3.3	9.4	25.6	74	52
AUC_{0-12}/D [ng/mL*hr/mg]	104	52.1	41.6	2.7	22.2	72.4	229.9	77	84
Ln(Cmax/D)	106	1.7	1.9	-0.7	1.2	2.2	3.2	46	4
Ln(AUC_{0-12}/D)	104	3.7	3.7	1.0	3.1	4.3	5.4	22	5

PK: pharmacokinetics, **LQ**: lower quartile, **UQ**: upper quartile, **CV**: coefficient of variation, C_{max}, peak plasma concentration, AUC_{0-12}, area under the curve from 0-12 hr after administration of first dose of sorafenib

Both metrics were highly inter-related (r=0.95, p<0.0001). The $AUC_{0\text{-}12}$/D and Cmax/D were reflective of CL/F and V_d/F, respectively. These exposure metrics can generally be described as function of the following underying pharmacokinetic properties:

$$AUC \propto F_{oral}, \frac{1}{CL_{total}}$$

$$C_{\max} \propto F_{oral}, k_a, \frac{1}{V_d}$$

where F_{oral} is absolute oral bioavailability, CL_{total} is total systemic clearance and k_a is the absorption rate constant. From these equations it is apparent that AUC/D and C_{max}/D are functions of F/CL_{total} and F/V_d.

4-5.2.2 Assessment of covariates

The screened covariates are summarized in **Table 4-8 (a), (b) and (c)**. Patients from four different trials were included in covariate analysis, but the numbers of patients in these trials were not equal. Approximately 77% of the patients received 400 mg BID, and the remaining patients were administered 200 mg BID. The proportion of males was higher than females (70% vs. 30%), and more than 8 out of 10 patients were Caucasians. These imbalances may obscure or bias the true effect of trial, dose, gender and ethnicity on exposure metrics. Among liver function markers, ALT, total bilirubin and total protein values were outside the normal limits for only 7%, 8% and 13% patients, which increased the possibility of bias in the effect size estimation and false negative findings. A total of 23%, 26% and 52% patients had abnormal values for AST, alkaline phosphatase and albumin. Thirty-nine percent (39%) patients had serum creatinine values outside the

normal limits, and only 13% patients had mild to moderate renal dysfunction based on the estimated creatinine clearance.

Patients' age varied from 30-85 years (approximately 3-fold variation with a median of 64 years), and their weight ranged from 35-132 kg (approximately 4-fold variation with a median of 81 kg). Height varied from 144 to 191 cm with 1.3-fold variation and a median of 171 cm, and the variability in BSA was 2.5-fold with range of 1.2-2.5 m^2 and q median of 1.9 m^2. Creatinine clearance values ranged from 25-150 mL/min (approximately 6-fold variation with a median of 91 mL/min). ALT, AST, alkaline phosphatase and bilirubin total had wide range of distribution with approx. 7-17 fold variation (%CV 40-60). Albumin and total protein had only 2-fold variation (%CV 9-12), but as mentioned earlier more than 50% of patients had albumin levels lower than normal.

Similar to the laboratory and demographic covariates, the genotype distributions for CYP3A4*1B, CYP3A5*3C, UGT1A9*3, UGT1A9*5, VEGFR2 H472Q and VEGFR2 V297I polymorphisms were also imbalanced. None of the patients in studied population carried the variant allele for UGT1A9*5 SNP; hence, it was not included in further analysis. Only 11% and 2% patients carried the variant allele for CYP3A4*1B and UGT1A9*3 SNPs, respectively, while the frequencies of variant allele for VEGFR2 H472Q and VEGFR2 V297I SNPs were 20% and 15%, respectively. For CYP3A5*3C, the frequency of wild-type (wt) allele was smaller compared to the variant allele, i.e., 13 %. Among these, CYP3A4*1B, CYP3A5*3 and both VEGFR2 polymorphisms were in Hardy-Weinberg equilibrium (**Table 4-8 (c)**, $p>0.05$), when evaluated for only Caucasian

patients. The deviation of UGT1A9*3 from Hardy-Weinberg equilibrium may be attributed to the small sample size, leading to increase in selection bias for study subjects.

Collinearity between these covariates was assessed by evaluating the multivariate correlations (**Table 4-9**). The relationship between nominal and continuous covariates or other nominal covariates were also assessed, a selected example of which is shown in **Fig 4-8**. The effect of BSA, gender and CL_{Cr} were confounded by body weight (**Table 4-9**), which were not unexpected given that BSA and CL_{Cr} were calculated by DuBois and DuBois and Cockroft-Gault formula, respectively; and females had significantly lower body weight (mean=71 kg, SD=18.3) than males (mean=87 kg, SD=17) ($p<0.0001$) (**Fig. 4-8**). Similarly, AST and ALT and SCr and CL_{Cr} were correlated (**Table 4-9**).

Table 4-8 (a) Summary of nominal, non-genetic covariates

	Level 1	**(%) No.**	**Level 2**	**(%) No.**	**Level 3**	**(%) No.**	**Total**
Trial[†]	mCRPC, (43) 46 / NSCLC, (17) 18 / CRC, (17) 18 and ST,(23) 24						
Dose [200/400 mg]	200	(23) 24	400	(77) 82			106
Gender [F/M]	F	(30) 32	M	(70) 74			106
Ethnicity	Cauc	(81) 86	AA	(9.5) 10	Asian/other	(9.5) 10	106
SCr [L/N/H]	L	(37) 39	N	(60) 64	H	(3) 3	106
CL_{Cr}^{CG}	Mild dysfunction	(10) 11	Moderate dysfunction	(3) 3	N	(87) 92	106
Albumin [L/N]	L	(52) 55	N	(48) 51	H	(0) 0	106
Protein, Total [L/N/H]	L	(11) 12	N	(87) 92	H	(2) 2	106
ALT [L/N]	L	(0) 0	N	(92.5) 98	H	(7.5) 8	106
AST [L/N]	L	(0) 0	N	(76.5) 81	H	(23.5) 25	106
Alk Phos [L/N/H]	L	(2) 2	N	(73.5) 78	H	(24.5) 26	106
Bilirubin, Total [N/H]	L	(0) 0	N	(92.5) 98	H	(7.5) 8	106

[†]**mCRPC**: Phase II trial of sorafenib in metastatic castrate resistant prostate cancer, **ST**: Phase I trial of sorafenib and bevacizumab combination in patients with solid tumors, **NSCLC**: Phase II trial of sorafenib in non-small cell lung cancer, **Bay-CRC**: Phase II trial of sorafenib and cetuximab combination in patients with colorectal cancer
SCr: serum creatinine; **CL_{Cr}**: creatinine clearance; **ALT**: alanine transaminase or SGPT, **AST**: aspartate transaminase or SGOT, **Alk Phos**: alkaline phosphatase, **L**: lower than normal lab values, **N**: normal lab values, **H**: higher than normal lab values.

Table 4-8 (b) Summary of continuous covariates

Covariate	N	Mean	Median	Min	LQ	UQ	Max	CV%	Fold range
Age [years]	106	62.8	64.2	30.4	55.3	71.4	85.0	18	2.8
Weight [kg]	106	82.7	81.3	35.2	69.0	97.7	132.5	23	3.8
Height [cm]	106	170.2	171.3	144.3	164.2	176.9	191.5	6	1.3
BSA [m^2]	106	1.9	1.9	1.2	1.7	2.2	2.5	14	2.1
SCr [g/dL]	106	0.95	0.9	0.4	0.8	1.05	1.9	25	4.8
CL_{Cr}^{CG} [mL/min]	106	92.3	90.6	25.5	74.4	109.7	150.0†	31	5.9
Albumin [g/dL]	106	3.6	3.6	2.2	3.3	3.9	4.4	12	2
Protein, Total [g/dL]	106	6.5	6.6	4.6	6.2	6.9	8.2	9	1.7
ALT [U/L]	106	23.4	20.5	8.0	15.0	28.0	75.0	52	9.4
AST [U/L]	106	28.4	26.0	13.0	21.0	34.0	90.0	39	7
Alk Phos [U/L]	106	99.8	81.5	34.0	64.0	115.5	414.0	58	12.2
Bilirubin, Total [mg/dL]	106	0.65	0.6	0.1	0.5	0.8	1.7	38	17

†CL_{Crea} values greater than 150 were truncated at 150.
LQ: lower quartile, **UQ**: upper quartile, **CV**: coefficient of variation
BSA: body surface area **SCr**: serum creatinine; **CL_{Cr}**: creatinine clearance; **ALT**: alanine transaminase or SGPT, **AST**: aspartate transaminase or SGOT, **Alk Phos**: alkaline phosphatase

Table 4-8 (c) Summary of pharmacogenetic covariates

	Genetic Variants	**N**	**Genotype Frequencies[a]**			**Allele Frequencies[b]**		
			Wt	**Het**	**Var**	**p**	**q**	**p-value[c]**
Metabolic Enzymes	CYP3A4*1B	104	88 (84.6)	9 (8.6)	7 (6.7)	0.88	0.12	0.19
	CYP3A5*3C	104	5 (4.8)	18 (17.3)	81 (77.9)	0.14	0.86	0.65
	UGT1A9*3	104	100 (96.1)	3 (2.9)	1 (1)	0.98	0.02	<0.01
	UGT1A9*5	102	102 (100)	0 (0)	0 (0)	1	0	NA
Sorafenib Target	VEGFR2 H472Q	103	66 (64.1)	32 (31.1)	5 (4.8)	0.8	0.2	0.76
	VEGFR2 V297I	102	74 (72.5)	25 (24.5)	3 (3)	0.85	0.15	0.99

NA: not accessible
Wt, wild type sequence; **Het**, heterozygous and **Var**, homozygous variant sequences;
p, q are standard Hardy-Weinberg nomenclature for allele frequencies
a. Number represents number of patients with percentages in parentheses
b. Data are given as relative frequency
c. p-value for evaluation of Hardy-Weinberg equilibrium for Caucasian subjects only

Table 4-9 Assessment of collinearity (correlation coefficient, r) between continuous covariates by evaluating the multivariate correlations

	BW	Age	BSA	Alb	Total Protein	Alk Phos	Total Bili	AST	ALT	SCr	CL_{Cr}
BW	1.00										
Age	-0.02	1.00									
BSA	**0.75**¶	0.20	1.00								
Alb	0.04	-0.24	-0.01	1.00							
Total Protein	-0.06	-0.27	-0.19	**0.53**	1.00						
Alk Phos	0.01	0.03	0.03	-0.32	-0.09	1.00					
Total Bili	0.09	0.04	0.05	0.10	0.01	0.00	1.00				
AST	0.06	0.14	0.10	-0.02	0.08	0.32	0.02	1.00			
ALT	0.11	0.01	0.14	0.17	0.17	0.27	0.02	**0.60**	1.00		
SCr	0.13	0.13	0.16	0.14	0.07	-0.07	0.17	0.09	0.00	1.00	
CL_{Cr}	**0.64**	-0.46	0.39	0.05	0.02	0.03	-0.01	-0.04	0.08	**-0.53**	1.00

¶The correlation coefficient above 0.5 are highlighted

BW: body weight, **BSA**: body surface area, **Alb**: albumin, **Alk Phos**: alkaline phosphatase, **Total Bili**: total bilirubin, **AST**: aspartate transaminase or SGOT, **ALT**: alanine transaminase or SGPT, **SCr**: serum creatinine, **CLCr**: creatinine clearance

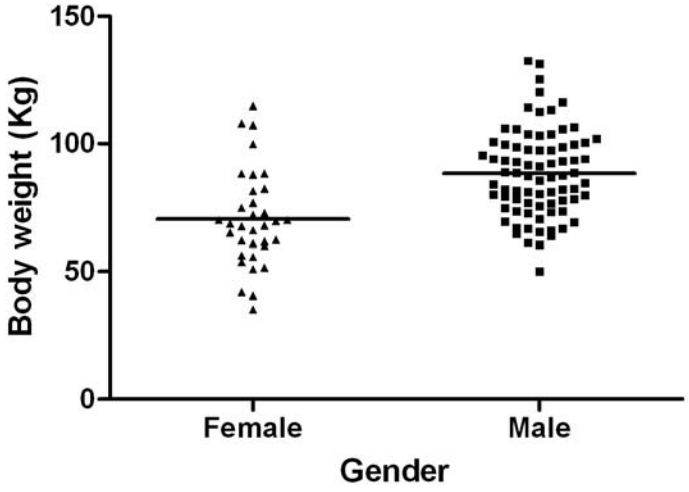

Fig 4-8 Comparison of body weight (continuous variable) between genders (nominal variable)

4-5.2.3 Covariate Screening

4-5.2.3.1 Characterization of extreme values for AUC_{0-12}/D and C_{max}/D

A Caucasian man of age 57 years with prostate cancer had the lowest values of AUC_{0-12}/D and C_{max}/D. His weight and BSA were 101 kg and 2.2 m^2, which were in the upper quartile of their respective distributions as shown in **Table 4-8 (b)**. Except serum albumin, which was marginally low, his liver and renal function markers were within the normal limits. He carried wild-type genotype for CYP3A4*1B, UGT1A9*3, UGT1A9*5 and VEGFR2 H472Q; heterozygous genotype for VEGFR2 V297I and variant genotype for CYP3A5*3C.

A 72 year old Caucasian woman with non-small cell lung cancer had the highest values of AUC_{0-12}/D and C_{max}/D. Her body weight and BSA were in the lower quartile of their respective distributions (**Table 4-8 (b)**), with values of 55.8 kg and 1.56 m^2, respectively. Her liver function markers were within the normal limits, but renal function markers, SCr and CL_{Cr}, were marginally lower than normal, 0.75 g/dL and 59.3 mL/min respectively. Her genetic makeup for metabolic enzymes was similar to the Caucasian man with lowest values of AUC_{0-12}/D and C_{max}/D, as discussed in previous paragraph.

Overall, comparison of these extreme values suggests an inverse relation between body weight or BSA and AUC_{0-12}/D and C_{max}/D, which is mechanistically plausible. Liver and kidney function markers and genetic polymorphisms in studied metabolic enzymes did not appear to be important for variability in AUC_{0-12} or C_{max}.

4-5.2.3.2 Covariate screening for ln (C_{max}/D) using linear regression or ANOVA

Results of covariate screening for ln (C_{max}/D) are summarized in **Table 4-10**. Gender, weight, BSA, CL_{Cr}, albumin, ALT, and VEGFR2 H472Q had a significant univariate effect on ln (C_{max}/D), but none of them had met the r^2>0.1 criterion. No other covariates met either of the pre-specified criteria, i.e., r^2>0.1 or p-value<0.05.

Gender, weight, BSA and CL_{Cr} accounted for 7.4%, 6.6%, 5.6% and 5.3% of the variation in ln (C_{max}/D). Among these, associations of ln (C_{max}/D) with gender, BSA and CL_{Cr} were confounded by weight, as described earlier and shown in **Table 4-9, Fig 4-8 and section 4-5.2.2**.

The C_{max}/D decreased by 10% per 10 kg increase in body weight, which is mechanistically understandable. An increase in body weight would increase the distribution volume, leading to a reduction in C_{max}.

The C_{max}/D increased with an increase in albumin from low to normal by 17.4%, which may have been reflective of a decrease in volume of distribution. Mechanistically, this may be the case for drugs with large distribution to peripheral tissues, where higher plasma protein binding may restrict the amount of drug distributing into tissues, as seem to be the case for sorafenib.

The decrease in C_{max}/D by 1.2% with each unit increase in ALT was statistically significant, but appeared to be inconsistent with our mechanistic expectations. Increased

ALT levels suggest liver dysfunction; mechanistically this would suggest a reduction in hepatic first-pass and systemic metabolism, which should increase C_{max} of sorafenib. However, this inverse trend was driven by ALT values from only 5-6 patients; exclusion of them would have made this relationship non-significant, suggesting that this observation may be artifactual.

The VEFR2 H472Q was also a significant covariate for ln (C_{max}/D), but the effect size of this relation was very small as shown in the JMP-generated factor profiler in **Fig 4-9**.

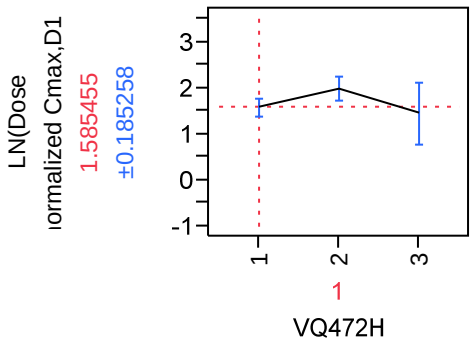

Fig 4-9 JMP predicted effect of VEGFR2 H472Q polymorphism on ln (C_{max}/D). 1=wild type (N=66), 2=heterozygous (N=32), 3=variant genotype (N=5). Least squares mean ± SE for 1 = 1.59 ± 0.09, 2 = 1.98 ± 0.13, and 3 = 1.45 ± 0.34.

Ln (C_{max}/D) was marginally higher for heterozygotes compared to wt or homozygous variant genotypes. Tukey's HSD test revealed that the mean ln (Cmax/D) for only heterozygotes was marginally different from wt carriers (p=0.048), and the difference between heterozygous and variant genotype was not significant. The small sample size and imbalances in number of subjects across genotype subgroups might have influenced this apparent association, which requires further evaluation with a larger sample size.

Table 4-10 Covariate screening for ln (C_{max}/D)

Candidate covariate	r^2	intercept	slope	Ref group	p-value	†slope*100
Dose	0.016	1.76	0.1166	200	0.1913	11.66
Trial	0.048	1.74			0.1637	
Gender	0.074	1.78	0.225	F	**0.0049**	22.5
Ethnicity	0.01	1.84			0.9019	
Age [years]	0.002	1.91	-0.0034		0.6059	-0.34
Weight [kg]	0.066	2.54	-0.01		**0.0078**	-1
Height [cm]	0.0177	3.42	-0.01		0.1733	-1
BSA [m2]	5.60E-02	2.93	-0.64		**0.0149**	-64
SCr [g/dL]	9.50E-04	1.6	0.099		0.7532	9.9
SCr [N/L]	0.053	1.99			0.0613	
CL_{Cr}^{CG} [mL/min]	0.053	2.26	-0.00613		**0.0174**	-0.613
CL_{Cr}^{CG} [H/N/L]	0.053	1.92			0.0601	
Albumin [g/dL]	0.023	0.69	0.2812		0.1196	28.12
Albumin [H/N/L]	0.052	1.7	-0.174	L	**0.0184**	-17.4
Protein, Total [g/dL]	0.0056	1.05	0.098		0.4437	9.8
Protein, Total [H/N/L]	0.0063	1.68			0.7211	
ALT [U/L]	0.037	1.98	-0.012		**0.047**	-1.2
ALT [H/N/L]	0.042	1.44	-0.29	H	**0.0342**	-29
AST [U/L]	0.0058	1.84	-0.005		0.4364	-0.5
AST [H/N/L]	7.40E-03	1.65	-7.70E-02	H	0.3795	-7.700
AP [U/L]	1.10E-03	1.74	-4.50E-04		0.7273	-0.045
AP [H/N/L]	0.012	1.56			0.5361	
Bilirubin, Total [mg/dL]	0.003	1.58	0.17		0.5763	17
Bilirubin, Total [H/N/L]	0.0001	1.71	0.019	H	0.8901	1.9
CYP3A4*1B	0.011	1.6			0.5613	
CYP3A5*3C	0.007	1.68			0.7003	
UGT1A9*3	0.036	2.2			0.1541	
VEGFR2 H472Q	0.059	1.7			**0.0471**	
VEGFR2 V297I	0.005	1.77			0.775	

Please check the footnotes on next page.

†Slopes are multiplied with 100 in order to interpret the ln-transformed data on normal scale.

p-value cut-off was <0.05 and r^2 cut-off was >0.1.

Ref: reference

4-5.2.3.3 Covariate screening for ln (AUC_{0-12}/D) using linear regression or ANOVA

The results of covariate analysis for ln (AUC_{0-12}/D) are summarized in **Table 4-11**. Gender, weight, BSA, SCr [L/N], albumin and VEGFR2 H472Q had significant univariate effects on ln (AUC_{0-12}/D) at $p<0.05$ level; but accounted for only 5.6%, 5.3%, 5.1%, 6.3%, 4.3%, 6.7% and 0.37% variability in ln (AUC_{0-12}/D), respectively. The r^2 values for none of these covariates met the pre-specified criteria of ≥ 0.1. No other covariate met either of the pre-specified criteria of r^2 values ≥ 0.1 or p-values of <0.05; hence, were not considered further.

As mentioned in **section 4-5.2.2**, the effects of gender and BSA were confounded by body weight. The effect of SCr [L/N] on ln (AUC_{0-12}/D) appeared to be artifactual, since the relationship between (AUD_{0-12}/D) and SCr was not in the expected rank order. The (AUC_{0-12}/D) increased in the order of $AUC_{\mathbf{SCr[H]}}$>$AUC_{\mathbf{SCr[L]}}$>$AUC_{\mathbf{SCr[N]}}$ for SCr groups. Mechanisticaly, we did not expect any association between sorafenib exposures and SCr, because the renal excretion of parent drug was negligible (33).

The effect of weight on ln (AUC_{0-12}/D) was mechanistically plausible, with a 9.4% decrease in AUC_{0-12}/D for each 10 kg increase in weight. Both volume of distribution and systemic clearance (metabolic activity) may increase with increase in weight, which could lead to decrease in sorafenib exposures.

Another mechanistically plausible relation was increase in ln (AUC_{0-12}/D) with increase in albumin. Sorafenib binds to human serum albumin, α-, β-globulin and the low density lipoproteins (LDL) with the fraction unbound in plasma ranging from 1.02 to 3.55 % (33). With elevated albumin levels, the concentration of sorafenib not bound to plasma proteins (f_u) will decrease, resulting in reduced distribution of free drug to peripheral organs including liver. Reduced distribution to liver may reduce the amount of drug undergoing metabolism (i.e., reduction in f_u*CL_{int}). For drugs with low hepatic extraction ratio, such as is likely the case for sorafenib, *f*u*CL_{int} is the main determinant of hepatic clearance (CL_{hep}) based on the Wilkinson-Shand well-stirred model:

$$CL_{hep} = Q.ER_{hep} = Q * \frac{f_u * CL_{int}}{Q + f_u * CL_{int}}$$

where Q is the hepatic blood flow and CL_{int} is the intrinsic rate at which liver clears the drug from blood in absence of any flow restrictions

AUC_{0-12}/D increased by approximately 4% per 0.1 g/dL increase in serum albumin, and the average (AUC_{0-12}/D) for patients with normal albumin levels was 20.4% higher than patients with low serum albumin levels.

The VEGFR2 H472Q was a significant covariate for ln (AUC_{0-12}/D), but similar to its effect on ln (C_{max}/D), effect size was small, and sample sizes in genotype subgroups were imbalanced. The factor profiler generated by JMP (**Fig 4-10**) shows that patients with heterozygous genotype had significantly higher ln (AUC_{0-12}/D) compared to wt carriers (p=0.0043); however, the variant genotype was not different from either of the remaining

genotypes. These results might have been influenced by imbalances in sample size across genotype groups and need to be further evaluated with larger sample size.

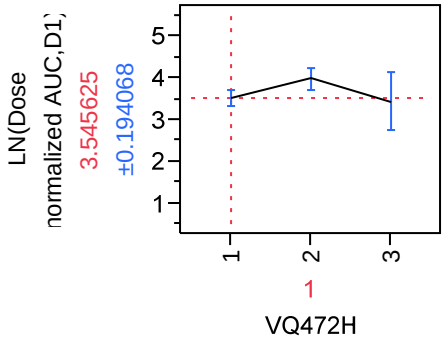

Fig 4-10 JMP predicted effect of VEGFR2 H472Q polymorphism on ln ($AUC_{0\text{-}12}$/D). 1=wild type (N=66), 2=heterozygous (N=32), 3=variant genotype (N=5). Least squares mean ± SE for 1 = 3.54 ± 0.10, 2 = 3.99 ± 0.14, and 3 = 3.44 ± 0.35.

Table 4-11 Covariate screening for ln (AUC_{0-12}/D).

Candidate covariate	r^2	intercept	slope	Ref group	p-value	†slope*100
Dose	0.008	3.71	0.086	200	0.3609	8.6
Trial	0.032				0.3524	
Gender	0.056	3.75	0.204	F	**0.0153**	20.4
Ethnicity	0.025				0.6357	
Age [years]	0.004	3.94	-0.004		0.5318	-0.4
Weight [kg]	0.053	4.45	-0.00900		**0.0191**	-0.9
Height [cm]	0.0169	5.44	-0.01		0.1876	-1
BSA [m2]	0.051	4.89	-0.63		**0.0215**	-63
SCr [g/dL]	6.11E-05	3.65	0.026		0.9372	2.6
SCr [L/N/H]	6.30E-02				**0.0372**	
CL_{Cr}^{CG} [mL/min]	0.034	4.14	-0.005		0.0614	-0.5
CL_{Cr}^{CG}	0.039				0.1356	
Albumin [g/dL]	0.043	2.26	0.395		**0.0342**	39.5
Albumin [L/N]	0.067	3.68	-0.204	L	**0.008**	-20.4
Protein, Total [g/dL]	0.012	2.73	0.145		0.2786	14.5
Protein, Total [H/N/L]	0.013	3.62			0.5084	
ALT [U/L]	0.019	3.89	-0.009		0.1162	-0.9
ALT [L/N]	0.016	3.49	-0.198	H	0.2018	-19.8
AST [U/L]	0.002	3.76	-0.003		0.6511	-0.3
AST [L/N]	0.012	3.62	-0.1033	H	0.2653	-10.33
AP [U/L]	1.55E-07	3.67	5.49E-06		0.9968	0.001
AP [L/N/H]	5.00E-03				0.7711	
Bilirubin Total [mg/dL]	0.001	3.59	0.121		0.7042	12.1
Bilirubin Total [N/H]	0.001	3.72	0.055	H	0.7087	5.5
CYP3A4*1B	0.0099	3.6			0.6082	
CYP3A5*3C	0.011	3.66			0.5606	
UGT1A9*3	0.034	4.01			0.1797	
VEGFR2 H472Q	0.069	3.65			**0.0298**	
VEGFR2 V297I	0.0037	3.63			0.8353	

Please check the footnotes on next page.

†Slopes are multiplied with 100 in order to interpret the ln-transformed data on normal scale

p-value cut-off was <0.05 and r^2 cut-off was >0.1.

Ref: reference

Table 4-12 Final model for ln (C_{max}/D)

Final Model	**SSQ_{tot}**	**r^2**	**p-value**
	37.8	0.2518	**<0.0001**

Final Covariate	**SSQ**	**intercept**	**Slope**	**p-value**	**†Slope*100**
BSA [m^2]	2.9	2.09	-0.6461	**0.0111**	-64.61
Albumin [g/dL]	2.9		0.6043	**0.0025**	60.43
AP [U/L]	1.5		0.0017	0.1781	0.17
ALT [U/L]	3.5		-0.0169	**0.0072**	-1.69
UGT1A9*3 (wt & het) vs. var	3.1		-1.0293	**0.0076**	-102.9
VEGFR2 H472Q (wt & het) vs. var	2.0		-0.1623	**0.0328**	-16.23

†Slopes are multiplied with 100 in order to interpret the ln-transformed data on normal scale

Table 4-13 Final model for ln (AUC_{0-12}/D)

Final Model	**SSQ_{tot}**	**r^2**	**p-value**
	39.1	0.2662	**<0.0001**

Final Covariate	**SSQ**	**intercept**	**Slope**	**p-value**	**†Slope*100**
BSA [m^2]	3.1	3.6	-0.6841	**0.009**	-68.41
Albumin [g/dL]	4.4		0.7429	**0.0003**	74.29
AP [U/L]	2.0		0.0021	0.1131	0.21
ALT [U/L]	3.1		-0.0171	**0.0134**	-1.71
UGT1A9*3 (wt & het) vs. var	3.1		-1.0488	**0.008**	-104.8
VEGFR2 H472Q (wt & het) vs. var	2.6		-0.1888	**0.0165**	-18.88

†Slopes are multiplied with 100 in order to interpret the ln-transformed data on normal scale

4-5.2.3.4 Final covariate model for ln C_{max}/D and ln (AUC_{0-12}/D)

Parameters from final covariate models for ln (C_{max}/D) and ln (AUC_{0-12}/D) are shown in **Tables 4-12 and 4-13.** Both models included BSA, albumin, alkaline phosphatase, ALT, UGT1A9*3 and VEGFR2 H472Q as covariates. Overall, these covariates together accounted for only 25% and 27% variability of the observed total variability in ln (C_{max}/D) [%CV, 45%] and ln (AUC_{0-12}/D) [%CV, 22%]. Except alkaline phosphatase, all other covariates were statistically significant at the $p<0.05$ level. BSA, albumin, ALT, UGT1A9*3 and VEGFR2 H472Q accounted for 18%, 18%, 22%, 19% and 13% of model SSQ for ln (C_{max}/D) and 17%, 24%, 17%, 17% and 14% of model SSQ for ln (AUC_{0-12}/D). All of these were very similar and minor effects.

An 0.1 m^2 increase in BSA resulted in a 6.5% decrease in C_{max}/D and 6.8% decrease in AUC_{0-12}/D, after correction for other covariates. The slopes and (inverse) directions of these relations were similar to the results of univariate covariate screening. BSA is a composite matrix of body weight and height, and increase in BSA would indicate increase in volume of distribution and/or metabolic rate. Sorafenib is primarily eliminated by hepatic metabolism and heptobiliary excretion, and has large apparent volume of distribution. An increase in volume of distribution would reduce the C_{max}, and increased metabolism may reduce the total drug exposure over time, i.e., AUC. Regardless of the underlying mechanism, the effect of BSA on C_{max} and AUC was likely to be of limited clinical relevance because of their minor contribution to overall variability in C_{max} and AUC – within the range of BSA included in this analysis, i.e., 1.2 to 2.5 m^2. Contribution of BSA in the overall variability explained by the model for ln (C_{max}/D) or ln (AUC_{0-12}/D)

was only 4.5% (i.e., 18% of 0.2518 for ln (C_{max}/D) and 18% of 0.2662 for ln (AUC_{0-12}/D)).

The effects of albumin levels on C_{max}/D and AUC_{0-12}/D were also previously detected during univariate covariate screening; however, after correction for other covariates, their sensitivity (effect size) was enhanced. The 0.1 g/dL increase in albumin resulted in 6% and 7% increase in C_{max}/D and AUC_{0-12}/D, respectively. This was likely an outcome of identification of alkaline phosphatase as separate covariate, which had weak inverse correlation (r=-0.32) with albumin (**Table 4-9**). Separation of effects for alkaline phosphatase and albumin in full model eliminated the confounding effects. As described earlier in **sections 4-5.2.3.2 and 4-5.2.3.3**, the increase in albumin may restrict the concentrations of sorafenib undergoing metabolism or distributing into tissues, which may result in decreased CL/F and/or V/F leading to increase in AUC and C_{max}. These effects are also not clinically relevant, considering their small contribution to overall variability in ln (C_{max}/D) (i.e., 4.5%) and ln (AUC_{0-12}/D) (i.e., 6.4%).

Although, the effects of alkaline phosphatase on C_{max}/D and AUC_{0-12}/D were statistically insignificant, they were mechanistically plausible. Each unit (1 U/L) increase in alkaline phosphatase resulted in 0.1% and 0.2% increase in ln (C_{max}/D) and ln (AUC_{0-12}/D). Increased alkaline phosphatase levels might indicate obstruction in bile duct, which would impede the biliary elimination of sorafenib. However, another more likely reason for the increase in alkaline phosphatase levels is bone metastases, and most of the patients on these trials had advanced metastatic disease. Regardless of the cause, clinical

relevance of this effect is negligible because of negligible effect size and negligible contribution to variation in ln (C_{max}/D) and ln (AUC_{0-12}/D).

The effects of ALT on both ln (C_{max}/D) and ln (AUC_{0-12}/D) were statistically significant, but it was unexpected for AUC_{0-12}/D because similar effect was not detected during univariate covariate screening. Both C_{max}/D and AUC_{0-12}/D decreased by 1.7% for per unit (1 U/L) change in ALT. Elevated ALT levels often suggest liver damage (e.g., cirrhosis) or bile duct obstruction, which would mechanistically indicate a reduction in hepatic metabolism/excretion of sorafenib. However, the findings in current analysis were not in agreement with this plausible mechanism. Some co-administered drugs such as statins, antibiotics, chemotherapy, aspirin and narcotics may also increase ALT with simultaneous displacement of sorafenib from plasma proteins, causing increase in its metabolism. In that case relationship between ALT and sorafenib exposures might be artifactual. Nevertheless, because of small effect size and small contribution to variability in C_{max}/D and AUC_{0-12}/D, effect of ALT on exposure metrics for sorafenib would not be clinically relevant. The distribution of ALT was skewed to the right; the number of patients with above normal values was higher than that of lower ALT levels. The effects of chronic liver dysfunction on sorafenib exposures was earlier studied in a prospective clinical trial. Patients with various degree of liver dysfunction, as determined by albumin, AST and bilirubin levels, were treated with sorafenib, and sorafenib pharmacokinetics was analyzed for patients. The AUC_{0-12} did not appear to be associated with liver dysfunction; however, based on long-term follow-up for safe dose, the tolerable dose for patients with moderate to severe liver damage was apparently lower than clinically

approved dose (i.e., 200 mg QD/BID compared to 400 mg BID) (94). Further studies with long-term exposure metrics might be needed to confirm the effects of liver damage on sorafenib disposition.

The effects of UGT1A9*3 polymorphism on both ln (C_{max}/D) and ln (AUC_{0-12}/D) were statistically significant, but were not detected during univariate covariate screening. Only 1 of 106 patients carried UGT1A9*3*3 variant genotype and 3 patients carried heterozygous UGT1A9*1*3 genotype; hence the estimated effects were likely biased towards UGT1A9*1*1 wild-type genotype. The C_{max}/D and AUC_{0-12}/D appeared to be 103% and 105% higher for carriers of UGT1A9*3*3 compared to UGT1A9*1*1 or UGT1A9*1*3 carriers. The UGT1A9*3*3 polymorphism has been shown to reduce the UGT1A9 glucuronidation activity (75)(see section **1-4.1.2**), which could mechanistically explain the current findings. However, these results should be interpreted with caution because of limited sample size (only 1 of 106 patients carried the UGT1A9*3*3 genotype) and requires further confirmation in a larger cohort.

Finally, VEGFR2 H472Q was statistically significant for both C_{max}/D and AUC/D, which was also identified during univariate covariate screening; however, these effects were mechanistically implausible. Based on the results, patients with variant genotype had 16.2 % lower C_{max}/D and 18.8% lower AUC_{0-12}/D compared to patients with wild type or heterozygous genotype. Imbalances in subgroup sizes based on genotype might also have biased these relationships.

4-5.3 Conclusions for non-compartmental pharmacokinetic analysis and covariate search by general linear modeling

1. As expected, sorafenib pharmacokinetics was highly variable among patients with various solid tumors. Inter-patient variability in C_{max} and AUC_{0-12} were respectively 46-87% and 45-79% for the 200/400 mg BID dose administered in patients with mCRPC, NSCLC, CRC and ST.
2. Co-administration of bevacizumab and ritonavir did not appear to have any significant effects on exposures of sorafenib.
3. Exposure metrics were normalized with the amount of administered drug (D) in order to account for the differences in dose levels. Dose-normalized pharmacokinetic metrics, C_{max}/D and AUD_{0-12}/D, were not statistically different between trials or two dose levels, which was consistent with linear pharmacokinetics. This justified pooling of data across trials, irrespective of administered dose.
4. Inter-patient variability in pooled exposure metrics C_{max}/D and AUD_{0-12}/D were 73% and 77%. Distributions for these metrics were skewed; hence, ln-transformation was performed prior to covariate analysis. The inter-patient variability for ln-transformed values was modest: 46% for ln (C_{max}/D) and 22% for ln (AUC/D).
5. Body size metrics, namely body weight and BSA, were statistically significant covariates for both exposure metrics, where ln (C_{max}) and ln (AUC_{0-12}) were inversely related with these covariates. The directions of these relations were mechanistically plausible, likely reflecting the impact of an increase in body size

on sorafenib's metabolic clearance and/or volume of distribution. However, these covariates accounted for only less than 7% of variability in exposure metrics and the effect sizes were also relatively small [~1% and ~6.5% decrease in pharmacokinetic metrics for each kg increase in weight and 0.1 m^2 increase in BSA]. These findings are of little clinical relevance and do not justify any dose adjustments. Minor effects of gender on ln (C_{max}/D) and ln (AUC_{0-12}/D), and effects of CL_{Cr} on ln (C_{max}/D) were statistically significant, but were confounded by weight.

6. Baseline serum albumin levels had a small univariate effect (<4%) on both the C_{max}/D and AUC_{0-12}/D; which increased to 6.5% after correcting for effect of other covariates. Although these effects can be explained mechanistically by increased distribution/clearance at low albumin levels due to increase in unbound fractions (*f*u), their small contribution to overall variability makes the effect clinically irrelevant.
7. Baseline serum levels of ALT and VEGFR2 H472Q genotype were statistically significant covariates for ln (C_{max}/D) and ln (AUC_{0-12}/D). However, the ALT distribution was imbalanced (slightly skewed to right) and the direction of its relation with exposure metrics (1.7% decrease in C_{max}/D and AUC_{0-12}/D per unit increase in ALT) were mechanistically implausible. The small effect size and mechanistic implausibility for relationship with target receptor (i.e., VEGFR2) polymorphism suggested that it was clinically irrelevant.
8. In the final model, UGT1A9*3 genotype was a significant covariate for both Cmax and AUC. The effect size was large; Cmax or AUC for homozygous

variant genotype (UGT1A9*3*3) increased by >100% compared to wild-type or heterozygous genotypes. However, these observations were strictly limited by small sample size (only 1 of 106 patients carried variant genotype), and needs further evaluation.

4-6 Population pharmacokinetic model building – non-linear mixed effect modeling approach

4-6.1 Introduction

The non-linear mixed effect modeling (NONMEM) is a one-stage (i.e., pooled analysis) approach, which considers the complete population study sample, rather than individuals, as a unit of analysis for estimation of pharmacokinetic parameters, their distribution and their relationship with covariates within the population. NONMEM methods estimate the pharmacokinetic model parameters (both structural and statistical) using the maximum likelihood approach. The probability of observed individual plasma concentration-time profiles conditioned to the model is written as a function of model parameters (i.e. log-likelihood function), also referred as objective function value, and estimates for parameters are chosen to maximize this probability (95). The best parameter estimates are those which makes the observed data most probable than under any other set of parameters (95).

The minimization of objective function requires various degrees of approximations (or generalizations), depending on the estimation method used in the analysis, each of which also determine accuracy and precision of estimated parameters and computational time.

The common parameter estimation methods are Laplacian, first-order conditional method (FOCE) with or without interaction (i.e., INTER), and the first-order (FO) method. The Laplacian method makes least approximations, whereas FO method is based on several assumptions, which significantly reduces the computational time. The FOCE with INTER is the most commonly used method, estimates of which are acceptably close to the true underlying values.

In order to find the best set of parameters, the selection of various values for vector of model parameters is guided by gradient minimization approaches such as simplex or steepest-descent algorithm and Gauss-Newton algorithm. Some times these algorithms converge into local maxima rather than global maxima, which would falsely indicate that likelihood function has been maximized. To avoid such possibilities, final models are always re-run after perturbing the initial estimates of model parameters, until stable parameter values are obtained. This ensures that estimated model-parameters are likely to represent the global maxima (or maximum possible likelihood function value) and not the local maxima.

Population pharmacokinetic analysis involves at least two hierarchical models. In the first stage, the observed plasma concentration-time profile data for a particular individual is modeled, conditioned to the individual specific parameters; and in the second stage the individual parameters are modeled as a function of individual-specific covariates to obtain the typical (population average) pharmacokinetic values (96).

1st hierarchy

For each subject, the observed plasma drug concentrations are modeled as below (97):

$$y_{ij} = f(x_{ij}, \phi_i) + \varepsilon_{ij}$$

where, i = 1, 2, 3, ….N individuals, from whom data are collected for population pharmacokinetic analysis.

y_{ij} is the observed concentration for i^{th} individual at j^{th} time point

$f(x_{ij}, \phi_i)$ is the model predicted concentration for i^{th} individual at j^{th} time point, where f stands for some pre-specified form of model such as monoexponential, biexponential etc.

x_{ij} indicates the known quantities for j^{th} time point for i^{th} individual such as time (t_{ij}) and dosing (d_i) information.

ϕ_i represents the individual (i) specific model parameters (individual's fixed effect parameters)

ε_{ij} denotes the random difference between observed (y_{ij}) and model predicted ($f(x_{ij}, \phi_i)$) concentrations, also known as residual error. It follows normal distribution with mean of 0 and variance of σ^2, i.e., $\varepsilon \sim N(0, \sigma^2)$.

2nd hierarchy

Individual pharmacokinetic model parameters, e.g., rate constants, V_d, CL_{total}, are modeled as a function of individual-specific covariates, as below (97):

$\phi_i = g(z_i, \theta) + \eta_i$

where, ϕ_i denotes the model parameters for individual i

z_i represents the fixed covariate effect for individual i, such as individuals weight and BSA

θ, represents the vector of population parameters

g (z_i, θ), is a function of fixed covariate effects, z_i , and fixed effects parameters, θ. It represents the typical population (mean) values of model parameters for an individual with z_i fixed effects (e.g., population CL for typical 70 kg weight male).

η_i denotes the random difference between typical population mean values of model parameters (g (z_i, θ)) and individual-specific model parameters. The η values are assumed to follow normal distribution with mean of 0 and variance of ω^2, i.e. $\eta \sim N(0, \omega^2)$. The ω represents the inter-individual or between subject variability in model-predicted parameters.

These two hierarchical models explicitly partition the variability between model-predicted and observed plasma concentration – time profiles into two components, namely inter-individual variability (ω) and within-subject or intra-individual variability (σ). The objectives of population pharmacokinetic modeling are (i) to identify the covariates which can explain these inter-individual variabilities, and (ii) to quantify and minimize the residual variability.

The population pharmacokinetic modeling approach consists of three basic components: (i) structural pharmacokinetic model, which describes the (compartmental) structure of pharmacokinetic model underlying the observed plasma concentration – time profiles, (ii) statistical error models or random effect models, which comprise the error models for inter- and intra individual and inter-occasion variability, and describe the random differences between observations and structural model predictions., and (iii) covariate

model, which describes the relationship between covariates (demographic, pathophysiological etc.) and pharmacokinetic parameters.

4-6.2 Structural models

Structural models are usually the pharmacokinetic models (e.g., one-compartmental, two-compartmental model) which describe the plasma concentrations across observation time-points. These models generate predictions of concentrations at appropriate time points as a function of model parameters (pharmacokinetic and non- pharmacokinetic), doses and observation time points (98). The structural model, if possible, should be selected based on *a-priori* available information about the drug; a less complex, but statistically significant model should be preferred over complex models. For example, if a drug follows entero-hepatic recycling, models with entero-hepatic recycling components should also be tested along with other simplified models. Structural models are usually expressed using primary pharmacokinetic parameters such as clearance (CL) and volume of distribution (V) rather than rate constants, which allow the direct assessment of impact of covariates on these parameters.

4-6.3 Statistical error models

4-6.3.1 Residual error model

This statistical model describes the distribution of random residual errors. Residual error is the difference between 'model predicted true subject concentrations' and 'observed concentrations'. It includes, but is not limited to, intra-individual variability, model

misspecifications, errors in assay method, dosing errors and errors in recording of dosing times. The three most common error structures are:

a. Additive error model: $Y = TY + \varepsilon 1$

b. Constant coefficient of variation or proportional error model:

$$Y = TY * (1 + \varepsilon 1)$$

c. Mixed additive + constant CV model:

$$Y = TY * (1 + \varepsilon 1) + \varepsilon 2$$

Where, Y represents the actual observation, TY is the 'model predicted true value' of the observation and $\varepsilon 1$ and $\varepsilon 2$ are the residual error terms used to describe the difference between Y and TY.

4-6.3.2 Inter-individual variability model

This is another type of statistical model, which describes the inter-individual variation in pharmacokinetic parameters after adjusting for fixed effects. Inter-individual variations are random differences between typical population mean values and true individual values, i.e. η. Commonly, the exponential or log-normal model is used to define this variability, such as:

$$CL = TVCL * \exp(\eta_{CL})$$

The other two less commonly used structures are:

Additive error model: $CL = TVCL + \eta_{CL}$

Proportional or constant coefficient of variation model:

$$CL = TVCL * (1 + \eta_{CL})$$

Where, TVCL is the typical value of clearance (CL) and η_{CL} is the difference of the patient-specific value from the typical (population mean) value.

4-6.3.3 Inter-occasion variability model

For data which are collected on multiple occasions for the same individual, such as plasma concentration – time profiles collected after single dose and at steady-state, an additional variability parameter, the inter-occasion variability, is sometimes used to describe the random variability in individual pharmacokinetic parameters across occasions. It is modeled as:

$$CL = TVCL * \exp(\eta_{CL} + BOV_1)$$

Where, $BOV_1 = \eta_k$ (k=number of occasions=1, 2,..N). η_k is a normally distributed random variable with mean of zero and variance π_k^2, i.e. η_k~N (0, π_k^2).

4-6.4 Covariate model

Covariate model building involves the quantitative assessment of relationship between covariates and structural pharmacokinetic model parameters, in order to evaluate the need for special dose adjustments in a subgroup of patients. The process for identification of covariates and steps used for their inclusion in the final model are summarized below:

4-6.4.1 Identification of covariates and inclusion in the model

Candidate covariates are selected based on graphical and statistical assessment of their relationship between covariates and post-hoc Bayesian estimates of individual random effects (η_i values). Statistical correlations are assessed by regression analysis or one-way

ANOVA, using statistical software such as JMP and S-plus. The covariates which are significant at a pre-specified significance level of $p<0.05$, and for which we have suitable mechanistic explanation, are included in the model using stepwise forward regression method. The hierarchical models (with and without covariates) are then compared using likelihood ratio test. Covariates, inclusion of which results in decrease in objective function value (OFV) by 3.84 (Chi-square statistics at p=0.05 and df=1), are retained in the model. The covariate search process is repeated until all significant covariates (at p=0.05 level), are included in the model, after which stepwise backward elimination is performed. A significance level of 0.01 is used for backward analysis, where covariates, elimination of which increases the OFV by 10.83 (Chi-square statistics at p=0.01 and df =1), are retained in the model. The backward elimination process is repeated until all the remaining covariates are significant at p=0.01 level. This approach is referred as a stepwise forward inclusion and backward elimination method. Alternatively, only stepwise forward inclusion or stepwise backward elimination approaches are used.

4-6.4.2 Covariate model structures

Several different structures can be used to enter the covariates into the model, depending on the form of relation between covariate and η_i values. Some examples of covariate model structures for continuous and categorical covariates are shown below:

Linear structure

Continuous covariate: $TVCL_i = \theta_{CL} + \theta_{Wt} * (Wt_i - Wt_{median})$

Categorical (binary) covariate: $TVCL_i = \theta_{CL,female} + \theta_{male} * Gender_i$

Power structure

Continuous covariate: $TVCL_i = \theta_{CL} * (Wt_i / Wt_{median})^{\theta_{Wt}}$

Categorical (binary) covariate: $TVCL_i = \theta_{CL,female} * (\theta_{male})^{Gender_i}$

Exponential structure

Continuous covariate: $TVCL_i = \theta_{CL} * \exp(\theta_{Wt} * Wt_i)$

Categorical (binary) covariate: $TVCL_i = \theta_{CL,female} * \exp(\theta_{male} * Gender_i)$

Where, θ_{CL} is the population mean for CL, θ_{Wt} is the effect size for weight's relation with CL, Wt_i is the individual weight and Wt_{median} is the median weight for study population. Similarly, $\theta_{CL,female}$ is the population (mean) CL for females and θ_{male} is the effect size for impact of (male) gender on CL. The gender variable was 1 for males and 0 for females.

4-7 Characterization of pharmacokinetics by population- pharmacokinetics analysis

4-7.1 Methods

4-7.1.1 Patients and data collection

Full plasma concentration-time profiles after initial-doses and at steady-state as well as sparse samples from 112 patients were used for population pharmacokinetic analysis, which included the 106 patients used for non-compartmental analysis, 2 patients with KS for which only day 7 pharmacokinetics was drawn and 4 additional solid tumor patients on sorafenib and bevacizumab combination trial for which non-compartmental analysis was not performed due to limited sampling (**Table 4-14**). Data from 6 patients with KS who received sorafenib in combination with ritonavir were not included in the analysis, because of the potential for drug interaction. Study design and dosing regimen for these

trials are described under non-compartmental analysis in **section 4-4.1.1**. Apart from samples for pharmacokinetics and pharmacogenetic analysis; demographic, liver and kidney function markers were collected at baseline. Data from both the dose levels, and from day 1 as well as steady-state were used together to perform this analysis.

4-7.1.2 Pharmacokinetic sampling and sample analysis

Sampling schedules for patients enrolled in sorafenib trials are summarized in **Table 4-2**. All the samples were analyzed by using the validated liquid chromatographic method with mass spectrometric detection described in chapter 3.

4-7.1.3 Genotyping analysis

As described in **section 4-4.1.3**, genotyping was performed for CYP3A4*1B, CYP3A5*3, UGT1A9*3, UGT1A9*5, VEFR2 H472Q and VEGFR2 V297I SNPs using PCR sequencing reaction. Details of these procedures are described in chapter 7.

Table 4-14 Details of sorafenib trials.

Therapy	Sorafenib dose	Cancer type	No. of patients with sampling after		Ethnicity		
			Initial doses	Steady-state	Cauc	AA	Others
Monotherapy	400 mg BID	mCRPC	46	NA	38	5	3
Monotherapy	400 mg BID	NSCLC	18	17	12	2	4
Combination	200 mg BID	ST	28	12	27	0	1
Combination	400 mg BID	CRC	18	NA	13	3	2
Monotherapy / Combination	200 mg QD/BID	KS	NA	2	2	0	0
Total			110	31	92	10	10

Cauc: Caucasian, AA: African-American, Others: Asians and Hispanics

mCRPC: metastatic castrate resistant prostate cancer, NSCLC: non-small cell lung cancer, ST: solid-tumor, CRC: colorectal cancer, KS: Kaposi's sarcoma

4-7.1.4 Software

Population pharmacokinetic model development and simulations were performed by non-linear mixed effect modeling approach. The software package used was NONMEM version VI level 2.0 (ICON Development Solutions, North Wales, PA). NONMEM was compiled by Intel Visual Fortran compiler version 10 (Intel Corporation, Santa Clara, CA) on Windows XP operating system. Data processing and statistical analyses were performed using JMP statistical software version 8.0 (SAS Institute, S Cary, NC). The appropriateness of models was assessed by graphical diagnostics, using Xpose version 4, an R-based model building software.

4-7.1.5 Estimation method

For initial models the FO POSTHOC estimation method was used, with the intent to identify the suitable initial estimates for vector of model parameters. After finding initial estimates, all NONMEM analyses were performed using the FOCEI. Estimates from FOCEI method were found to be close to the real values compared to FO method (99).

4-7.1.6 Selection of structural model

Previously, a two-compartmental model with first-order absorption, first-order elimination and absorption lag time has been shown to describe the sorafenib pharmacokinetics, using a much larger data set than used in current analysis (51).

However, in our NCI trials, insufficient samples were drawn during the drug distribution phase, resulting in unstable estimates for distribution phase parameters during testing of two-compartment models. To account for entero-hepatic recycling and GI solubility limited absorption, entero-hepatic recycling, mixed zero- and first-order absorption, and GI absorption transit compartments were evaluated with one- or two-compartment models. A log-transformation of both side (LTBS) approach was used, where logarithm of observed concentrations were fitted to the model to predict the log-transformed concentrations.

4-7.1.7 Statistical models

The difference between model-predicted individual concentrations, $\hat{C}_{ij}$, and observed plasma concentrations, C_{ij}, i.e. residual error, was modeled using a combined proportional $(\varepsilon 1_{ij})$ and additive error $(\varepsilon 2_{ij})$ model:

$$\ln(C_{ij}) = \ln(\hat{C}_{ij}) + \sqrt{\varepsilon 1_{ij}^{\,2} + \frac{\varepsilon 2_{ij}^{\,2}}{\hat{C}_{ij}^{\,2}}}$$

$$\hat{C}_{ij} = f(p_i, t_{ij})$$

where C_{ij} [ng/mL] and $\hat{C}_{ij}$ [ng/mL] are the observed and predicted concentrations at j_{th} time point measured in the i_{th} patient, and the (εk_{ij}) (k=1, 2) are random error terms. These errors follow normal distribution with mean of zero and variance of $\sigma_k^{\,2}$, and the variance $\sigma_k^{\,2}$ is estimated during analysis. Predicted concentrations $\hat{C}_{ij}$ are modeled as a

function of individual pharmacokinetic variables for i_{th} subject, p_i (described below), at a time t_{ij}.

The difference between 'model-predicted individual true pharmacokinetic parameters' and 'mean population pharmacokinetic parameters', i.e. inter-individual variability, was modeled using an exponential error model:

$$p_i = \theta * \exp(\eta_i)$$

Where, θ denotes the typical value of pharmacokinetic parameter P (e.g., CL, V) in the population, p_i is the individual value for P for i_{th} individual, and η_i is a random variable with a mean of zero and variance ω_p^2. The variance ω_p^2 is estimated during analysis.

The inter-occasion variability was modeled as third type of random effect, where day 1 and steady-state were defined as two separate occasions:

$$p_{ik} = \theta * \exp(\eta_i + \eta_{ik})$$

Where, p_{ik} is the individual value of pharmacokinetic parameter P (e.g., CL, V) in i_{th} individual at occasion *k*, η_i is a random variable with a mean of zero and variance ω_p^2, and η_{ik} is a random variable with a mean of zero and variance π_p^2 at occasion *k* and zero otherwise.

4-7.1.8 Model building criteria

Model selection was guided by the following goodness-of-fit criteria:

i) The likelihood-ratio test, also known as the log-likelihood criteria, was used to compare nested alternative models. The difference in log-likelihood [-2 (log L_1 - logL_2)] or the ratio of the NONMEM objective function values [-2 log (L_1/L_2)] follows a Chi-square distribution. Hence the reduction in objective function by 3.84 units (Chi-square distribution value at probability of 0.05, df=1) was considered significant for the selection of the alternative model. For non-nested models, the Akaike Information Criteria (AIC) was used, which was derived as follows:

AIC= -2 log likelihood + 2*k where k = no. of model parameters

ii) Diagnostic plots: The following diagnostic plots were used to evaluate the goodness of fit.

- scatter plot of observed and predicted concentrations vs. time (DV, PRED and IPRED vs. Time)
- Observed vs. population or individual predicted concentration (DV vs. PRED or DV vs. IPRED)
- Weighted residuals vs. time
- Weighted residuals vs. PRED

iii) Precision of parameter estimates. The covariance matrix was used to assess the standard errors on estimated (population mean and inter- and intra-individual variability) parameters. Large standard errors could indicate over-parameterization.

4-7.1.9 Covariate model

The covariates which were explored are summarized in **Table 4-15**. There were no missing values for any of the continuous covariates. Candidate covariates were first

identified by evaluating the graphical and statistical relationship between covariate and empirical Bayesian estimates of the relevant individual random effects (η). The covariates which met the pre-specified significance criteria of $p<0.05$ were included in the model, one-by-one, using the stepwise-forward regression method. Body weight was included in an allometric model on volume with allometric quotient fixed to the literature value of 1 (100, 101). Other candidate, continuous covariates were entered using the linear models. If there were multiple covariates for the same parameter, their combined effect was described by multiplicative equations. For example, if both BW and albumin were covariates for volume of distribution (V), the covariate model for typical value of V (TVV) was describes as below:

$$TVV_i = \theta_v * (WT_i / WT_{median})^1 * (1 + \theta_{ALB} * (ALB_i - ALB_{median}))$$

where body weight (BW) is standardized by median value and albumin (ALB) is centered at median value.

Categorical covariates, if found significant, were included in linear form in the model, as shown in example below:

$$CL_i = TVCL_{female} * (1 + \theta_{male\_diff} * Gender_i)$$

Where, Gender variable is 1 for males and 0 for females, and θ_{male_diff} indicates the percentage by which male clearance is higher than females.

After all the significant covariates were entered into the model, the model was further refined by stepwise backward elimination. The covariates that already existed in the model were removed; one at a time, and the resulting objective function values were compared with the previous models, with a significance level of 0.001. If the increase in objective function value was ≥10.83, the covariate was retained in the model.

Graphical goodness-of-fit assessments, as described in section **4-7.1.8**, were also performed simultaneously with statistical testing.

4-7.1.10 Model evaluation

The predictive performance of the model was tested by performing the visual and posterior predictive checks. The final model and the final parameter estimates were used to simulate the data for 10000 virtual patients. The 5^{th}, 50^{th} (median) and 95^{th} percentiles were estimated for simulated concentrations at each time point. The distribution of simulated concentrations was then compared with the distribution of actual observed sorafenib concentrations (102).

For the posterior predictive check 500 Monte Carlo simulation replicates of the original dataset were created using the final model. Average dose normalized concentrations for one dosing interval ($Cav_{i\,(0\text{-}12)}$) were estimated for each individual, after initial doses and at steady-state. For each simulated data replicate, summary statistics such as first quartile, median and third quartile were calculated, which were referred to as the prediction test quantities. Prediction distribution for each test quantity was generated using the data from 500 replicates. These were compared with the similar test quantities calculated using the observed dataset (dose normalized concentrations), which were referred to as the realized test quantities. A prediction P value (P_p) was calculated for each test quantity as the fraction of simulated values that were equal or greater than the realized values (equation 1) (103). The Bayesian P_p value was the probability of replicated data being equal or more extreme than the observed data.

$$P_p = \frac{1}{N_{rep}} \sum_{i=1}^{N_{rep}} I\left(T\left(y_i^{rep}, \theta\right) \geq T\left(y^{od}, \theta\right)\right) \qquad (1)$$

where, I(•) is an indicator function with value of 1 when its argument is true or zero otherwise, y_i^{rep} is the value of test quantity for i^{th} replicate data set, y^{od} is the respective test quantity for observed data set, θ represents individual specific pharmacokinetic parameters, and N_{rep} is the total number of replicates.

We also calculated the probability of equivalence (P_{eqv}) for dose normalized trough concentrations, i.e, concentrations at 12^{th} and 24^{th} hr (C12 and C24), both after initial doses and at steady-state, using the following equation (103):

$$P_{eqv} = \frac{1}{N_{rep}} \sum_{i=1}^{N_{rep}} \frac{1}{N_{sub}} \sum_{j=1}^{N_{sub}} I\left(0.80 \leq \frac{T(y_{ij}^{rep})}{T(y_j^{obs})} \leq 1.25\right) \qquad (2)$$

where N_{sub} is the total number of subjects in one replicate data set, and y_{ij}^{rep} is a test quantity for the j^{th} patient in the i^{th} replication.

In this approach, the ratio of test quantity for simulated data set ($T(y_{ij}^{rep})$) and observed data were determined for each subject. Indicator function was assigned a value of 1, when this ratio was between 0.8 – 1.25 (both inclusive), or zero otherwise, as shown in equation 2. The proportion, for which the test statistic for replicated data set was between 0.8-1.25 times of realized test statistic, was indicative of probability of equivalence.

4-7.2 Results

4-7.2.1 Patient demographics and genotypes

The population pharmacokinetic analysis was started with 112 patients; however, one patient was excluded during analysis because of an extremely high value (outlier) for

volume of distribution, which caused destabilization of the model. As mentioned earlier, patients were enrolled in 5 different phase I/II clinical trials, and sorafenib was administered as either single agent or in combination with chemotherapies at 200 or 400 mg BID dose levels. The demographic and clinical characteristics of 111 patients used in final analysis are summarized in **Table 4-15**. Genotype and allelic frequencies for polymorphisms in metabolic enzymes and drug target are described in **Table 4-16**. In total, 1276 plasma concentrations were used in the analyses. Initial-dose plasma concentration data were available from 110 patients and steady-state data were available from only 31 patients (**Table 4-14**). There were no missing values for continuous covariates, but genotype data were missing for 4 to 6 patients because of difficulties in PCR amplification.

Table 4-15 Patient characteristics

	Mean ± SD	Median	Range
Number of patients	111		
Trial / Tumor type[†]	mCRPC, 45 (stage 1, 22; stage 2, 23);		
	NSCLC, 18		
	CRC, 18		
	KS, 2		
	ST, 28 (Arm A, 13; Arm B, 15)		
Dose	400 mg BID, 81		
	200 mg BID, 30		
Occasion	Single dose, 109		
	Steady-state, 31 (patients with only steady-state, 2)		
Ethnicity	Caucasian, 90; African-Americans, 12; Others, 9		
Age, years	62.6 ± 11.1	63.9	30.3 – 84.9
Sex, male/female	77 / 34		
Body weight, kg	82.7 ± 19.4	81.4	35.2 – 132.5
BSA, m^2	1.9 ± 0.27	1.9	1.2 – 2.5
Biochemical Parameters			
Albumin, g/dL	3.6 ± 0.4	3.6	2.2 – 4.4
Total protein, g/dL	6.6 ± 0.6	6.6	4.6 – 8.0
Alk phosp, U/L	99.5 ± 57.3	82	34 – 414
Total bilirubin, mg/dL	0.65 ± 0.25	0.6	0.1 – 1.7
AST, U/L	28.6 ± 11	26	13-90
ALT, U/L	23.9 ± 12.6	21	8 – 75
SCr, g/dL	0.96 ± 0.23	0.9	0.4 – 1.9
CL_{Cr}, mL/min	97.7 ± 34.3	95.3	25.6 – 225.7

[†]Each trial evaluated the sorafenib's efficacy in different type of solid tumors
mCRPC: metastatic castrate resistant prostate cancer; NSCLC: non-small cell lung cancer; CRC: colorectal cancer; KS: Kaposi's sarcoma; ST: solid tumors; BID: twice-a-day; Alk phos: alkaline phosphatase; AST: aspartate transaminase or SGOT; ALT: alanine transaminase or SGPT; SCr: serum creatinine; CL_{Cr}: creatinine clearance

Table 4-16 Summary of genotype distribution for patients on sorafenib trials

Genetic Variants	N	Genotype Frequencies[a]			Allele Frequencies[b]		
		Wt	Het	Var	P	q	p-value[c]
CYP3A4*1B	108	89 (82.4)	10 (9.3)	9 (8.3)	0.87	0.13	0.14
CYP3A5*3C	108	8 (7.4)	17 (15.7)	83 (76.9)	0.15	0.85	0.12
UGT1A9*3	107	103 (96.3)	3 (2.8)	1 (0.9)	0.98	0.02	<0.01
UGT1A9*5	107	107 (100)	0 (0)	0 (0)	1	0	NC
VEGFR2 H472Q	106	66 (62.2)	35 (33.1)	5 (4.7)	0.79	0.21	0.87
VEGFR2 V297I	106	78 (73.6)	25 (23.6)	3 (2.8)	0.85	0.15	0.99

Wt, wild type sequence; **Het**, heterozygous and **Var**, homozygous variant sequences;
p, q are standard Hardy-Weinberg nomenclature for allele frequencies
a. Number represents number of patients with percentages in parentheses
b. Data are given as relative frequency
c. p-value for evaluation of Hardy-Weinberg equilibrium for Caucasian subjects only
NC-Not calculated

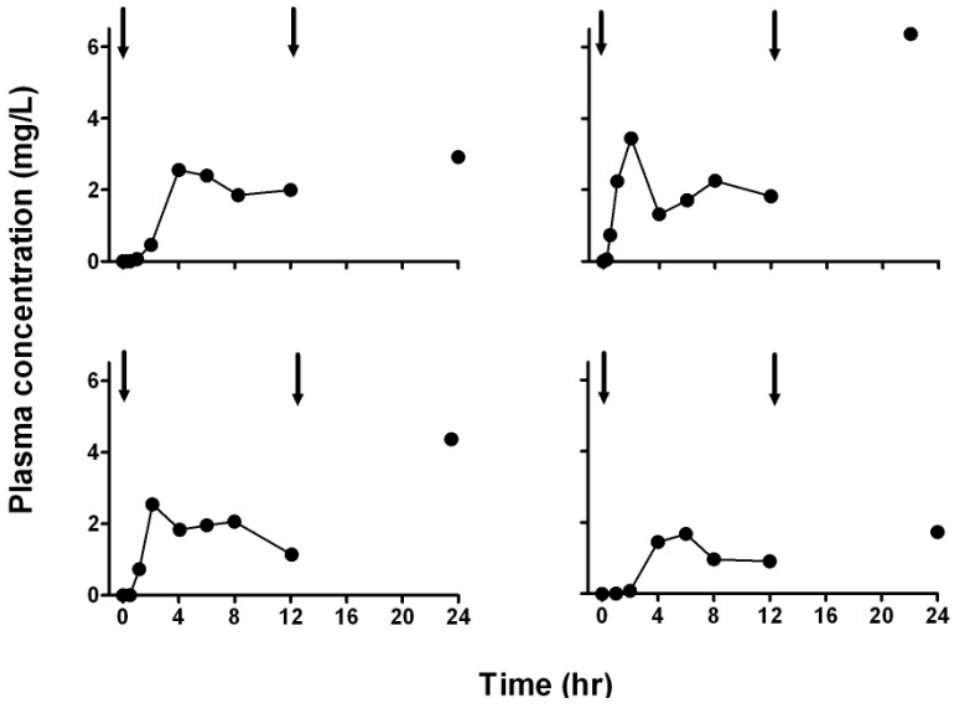

Fig 4-11 Representative plasma concentration – time profiles for patients included in current population pharmacokinetic analysis. Arrows represent the dose administration times.

4-7.2.2 Model building

Typical plasma-concentration time profiles from patients on these trials are shown in **Fig. 4-11**. Double peaks were observed for almost 8% patients on these trials, which is characteristic of drugs undergoing entero-hepatic recycling. For other patients, although distinct double peaks were not observed, the rate of decline in plasma concentrations was reduced after 5-6 h, suggesting that loss of drug from central compartment may have been hampered by EHR or re-distribution of drug from peripheral compartment. Earlier the pharmacokinetics of sorafenib was described by a two compartment model, with absorption lag-time and first order elimination (51).

When we began the population pharmacokinetic modeling for sorafenib, data from only 109 patients were available. One-compartment, two-compartment and entero-hepatic recycling models were tested using plasma concentration-time profiles on normal scale. Due to limited sampling in distribution phase, the estimated distribution parameters for two-compartment model were unstable; therefore, those parameters were fixed to previously reported values (51). Several different GI absorption models, including the absorption lag-time and sequential zero- and first-order absorption were tested to describe the solubility limited absorption for sorafenib. With data from 109 patients, when concentrations on a normal scale were fitted to the pharmacokinetic model to predict the normal scale concentrations, a one compartment model with sequential zero- and first-order absorption, absorption lag time and first order elimination was found to adequately describe the observed plasma concentration-time profiles. The schema of this final model and parameters estimates are presented in **Fig 4-12** and **Table 4-17**, which was also

presented at 2009 annual meeting of American Society of Clinical Pharmacology and Therapeutics (ASCPT) (104).

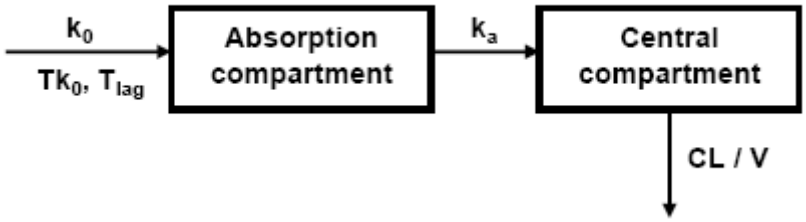

Fig 4-12. Structural model for the initial population pharmacokinetic model, describing the plasma concentration – time profiles for sorafenib (104).

Table 4-17. Parameter estimates from the initial population pharmacokinetic model (N=109)

Parameter	**Population mean (%RSE)**	**% BSV (%RSE)**
CL/F, L/h	4.74 (11.6)	45 (27.9)
V/F, L	156 (9.8)	80 (20.9)
ka, 1/h	1.04 (17.0)	136 (35.6)
Tk0, h	1.92 (16.5)	30 (39.4)
ALAG1, h	0.196 (11.5)	145 (55.9)
ALAG1~African American	0.696 (5.9)	
Residual error		
Additive (ng/mL)	68.3 (44)	
Proportional (%CV)	48 (12)	

% Relative standard error (RSE) = (SE/Mean)*100

However, there were few limitations to this model, including (i) high residual errors in the predicted plasma concentrations (i.e., additive, 44 ng/mL and proportional, 50%), (ii) high imprecision for absorption parameters (i.e. standard error of 55% for Ka, 62% for

absorption lag-time, and 41% for duration of zero order absorption), and (iii) large residuals for the steady-state profiles.

In continuing with model development, we updated the above model with data from a total of 112 patients; however, one patient was excluded from model building because of extremely high value (outlier) for volume of distribution, causing destabilization of the model. A total of 1276 plasma concentrations were used in updated analysis. To resolve the problem of large residuals, limitations (i) and (iii) above, both side log-transformation approach was used. The log-transformed observed concentrations were fitted with the model to make predictions of log-transformed concentrations. The poor description of absorption profile, limitation (ii) above, might have been because of model misspecification or estimation of delay in absorption as lag-time. At the point of lag-time, the differential equation solver in NONMEM attempts to integrate over a discontinuity, which may result in numerical problems (105). To resolve this problem, the apparent delay in absorption was modeled with GI transit absorption compartments, which described the concentration-time profile as a gradually increasing continuous function. This was also a better model to reflect the physiological absorption process. Hence, the GI transit compartments absorption model was tested as a replacement of mixed-order absorption process with lag-time, to overcome the limitation (ii) (see above).

With these modifications, one- and two-compartment models with and without entero-hepatic recycling were re-tested. Although several EHR models (106-108) had been tested initially, before we finalized the initial one-compartment model, a few additional

EHR models were also evaluated during this modification stage. Initial estimations were performed with FO POSTHOC method. Graphical and statistical assessment of evaluated models revealed that addition of EHR improved the model predictability for observed plasma concentration-time profiles both after initial-doses and at steady-state. Therefore, the EHR component was retained for further analyses. The number of GI transit compartments was adjusted (N=2, 3 or 4), and different arrangements (parallel vs. sequential) were tested. A model with four serial transit compartments was found to adequately describe the absorption phase.

The best model from this stage, a one-compartment model with entero-hepatic recycling, GI transit absorption compartments (N=4) and first order elimination, was re-assessed with FOCE INTER estimation method. The number of GI transit compartments were also re-adjusted, but N=4 remained superior. The scheme of this optimized, final structural model is shown in **Fig 4-13**. Four transit-compartments, each of them receiving drug from the antecedent and releasing drug into the subsequent transit-compartment with a first-order rate constant k_a, accommodated the apparent lag time and a highly variable T_{max}. EHC was modeled with a semi-mechanistic model, where a fraction of drug from the central compartment (F_{ent}) was hepatobiliarily excreted (transferred) into a gall-bladder compartment with a first-order rate k_b, which, in turn, periodically emptied drug into the last GI transit-compartment at a first-order rate of k_{Ehc}. For modeling purposes, F_{ent} was logit-transformed, to constrain its value between 0 and 1, and to allow typical parameters to be estimated as a continuous function (between -infinity to +infinity). The periodic drug release from the gall bladder compartment was regulated by the "on-off"

switch '*Ehc*', modeled by a square-wave function. The remaining fraction of drug in the central compartment, (1-F_{ent}), was eliminated by a first-order rate process, characterized by k_e and reflecting hepatic metabolism and irreversible biliary excretion; ke was parameterized in terms of clearance (CL/F) and volume of distribution (V/F).

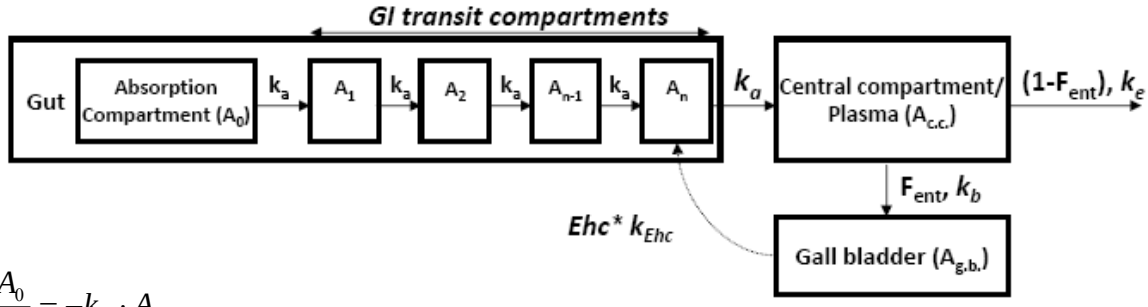

$$\frac{dA_0}{dt} = -k_a \cdot A_0 \quad \textbf{(1)}$$

$$\frac{dA_1}{dt} = -k_a \cdot (A_1 - A_0) \quad \textbf{(2)}$$

:

:

$$\frac{dA_{n-1}}{dt} = -k_a \cdot (A_{n-1} - A_{n-2}) \quad \text{, n = 2, 3…..N} \quad \textbf{(3)}$$

$$\frac{dA_n}{dt} = -k_a \cdot (A_n - A_{n-1}) + Ehc \cdot k_{Ehc} \cdot A_{g.b.} \quad \textbf{(4)}$$

$$\frac{dA_{c.c.}}{dt} = k_a \cdot A_n - F_{ent} \cdot k_b \cdot A_{c.c.} - (1 - F_{ent}) \cdot \frac{CL}{V} \cdot A_{c.c.} \quad \textbf{(5)}$$

$$\frac{dA_{g.b.}}{dt} = F_{ent} \cdot k_b \cdot A_{c.c.} - Ehc \cdot k_{Ehc} \cdot A_{g.b.} \quad \textbf{(6)}$$

$$Ehc = \frac{(t - DOST)^{40}}{(t - DOST)^{40} + (ADT)} \quad \textbf{(7)}$$

Fig 4-13 Final base model for describing the plasma concentration – time profiles for sorafenib. k_a: first-order absorption rate constant, k_e: first-order elimination rate constant, k_b: first-order rate constant for transfer of sorafenib to gall-bladder, k_{EHR}: first-order rate constant for secretion of sorafenib in bile to GI transit compartments, F_{ent}: fraction undergoing entero-hepatic recycling, *Ehc*: switch to regulate the bile secretion, which

was turned-on at ADT time after administration of dose. $A_{0,}$ $A_{c.c.}$and $A_{g.b.}$ are amounts of drug in absorption, central and gall-bladder compartment, and their initial conditions were set to zero except A_0, which was assumed to contain the entire dose at time zero.

During initial modeling, k_b and k_e were estimated independently, but assuming $k_b = k_e$ (i.e., F_{ent} =50%) adequately described the EHC for sorafenib. IIV was estimated only for CL/F, V/F and ka. For all other parameters, η's had either high shrinkage (i.e., >30 %) or low precision; therefore, these η's were fixed to zero. All the model parameters were estimated; however, BSV was estimated only for pharmacokinetic parameters, i.e., CL/F, V/F and k_a. Incorporation of correlation between CL/F and V/F resulted in 30-units ($p<0.001$) decrease in objective function value compared to the base model, and introduction of inter-occassion variability in CL/F further reduced the objective function value by 44-units ($p<0.001$) compared to model without this variability. Since both these changes were statistically significant, they were retained in the model. Additional introduction of inter-individual or inter-occasion variability either de-stabilized the model and/or was not significant. These optimization steps are summarized in **Table 4-18**.

After optimization of the base model, the covariate search was initiated using the *post-hoc* Bayesian estimates of individual random effects (η_i values) from final base model. In first covariate screening, body weight, BSA, gender, albumin, ALT, VEGFR2 H472Q and Trial showed up as significant ($p<0.05$) covariates for $\eta_{V/F}$; only VEGFR2 H472Q and VEGFR2 V297I were significant for $\eta_{CL/F}$ and η_{ka}, respectively. The same covariates were significant for peak plasma concentrations (C_{max}) and exposures (AUC_{0-12}) during

covariate screening by non-compartmental analysis-general linear modeling (**Section 4-5.2.3.4**, **Tables 4-12 and 4-13**). As described earlier in **section 4-5.2.3.2**, correlation of BSA and gender with $\eta_{V/F}$ were confounded by body weight. In covariate model 1, the most apparent mechanism-based covariate, body weight, was included in V/F as an allometric model. The allometric coefficient (power) was fixed to the literature value of 1.0, which has been derived based on structural and function properties of biological system (100, 101). The inclusion of weight on V/F resulted in 14-units ($p<0.001$) decrease in objective function value and inter-individual variability declined from 72% to 69%.

Covariate screening was re-performed for *post-hoc* Bayesian estimates of individual random effects from covariate model 1. Albumin and VEGFR2 H472Q were significant for both $\eta_{V/F}$ and $\eta_{CL/F}$, and only VEGFR2 V297I was significant for η_{Ka}; no other covariates were significant for all three parameters. Among these, only the relationship of albumin with and $\eta_{V/F}$ and $\eta_{CL/F}$ were mechanistically plausible. There appeared be a lack of gene-dose-response relationship for polymorphism in receptor for sorafenib, i.e., VEGFR2. It did not appear to be clinically important. Serum albumin was tested on both CL/F and V/F, separately. Incorporation of serum albumin in V/F, in a log-linear model with median centered covariate values, resulted in decrease in objective function value by 5.9-units ($p<0.05$), while objective function value was not altered following inclusion of serum albumin in CL/F. Hence, in covariate model 2, serum albumin was retained as covariate for V/F in addition to body weight, which also reduced the inter-individual variability on V/F from 69% to 66%.

Table 4-18 Summary of selected modelssequentially tested for population pharmacokinetic analyses and their objective function values.

S.N.	Model description	Remarks	OBF	ΔOBF[†]
	Normal scale (For initial model with data from 109 patients)			
1	One compartment model with sequential zero and first order absorption (HYBRID method)	Base model on Normal scale	16372.5	
2	Two compartment model sequential zero and first order absorption (HYBRID method)	Normal scale	16878.2	505.7
3	Entero-hepatic recycling models	Normal scale	>16500	>125
	Log-tranformed data (For final model with data from 112 patients)			
4	One compartment with entero-hepatic recycling and GI transit absorption model (N=4) (method=FOCEI)	Base model on log scale	423.9	
5	Model 4, after exclusion of one subject[*] and inclusion of correlation between CL and V in $OMEGA block		393.5	(-)30.4
6	Model 5 + IOV on CL		349.4	(-)44.1
7	Model 6 + BW as covariate for V/F (allometric model)	CM[‡] 1	335.0	(-)14.4
8	Model 7 + Albumin as covariate for V/F (log linear model with albumin centered at median value)	CM 2	329.1	(-)5.9
9	Model 8 + ALT as covariate for V/F (linear model with ALT normalized with median)	CM 3	320.8	(-)9.1
10	Model 9, with exclusion of BW from V/F	CM 4	355.7	34.9
11	Model 9, with exclusion of albumin from V/F	CM 4	330.5	9.7
12	Model 9, with exclusion of ALT from V/F	CM 4	329.7	8.9
13	**Final model[§], model 6 + BW as covariate in V/F**	**Final model**	**333.9**	

[*]One subject with very high volume of distribution was excluded to stabilize the model
[†]ΔOBF = Objective function value for base model – alternate model

‡CM: Covariate model
§Final model is presented below:

$$CL/F_i = \theta_{CL/F} \cdot \exp(\eta_{CL/F_i} + \kappa_{CL/F_{ij}})$$

$$V/F_i = \theta_{V/F} \cdot (weight/81.5)^1 \cdot \exp(\eta_{V/Fi})$$

$$k_a = \theta_{k_a} \cdot \exp(\eta_{k_{ai}})$$

$$k_b = k_e = CL/V$$

$$F_{ent} = 1/(1+\exp(-\theta_{F_{ent}}))$$

$$k_{Ehc} = \theta_{Ehc}$$

$$\text{Ehc} = \frac{(\text{T} - \text{DOST})^{40}}{(\text{T-DOST})^{40} + \text{ADT}^{40}}$$

$$ADT = \theta_{ADT}$$

where θ are fixed effect parameters and η represents random inter-individual variability. T is observation time point, DOST is dose administration time and ADT is absolute time after dose administration at which EHR switch turns on.

Method = FOCE INTER

NONMEM Subroutine: ADVAN9 TOL=4

In covariate model 3, the covariate screening was repeated for individual *post-hoc* Bayesian estimates of random effects from covariate model 2, and ALT, UGT1A9*3, VEGFR2 H472Q and Trial came out as significant covariates for both CL/F and V/F, and only VEGFR2 V297I was significant for Ka. For UGT1A9*3, only 1 patient carried the homozygous variant genotype (UGT1A9*3*3); therefore, it was not possible to evaluate

its impact on pharmacokinetic parameters. The effects of VEGFR2 polymorphisms on CL/F, V/F and Ka were considered artifactual.

For the covariate "Trial", patients who were treated on stage 2 of mCRPC trial and arm B of ST trial had relatively low V/F and CL/F compared to the other patients. However, comparing the typical values for the pharmacokinetic parameters across entire trials, rather than their subdivisions into stages or arms, no significant differences in pharmacokinetics were observed. Stages 1 and 2 of mCRPC trial were different only in terms of the efficacy endpoints, and administered treatments and pharmacokinetic sample collection timepoints were similar between these two stages. In the ST trial, arm B patients received sorafenib in combination with bevacizumab after four weeks of receiving only bevacizumab (5 mg/m^2 IV QS 2 week); while arm A patients first received sorafenib for 4 weeks, which was followed by administration of combined therapy (**Fig 4-3**). No difference in pharmacokinetics was observed between arm A and arm B by non-compartmental analysis, and *in-vitro* plasma protein binding studies also did not show any significant change in unbound fraction of sorafenib in plasma following co-administration with bevacizumab (data not shown). Based on these reasons, the significant effect of Trial on CL/F and V/F was thought to be artifactual or associated with the small sample sizes and was not considered further.

The ALT values were directly related with $\eta_{CL/F}$ and $\eta_{V/F}$; however these relations were driven by observations from 5-6 individuals and also appeared to contradict the mechanistic expectations. Regardless of mechanistic contradiction, ALT was tested for

both CL/F and V/F, to check for any statistical influence. Inclusion of ALT on V/F in a linear model with median normalized values reduced the objective function value by 9 units ($p<0.05$), while its inclusion on CL/F was not significant ($\Delta_{obj} \leq 1$). Hence ALT was retained on V/F.

During re-screening by using the individual *post-hoc* Bayesian estimates of random effects from covariate model 3, no other covariate was found to be significant, except mechanistically implausible effects of VEGFR2 H472Q polymorphism on $\eta_{CL/F}$ and $\eta_{V/F}$, and VEGFR2 V297I polymorphism on η_{Ka}.

After inclusion of all significant covariates into the model, the step-wise backward elimination process was started: In three alternate models, each of these covariates was excluded individually from the full model, and their objective function values were compared with that of full model. Exclusion of weight increased the objective function value by approximately 36 units, which was significant at $p<0.001$. Omission of serum albumin and ALT resulted in a 9.7 and 8.9 units increase in objective function value, which were statistically insignificant ($p>0.001$). Hence, only body weight was retained in the final model. Explicitly, the final model was a one-compartment model with following features: first-order absorption, GI transit absorption compartments (N=4), entero-hepatic recycling, first-order elimination, covariance between CL/F and V/F, BSV for CL/F, V/F and ka, inter-occassion variability on CL/F, body weight as covariate on V/F, and combined additive and proportional residual error model.

4-7.2.3 Goodness-of-fit plots and parameter estimates for the final base and covariate model

Goodness-of-fit plots for sorafenib plasma concentrations predicted from final base and covariate model are shown in **Fig 4-14 and 4-15**. Model predictions were in reasonable agreement with observed concentrations. The individual weighted residuals did not reflect any systematic deviations. The parameter estimates from the final model are summarized in **Table 4-19**. For a patient with body weight of 81.5 kg, typical population clearance (CL/F) was estimated as 8.05 L/h with a volume of distribution of 217 L. However, these pharmacokinetic parameters were inter-related with a correlation coefficient of 0.77, and were associated with moderate to high inter-individual variability ranging from 18-69%. The between occasion variability on CL/F was 48%.

The estimated typical value for CL/F of 8.05 L/h suggests low hepatic extraction, when compared to the hepatic blood flow of 90 L/h, which is in accordance with sorafenib's known pharmacokinetic properties with oral bioavailability in rats and dogs ranging from 67 to 80%, i.e., low hepatic first-pass metabolism. Similarly, the estimated typical value for volume of distribution (V/F) of 217 L is in accordance with estimates in rats and dogs after IV administration (0.65 to 0.74 L/kg) (33) and with population pharmacokinetic estimates in humans after oral administration (109.8 L) (51) observations. This high volume of distribution suggests extensive tissue distribution despite high plasma-protein binding. The significant relationship of body weight with volume of distribution might be explained based on physiological rationale that body volume increases with body weight, as dicussed previously.

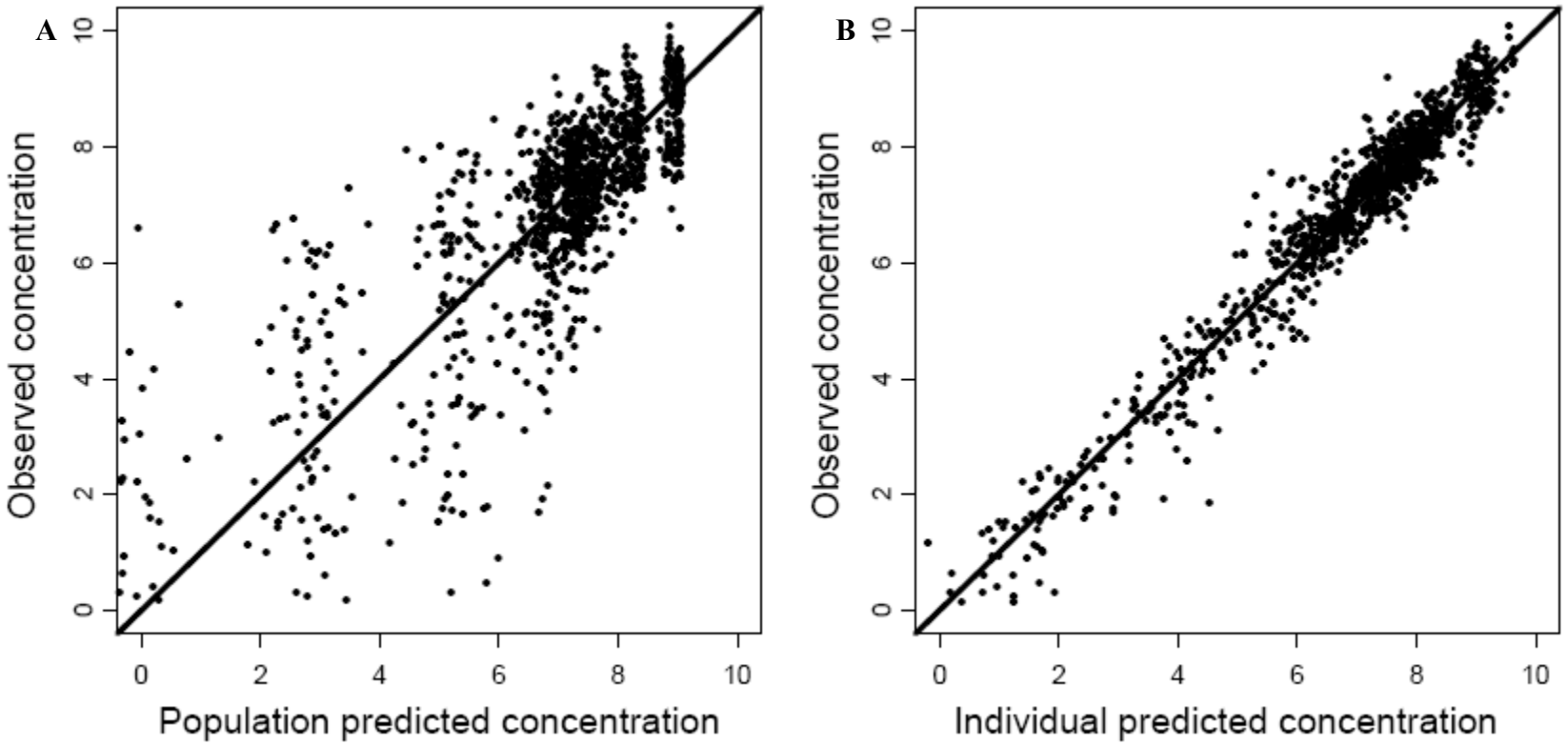

Fig 4-14 Diagnostic plots for the final population pharmacokinetic model on a log-log scale. (A) Population-predicted concentrations vs. observed concentrations, and (B) Individual-predicted concentrations vs. observed concentrations

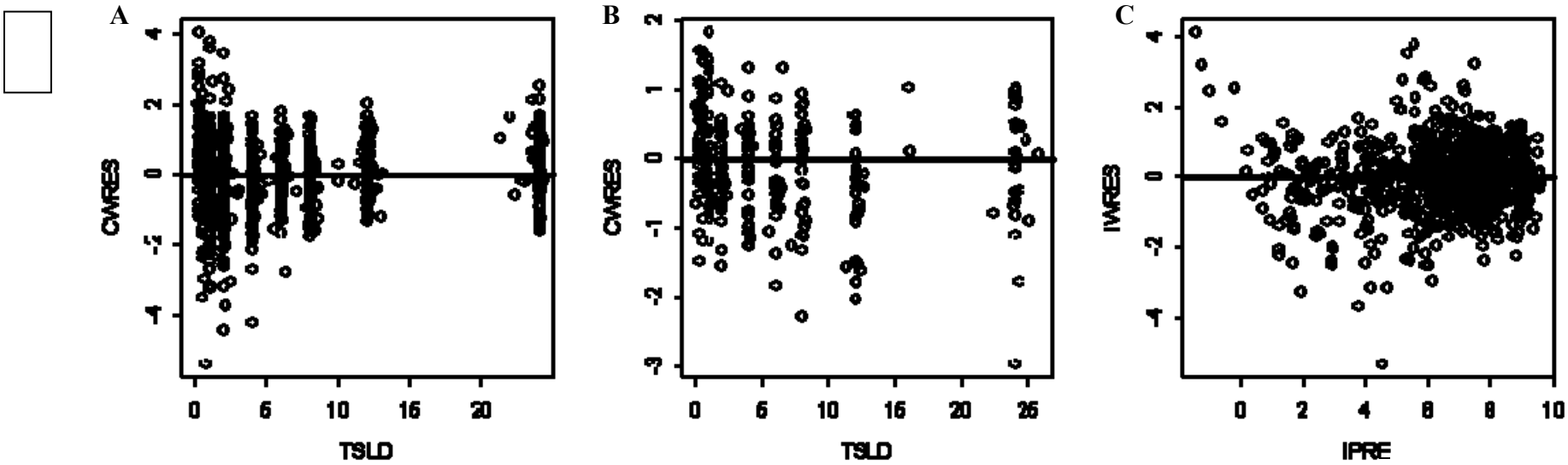

Fig 4-15 Diagnostic plots for the final population pharmacokinetic model. Conditional weighted residuals vs. time since last dose (TSLD, hours) after (A) initial doses and (B) at steady-state, and (C) Individual-weighted residuals vs. individual predicted concentrations

The typical value for absorption transit time was 1.98 h, which is the average time spent by sorafenib in traveling from gut compartments to the central compartment. The typical value for plasma half-life - based on NONMEM estimated parameters - was 18.7 h, which was slightly lower than the previously reported range of 25-48 h (49); however, plasma sampling in our trials was limited to 12 hours post-dose because sorafenib was administered in BID dosing schedule compared to sampling upto 168 hours post-dose in selected patients in previous analysis (51). On an average, 50% of the sorafenib reaching the central (plasma) compartment underwent entero-hepatic recirculation. The typical value for the time of gall-bladder emptying (ADT) was 6.7 h post-dose.

Table 4-19 Estimated NONMEM model parameters

Parameter	**NONMEM estimate**	**IIV (%CV)**	**IOV (%)**
CL/F (L/h)	8.05	21%	48%
V/F (L)	217	66%	NE
Mean transit time* (h)	1.98	62%	NE
K_{EHR} (h^{-1})	0.998	NE	NE
F_{ent}	0.50	NE	NE
ADT	6.66	NE	NE
Correlation $_{CL/F–V/F}$	0.77	NE	NE
Proportional residual error (%CV)	51.4%		
Additive residual error	0.0003		

*Mean transit time = (n+1)/ K_a = 5/2.51 = 1.98. NE: Not estimated

4-7.2.4 Model evaluation

The pharmacokinetic model evaluation, including the visual and posterior predictive checks, revealed that the final model predictions were in reasonable agreement with

observed concentrations. The **Fig 4-16** represents the visual predictive check showing the median and 90% prediction intervals of model-predicted and observed plasma-concentration time profiles, after initial doses and at steady-state. The Cav predictions from the final population pharmacokinetic model are shown in **Fig 4-17**. The model-derived simulations appeared to be in agreement with observed data with P_p values of 0.90, 0.67, 0.13 and 0.95, 0.66, 0.83 for first quartile, median and third quartile $C_{av(0-12)}$ after initial doses and at steady-state. At both occasions, the P_P values for median $C_{av(0-12)}$ were close to 0.5, suggesting that distribution of predicted $C_{av(0-12)}$ was approximately centered around the observed median $C_{av(0-12)}$.

The distributions of P_{eqv} for trough concentrations are shown in **Fig 4-18**. Range of P_{eqv} for C12 and C24 was 0.75-1, suggesting that on an average more than 75% of replicated simulations met the equivalence criteria. Overall, these results suggest that model-simulated exposures from the final model were reasonably close to the observed exposures that were used for population pharmacokinetic modeling.

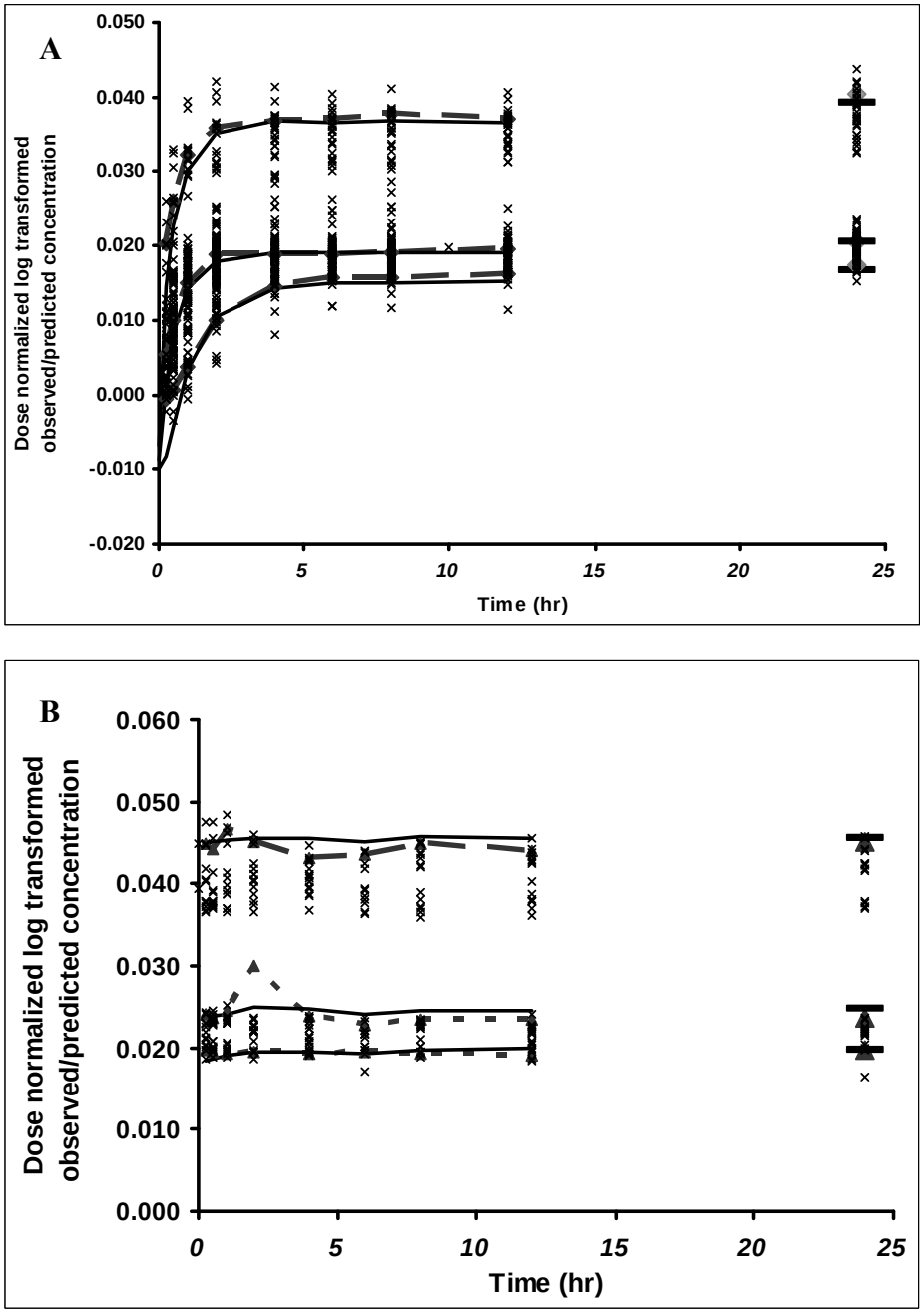

Fig 4-16 Visual predictive check for pharmacokinetic model. (A). after initial doses and (B) at steady-state. Solid (─) and dotted (---) black lines represents the median and 90% interval for dose-normalized model-predicted concentrations and observed concentrations, respectively; and crosses (x) depicts the actual dose-normalized observed concentrations.

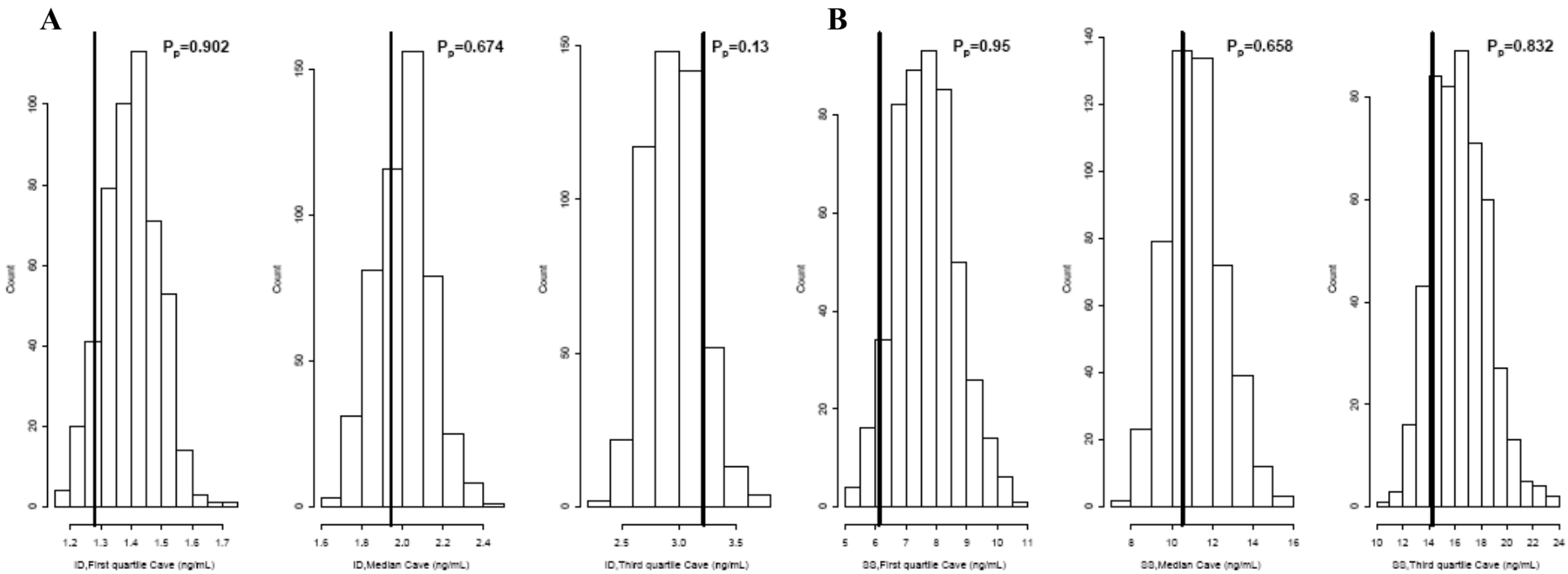

Fig 4-17 Results of the predictive check for final sorafenib population pharmacokinetic model: Histograms showing distributions of C_{ave} for 500 replicate simulated data sets, after single dose (A) and at steady-state (B), calculated using the back-transformed (normal scale), dose normalized data.

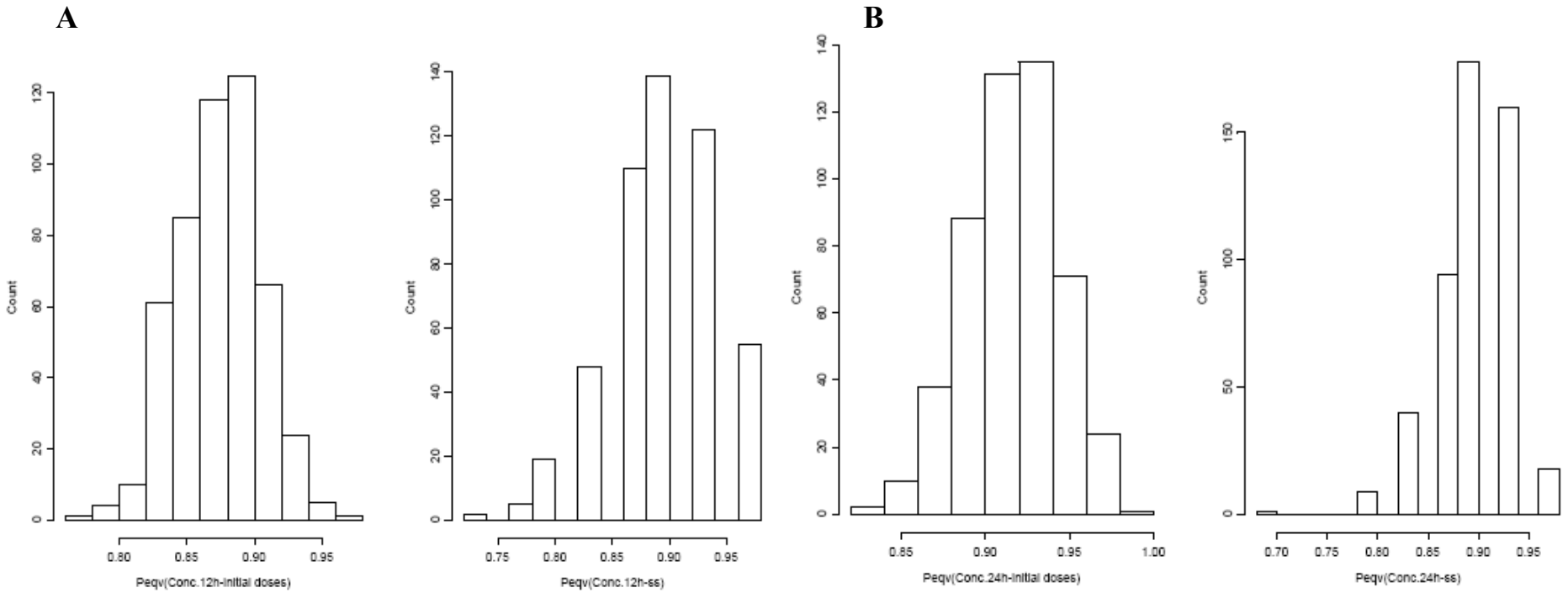

Fig 4-18 Results of the predictive check for final sorafenib population pharmacokinetic model: Histograms showing distributions of P_{eqv} for trough concentrations at 12^{th} hr (A) and 24^{th} hr (B) for 500 replicate simulated data sets, plotted separately for single dose and steady-state. Predictions on log-scale were dose normalized for the plot.

4-7.3 Discussion

A mechanism-based pharmacokinetic model was developed and validated to describe the sorafenib plasma concentration – time profiles in patients with solid tumors. The description of sorafenib pharmacokinetics in most of the currently reported studies was based on non-compartmental pharmacokinetic analysis. The reported half-life of sorafenib was 25-48 hrs, however, it is mostly administered in a BID dosing schedule, making the collection of terminal phase samples unfeasible. Therefore, most pharmacokinetics parameters such as exposures upto 12 h (AUC_{0-12}), peak plasma concentration (C_{max}) and time to peak plasma concentration (t_{max}) were reported. Only one earlier population pharmacokinetic analysis has been reported, which included 226 cancer patients and 69 healthy subjects and determined that two-compartment model with absorption lag-time was descriptive of observed plasma concentration-time profiles (51)

Sorafenib shows a complex pharmacokinetic disposition profile after oral administration, where its GI absorption is limited by poor GI solubility and complicated by entero-hepatic recirculation. High inter-patient variability was reported in sorafenib pharmacokinetics after initial doses, the magnitude of which further increased after multiple dosing. A mechanism-based pharmacokinetic model for sorafenib was developed, taking into account its known pharmacokinetic characteristics. Similar to the previous study (51), the impact of demographic and (patho-) physiological variables on sorafenib pharmacokinetics was evaluated; in addition, we also examined the impact of genetic variation in metabolic enzymes on sorafenib's disposition. To best of our

knowledge, no other study has evaluated the impact of genotype on sorafenib pharmacokinetics.

The final population pharmacokinetic model was a one-compartmental model with entero-hepatic recycling, serial GI transit absorption compartments (N=4) and first-order elimination and absorption. Goodness-of-fit plots showed that the predictions from the final model were reasonably consistent with observed data with no systematic bias. The implementation of entero-hepatic recycling component improved the predictions at steady-state concentrations compared to a one- or two-compartment model without this component (or compared to the initial model (104)). Characterization of the sorafenib pharmacokinetics with the current data was largely dependent on steady-state plasma concentration – time profiles, because collection of terminal phase pharmacokinetic samples was not feasible given its BID dosing schedule. Hence, adequate description of both plasma concentration-time profiles at steady-state as well as after initial doses was desirable. Population mean values for CL/F, V/F and transit rate constant in the absorption model (K_a) were estimated, along with parameters used to describe the entero-hepatic recycling. Inter-patient variability was estimated only for CL/F, V/F and K_a, and between-occasion variability was characterized only for CL/F. The between-occasion variability for CL/F was larger than the inter-patient variability. Model evaluation by visual and posterior predictive checks confirmed that model predictions were consistent with the observed data.

The results from three different population pharmacokinetic models are compared in **Table 4-20**.

Table 4-20 Compariosn of study design and parameter estimates from three population pharmacokinetic models

Property	**Prior published model** (51)	**Initial model (N=109)** (104)	**Final model (N=111)**
No. of patients	229 patients, 69 healthy subjects	109 patients	111 patients
Dose range	50-800 mg BID	200-400 mg QD/BID	200-400 mg QD/BID
Pharmacokinetic samples	**SD**: serial/sparse samples upto 12 hr or upto 168 hrs (few patients) **SS**: upto 12 hrs post-dose selected patients	**SD**: serial samples upto 12 hr (N=106) **SS**: serial samples upto 12 hr (N=30)	**SD**: serial samples upto 12 hr (N=110) **SS**: serial samples upto 12 hr (N=31)
Structural (Base) model	Two-compartment model with absorption lag time and first-order absorption and elimination. F_{rel} modeled as a function of dose to incorporate the observed infra-proportional increase in sorafenib exposure	One-compartment model with absorption lag time and sequential zero- and first-order absorption	One-compartment model with serial GI transit absorption compartments (N=4) model and EHC
Final Parameter estimates	CL/F = 3.31 L/hr (IIV, 25%) V_c/F = 85.2 L (IIV, 10%) V_p/F = 24.6 L (IIV, 45%)	CL/F = 4.74 L/hr (IIV, 45%) V/F = 156 L (IIV, 80%)	CL/F = 8.05 L/hr (IIV, 18%; IOV, 48%) V/F = 217 L (IIV, 68%) Mean transit time = 1.98 hr

	k_a = 0.229 hr^{-1} (IIV, 104%)	k_a = 1.04 hr^{-1} (136%)	
Covariates	Ethnicity (Japanese vs. non-Japanese) for k_a and F_{rel}	Body weight for V/F	Body weight for V/F
Comments	-Body weight (range 36-155 kg) was screened as a covariate for both V_c/F and V_p/F. Because two different volumes were estimated, weight may not have been identified as a significant covariate. -None of the studied covariates were clinically relevant.	-Considering the IIV, estimated parameters are reasonably close to the previously reported values. -None of the studied covariates were clinically relevant.	-Both CL/F and V/F are almost double than the previously reported values, which could be explained by 50% drug undergoing EHC. If we consider that 50% of the bioavailability is because of EHC, the estimated parameters would be reasonably close to previous reports. -None of the studied covariates were clinically relevant.

The clearance estimates from the final (8.05 L/h) were clearly different from the previously reported population pharmacokinetic analysis (3.31 L/h) and our initial model (4.74 L/h). Comparison with the previous analysis was limited by their dose-dependent relative bioavailability assumptions (across a large dose range) and better representation of terminal phase in their model (samples upto 168 hrs were collected for selected patients after single dose) (51). These differences can further be explained by the involvement of EHC in the final model (**Table 4-20**). On average, 50% of the sorafenib reaching systemic circulation underwent EHC; this suggests that EHC provides a major contribution to the overall plasma exposure of sorafenib. Steady-state concentrations were highly variable for these patients, which could not be properly described by our initial model. Therefore, pharmacokinetic parameters from our initial model should be carefully considered with this limitation. Nevertheless, all clearance estimates were indicative of low hepatic extraction ratio for drugs cleared by hepato-biliary elimination, which is consistent with predictions based on clearance from preclinical studies (33). Similarly, the estimate for apparent volume of distribution from our study (217 L) was different from previous analysis (volume of central compartment, 85.2 L and peripheral compartment, 24.6 L) and our initial model (156 L), but all of them suggest extensive tissue distribution. Again, these differences can be explained by involvement of EHC in the final model (**Table 4-20**). Mean transit time was estimated as 1.98 h. The BSV on these parameters ranged from 18-69% and IOV on CL/F was 48%. High variability estimates were in agreement with results of non-compartmental analysis (35, 38-40) and previously reported population pharmacokinetic analysis, where estimated BSV ranged between 10-104% (51). Potential reasons for this high pharmacokinetic variability were

mentioned above, including the poor GI solubility, differences in extent of entero-hepatic recycling among patients, high plasma protein binding and the possible effect of food on bioavailability. Sorafenib administration was not controlled or monitored in terms of food consumption in these trials. Pharmacokinetic parameters were not different based on studied dose levels (200 and 400 mg BID) which was in agreement with previous report (51) , and estimates of parameters were not altered significantly over multiple dosing, except CL/F.

The previous study reported ethnicity (Japanese vs. Non-Japanese) as a significant covariate for absorption rate constant and relative oral bioavailability (51), which was not assessable with the current data since no Japanese patients were enrolled in trials at NCI. Our results show body weight as a significant covariate for V/F, which was not true in the previous analysis (51). However, inclusion of body weight explained less than 4% of the inter-patient variance on V/F and approximately 68% remained unaccounted for. Therefore, clinical dose adjustments based on weight are not recommended. The other examined demographic, physiological and pharmacogenetic covariates appeared to be unimportant for description of sorafenib pharmacokinetics, which is supported by the findings from previous population pharmacokinetic analysis (51) and clinical studies (37, 94).

Other potential covariates which were not studied, but could conceivably contribute to the variability in sorafenib pharmacokinetics include co-medications: Co-administration of sorafenib with antibiotics and/or proton-pump inhibitors may influence its GI

solubility and/or the extent of EHC, by altering the GI pH and deconjugation activity (mediated by intestinal bacteria). Information about co-administered medications was not available from all the trials involved in current analysis; hence, its impact could not be evaluated. Genetic polymorphism in drug transporters involved in hepatobiliary elimination, such as P-gp and MRP2, which were not measured in the study may also have contributed to EHC and be responsile for at least part of the remaining, unexplained pharmacokinetic variability/model imprecision. Co-administered drugs may also induce or inhibit the activity of transporters and metabolic enzymes (109).

A recent clinical study prospectively enrolled 138 cancer patients with various degrees of liver and kidney dysfunctions (9 different cohorts) to study their impact on sorafenib pharmacokinetics (94). The majority of patient cohorts in this study were defined based on laboratory values for total bilirubin, AST and CLCr; serum albumin was also used to define one of the cohorts. Pharmacokinetics was measured after single-dose by non-compartmental analysis and no significant differences in AUC_{0-12} of sorafenib or its N-oxide metabolite were apparent between these patient cohorts (94). However, lower maximum tolerable doses of 200 mg BID to 200 mg QD were recomended for patients with moderate to very severe liver dysfunction based on long-term toxicity profile, in contrast to the clinically approved dose of 400 mg BID (94). These differences in tolerable dose may have been related with long-term sorafenib exposures (i.e., cumulative sorafenib exposures or steady-state pharmacokinetics), which was not assessed for these patients. The limitation of this study was that only two laboratory parameters (i.e., total bilirubin and AST) were considered to determine the functional state of the liver, as

against the five criteria (i.e., total bilirubin, serum albumin, INR, ascites and hepatic encephalopathy) used in Child-Pugh scoring system generally used to assess the severity of chronic liver disease. Further studies might be needed to better understand the impact of chronic hepatic impairment on long-term sorafenib exposures. Another study comparing the systemic exposure of sorafenib in patients with Child-Pugh A and B hepatocellular carcinoma, failed to find any statistical difference between two groups, although, the geometric mean for AUC_{0-8} and C_{max} were higher for patients with Child-Pugh B disease (44)(**section 1-2.2.6**). No dose adjustments were recommended for patients with renal impairment, which were not unexpected, given that only a small proportion (i.e., ~19%) of sorafenib is eliminated in urine as metabolites (33).

Patients in current analysis were genotyped for single nucleotide polymorphisms in metabolic enzymes for sorafenib, namely CYP3A4*1B, CYP3A5*3C, UGT1A9*3 and UGT1A9*5. In studied population, no one carried the variant allele for UGT1A9*5, hence it was not included in covariate analysis. CYP3A4*1B and CYP3A5*3 were not related with sorafenib pharmacokinetics. These results were in agreement with findings from a clinical study where co-administration of ketoconazole, a potent CYP3A4 inhibitor, had no significant effect on sorafenib pharmacokinetics (37). UGT1A9*3 was significant for both CL/F and V/F in third step of covariate analysis, but its impact on these pharmacokinetic metrics could not be studied because very few patient carried the homozygous or heterozygous variant genotype. This polymorphism also appeared to be important during non-compartmental analysis, where the patient who carried the UGT1A9*3*3 genotype had significantly high AUC_{0-12} and C_{max} (between 90^{th}-100^{th}

percentile considering all patients), which was highest among patients with similar indication (mCRPC) (110). This polymorphism has been shown to result in reduced glucuronidation activity with only 3.8% glucuronidation activity for SN-38 in UGT1A9*3*3 genotype carriers compared to carriers of UGT1A9*1*1 genotype (75). Therefore, UGT1A9*3 polymorphism might be important for sorafenib disposition, but may not require clinical dose adjustments because of its low frequency and considering that toxicities associated with sorafenib treatment are not life-threatening.

In summary, this study presents a mechanism-based population pharmacokinetic model of sorafenib in patients with various solid tumors. This is the only report where pharmacokinetic model based on prior understanding of sorafenib disposition has been developed; therefore results of this analysis are important addition to our current knowledge of sorafenib pharmacokinetics. Body weight was found to be a statistically significant covariate for volume of distribution, but its clinical relevance was minimal. Genetic variation in CYP3A4 and CYP3A5 did not appear to alter the sorafenib disposition. The UGT1A9*3 polymorphism might be an important determinant for sorafenib pharmacokinetics, but this effect needs further evaluation in a prospective clinical trial.

CHAPTER FIVE

EVALUATION OF EXPOSURE-EFFICACY RELATIONSHIP, AND LABORATORY MARKERS FOR EFFICACY IN SOLID TUMOR PATIENTS TREATED WITH SORAFENIB

5-1 Introduction

A major goal of cancer therapy has been to obtain adequate clinical efficacy at the expense of tolerable toxicity. Biomedical scientists have long sought to identify the optimal therapy for individual patients – also known as personalized medicine. It will be easy to realize these goals if we have a quantitative exposure-response relationship or if validated markers are available to make predictions about response based on patient characteristics prior to start of therapy or in early stages of treatment.

Because of heterogeneity among different cancer types and patients, most cancer treatments are only effective in a minority (selected group) of patients undergoing therapy. Thus, there are great challenges and tremendous opportunities to improve the treatment outcome by discovering new treatment approaches, possibly involving the use of biomarkers / surrogate efficacy markers / surrogate toxicity markers / prognostic disease markers / pharmacogenetic markers etc. that will help in prediction of the right dose for right patient at right time. A biomarker is defined as any characteristic that can

be objectively measured and evaluated to indicate the normal biological or pathological process, or pharmacological response to a therapeutic intervention, and has putative diagnostic or prognostic value (111).

Several such markers have been described in literature and included in drug prescribing information. These markers are generally identified by assessment of exposure-response relationships and by correlative studies for response variables. In oncology; however, most of the studies are focused on assessment of exposure-toxicity relationships, and only few have studied the impact of exposure on activity of an agent or efficacy. One such example is association of steady-state concentrations of methotrexate with therapeutic outcome in pediatric patients with acute lymphoblastic leukemia (ALL). Monitoring of steady-state drug concentrations and dose adjustments based on that were helpful in improving the treatment outcome (86). Robert and colleagues reported a linear relationship between plasma doxorubicin exposures and short-term tumor response in patients with breast cancer (112). Santini and colleagues demonstrated a trend of higher 5-FU exposure in patients with complete response. A threshold exposure was identified which was later used to determine the 5-FU dosage in a prospective study. Patients who received the individualized dose had significantly better response rate than the group receiving the standard dose of 5-FU (47% complete response vs. 31%) (113). These examples highlight the importance of conducting the exposure-efficacy analysis.

With advent of new targeted anticancer therapies use of molecular markers has become usual in identifying the likely responders to selected agents. Few examples of such anticancer agents are listed in **Table 1-1**. One example of molecular markers for efficacy

is the expression of ERCC1 mRNA along with thymidylate synthase, which was identified as an independent predictive marker of survival for 5-FU/oxaliplatin chemotherapy ($p<0.001$) (114). Pharmacogenetic markers are also being increasingly used to individualize the treatment.

As described in **chapter 1, sections 1-2.4 and 1-2.5**, sorafenib treatment is associated with huge inter-patient variability in treatment outcome or efficacy, which may be caused by high variability in plasma drug concentrations and/or other factors such as pharmacogenetic variation. In order to maximize the efficacy and improve overall treatment outcome, we assessed the impact of exposure on efficacy, and explored pharmacogenetic and laboratory markers for efficacy. The results of association of pharmacogenetic variation and efficacy are described in chapter 7. Other efficacy markers evaluated are described below:

i. use of prostate specific antigen (PSA) as a surrogate end point of efficacy in patients with mCRPC treated with sorafenib, and
ii. use of *ex-vivo* anti-angiogenic activity for patient's steady-state serum samples as a marker of clinical outcome in patients treated with sorafenib and bevacizumab combination

The methodologies used for these analyses along with results are described in this chapter.

5-2 Evaluation of exposure-efficacy relationship

5-2.1 Methods

5-2.1.1 Patients and study design

Data from 104 patients enrolled in phase II trial in mCRPC, phase II trial in NSCLC, phase II trial in CRC and phase I trial in ST were included in exposure-efficacy analysis. These patients were also a part of population pharmacokinetic analysis, described in chapter 4. Exposure-efficacy evaluation was performed separately for each clinical trial to account for the differences in tumor type and treatment regimen. The dosing regimen and design of these phase I / II clinical trials are described in detail in **section 4-4.1**. The phase I trial in KS was not included in this analysis, because, at the time of this analysis, only eight patients have been enrolled in this trial: Two received only sorafenib, while the remaining six received sorafenib along with ritonavir.

5-2.1.2 Pharmacokinetic metrics

The sorafeinb exposures (AUC = Dose/(CL/F)) calculated from the individual predictions of systemic clearances (CL/F) from the final population pharmacokinetic model were used to evaluate the exposure-efficacy relationships. Single-dose exposures were predicted for the 400 mg dose for patients with mCRPC, CRC and NSCLC, and for the 200 mg dose for patients enrolled in ST trial. In case of dual therapy, exposures of the co-administered agents (i.e., bevacizumab or cetuximab) were not available for use in evaluation of the exposure-efficay relationships.

5-2.1.3 Efficacy metrics

Treatment response, measured using the response evaluation criteria in solid tumors (RECIST), and the duration of progression-free survival (PFS) were used as efficacy metrics. Treatment responses were determined based on the change in tumor dimensions

and were divided into five groups – CR, PR, PD, not evaluable/refused further treatment (NE) and death. PFS was defined as the duration for which disease did not progress based on clinical (symptomatic/radiological/molecular) end points from the start of treatment.

5-2.1.4 Statistical analysis

Patients from each trial were divided into four exposure groups which were created based on the four quartiles of the sorafenib AUC distribution. Incidence rates (%) of clinical responses (CR, PR and PD) were compared among these exposure quartiles, separately for each clinical trial. Direct correlations between AUC and PFS were also assessed. The statistical analyses were performed using JMP 8.0 (SAS Institute Inc., Cary, NC, USA) statistical software.

5-2.2 Results

The observed best response for solid tumor patients treated with sorafenib as a single agent or in combination therapy is summarized in **Table 5-1**. Sorafenib had moderate activity in patients with mCRPC, with a median PFS of 3.7 months and median overall survival time of 18.3 months for a median follow-up for 27.2 months (110). Sorafenib appeared to benefit patients with NSCLC with upto 50% of treated patients responding with partial response or stable disease. Combination therapy with sorafenib and bevacizumab had promising clinical activity in patients with solid tumors including the ovarian cancer (N=13), renal cell carcinoma (N=3), melanoma (N=7), colon cancer (N=2), sarcoma (N=5) and others (N=9) (115). Six of thirteen ovarian cancer patients (i.e. 46%) had PR and three (i.e. 23%) had disease stabilization for at least 4 months (115).

This combination is further being evaluated in a phase II clinical trial in patients with ovarian cancer (115). Another combination therapy trial, involving sorafenib and cetuximab, also appeared to have significant activity in patients with CRC, where eleven of the fourteen evaluable patients (78.6%) had PR or SD. So far only few patients were enrolled in KS trial; hence, it was not possible to make conclusions about sorafenib's efficacy in those patients.

Overall, it appears that the combined inhibition of multiple proteins in signaling pathways shows better clinical activity than treatments with single agents alone. However, the incidence of treatment-associated toxicities may also increase with combination therapy, hence, assessment of benefit-risk ratio for each individual patient, based on their characteristics, is important in order to achieve the optimal therapeutic benefit. Results of exposure-efficacy analysis for each clinical trial are separately discussed in following sections.

Table 5-1 Summary of best clinical response for solid tumor patients treated with sorafenib alone or in combination with other agents

Tumor type	**Treatment**	**N**	**Best clinical response %, (N)**					
			PR	**SD**	**PD**	**REF/Not assessable**	**Death**	**Response not available**
mCRPC	Sorafenib	46	2 (1)	43 (20)	35 (16)	13 (6)	2 (1)	4 (2)
NSCLC	Sorafenib	18	11 (2)	39 (7)	50 (9)	0 (0)	0 (0)	0 (0)
ST	Sorafenib + bevacizumab	28	18 (5)	61 (17)	14 (4)	4 (1)	0 (0)	4 (1)
CRC	Sorafenib + cetuxiamb	18	6 (1)	56 (10)	17 (3)	6 (1)	0 (0)	17 (3)
KS	Sorafenib +/- ritonavir	8	25 (2)	38 (3)	13 (1)	25 (2)	0 (0)	0 (0)

mCRPC: metastatic castrate resistant prostate cancer; **NSCLC**: non-small cell lung-cancer; **ST**: solid tumors; **CRC**: colorectal cancer; **KS**: Kaposi's sarcoma; **PR**: partial response; **SD**: stable disease; **PD**: progressive disease; **REF**: refused further treatment

5-2.2.1 Phase II trial in patients with mCRPC treated with sorafenib as a single agent

Results of exposure-efficacy analysis for patients with mCRPC are shown in **Fig. 5-1 and 5-5**. No major change in frequency of SD was observed with increase in exposure from the lower to the upper quartile, as shown in **Fig 5-1**. Incidence rate of PD declined and refusals of treatment were unaltered from 2nd to 4th exposure quartile, and one patient with exposure in 4th quartile expired on the trial. This patient was 85 years old, with a pre-existing cerebrovascular accident within the past 5 years, and was on study for only 20 days when he had a recurrent haemorrhagic cerebrovascular accident (110). Notably, this patient was one among the three who had relatively high sorafenib exposures in mCRPC trial. No significant correlation was observed between AUC and PFS (**Fig 5-5 (A)**). These results suggest a lack of exposure-efficacy relationship in mCRPC patients treated with sorafenib.

5-2.2.2 Phase II trial in patients with NSCLC treated with sorafenib as a single agent

The exposure-efficacy analysis results for patients with NSCLC are shown in **Fig 5-2 and 5-5**. No change in PR, increase in SD and decrease in PD was observed with an increase in sorafenib exposure from the lower quartile to the upper quartile, as shown in **Fig 5-2**. These observations were indicative of a positive exposure-efficacy relationship; however, the sample size in these groups was too small to draw definitive conclusions. The lack of correlation between AUC and PFS (**Fig 5-5 (B)**) also fails to demonstrate a favorable exposure-efficacy relationship based on **Fig 5-2**. The exposure-efficacy

relationship in patients with NSCLC needs to be evaluated with a larger sample size. This trial is currently (after this analysis) enrolling patients with a targeted accrual of 37 patients.

5-2.2.3 Phase I trial in patients with ST treated with sorafenib and bevacizumab in combination

In patients with ST treated with sorafenib and bevacizumab combination, we observed no significant change in PR, SD and PD across sorafenib's exposure quartiles, as shown in **Fig 5-3**. Also, PFS was not significantly correlated with AUC of sorafenib for these patients (**Fig 5-5 (C)**). The exposures of sorafenib appeared not to be associated with efficacy in patients with ST, following treatment with the sorafenib and bevacizumab combination. Note that addition of bevacizumab had improved the response rate of sorafenib. Hence, a non-significant relation of only sorafenib exposure with efficacy is not unlikely. A surrogate marker of efficacy, accounting for both sorafenib and bevacizumab exposures, would possibly be a better predictor of treatment outcome. We evaluated *ex-vivo* anti-angiogenic activity using patient serum samples, a laboratory marker assumed to account for both sorafenib and bevacizumab exposures, as one potential surrogate of clinical response, which is described in **section 5-3**.

5-2.2.4 Phase II trial in patients with CRC treated with sorafenib and cetuximab in combination

For patients with CRC, with increase in sorafenib exposure, we observed no change/decrease in SD, increase in PD and one treatment refusal (**Fig 5-4**), which is the

opposite of what would be expected in a positive exposure-response relationship. Also the sorafenib AUC was not predictive of PFS (**Fig 5-5 (D)**). These results suggest a lack of significant association between sorafenib exposure and efficacy for patients with CRC treated with sorafenib and cetuximab combination. Again, we need to identify some surrogate markers accounting for both sorafenib and cetuximab exposures, for an appropriate assessment of the true, underlying exposure-efficacy relationship. Note that addition of cetuximab to sorafenib also appears to increase the response rate compared to the historical 10% response rate with only cetuximab (27).

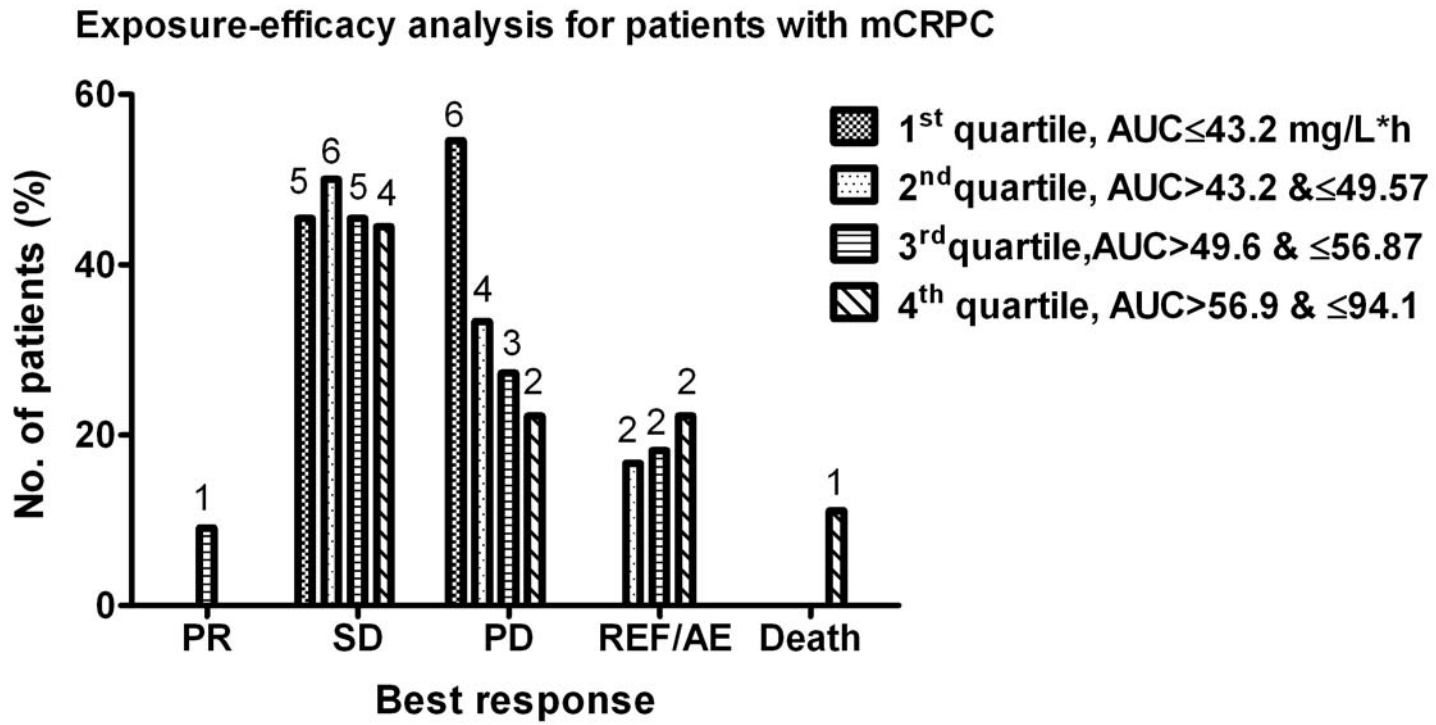

Fig 5-1 Evaluation of exposure response relationship for patients with metastatic castrate resistant prostate cancer (mCRPC) following treatment with single agent sorafenib

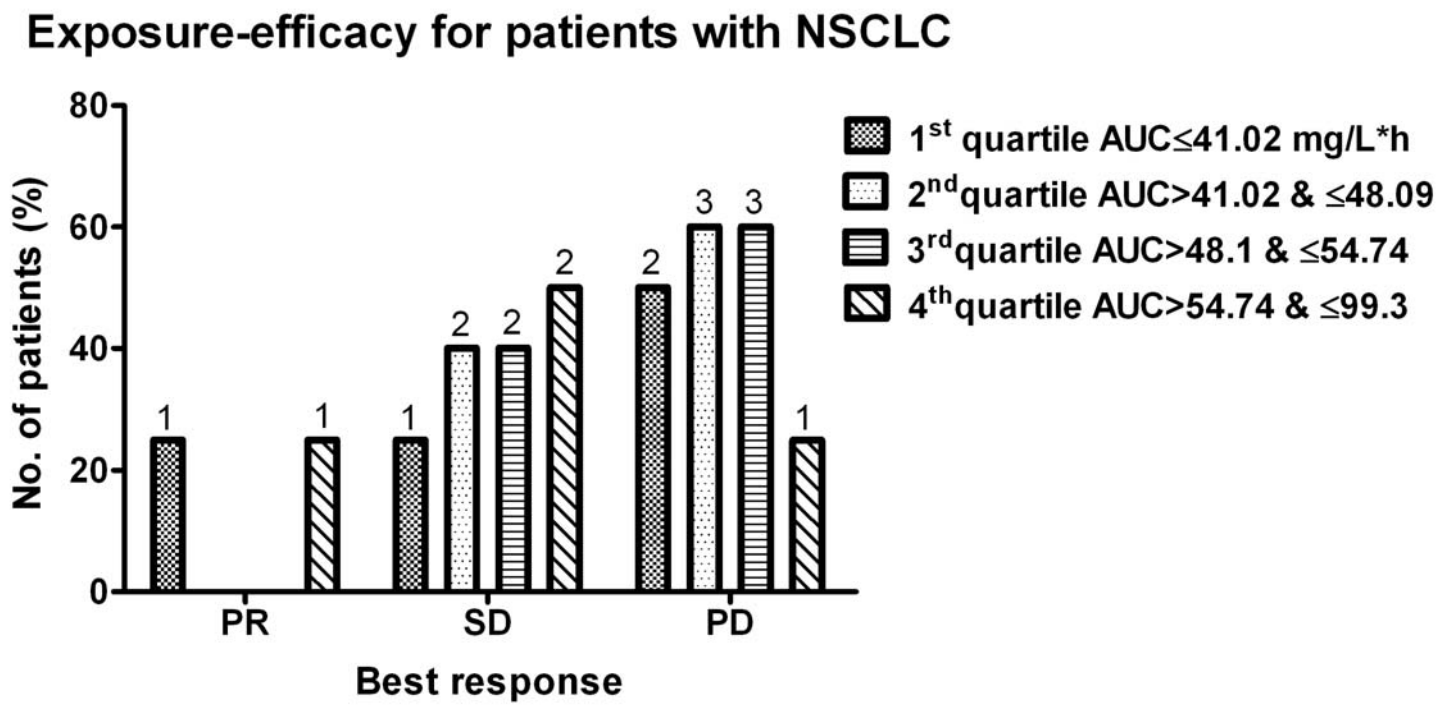

Fig 5-2 Evaluation of exposure response relationship for patients with non-small cell lung cancer (NSCLC) following treatment with single agent sorafenib

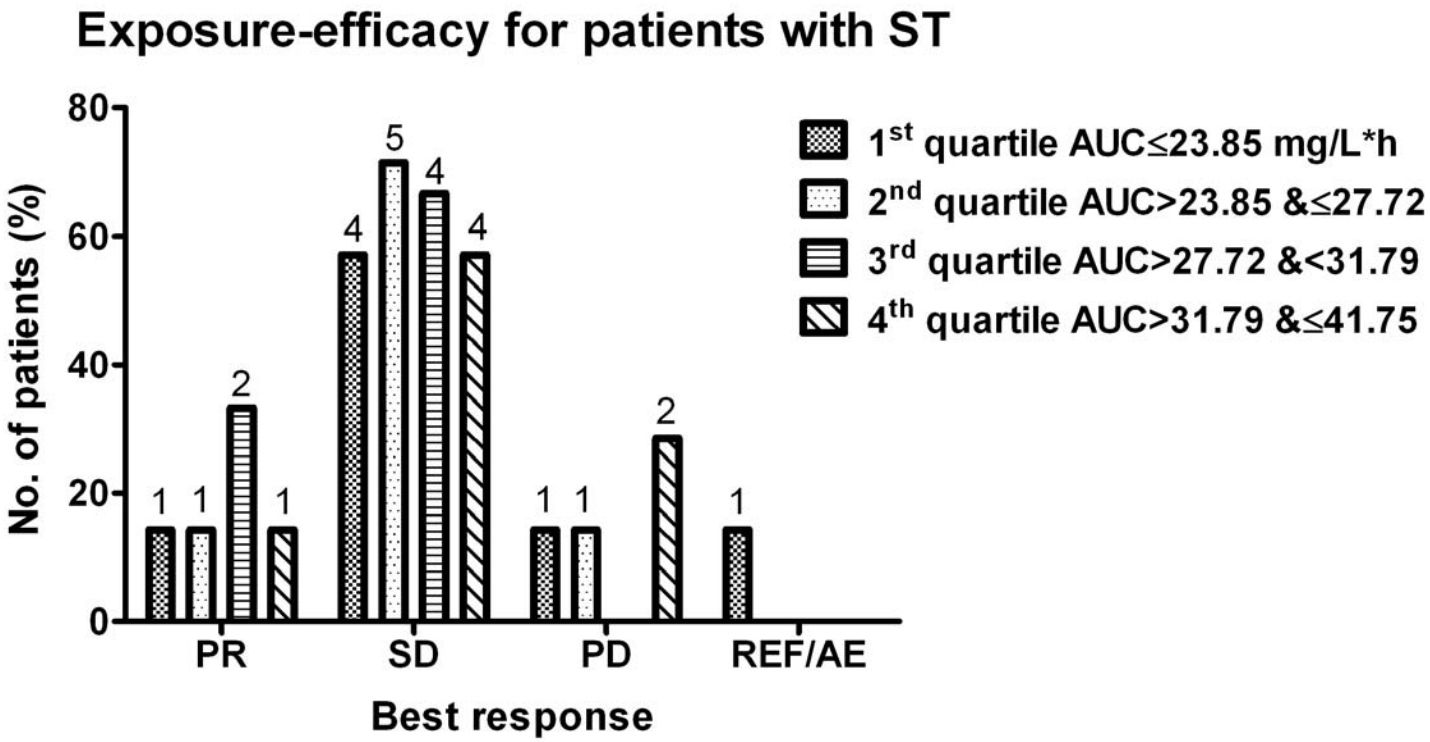

Fig 5-3 Evaluation of exposure response relationship for patients with solid tumor (ST) following treatment with sorafenib and bevacizumab combination

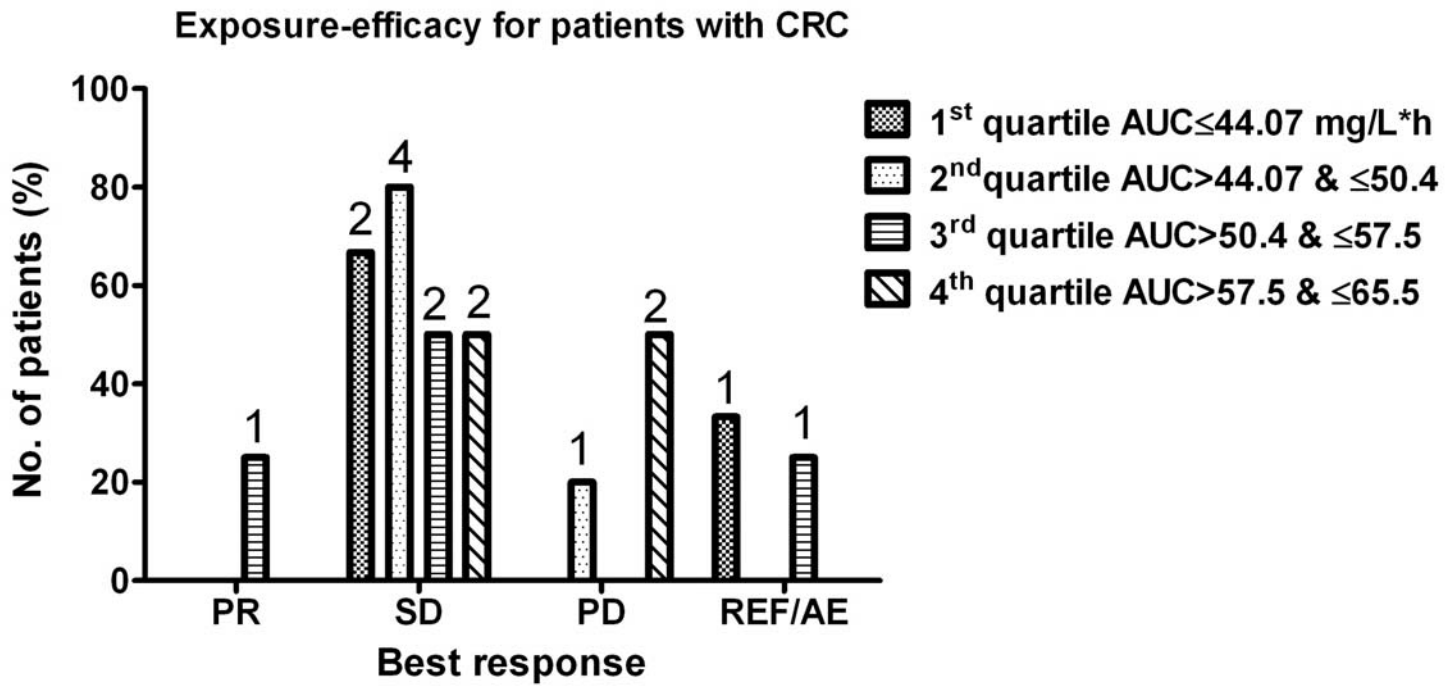

Fig 5-4 Evaluation of exposure response relationship for patients with colorectal cancer (CRC) following treatment with sorafenib and cetuximab combination

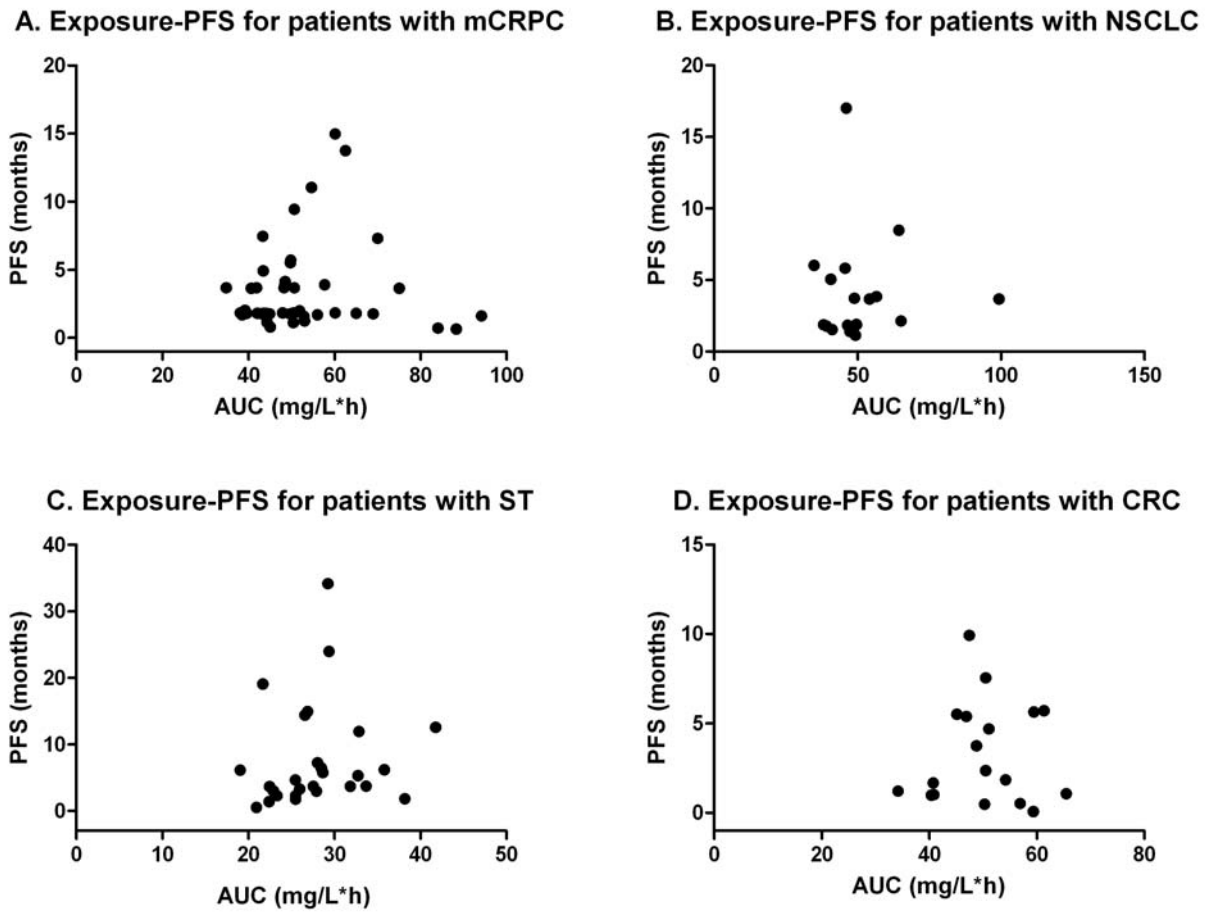

Fig 5-5 Evaluation of correlation between exposure (AUC) and progression free survival (PFS) for patients with **(A)** metastatic castrate resistant prostate cancer (mCRPC), **(B)** non-small cell lung cancer (NSCLC), **(C)** solid tumors (ST) and **(D)** colorectal cancer (CRC)

5-2.3 Conclusions

Sorafenib was found to have moderate efficacy in patients with mCRPC. Addition of bevacizumab and cetuximab appears to have a synergistic effect on sorafenib's efficacy. The combination of agents with the activity against upstream and downstream targets in the same signaling pathway seems to result in better treatment outcomes than single-agent treatment. However, the frequency of treatment-associated toxicities may also increase. Sorafenib's activity in NSCLC cannot be determined definitively because of the small sample size of the trial. Further evaluation with a larger sample size is required.

No significant exposure-efficacy relationship was observed based on sorafenib exposures for trials studying the patients with mCRPC, CRC and ST. It is less likely to explain the differences in response by exposure of just one drug, when patients are treated with more than one drug. A combined exposure metrics or a surrogate marker accounting for exposure of all the administered agents would be more useful. Patients with NSCLC had higher incidences of stable disease and reduced numbers of progressive disease, with increase in sorafenib exposure. But data from only 18 patients were evaluable, which weakens the credibility of these results and requires further evaluation with a larger number of subjects. The results of these exposure-efficacy analyses may not be conclusive, because of (i) lack of random assignment for exposures, and (ii) lack of clear evidence for sorafenib's activity in studied indications. An exposure-efficacy analysis for sorafenib could be performed for tumor types for which there is a clear evidence of sorafenib's activity (with a known plausible mechanism of action), by enrolling the

patients prospectively, and by their random assignment into different dose/exposure groups followed by comparison of response rate in these groups.

Sorafenib is a cytostatic agent, which requires long-term administration to achieve therapeutic benefit. For such agents, there is a low probability of significant correlation between exposure after a single-dose and treatment outcome. Alternative metrics such as cumulative dose or cumulative drug exposure would possibly be a better predictor of clinical response. However, the disadvantage of using these metrics would be that their correlation with PFS will not be informative, because it will always be forced positive, such as patients with longer PFS would always have longer duration on treatment and higher cumulative dose or cumulative drug exposure.

Another reason for the lack of exposure-efficacy relationship in cancer patients is that, it is a heterogeneous disease with significant inter-patient variability in tumors, which may also vary considerably in their responsiveness towards treatments.

5-3 *Ex-vivo* anti-angiogenic activity as a biomarker of clinical response

5-3.1 Introduction

A correlative study was conducted to study the association of *ex-vivo* anti-angiogenic activity for steady-state serum samples from patients on sorafenib and bevacizumab combination and observed best clinical response. It was hypothesized that patients with higher steady-state concentrations of these drugs will likely have better clinical response, assuming no major differences in responsiveness for this drug combination between

subjects. If these steady-state serum samples were to be used for *ex-vivo* angiogenesis assay (rat aortic ring assay), we would also observe a higher percent anti-angiogenic activity for samples with high drug concentrations and vice versa. Hence, the percent anti-angiogenic activity in this assay could possibly predict the clinical response, assuming no significant difference in responsiveness towards sorafenib and bevacizumab combination between rat aortas and human endothelial cells (**Fig 5-6**). For example, a patient with higher steady-state drug concentrations would be expected to have a better clinical response, and serum samples from these patients will also possibly show a higher percent anti-angiogenic activity in *ex-vivo* assay. If this hypothesis were to prove true, it would be possible to predict the clinical response based on activity in *ex-vivo* assay, which may also guide the dose adjustments to achieve the optimum therapeutic outcome.

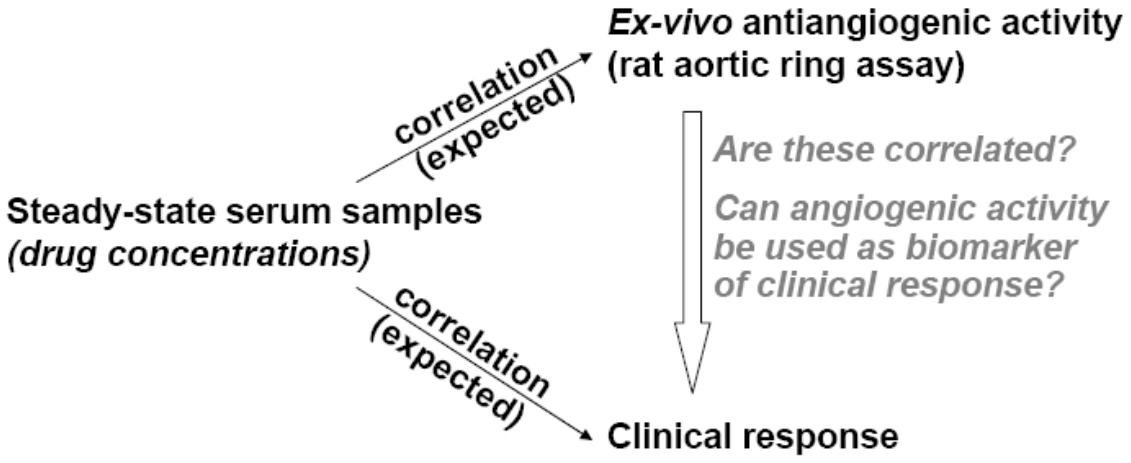

Fig 5-6 Illustration of hypothesis for testing the ex-vivo anti-angiogenic activity as biomarker of clinical response

Ex-vivo Rat aortic ring assay was originally developed by Nicosia and colleagues (116). It combines together the advantages of both the *in-vitro* and *in-vivo* systems. This assay

avoids the effect of inflammatory reactions seen in *in-vivo* assays (117) and makes it possible to collectively examine the different stages of angiogenic development, which is difficult to monitor with *in-vitro* system (118). In addition, multiple assays can be conducted per animal (117). This assay has previously been used with human serum samples to study the effect of protein binding on anti-angiogenic activity of suramin, carboxyamidotriazole and UCN-01 (119). We used the same assay procedure (119) to test the current hypothesis.

5-3.2 Methods

5-3.2.1 Patients and samples

Baseline and steady-state serum samples from patients with solid tumors treated with sorafenib and bevacizumab combination were used to perform the rat aortic ring assay. Baseline samples were collected prior to start of treatment, and most of the steady-state samples were collected in treatment cycle 4, where each cycle was 28 days long. By cycle 4, steady-state for both sorafenib and bevacizumab were reached, based on their half-lives of 25-48 h (49) and 20 days (range 11-50 days) (120), respectively.

5-3.2.2 Rat-aortic ring assay

Twelve-well tissue culture grade plates were covered with 250 μL of Matrigel and allowed to gel for 30 to 45 min at 37 °C, 5%CO_2. Thoracic aortas were excised from 8-10 week old male Sprague Dawley rats, and the fibroadipose tissue was removed. 1 mm long cross-sections of aorta were cut and placed in the center on the Matrigel coated wells. These were then covered with an additional 250 μL of Matrigel and allowed to gel for

additional 30 to 45 min at 37 °C, 5%CO_2. The rings were cultured for 24 h in 1 mL of EGM-II medium, which is a mixture of EBM-II medium (endothelial cell basal medium) and growth factors provided in the EGM-II Bullet kit (Cambrex Bio Science, Walkersville, MD). After 24 h, the medium was aspirated out and replaced with 1 mL of control or patient serum. Negative and positive control rings were treated with control serum containing 0.05% DMSO and 240μg/mL CAI, respectively. Serum samples from patients with solid tumors, collected at baseline and steady-state (for both sorafenib and bevacizumab) were used for the analysis. Sorafenib was stable for at least 4 days, the duration of assay, under incubator conditions; hence, the cells were treated only once. After 4 days of incubation with patient serum samples, on day 5, supernatant was removed and rings were pictured. The angiogenic vascular outgrowth was quantified in pixel counts using Adobe Photoshop (Adobe systems, Inc., San Jose, CA). The percentage inhibition was calculated as the ratio of growth for steady-state serum samples to that of growth for baseline serum samples. The ex-vivo anti-angiogenic activity was then used as an assessment of the relationship with clinical response.

5-3.2.3 Statistical analysis

The anti-angiogenic activity between different clinical response groups was compared using one-way ANOVA. The anti-angiogenic activity was considered as a marker of serum drug concentrations for the active circulating moieties; hence, the direct correlation between sorafenib exposures and anti-angiogenic activity was also assessed using linear regression. The bevacizumab exposures were not available to conduct the similar exposure-activity assessment. We also compared the sorafenib exposures between

clinical response groups using one-way ANOVA, to examine whether serum concentrations between these groups were considerably different to translate into significant differences in *ex-vivo* anti-angiogenic activity. The statistical analyses were performed using JMP 8.0 (SAS Institute Inc., Cary, NC, USA) statistical software.

5-3.3 Results and Discussion

The *ex-vivo* anti-angiogenic activity (or percent angiogenic inhibition) and clinical response for solid tumor patients treated with sorafenib in combination with bevacizumab are shown in **Table 5-2**. As shown in **Fig 5-7**, the *ex-vivo* anti-angiogenic activity ranged from 10 to 75%; and no specific cut-off for percent angiogenic inhibition was apparent, which would result in a favorable clinical response (stable disease or partial response), at least based on patients included in this analysis. Also, the association between percent angiogenic inhibition and observed best clinical response was not statistically significant (p=0.58).

The sorafenib exposures after the first dose were not related with the *ex-vivo* anti-angiogenic activity calculated using corresponding sorafenib/bevacizumab steady-state samples (**Fig 5-8**). Comparison of sorafenib exposures between clinical response groups revealed marginally significant differences in mean exposures for PR, SD and PD groups (p=0.045; **Fig 5-9**). Tukey's HSD test showed that the exposures between only PR and SD groups were statistically different, and both of them were not significantly different from the PD group. There were only three patients in the PR group and the higher mean

for this group was driven by only one patient. Hence, it was difficult to conclude the relationship between exposure and efficacy based on limited sample size.

Table 5-2 Summary of results for *ex-vivo* anti-angiogenic activity, clinical response and sorafenib exposures for solid tumor patients treated with sorafenib and bevacizumab

Pt Id	% Angiogenic Inhibition (*ex-vivo*)[†]	Best clinical response	Sorafenib AUC_{0-12} (mg/L*h), *in-vivo*
1	29.15	SD	17.33
2	28.57	SD	4.61
3	10.47	PR	14.49
4	56.87	SD	3.06
5	10.76	PR	17.43
6	21.02	SD	4.04
7	20.10	SD	11.7
8	24.31	SD	7.03
9	11.48	SD	7.89
10	44.71	SD	17.18
11	11.27	SD	4.49
12	*	SD	14.72
13	*	PR	
14	*	SD	12.81
15	11.17	SD	1.26
16	75.27	SD	13.71
17	21.01	SD	18.68
18	13.77		
19	46.11	PR	39.72

[†] % angiogenic inhibition = (pixel counts for ring with steady-state serum sample/pixel counts for ring with baseline serum sample)*100
*There were technical problems with the rings from these patients.
SD, stable disease; PR, partial response; AUC_{0-12}, area under the curve after first dose of sorafenib, calculated by non-compartmental analysis

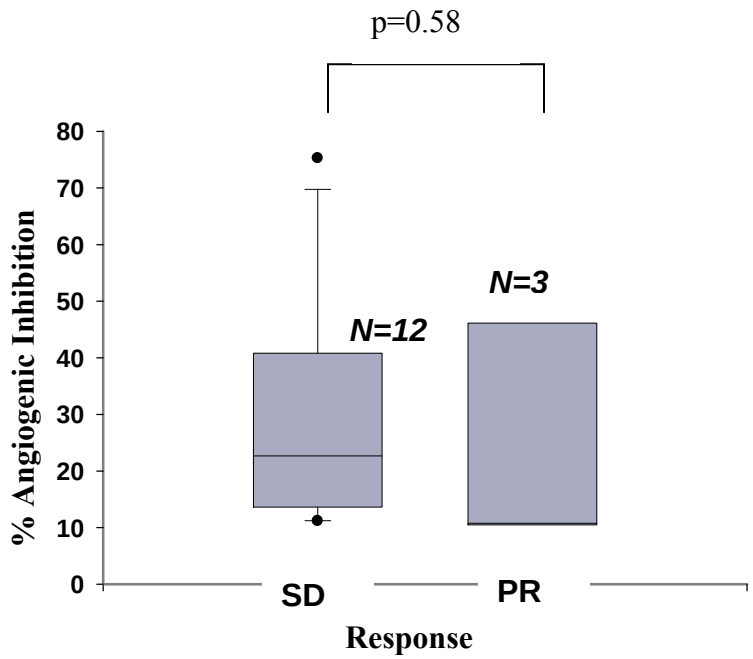

Fig 5.7 Box plot comparing the *ex-vivo* anti-angiogenic activity for patients with stable disease (SD) and partial response (PR).

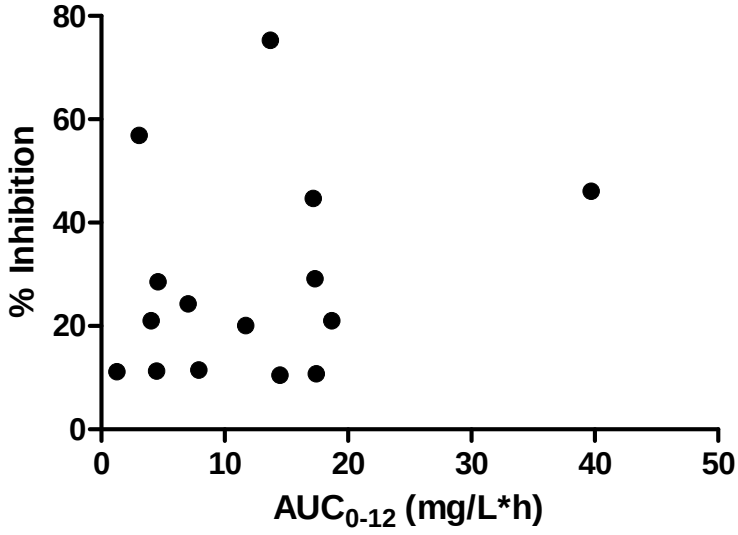

Fig 5-8 Assessment of relationship between sorafenib exposures after first dose (AUC_{0-12}, calculated by non-compartmental analysis) and *ex-vivo* anti-angiogenic activity for corresponding steady-state samples

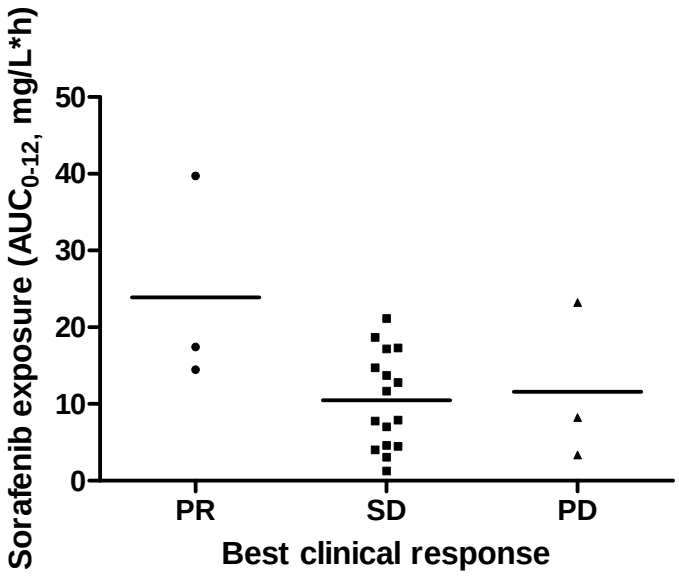

Fig 5-9 Distribution of sorafenib exposures for different clinical response groups. (PR: Partial response; SD: stable disease; PD: progressive disease)

5-3.4 Conclusions

We evaluated *ex-vivo* anti-angiogenic activity for patient serum samples in rat aortic ring assay as a (laboratory) biomarker of clinical response. The *ex-vivo* anti-angiogenic activity was not apparent to be predictive of clinical outcome, at least based on available limited data. This *ex-vivo* anti-angiogenic activity for steady-state serum samples from patients treated with sorafenib and bevacizumab combination was also not apparently associated with only sorafenib exposures after first dose. Sorafenib exposures between different clinical response groups were also not statistically different. The major limitation of these correlative studies is the small sample size.

In addition to the earlier described advantages of the rat-aortic ring assay (**section 5-3.1**), there are few limitations to its use which might have partly influenced the results.

Animals may have inherent variability among themselves in responsiveness towards drugs. Drug responsiveness between animals and humans may also vary, which might mask the true correlation between this laboratory marker and clinical response. Also, technical variability in implementation of this assay, may introduce some inconsistencies between experiments.

5-4 Prostate specific antigen as a marker of efficacy in mCRPC patients treated with sorafenib

5-4.1 Introduction

Prostate cancer is the second leading cause of death by cancer among men in the United States. In 2009, number of prostate cancer cases are expected to be 192,280 and of them approximately 27630 will succumb to death because of disease (13). Patients with prostate cancer initially respond well to hormonal and radiation therapy, but unfortunately, most of them eventually become resistant. After a median duration of 18-24 months on androgen deprivation therapy, tumor growth in these patients with metastatic disease becomes androgen-independent (121). This stage of disease is commonly referred to as 'hormone refractory prostate cancer (HRPC)' or 'metastatic castrate-resistant prostate cancer (mCRPC)'.

Only limited treatment options are available for patients with mCRPC. In 2004, the FDA approved docetaxel in combination with prednisone as first-line chemotherapy for mCRPC. Docetaxel 75 mg/m^2 administered IV every 21 days and oral prednisone twice a day offered a statistically significant survival advantage over the mitoxantrone and

prednisone combination (18.9 vs. 16.5 months) (89). However, this regimen is not universally effective, and nearly all patients have tumor progression after docetaxel treatment (89). There is urgent need to identify new therapeutic options (second-line therapies) for these patients. Molecularly targeted therapies have emerged as potential drug candidates with shift in focus of drug discovery from conventional cytotoxic drugs towards rationally designed targeted therapies with activity against cancer-specific pathways.

Angiogenesis has shown to play an important role in several human cancers including the breast, non-small cell lung, colorectal and prostate cancers (122-125). Angiogenesis is a fundamental event in tumor growth and metastatic dissemination. Simultaneous blocking of cell growth and angiogenesis by inhibition of Ras/Raf kinases and VEGF signaling by sorafenib has been considered as a potential method to restrict the growth of prostate tumors. To evaluate the efficacy of sorafenib as a second-line treatment for mCRPC, a phase II trial was initiated at NCI, Bethesda, MD, USA (83). Three other phase II trials, conducted in Iran, Europe and Canada, also assessed the role of sorafenib in the treatment of patients with mCRPC (56, 126, 127). All four trials had prostate specific antigen (PSA) as one of the determinants for primary end point. Sorafenib was reported to have limited activity as second line treatment in mCRPC, and almost half of the patients on sorafenib trials showed an increase in PSA concentrations while undergoing treatment. Historically, PSA concentrations have been shown to decline after treatment with cytotoxic agents and have long been used as a surrogate endpoint to evaluate the efficacy of these agents in mCRPC (128). Many published studies have noted a survival

advantage for patients with a >50% post-treatment decline in serum PSA levels (129) and its levels were also found to correlate with the tumor stage (130). Contrary to the conventional therapies, serum PSA concentrations increased following treatment with sorafenib. However, of note, serum PSA concentrations for these patients declined after discontinuation of sorafenib therapy (83, 126). Clinical responses for some of these mCRPC patients on sorafenib trials were also in disagreement with PSA responses.

In the first stage of a mCRPC trial at NCI we observed an increase in PSA concentrations from baseline after the first cycle of treatment for seventeen of the twenty-two enrolled patients. Thirteen of the twenty-one evaluable patients progressed only by PSA criteria and PSA concentrations for six of them declined after discontinuation of sorafenib (in absence of initiating another treatment) (83). Also, two patients showed improvement in metastatic bone lesions despite of continuous increase in PSA levels after two and four cycles of sorafenib treatment (83). For one patient, the requirement of narcotics for pain management was significantly reduced (83).

Similar results about change in PSA concentrations following treatment with sorafenib in patients with mCRPC were reported by Chi and colleagues (126) which are shown in **Figures 5-10** and **5-11.** Notably, they also observed 7-52% decline in PSA levels in 10 of the 16 patients who did not receive any immediate treatment after discontinuation of sorafenib therapy (126). Another ten patients who received radiation therapy or chemotherapy had larger PSA decline of 14-91% (126).

These observations indicate that sorafenib may itself increase the PSA concentrations - independent of its effect on cellular-growth - and it may not be a suitable surrogate of efficacy in prostate cancer patients treated with sorafenib. We evaluated this hypothesis in *in-vitro* cell line experiments. Methods used for evaluation, observed results and their discussions are summarized in this section.

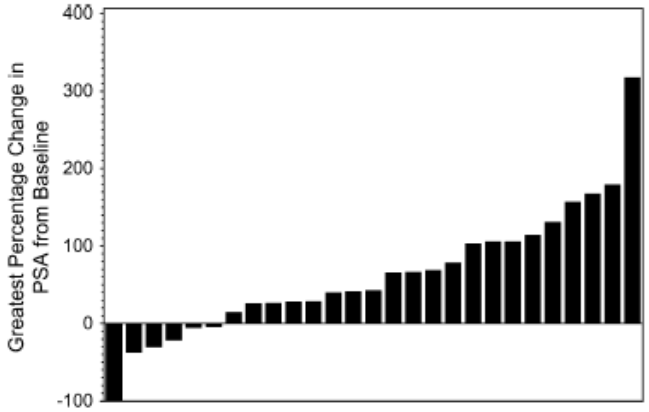

Fig 5-10 Plot of greatest percentage change in prostate-specific antigen (PSA) of individual patients while on sorafenib therapy (reproduced by permission of Oxford University press from Chi et al. (126))

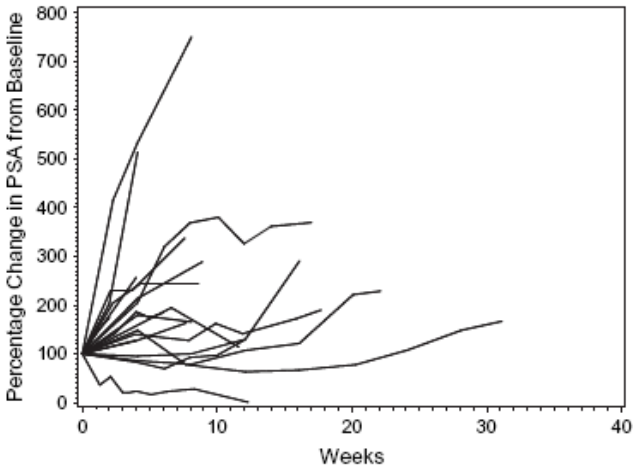

Fig 5-11 Plot of percent change in prostate-specific antigen (PSA) of individual patients over time while on sorafenib therapy (reproduced by permission of Oxford University press from Chi et al.(126))

5-4.2 Methods

5-4.2.1 Experimental procedure

The LNCaP human prostate carcinoma cell line was treated with RPMI medium containing sorafenib (freshly prepared dilutions). Final concentrations of sorafenib in the medium were 0, 2.5, 5 and 10 μM, which covered the range of measured peak plasma concentrations (C_{max}) for stage 1 of phase II trial in patients with mCRPC, i.e. 1.8-4.1 μM. The dilutions used to prepare these solutions are shown in **Table 5-3**. The treatment was repeated every 24 h until the final time points of 24, 48 and 72 h. For each concentration and each time point, cells were treated in quintuplicate. During repetition of treatment with sorafenib, the old medium was removed, and fresh medium containing sorafenib was supplemented. PSA levels in media supernatant were measured using PSA ELISA kit (Alpha diagnostic international, San Antonio, TX). Cell counts were performed with a Dojindo cell counting kit (Dojindo molecular technologies, Rockville, MD).

Table 5-3 Summary of dilutions for assessment of effect of sorafenib treatment on PSA release

Primary stock: 10 mM

Secondary stock: 500 µM (200 µL of 10 mM stock + 3.8 mL of media)

Day 1 (35 mL each of 2.5, 5 and 10 µM)

Concentration	Qty of 500 µM stock	Media	Total volume	% DMSO
DMSO only	175 µL of 100% DMSO	34 mL and 825 µL	35 mL	0.5 %
2.5 µM	175 µL	34 mL and 825 µL	35 mL	0.025%
5.0 µM	350 µL	34 mL and 650 µL	35 mL	0.05 %
10.0 µM	700 µL	34 mL and 300 µL	35 mL	0.10 %

Day 2 (25 mL each of 2.5, 5 and 10 µM)

Concentration	Qty of 500 µM stock	Media	Total volume	% DMSO
DMSO only	125 µL of 100% DMSO	24 mL and 875 µL	25 mL	0.5 %
2.5 µM	125 µL	24 mL and 875 µL	25 mL	0.025%
5.0 µM	250 µL	24 mL and 750 µL	25 mL	0.05 %
10.0 µM	500 µL	24 mL and 500 µL	25 mL	0.10 %

Day 3 (15 mL each of 2.5, 5 and 10 µM)

Concentration	Qty of 500 µM stock	Media	Total volume	% DMSO
DMSO only	75 µL of 100% DMSO	14 mL and 925 µL	15 mL	0.5 %
2.5 µM	75 µL	14 mL and 925 µL	15 mL	0.025%
5.0 µM	150 µL	14 mL and 850 µL	15 mL	0.05 %
10.0 µM	300 µL	14 mL and 700 µL	15 mL	0.10 %

5-4.2.2 Cell culture

The LNCaP cell lines were obtained from American Type Culture Collection (Manassas, VA, USA) and were grown in incubator at 37 ˚C, 5% CO_2 using the cell-culture procedure mentioned below. Approximately 50,000 cells were plated per 2 cm well in five, twelve-well tissue culture plates. When the wells were almost 60% confluent, the

cell medium was replaced with medium containing sorafenib. The layout of a tissue culture plate is shown in **Fig 5-12**.

Cell culture procedure:

a) Warm up RPMI medium, 0.25% trypsin and PBS in water bath.
b) Prepare 50 mL tube for 125 cm flask (1 tube for each flask).
c) Gently wash cells with medium in the flask and transfer the medium into 50 mL falcon tube.
d) Add 1-2 mL trypsin and incubate the flask for 5-10 minutes to segregate the cells.
e) Add 10 mL of medium to neutralize the trypsin and use 1 mL disposable pipette to separate the cells into single cells (by gently pipetting in and out). Transfer the medium into tube.
f) Centrifuge tube at 1000 rpm for 5 minutes at 4 ˚C.
g) Discard the supernatant.
h) Add 10 mL PBS to the pellet in bottom and centrifuge again.
i) Discard the supernatant.
j) Add 1 mL trypsin and mix cells gently with 1 mL pipette tip to segregate the cells.
k) Add fresh medium to neutralize the trypsin (medium : trypsin > 5:1).
l) Centrifuge tube at 1000 rpm for 5 minutes at 4˚C.
m) Discard the supernatant.
n) Add fresh medium to the tube and split the cells into new flasks (3 to 5 flask for one original flask).

The composition of RPMI medium used in above procedure was as below:

To 500 mL of RPMI medium following ingredients were added:

i. 2.8 mL of 45% glucose solution (RPMI stock contains 2 gm/L of glucose and we need to add additional 2.5 gm/L or 1.25 gm/500 mL)

ii. 5 mL of 1M HEPES

iii. 5 mL of 10 mM sodium pyruvate

iv. 50 mL fetal bovine serum

v. 5 mL penicillin streptomycin solution

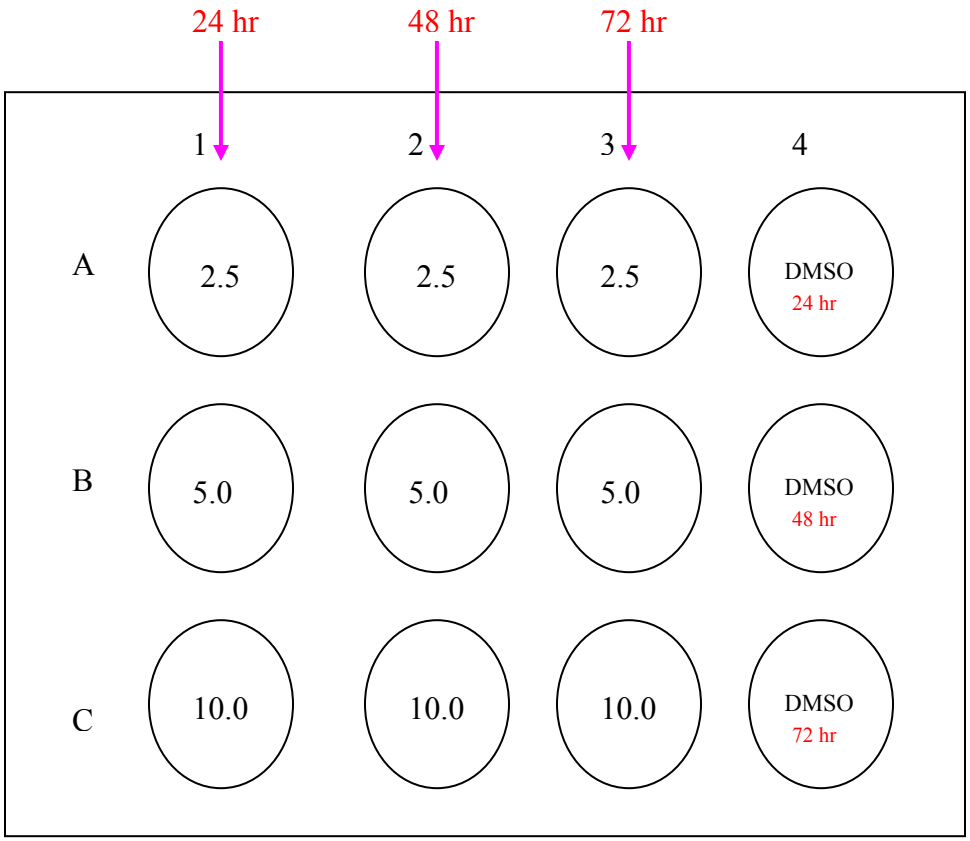

Fig 5-12 Layout of twelve-well tissue culture plate and allocation of samples

5-4.2.3 PSA quantification

Supernatant medium from cell culture plates were collected, and a 12.5 µL aliquot was mixed with 12.5 µL of fresh medium in Eppendorf tubes to dilute PSA concentrations, so that it falls into the range of the calibration curve for the PSA ELISA assay. Immediately after their collection, PSA levels in the supernatant were measured using the procedures for the PSA ELISA kit (131). A standard curve was run for each set of samples analyzed.

5-4.2.4 Cell counting

Cell counting was performed using the CCK cell counting kit (132). First, a reference standard curve was developed. Known cell counts of LNCaP cells were plated in twelve-well plates (2 mL/well). These cells were treated with 50 µL of CCK reagent and were incubated for 1 h at 37 ˚C, 5% CO_2. After 1 h, 200 µL of supernatant was transferred to a 96-well plate (in duplicate), and absorbance was read at 450 nm using the plate reader. A standard curve was constructed by fitting the measured absorbance against the nominal cell-counts using linear regression. Samples with unknown cell-counts were processed similar to the samples with known cell counts, and calibration curve was used to estimate the cell count against the measured absorbance.

5-4.3 Results and discussion

5-4.3.1 Standard curve for cell counting

Three replicates of cell counts ranging from 100 to 1,600,000 were treated with CCK cell counting reagent. The measured absorbance readings for these samples are listed in **Table 5-4.** The linear and polynomial standard curves for cell counting are shown in **Fig**

5-13 and **5-14**. Cell count predictions from either of these curves were almost the same for the range of data observed in this study. Predictions based on linear curves are reported in this chapter.

Table 5-4 Absorbance readings for construction of cell counting standard curve using CCK reagent

Plate	Cell count	Replicate 1			Replicate 2			Replicate 3		
		Absorbance 450 nm			Absorbance 450 nm			Absorbance 450 nm		
		CR† 1	CR 2	Average 1	CR 1	CR 2	Average 2	CR 1	CR 2	Average 3
1	100	0.189	0.187	0.188	0.188	0.187	0.188	0.191	0.197	0.194
1	500	0.172	0.184	0.178	0.175	0.178	0.177	0.185	0.195	0.190
1	1000	0.177	0.183	0.180	0.183	0.184	0.184	0.187	0.188	0.188
1	2000	0.177	0.188	0.183	0.179	0.203	0.191	0.186	0.190	0.188
1	5000	0.183	0.188	0.186	0.176	0.180	0.178	0.184	0.196	0.190
1	10000	0.187	0.194	0.191	0.185	0.188	0.187	0.203	0.196	0.200
1	20000	0.190	0.190	0.190	0.207	0.191	0.199	0.199	0.215	0.207
1	30000	0.192	0.201	0.197	0.188	0.194	0.191	0.205	0.214	0.210
1	40000	0.204	0.205	0.205	0.207	0.195	0.201	0.213	0.211	0.212
1	50000	0.208	0.212	0.210	0.210	0.209	0.210	0.219	0.219	0.219
1	60000	0.219	0.214	0.217	0.211	0.219	0.215	0.216	0.220	0.218
1	80000	0.226	0.225	0.226	0.219	0.228	0.224	0.239	0.238	0.239
2	75000	0.248	0.260	0.254	0.263	0.259	0.261	0.273	0.274	0.274
2	100000	0.321	0.271	0.296	0.270	0.263	0.267	0.281	0.278	0.280
2	150000	0.317	0.330	0.324	0.323	0.305	0.314	0.313	0.315	0.314
2	200000	0.320	0.322	0.321	0.344	0.335	0.340	0.379	0.367	0.373
2	400000	0.447	0.437	0.442	0.435	0.445	0.440	0.429	0.445	0.437
2	500000	0.571	0.560	0.566	0.607	0.595	0.601	0.544	0.540	0.542
2	600000	0.516	0.522	0.519	0.670	0.618	0.644	0.710	0.651	0.681
2	800000	0.635	0.666	0.651	0.714	0.737	0.726	0.776	0.814	0.795
2	1000000	0.801	0.761	0.781	0.841	0.844	0.843	0.853	0.877	0.865
2	1200000	0.856	0.930	0.893	0.984	0.883	0.934	1.038	1.075	1.057
2	1400000	0.951	0.969	0.960	1.059	1.037	1.048	1.184	1.129	1.157
2	1600000	1.117	1.076	1.097	0.972	1.055	1.014	1.182	1.203	1.193

†**CR:** counting replicate (for each well absorbance was measured twice)

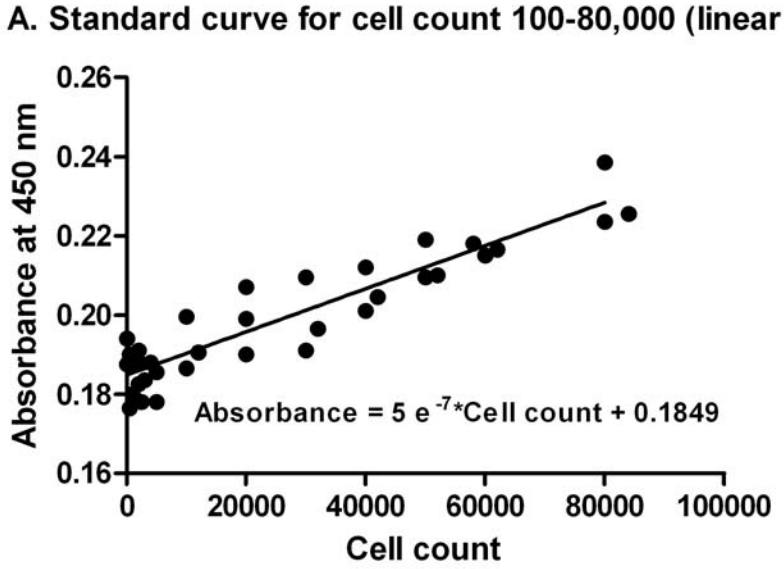

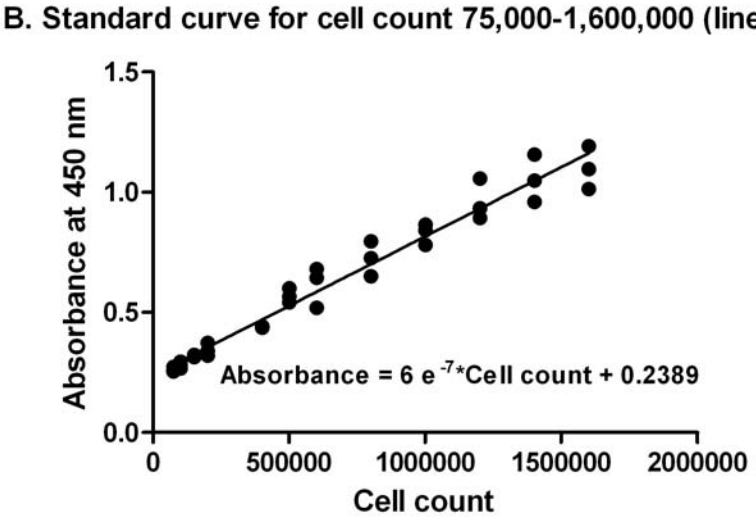

Absorbance	Equation to be used for back predictions
<0.1849	Below limits of quantification
≥0.1849 but <0.2389	$Y = 5\ e^{-7}\ X + 0.1849$
≥0.2389	$Y = 6\ e^{-7}\ X + 0.2389$

X: cell count; **Y**: absorbance

Fig 5-13 Linear fit for standard cell counting calibration curves for cell counts in range of (A) 100 to 80,000 and (B) 75,000 to 1,600,000

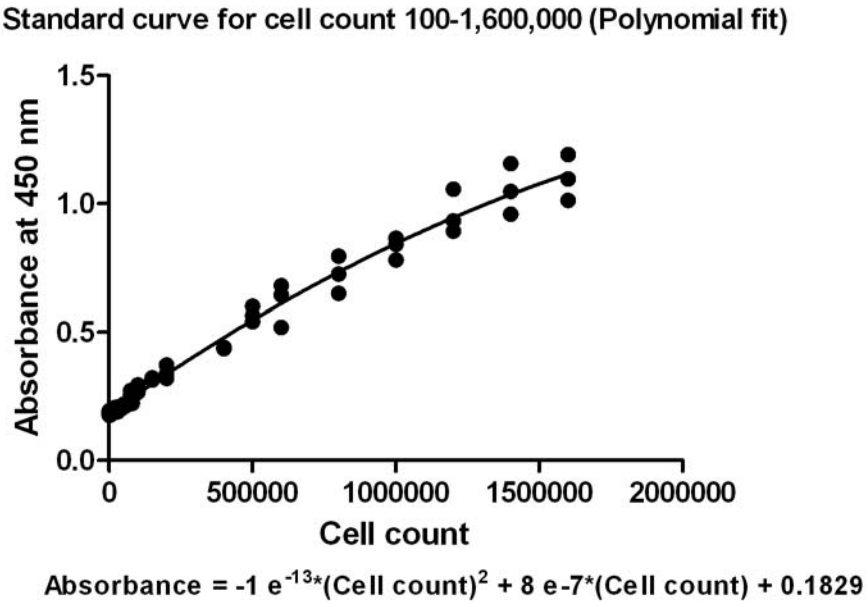

Fig 5-14 Polynomial fit for standard cell counting calibration curves for cell count in range of 100 –1,600,000

5-4.3.2 PSA quantification

The standard calibration curve for each day and PSA concentrations for sorafenib treated cell-supernatant samples are shown in **Figures 5-15, 5-16 and 5-17** and **Tables 5-5, 5-6 and 5-7**. The cumulative concentrations of PSA secreted from LNCaP cells following treatment with four different concentrations of sorafenib are shown in **Fig 5-18 (A)**. Cell count-normalized concentrations of PSA increased with an increase in sorafenib concentrations. Comparison of cell count-normalized PSA concentrations for each treatment duration, as shown in **Fig 5-18 (B)**, demonstrated that PSA secretion increased from the first treatment (0-24 h) to the second treatment duration (24-48 h), but declined for the third treatment duration (48-72 h). The decline in PSA for the third treatment duration was more prominent for higher (i.e. 5 μM) sorafenib concentrations. This may

be because fewer cells were viable for PSA secretion during 48-72 h duration compared to 24-48 h duration, and these cells may have already been exhausted out of PSA by 48 h. Cell counts for 10 μM concentration were below the limit of quantification; hence secreted PSA concentrations were undetectable.

These *in-vitro* results are in agreement with clinical findings and do confirm our hypothesis that sorafenib increases PSA concentrations - independent of its effect on cellular-growth – and, thus, may not be a suitable surrogate of efficacy in prostate cancer patients treated with sorafenib.

5-4.3.3 Cell counts following treatment with sorafenib

Cell counts following treatment with escalating sorafenib concentrations over 72 h periods are shown in **Table 5-8** and **Fig 5-19**. As expected, the ascending order of cell-counts was:

10 μM (undetectable) < 5 μM < 2.5 μM < only DMSO

Cell counts for 10 μM concentration were undetectable using the standard cell-counting calibration curves (**Fig 5-13**). These results demonstrate dose-dependent antitumor activity of sorafenib in LNCaP cell lines.

Day 1

	PSA concentration ng/mL	Absorbance at 450 nm
Std A	0	-0.031
Std B	1.5	0.471
Std C	5	1.209
Std D	15	2.822
Std E	30	4.028
Std F	40	4.943

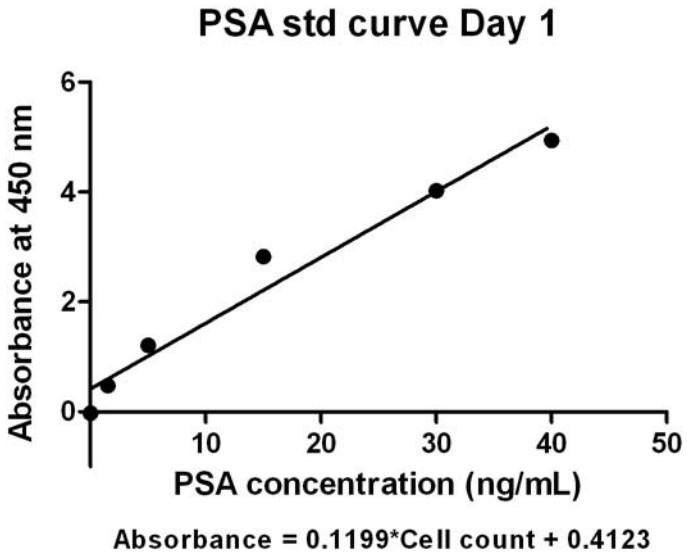

Fig 5-15 Standard curve for PSA estimation on day 1 (at 24 hrs).

Table 5-5 PSA concentrations at 24-hr time-point

Absorbance at 450 nM						**Mean**	**SD**
Sorafenib concentration	**Plate 1**	**Plate 2**	**Plate 3**	**Plate 4**	**Plate 5**		
DMSO	3.442	3.869	3.924				
2.5 uM	4.221	3.807	3.942	4.075	3.304		
5 uM	2.732	2.658	3.109	2.902	2.865		
10 uM	1.537	1.58	1.504	1.523	1.636		
Back-calculated PSA concentrations							
	Plate 1	**Plate 2**	**Plate 3**	**Plate 4**	**Plate 5**		
DMSO	25.27	28.83	29.29				
2.5 uM	31.77	28.31	29.44	30.55	24.12		
5 uM	19.35	18.73	22.49	20.76	20.46		
10 uM	9.38	9.74	9.11	9.26	10.21		
Cell count normalized PSA concentrations							
	Plate 1	**Plate 2**	**Plate 3**	**Plate 4**	**Plate 5**		
DMSO	0.0000634	0.0000699	0.0000547			0.0000627	0.0000076
2.5 uM	0.0000737	0.0000984	0.0000702	0.0000603	0.0000429	0.0000691	0.0000203
5 uM	0.0001656	0.0000736	0.0000686	0.0000560	0.0000653	0.0000858	0.0000451
10 uM	0.0001726	0.0001739	0.0000426	0.0000443	0.0000480	0.0000963	0.0000703

Day 2

	PSA concentration ng/mL	Absorbance at 450 nm
Std A	0	-0.009
Std B	1.5	0.471
Std C	5	1.296
Std D	15	3.117
Std E	30	4.454
Std F	40	5.7

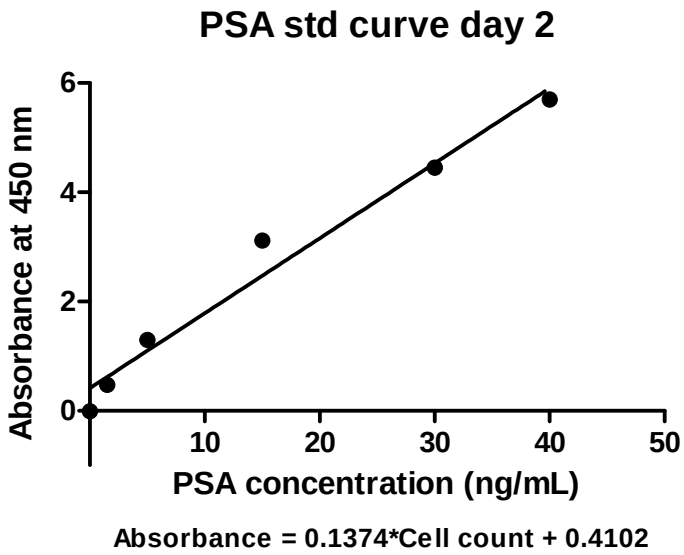

Fig 5-16 Standard curve for PSA estimation on day 2 (at 48 hrs).

Table 5-6 PSA concentrations at 48 hr time-point

Absorbance at 450 nM						**Mean**	**SD**
Sorafenib concentration	**Plate 1**	**Plate 2**	**Plate 3**	**Plate 4**	**Plate 5**		
DMSO	5.003	4.661	4.97				
2.5 uM	4.202	4.812	5.382	4.612	4.932		
5 uM	1.139	1.156	1.427	0.891	1.391		
10 uM	0.133	0.159	0.296	0.277	0.2		
Back-calculated PSA concentrations							
	Plate 1	**Plate 2**	**Plate 3**	**Plate 4**	**Plate 5**		
DMSO	33.43	30.94	33.19				
2.5 uM	27.60	32.04	36.18	30.58	32.91		
5 uM	5.30	5.43	7.40	3.50	7.14		
10 uM	*	*	*	*	*		
Cell count normalized PSA concentrations							
	Plate 1	**Plate 2**	**Plate 3**	**Plate 4**	**Plate 5**		
DMSO	0.0000818	0.0000747	0.0000739			0.0000768	0.0000044
2.5 uM	0.0000742	0.0000794	0.0001012	0.0001788	0.0000550	0.0000977	0.0000482
5 uM	0.0000551	0.0001850	0.0002675	0.0002302	0.0001095	0.0001695	0.0000869
10 uM	*	*	*	*	*	*	*

* Cell count for these time points were below the limits of quantitation

Day 3

	PSA concentration ng/mL	Absorbance at 450 nm
Std A	0	-0.051
Std B	1.5	0.481
Std C	5	1.58
Std D	15	3.033
Std E	30	4.004
Std F	40	5.096

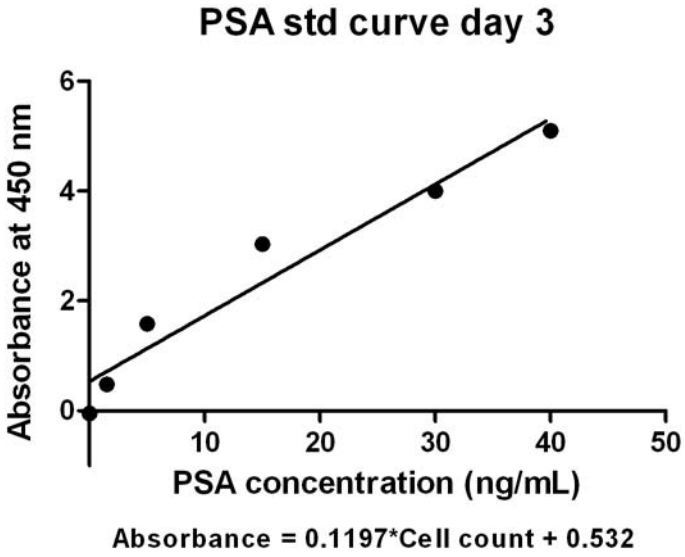

Fig 5-17 Standard curve for PSA estimation on day 3 (at 72 hrs).

Table 5-7 PSA concentrations at 72 hr time-point

Absorbance at 450 nM						**Mean**	**SD**
Sorafenib concentration	**Plate 1**	**Plate 2**	**Plate 3**	**Plate 4**	**Plate 5**		
DMSO	5.995	6.048	5.543				
2.5 μM	5.715	5.448	5.838	5.488	5.542		
5 μM	0.639	0.656	1.124	0.83	1.981		
10 μM	-0.023	-0.006	-0.015	-0.029	-0.024		
Back-calculated PSA concentrations							
	Plate 1	**Plate 2**	**Plate 3**	**Plate 4**	**Plate 5**		
DMSO	45.64	46.08	41.86				
2.5 μM	43.30	41.07	44.33	41.40	41.85		
5 μM	0.89	1.04	4.95	2.49	12.11		
10 μM	*	*	*	*	*		
Cell count normalized PSA concentrations							
	Plate 1	**Plate 2**	**Plate 3**	**Plate 4**	**Plate 5**		
DMSO	0.0000672	0.0000510	0.0000589			0.0000590	0.0000081
2.5 μM	0.0000664	0.0000669	0.0000855	0.0000708	0.0000452	0.0000670	0.0000144
5 μM	0.0000090	0.0000200	0.0000403	0.0000301	0.0000802	0.0000359	0.0000273
10 μM	*	*	*	*	*	*	*

* Cell count for these time points were below the limits of quantitation

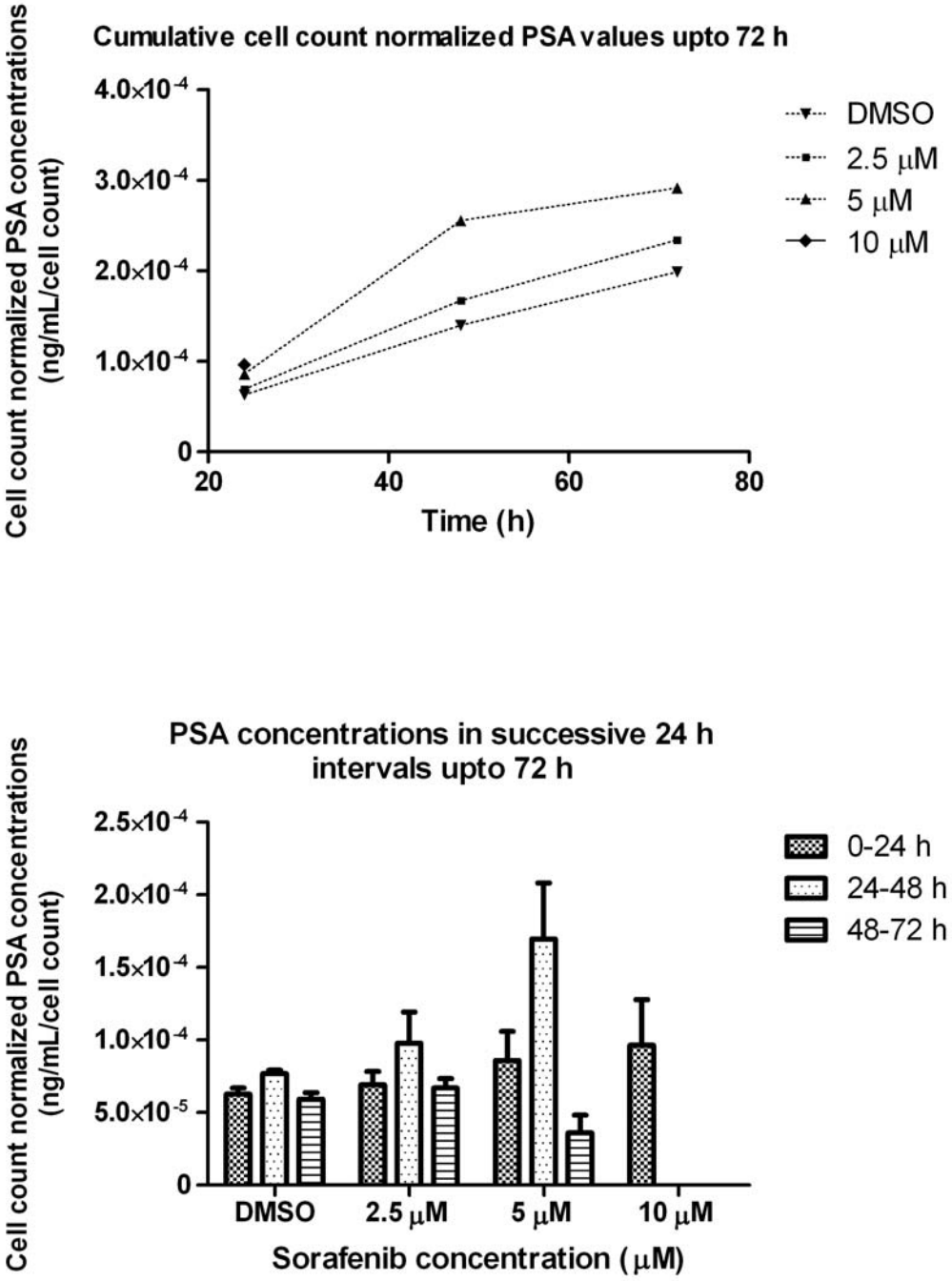

Fig 5-18 (A) Cumulative PSA (normalized to cell count) over 72 hrs. **(B)** Cell count-normalized PSA in successive 24-hr intervals after treatment of LNCaP cells with DMSO (control), 2.5, 5 and 10 μmol/L sorafenib. **Note**: For the 10 μM sorafenib concentration, cell counts and PSA levels were below the limits of quantification for cell counting reference curve and PSA ELISA assay, respectively.

Table 5-8 Cell counts at 24-hr 48-hr and 72-hr time-points following treatment with sorafenib

Cell counts at 24-hr time-point							
	Plate 1	**Plate 2**	**Plate 3**	**Plate 4**	**Plate 5**	**Mean**	**SD**
DMSO only	398500.00	412666.67	535166.67			448777.78	75149.54
2.5 µM	431000.00	287666.67	419333.33	506833.33	561833.33	441333.33	103699.95
5 µM	116833.33	254333.33	327666.67	371000.00	313500.00	276666.67	98617.88
10 µM	54333.33	56000.00	213500.00	209333.33	212666.67	149166.67	85826.05
Cell counts at 48-hr time-point							
DMSO only	408500	414333.333	449333.333			424055.56	22084.64
2.5 µM	371833.33	403500	357666.667	171000	598500	380500.00	152101.71
5 µM	96200	29333.3333	27666.6667	15200	65166.6667	46713.33	33344.36
10 µM	*	*	*	*	*	*	*
Cell counts at 72-hr time-point							
DMSO only	679333.33	903500	711000			764611.11	121318.95
2.5 µM	651833.33	613500	518500	585166.67	926000	659000.00	157004.95
5 µM	99333.333	51833.3333	122666.667	82666.667	151000	101500.00	37830.03
10 µM	*	*	*	*	*	*	*

* Cell count for these time points were below the limit of quantitation

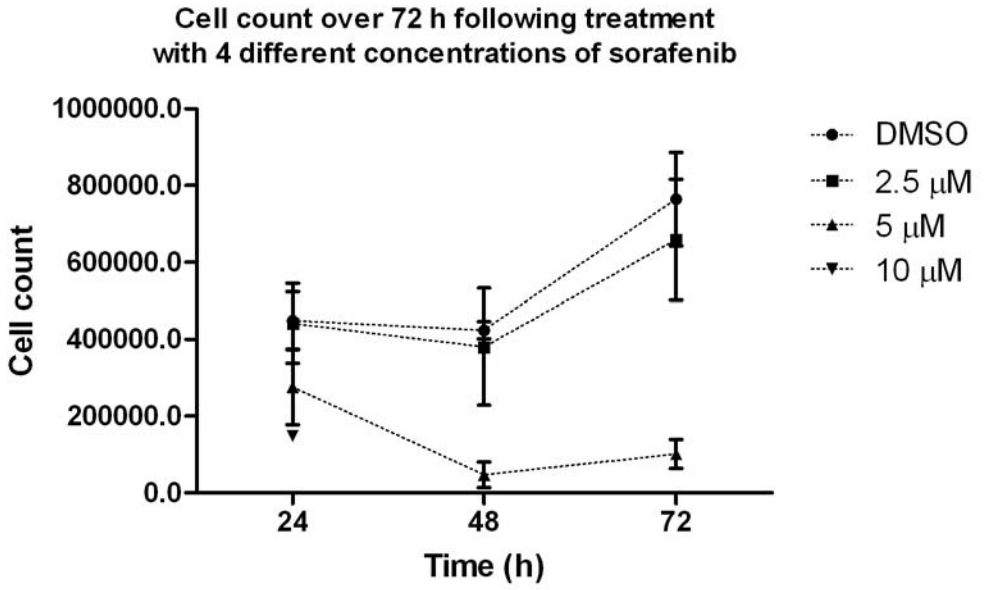

Fig 5-19 Cell counts upto 72 hrs, following treatment with four different concentrations of sorafenib and DMSO (negative control)

5-4.4 Conclusions

We demonstrated that sorafenib dose-dependently increases PSA secretion from LNCaP prostate cancer cell lines - independent of its effect on cell-growth inhibition. Similar findings were observed in clinical studies evaluating the efficacy of sorafenib in metastatic castrate resistant prostate cancer (mCRPC). These results indicate that PSA is not a suitable surrogate of efficacy for mCRPC patients treated with sorafenib.

Use of PSA as surrogate endpoint of efficacy has been debatable since it was first identified by Ferro and colleagues (133). A decline in serum PSA concentrationswas shown to be a useful indicator of treatment outcome for many anticancer drugs tested in patients with mCRPC (129). However, contrary outcomes have been observed for agents such as TNP-470, sodium phenylacetate and phenylbutyrate, which increase PSA

expression in *in-vitro*, *in-vivo* models and clinical studies (134). These agents have shown to affect the PSA expression or secretion independent of alterations in tumor growth or volume (134).

The exact mechanism by which these drugs increase PSA secretion is not known, but in part, it is thought to be an outcome of drug-induced increase in PSA transcription activity. Hence, it is important to validate the use of PSA for specific clinical settings and agents prior to its use as a surrogate marker for efficacy.

CHAPTER SIX

EVALUATION OF THE EXPOSURE-TOXICITY RELATIONSHIP AND LABORATORY MARKERS FOR TOXICITY IN SOLID TUMOR PATIENTS TREATED WITH SORAFENIB

6-1 Introduction

The greatest challenge in oncology drug development is the identification of agents with optimum activity and a tolerable side effect profile. Therefore, therapeutic advances in the last several years have focused on development of agents with improved selectivity for their antitumor effect with the hope of reducing toxicities. However, the utility of these treatments remain limited, and a significant proportion of patients experience treatment-associated toxicities while deriving little or no benefit. These differences among patients are evident because of inherent heterogeneity. The findings in the areas of pharmacology, pathology and pharmacogenetics have shown that general population is a mix of subpopulations which differ from the population average with respect to disposition of drugs or response to treatment. Therefore, the individualization of treatment is increasingly being sought to optimize the therapeutic outcome, which includes the identification of patients who are likely to respond favorably to a specific therapy or those who will suffer from toxicities.

Individualization of therapy involves, among others, identification of predictive markers for toxicity and evaluation of exposure-(toxicity) response relationship. Several studies have evaluated such markers for oncology drugs. Methotrexate plasma concentrations have shown to be correlated with gastrointestinal and hematological toxicity (135, 136), and its concentrations were prospectively measured in patients for adjusting the leucovorin rescue (folic acid analogs used to prevent harmful effects of methotrexate) and preventing the toxicity (136). Similarly, exposures of a methotrexate analogue, trimetrexate, were also shown to be related with hematological toxicity (137-139). Etoposide's steady-state plasma concentrations were higher in patients with significant hematological toxicity (140). Platelet counts following carboplatin treatment correlated with its exposure, which in turn was related with its renal clearance (141). An equation was devised to prospectively determine the dose of carboplatin, which would result in non-toxic exposures (142).

Pharmacogenetic variations were also shown to be related with toxicities. For example, genetic variation in TPMT was related with the concentrations of thioguanine nucleotides, which also correlated with the hematologic toxicities (143). Polymorphisms in the UGT1A1 gene correlated with SN-38 glucuronide concentrations, which in turn were related with treatment-associated neutropenia and diarrhea (144). Molecular and laboratory markers have also been evaluated to predict the efficacy and toxicity. For example the use of the HER2 and the estrogen receptor expression for decision of suitable chemotherapy in patients with breast cancer (145), and correlation of sweat

concentrations of doxorubicin with the occurrence of palmar-plantar erythrodysthesia syndrome (146), also known as the hand-foot syndrome.

We evaluated the impact of exposure, and genetic and non-genetic markers on the frequency and/or severity of toxicities in patients with solid tumor treated with sorafenib as single agent or in combination therapy. The sorafenib treatment-associated toxicities observed in selected phase II/III clinical trials and their plausible mechanisms are described in **section 1-3.7** and **Table 1-4**. The results of association between genetic markers and toxicities are described in chapter 7. The non-genetic marker evaluated was: sweat concentrations of sorafenib as a marker for the treatment-associated hand-foot skin reaction syndrome (HFSR). The methodologies, results and discussion of these correlative studies are described in this chapter.

6-2 Evaluation of exposure-toxicity relationship

6-2.1 Methods

6-2.1.1 Patients and study design

Data from a total of 112 patients included in the population pharmacokinetic analysis were used to assess the exposure-toxicity relationships. These patients were enrolled in a phase II clinical trial in mCRPC for single agent sorafenib (N=45), a phase II clinical trial in NSCLC receiving sorafenib only (N=18), a phase II trial in CRC receiving sorafenib in combination with cetuximab (N=18), a phase I trial in patients with ST receiving sorafenib in combination with bevacizumab (N=28), and a phase I trial in patients with KS receiving sorafenib only (N=2). Six patients in the KS trial receiving sorafenib with

ritonavir were not included in the current analysis because of the potential for a drug interaction (**section 1-3.3**). The exposure-toxicity analysis was separately performed for patients receiving only sorafenib (N=65), sorafenib with bevacizumab (N=28), and sorafenib with cetuxiamb (N=18). The dosing regimen and design of these phase I / II clinical trials have been described in **section 4-4.1**.

6-2.1.2 Pharmacokinetic metrics

The sorafeinb exposures (AUC = Dose/CL) calculated using the individual predictions of systemic clearances from population pharmacokinetic analysis were used to evaluate the exposure-toxicity relationships. Single-dose exposures were calculated using the 400 mg dose for patients with mCRPC, CRC and NSCLC, and with the 200 mg dose for patients enrolled in ST and KS trial. In case of dual therapies, exposures of the co-administered agents (i.e., bevacizumab and cetuximab) were not available to perform the similar analysis.

6-2.1.3 Toxicity metrics

In all of these trials, toxicities were reported using the Common Toxicity Criteria for Adverse Events (NCI CTC) version 3. The exposure-toxicity analysis was performed for most common sorafenib treatment-associated toxicities, which included fatigue, diarrhea, hand-foot skin reaction syndrome (HFSR), rash, desquamation and hypertension. The most severe grades of these toxicities observed anytime during the treatment were used for analysis.

6-2.1.4 Statistical analysis

Patients from each analysis category (single dose sorafenib, sorafenib + bevacizumab, and sorafenib + cetuximab) were divided into four exposure groups which were created based on four quartiles of sorafenib AUC distribution. Incidence rates (%) of toxicities (grade ≥ 2) were compared among these exposure quartiles using the Chi-square statistics. The statistical analyses were performed using JMP 8.0 (SAS Institute Inc., Cary, NC, USA) statistical software.

6-2.2 Results

The incidences of the most common toxicities for sorafenib clinical trials included in current analysis are summarized in **Table 6-1**. The incidences of these toxicities in patients receiving only sorafenib were normally less than 50%. However, co-administration of bevacizumab with sorafenib increased both the incidences (up to approximately 75%) and the severity of these toxicities, despite administration of half of the FDA approved dose of sorafenib (i.e., 200 mg BID) and bevacizumab (i.e., 5 mg/kg every other week). Up to 74% patients on dual therapy required dose reductions to 200 mg QD levels (115). The exposure-toxicity analyses for sorafenib alone and combination therapy trials are discussed below:

6-2.2.1 Combined single agent studies

The combined results of single agent sorafenib trials are shown in **Fig 6-1**. With an increase in exposure from the lower quartile to the upper quartile, there was no major change in incidence rates of fatigue and HFSR. The incidence of diarrhea doubled from

exposures below the median to the 3rd quartile, but was absent in the 4th quartile. The incidence of rash significantly increased with increased exposures from below the median to above the median (p=0.0201), while the frequency of hypertension decreased with increased exposures. These results suggest an exposure-toxicity relationship only for treatment-associated rash, but not for other common toxicities following administration of single agent sorafenib in patients with solid tumors.

6-2.2.2 Phase I trial in patients with solid tumors treated with sorafenib and bevacizumab combination

In patients with solid tumor treated with the sorafenib and bevacizumab combination, only sorafenib exposures were available to assess the impact on toxicity, results of which are shown in **Fig 6-2**. With increased exposures from the lower quartile to the upper quartile, the incidence of fatigue decreased, and there was no major change in the frequency of rash, diarrhea and hypertension. Incidence rates of HFSR increased significantly from below the median to above the median exposures (p=0.0039). From **Fig 6-2** and **Table 6-1**, we observe that, although sorafenib exposures for patients enrolled in the ST trial were comparatively low, the percent incidences of HFSR and hypertension toxicities were same or higher.

Note that the use of bevacizumab monotyherapy has not been associated with HFSR, but the addition of bevacizumab to sorafenib reduced the dose at which highest-grades of HFSR toxicity appeared (60). Hypertension is a common toxicity for both sorafenib and

bevacizumab, and for all the agents with activity against VEGF pathway; hence, the increase in the frequency of hypertension with combination therapy is not unexpected.

These results suggest that addition of bevacizumab intensifies the sorafenib treatment-associated HFSR; it shifts the occurrence of HFSR to a lower dose level, and also following addition of bevacizumab incidences of HFSR appear to increase with increase in sorafenib exposure. We observed an exposure-toxicity relationship for sorafenib / bevacizuamb combination, but not for sorafenib monotherapy.

6-2.2.3 Phase II trial in patients with colorectal cancer treated with sorafenib and cetuximab combination

The number of patients in the CRC trial was limited; hence it was not possible to evaluate (sorafenib) exposure-toxicity analysis for fatigue, HFSR and hypertension (**Fig 6-3**). Rash and diarrhea are common toxicities for both sorafenib and cetuximab (49, 147). Therefore, the frequency of these side-effects was relatively higher in patients on this combination than in other patients (**Table 6-1**). The incidence of rash was not altered significantly, but the incidence of diarrhea appeared to decrease with increased exposures from below median to above median. One possible explanation is that, if sorafenib systemic exposures are high, it would suggest a low concentration of unabsorbed drug in the GI tract and, hence, lower the incidence of diarrhea. However, for the combination of drugs with common toxicities it is less likely to see a positive correlation between toxicities and exposure (pharmacokinetics) of only one drug, when both are administered together. Alternative metrics or markers, integrating plasma concentrations for all the

drugs in combination would be a better measure to assess the relationship with treatment-associated toxicities.

The sample size for this trial is small, and further evaluation with larger sample size is required to draw conclusions about impact of sorafenib exposure on toxicity. This trial is currently (at the time of analysis) enrolling the patients with targeted cohort size of 50.

Table 6-1 Summary of toxicities in sorafenib clinical trials

Trial	Fatigue % (N)			Rash: desquamation % (N)			Hand-foot skin reaction % (N)			Diarrhea, % (N)			Hypertension % (N)		
	Gr1	**Gr2**	**Gr≥3**	**Gr1**	**Gr2**	**Gr≥3**	**Gr1**	**Gr2**	**Gr≥3**	**Gr1**	**Gr2**	**Gr≥3**	**Gr1**	**Gr2**	**Gr≥3**
mCRPC	24	9	0	4	20	9	41	13	2	9	13	2	33	15	4
(N=46)	(11)	(4)	(0)	(2)	(9)	(4)	(19)	(6)	(1)	(4)	(6)	(1)	(15)	(7)	(2)
NSCLC	22	6	0	33	28	0	11	39	11	28	11	0	11	28	6
(N=18)	(4)	(1)	(0)	(6)	(5)	(0)	(2)	(7)	(2)	(5)	(2)	(0)	(2)	(5)	(1)
CRC	44	6	0	11	22	17	22	11	0	17	28	17	6	6	0
(N=18)	(8)	(1)	(0)	(2)	(4)	(3)	(4)	(2)	(0)	(3)	(5)	(3)	(1)	(1)	(0)
ST	33	30	7	33	22	0	26	48	0	41	4	15	11	26	30
(N=28)	(9)	(8)	(2)	(9)	(6)	(0)	(7)	(13)	(0)	(11)	(1)	(4)	(3)	(7)	(8)
KS[†]	12.5	12.5	12.5	12.5	0	0	0	0	25	25	0	0	0	0	37.5
(N=8)	(1)	(1)	(1)	(1)	(0)	(0)	(0)	(0)	(2)	(2)	(0)	(0)	(0)	(0)	(3)

[†] Data from only 2 of these patients on sorafenib without ritonavir were included in exposure-toxicity analysis.

Gr: toxicity grade based on NCI CTC version 3, **mCRPC**: Phase II trial of sorafenib in metastatic castrate resistant prostate cancer, **NSCLC**: Phase II trial of sorafenib in non-small cell lung cancer, **CRC**: Phase II trial of sorafenib and cetuximab combination in patients with colorectal cancer, **ST**: Phase I trial of sorafenib and bevacizumab combination in patients with solid tumors. **KS**: Phase I trial of sorafenib (with or without ritonavir) in patients with Kaposi's sarcoma.

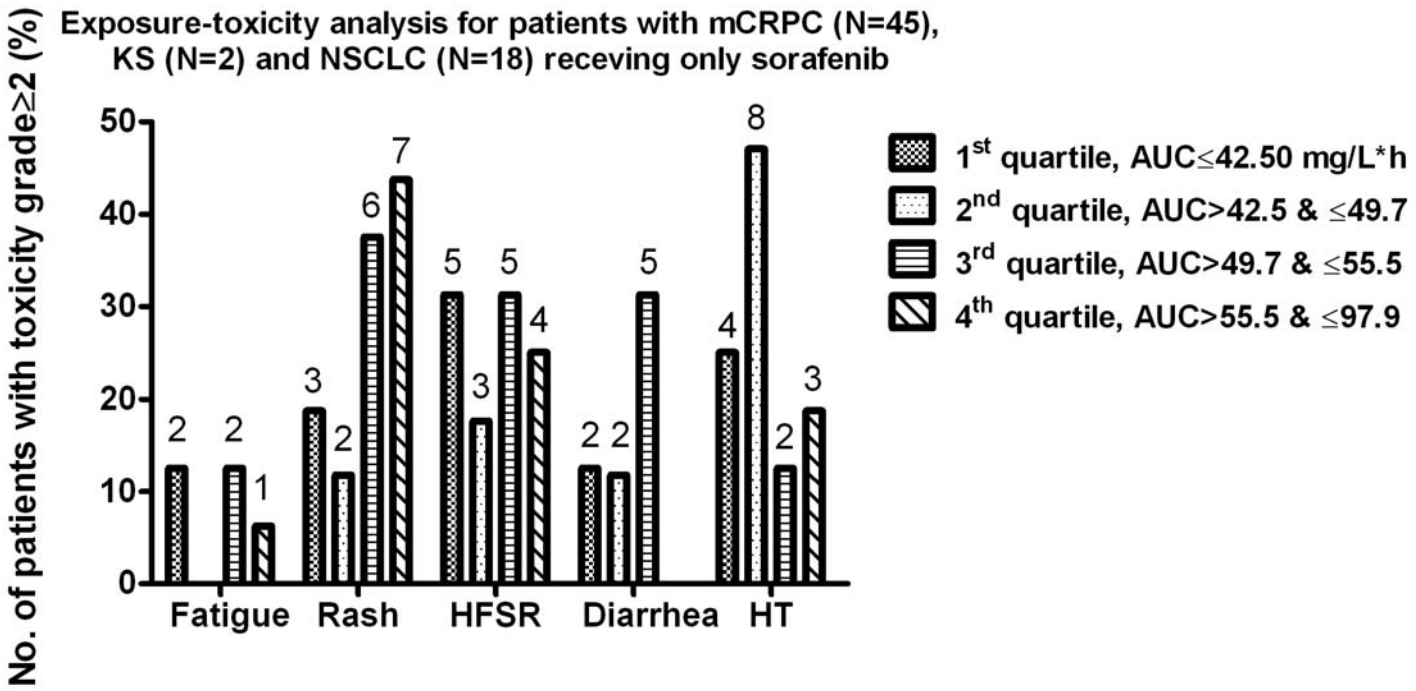

Fig 6-1 Evaluation of exposure-toxicity relationship for clinical trials involving administration of only sorafenib

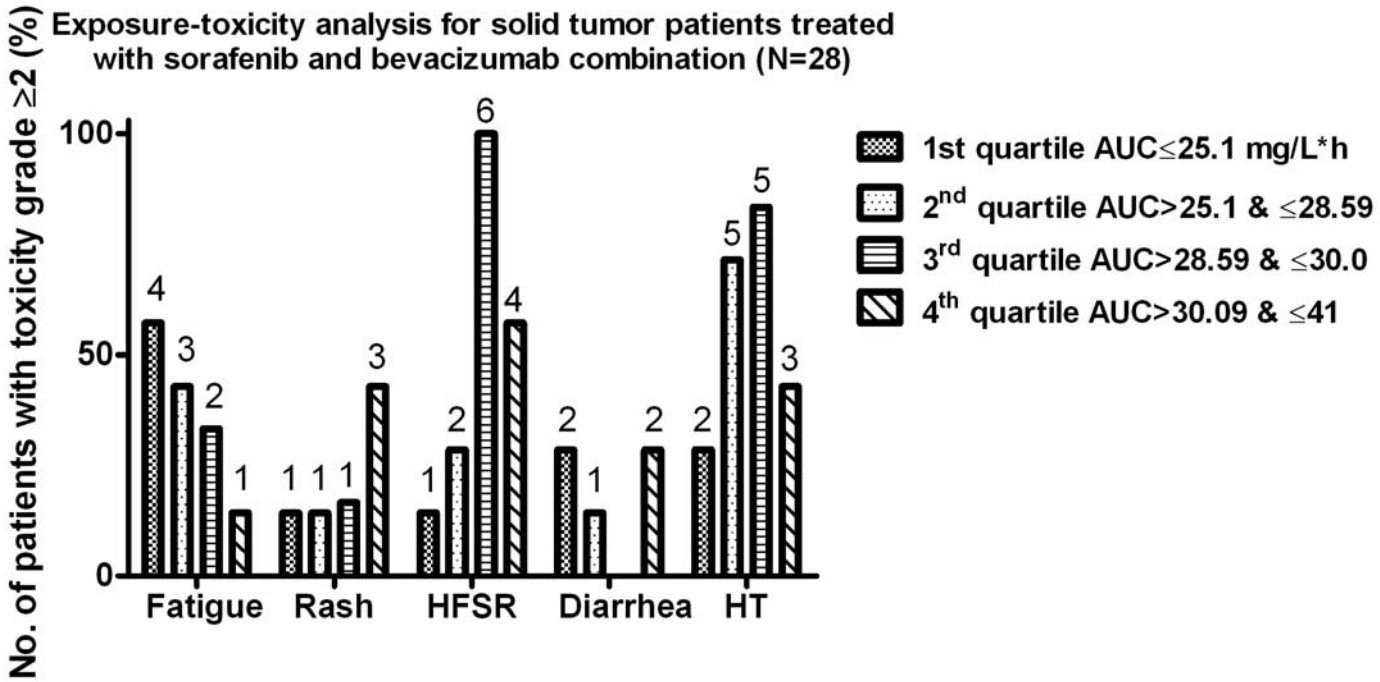

Fig 6-2 Evaluation of exposure-toxicity relationship for ST trial involving administration of sorafenib in combination with bevacizumab

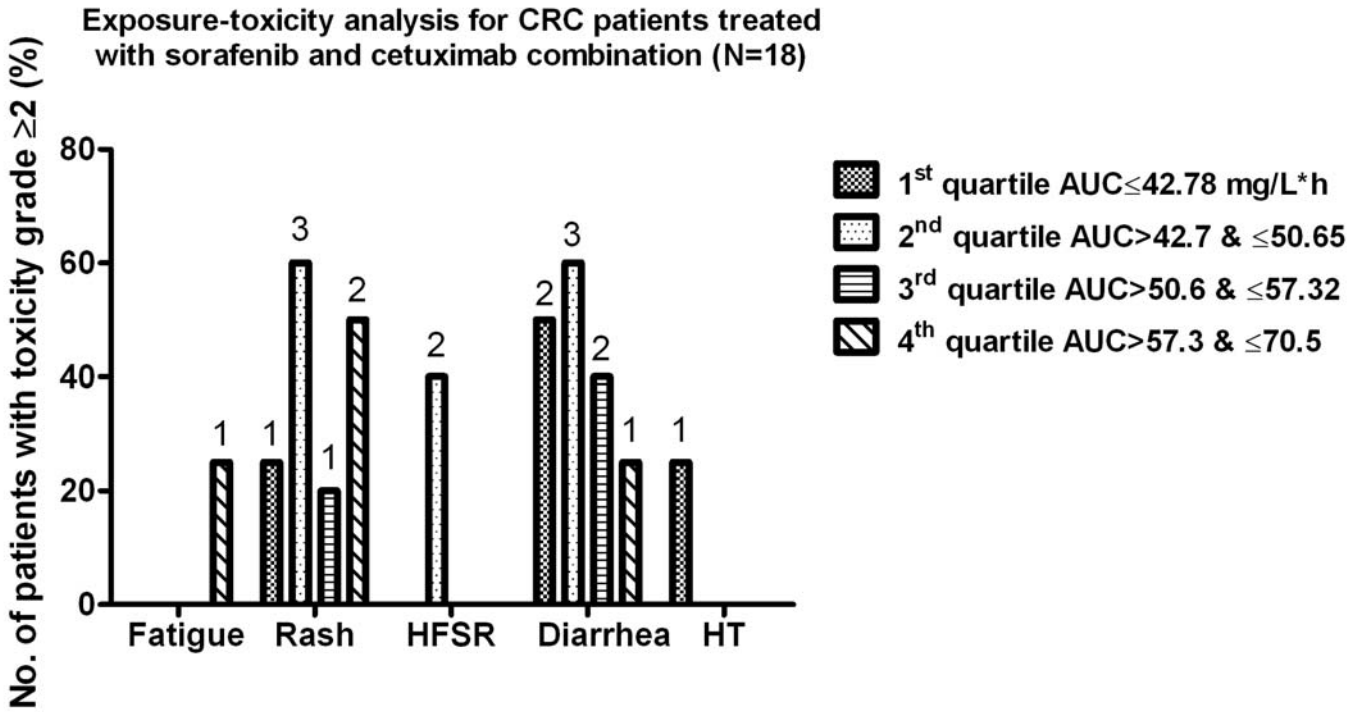

Fig 6-3 Evaluation of exposure-toxicity relationship for CRC trial involving administration of sorafenib in combination with cetuximab

6-2.3 Discussion

The majority of treatment-related toxicities associated with oral sorafenib administration were mild to moderate in severity. These toxicities were constitutional (such as fatigue), dermatological (such as rash, desquamation and HFSR), gastrointestinal (such as diarrhea) and cardiovascular (such as hypertension) in nature. Sorafenib monotherapy at a standard dose of 400 mg BID was well tolerated, and treatment-associated toxicities were manageable with the supportive therapies (91). However, even lower grades of these toxicities are of concern because sorafenib is a cytostatic agent and requires long-term administration for therapeutic benefit; recurrence of even lower grades of toxicities for a long time could adversely affect patient's quality of life and/or lead to treatment disruption/discontinuation.

Co-administration of bevacizumab, another anti-angiogenic agent, increased the incidence and severity of selected treatment-associated side effects. There is some overlap in toxicity profiles of these drugs; for example, both sorafenib and bevacizumab can cause hypertension, diarrhea and gastrointestinal perforation (49, 120). However, skin rash and HFSR are not common toxicities of bevacizumab (60, 120). Many patients on this dual-drug trial required reduction in sorafenib dose to 200 mg QD (one fourth of the clinically approved dose) because of treatment-associated toxicities (115). Similarly, administration of sorafenib in combination with cetuximab increased the incidence of their common toxicities, rash and diarrhea.

The incidence rate of rash increased with increased exposures following administration of sorafenib monotherapy. A pooled analysis of four phase I trials also found an increase in the severity of rash with a higher starting dose of single-agent sorafenib (91). The exposures for erlotinib, a tyrosine kinase inhibitor which belongs to the same class of drug as sorafenib, have also been shown to be related with incidence of skin rash (88, 148)

The frequency and severity of HFSR were reported to be significantly associated with a sorafenib dose in the range of 300-600 mg BID (91). However, no significant correlation was found between sorafenib exposures (pharmacokinetics) and HFSR, for single agent sorafenib trials. These results suggest that with cytostatic agents metrics which relates to extended exposures, such as cumulative dose, might be more useful for assessment of exposure-response relationship than the single dose exposures. Earlier, a report based on (part of) patients involved in current analysis has shown rise in incidences of HFSR with increasing cumulative sorafenib dose in single-agent sorafenib studies (60). The incidence of diarrhea and fatigue was determined not to be associated with dose based on pooled analysis of phase I studies (91), and we did not find any significant correlation with sorafenib exposures, too.

The incidence of HFSR increased significantly with increased sorafenib exposures, when administered in combination with bevacizumab. Sorafenib exposures at which HFSR was seen appeared to be lower for combination therapy compared with single agent therapy. Earlier investigations based on patients involved in current analysis have shown an increased frequency of high-grade HFSR for combined sorafenib and bevacizumab

therapy compared to treatment with sorafenib monotherapy (p=0.0006), as well as a lower dose was required for onset of highest grades of HFSR (60). Cumulative median dose of sorafenib for HFSR toxicity in combination therapy was 21,117 mg, while that dose level was not reached for treatment with single-agent sorafenib (60). The incidence and severity of HFSR were higher with combined sorafenib and bevacizumab therapy compared with single agent sorafenib at any given cumulative dose of sorafenib (60). Together, these results indicate higher incidences of HFSR with increased sorafenib exposure and cumulative sorafenib dose in the sorafenib/bevacizumab combination study, suggesting that the anti-VEGF effects of bevacizumab potentiates the sorafenib treatment-associated HFSR. The role of VEGF pathway in induction of HFSR has also been supported by several other observations reported by Azad et al (60). The risk of HFSR was not found to be related with other factors such as the number and type of prior therapies, including exposure to pegylated liposomal doxorubicin, previous toxicities, baseline neuropathy, or dermatological toxicities from prior treatments (60).

No significant correlations were found between the incidence of hypertension/fatigue and sorafenib exposures in single-agent or combination sorafenib trials, which was in agreement with results from pooled analysis for phase I studies (91).

6-3 Sweat concentrations of sorafenib as a marker of HFSR

6-3.1 Introduction

In Table 6-1 it is reported that HFSR is a common toxicity associated with sorafenib and combined vascular endothelial growth factor therapy. . Pain and disability associated with HFSR caused by sorafenib and sunitinib affects up to 62% of patients and can limit treatment dose and duration (53, 54, 60, 149). In phase III clinical trials of sorafenib in renal cell carcinoma and hepatocellular carcinoma, 10-38% patients required treatment discontinuation and 13-44% patients required dose reductions or interruptions because of treatment-related toxicities, which may compromise efficacy (53, 54). In phase II studies, patients treated with sorafenib for prostate cancer and lung cancer experienced dose reductions for HFSR toxicity (10% and 31%, respectively) (60). However, the mechanism underlying HFSR is not clearly understood.

Traditional chemotherapeutics such as cytarabine and liposomal doxorubicin, also cause acral erythematous plaques and dysesthesia, also known as hand-foot syndrome/HFS, acral erythema, or palmar-plantar erythrodysesthesia (150, 151). Based on anatomical distribution and eccrine histological changes of traditional HFS, others have postulated and studied sweat excretion of these toxic drugs as the etiology of traditional HFS (146). Similarly, we hypothesized that excretion of sorafenib in sweat might be a causal factor for HFSR. We sought to investigate this hypothesis to understand the mechanism of HFSR, which would also provide the basis for its prevention and effective treatment.

6-3.2 Methods

6-3.2.1 Patients and study design

Sweat was collected from hands of two patients with HFSR: a) a 62 year old female with ovarian cancer and active grade 1 HFSR on day 30 of sorafenib 200mg twice daily and bevacizumab 5mg/kg and b) a 62 year old male with prostate cancer, who had prior grade 2 HFSR, which improved after treatment was held for grade 3 hypophosphatemia, and had active grade 1 HFSR on day 197 of sorafenib 400mg twice daily at time of sweat collection. In addition, sweat samples were collected from two healthy volunteers, which were used to set-up the quantitation method using plasma samples as calibrators.

6-3.2.2 Sweat collection

Sweat excretion was stimulated with pilocarpine iontophoresis and was collected using a capillary macroduct collector (Wescor Macroduct® kit, Wescor, Inc., Logan, Utah). Immediately after collection sweat was transferred to a small sealable container, which was stored at -80 ˚C till the time of analysis.

6-3.2.3 Quantitation of sorafenib in sweat

A LC/MS)/MS method, originally developed and validated for plasma matrix (152) was used for analysis of sweat samples. For this analysis, sweat samples were measured against plasma calibrators. Precipitation agent was added to sweat in a 1:10 ratio. Sweat samples from healthy volunteers were spiked with known concentrations of sorafenib and were analyzed to determine the lower limits of quantitation (LOQ).

6-3.3 Results

The chromatograms of sweat samples from healthy subjects with externally spiked 2, 5 and 10 ng/mL concentrations are shown in **Fig 6-4**. The LOQ was determined to be 5 ng/mL. The sorafenib in sweat samples was found to be stable for at least 3 months, when stored at -80 ˚C.

Chromatograms for sweat samples collected from patients are shown in **Fig 6-5**. No sorafenib was detected in sweat collected from the hands of two patients with HFSR. The plasma concentrations for both the patients were at steady-state given that sorafenib's half-life is 25-48 h (49) and samples were collected on day 30 and 197. The plasma concentration for patient with prostate cancer during sweat collection was 7468.6 ng/mL. No pharmacokinetic blood samples were collected from the patient with ovarian cancer. Neither patient received prior HFS-associated chemotherapeutics. These results suggest that HFSR may not be associated with excretion of sorafenib in sweat, at least in concentrations of 5ng/mL and above.

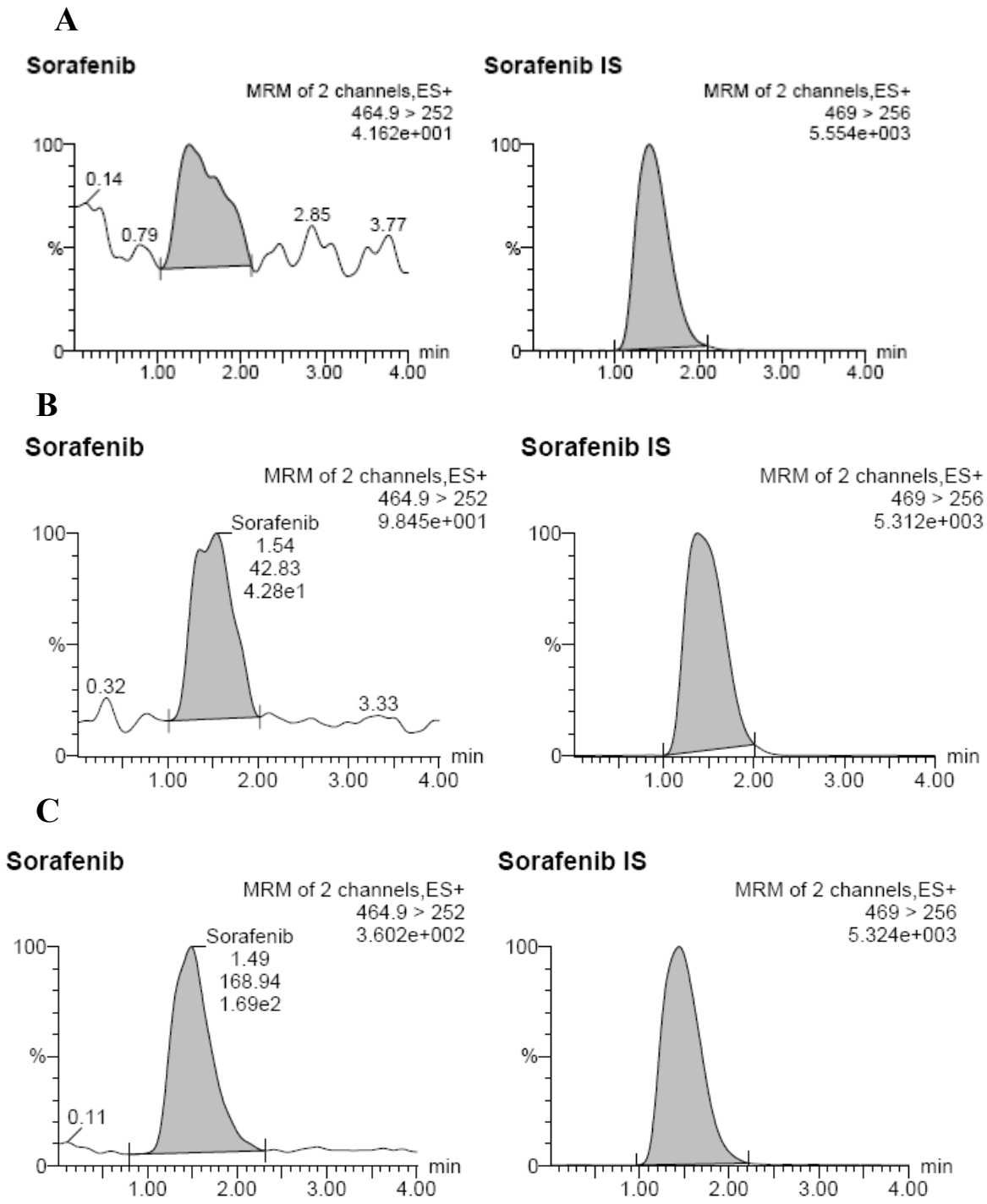

Fig 6-4 Chromatograms for sorafenib concentrations of (A) 2 ng/mL (B) 5 ng/mL and (C) 10 ng/mL when drug was spiked externally in sweat samples collected from healthy subjects.

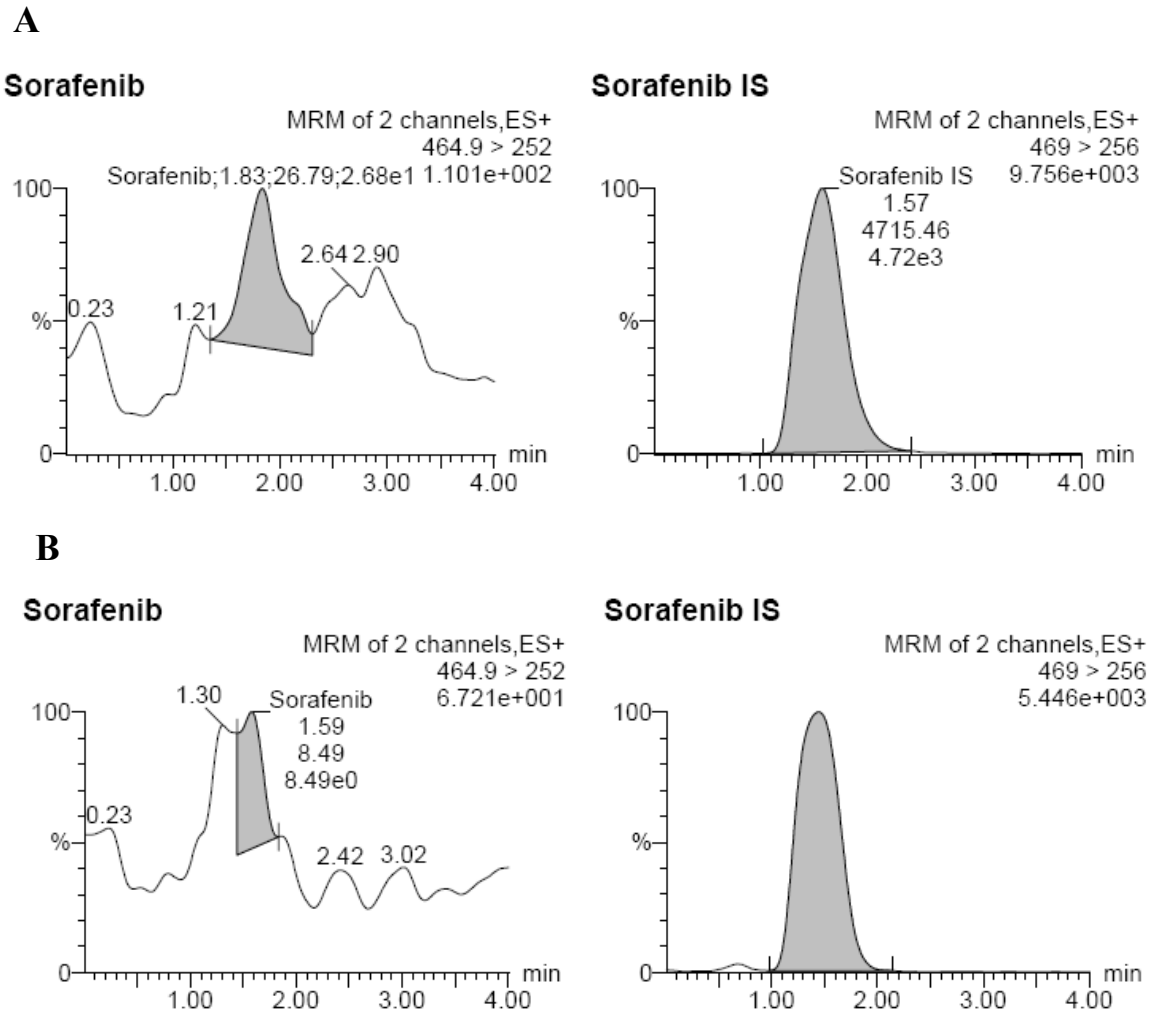

Fig 6-5 Chromatograms for sweat samples from; (A) collected from patient with active HFSR grade 1 on day 30 of phase II trial of sorafenib and bevacizumab in patients with epithelial ovarian, fallopian, and peritoneal cancer, (B) collected from patient with active HFSR grade 1 on day 197 of phase II trial of sorafenib in patients with androgen-independent prostate cancer.

6-3.4 Discussion

Sorafenib is a lipophilic compound with experimentally determined lipophilicity (logP) value of 3.8 (153). The sweat secreted from eccrine sweat glands, which are abundant on the palms of the hands and soles of the feet - the sites of HFSR, is mainly composed of water, various salts, and minute amounts of fatty material, urea and other waste. Based on the sweat composition sorafenib, being lipophilic, is less likely to be excreted via eccrine sweat glands. Sunitinib, another agent associated with HFSR, is also relatively lipophilic (logP: 2.5) (153). Conversely, most other HFS-causing drugs are relatively hydrophilic; the logP values for these drugs are -0.5: doxorubicin, -0.8: fluorouracil, -2.8: cytarabine, -1.6: hydroxyurea and capecitabine, 0.4 (153). Of note, sweat excretion has been shown to act as a carrier of doxorubicin to skin surfaces, which would then possibly be stored in stratum corneum and react with epidermal cells, resulting in HFSR (146).

Histologic examination of HFSR lesions has demonstrated focal horizontal zones of necrotic keratinocytes, dilated blood vessels, mild perivascular lymphohistiocytic inflammation, and eccrine gland abnormalities including dilatation and dysmorphic eccrine cells.(154, 155) The multi-kinase inhibitors target platelet-derived growth factor receptor (PDGFR) and c-KIT, which are both expressed on eccrine glands. Our findings demonstrate no association of HFSR with sorafenib sweat excretion ≥5 ng/mL. An alternative hypothesis is that the leakage of drug from blood capillaries damaged by subclinical trauma may cause HFSR, which is partly supported by the worsening severity of HFSR with increased activity and friction. However, to the best of our knowledge, there are no published studies which confirm this mechanism. Sorafenib and sunitinib

target tyrosine kinase receptors expressed on endothelial cells (PDGFR, c-KIT, and vascular endothelial growth factor receptor). Furthermore, combined anti-vascular endothelial growth factor therapy of sorafenib and bevacizumab is associated with a higher incidence of HFSR.(60)

CHAPTER SEVEN

EVALUATION OF VEGFR2 POLYMORPHISMS AS A MARKER OF THE RISK OF PROSTATE CANCER, AND SURVIVAL AND TOXICITY IN SOLID TUMOR PATIENTS RECEIVING ANTI-VEGF/VEGFR2 THERAPY

7-1 Introduction

The process of new blood vessel formation from the pre-existing blood vessels, or angiogenesis, is crucial for development of tumor, invasiveness and metastasis (156). This process is governed by an array of growth factors favoring or opposing the new blood vessel formation; however, vascular endothelial growth factor (VEGF) is the major regulator of this process (156). Angiogenesis has been implicated in several tumor types including the prostate cancer, NSCLC, CRC and other solid tumors. Raising interest in angiogenic modulators have led to the design and synthesis of several new molecules that target VEGF signaling pathway. These agents have shown promising anticancer activity and some of them, such as sorafenib, bevacizumab and sunitinib, are currently used clinically for various solid tumors.

So far, three VEGF receptors have been identified, namely VEGFR1 (or the fms-like tyrosine kinase (Flt-1)), VEGFR2 (or Kinase domain receptor (KDR)/ the murine fetal liver kinase (Flk-1)) and VEGFR3 (157). The VEGFR1 and 3 receptors are expressed in selected vascular beds, whereas the VEGFR2 receptor is expressed on almost all endothelial cells (158). Among these, VEGFR2 has the strongest kinase activity (157) and its interaction with VEGF is believed to be of utmost importance for angiogenesis during tumor development. Independent expression of only VEGF or VEGFRs does not always relate to increased tumor-angiogenesis, but the expression of their VEGF/VEGFR2 complex appears to be a better predictor of VEGF angiogenic activity (159). The VEGF/VEGFR2 complex was prominently localized in cancer cells and intra-tumoral vasculature in non-small cell lung and endometrial carcinomas (159, 160). The expression of this complex was related with poor prognosis and increased vascularization at the invading tumor-front regardless of VEGF levels (159), and appeared to be a strong prognostic factor than VEGF expression alone. These findings suggest that VEGFR2 plays a major role in VEGF signaling pathways by mediating the biological effects of VEGF. VGEF has shown to play an important role in both localized and metastatic prostate cancer (161-163) and its over-expression was shown to be associated with poor disease outcomes (164, 165). Microvessel density (MVD), a marker of angiogenic activity, and VEGFR2 expression was higher in prostate tumor cells compared to normal prostatic glands (166, 167).

Functional SNPs affecting the expression of genes or function of coded proteins may result in differences in an individual's susceptibility and severity of disease. These effects

might be caused by a single SNP or by coinheritance of multiple SNPs (also known as haplotypes) in a signaling pathway. Compared to the introduction of new VEGF/VEGFR2 targeted therapies, only few studies have investigated the impact of VEGFR2 SNPs on risk and prognosis of disease and drug response. The new targeted therapies are not equally tolerated by all patients, and some side-effects do not appear to be related with administered dose; suggesting that exploration of factors other than dose will be important to predict the occurrence of these side-effects. The etiology of common side-effects associated with anti-angiogenic class of compounds, such as hypertension and proteinuria, is not well understood (168). However, *in-vitro* and *in-vivo* evidence supports that these side-effects most probably result from inhibition of the VEGF pathway (168).

There is a critical need to identify molecular and pharmacogenetic markers to recognize patients who will likely benefit or develop toxicities from anti-angiogenic therapies. In the current study we evaluated the possible association between two SNPs in the VEGFR2 gene, namely rs2305948 (C/T) and rs1870377 (T/A), and (i) risk of prostate cancer, (ii) toxicities related with anti-VEGF/VEGFR2- inhibitor therapies, (iii) survival in solid tumor patients treated with anti-VEGF/VEGFR2- inhibitor therapies. These SNPs are located on exon 7 and 11 and result in nonsynonymous amino acid changes at residue 297 Val>Ile and 472 His>Gln, respectively.

7-2 Methods

7-2.1 Patients and controls

The analyses were performed on genomic DNA from 184 patients (144 males and 40 females) with solid tumors who received sorafenib (VEGFR2 inhibitor) and/or bevacizumab (anti-VEGF) with or without other agents. These patients were enrolled in six phase I/II clinical trials and their characteristics are summarized in **Table 7-1**. Sixty-one patients with castrate resistant prostate cancer not treated with anti-angiogenic therapies (i.e., bevacizumab or sorafenib) were used as controls for survival analysis. DNA samples from 292 control subjects with no known diagnosis of prostate cancer, obtained from Valley Biomedical (Winchester, VA, USA), were used as controls for risk analysis. Characteristics for survival and risk controls are also summarized in **Table 7-1**. This retrospective analysis was approved by the NCI Institutional Review Board. Information about survival and treatment-associated toxicities were collected from all patients treated with sorafenib and/or bevacizumab. Toxicities were graded based on NCI common toxicity criteria version 3.0.

7-2.2 Genotyping

DNA was extracted from plasma or whole blood samples using a QiaBlood extraction kit (Qiagen, Valencia, CA) and stored at 4°C. The primers were obtained from Invitrogen Corp (Carlsbad, CA). Genotyping for two VEGFR2 loci, VEGR2 H472Q and VEGFR2 V297I, was performed by single/nested PCR using the PCR primers shown in **Table 4-3**. The single PCR samples were subjected to an initial 40-cycle reaction with the following temperature cycle: 5 minutes at 94 ºC, 30 seconds(s) at 94 ºC, 30 s at annealing temperature (**Table 4-3**), 30 s at 72 ºC, and 7 minutes at 72 ºC. The nested PCR reaction consisted of a primary 20-cycle round of amplification using F1, R1 primers followed by

a second round of amplification for 40 cycles using F2, R2 primers with the same conditions as above. All samples were checked via 2% agarose gel electrophoresis for the presence of products.

PCR products were cleaned by treatment with Shrimp Alkaline Phosphatase (SAP) and Exonuclease I (Exo I) (USB Corporation, Cleveland, OH). These enzymes were deactivated by PCR cycle run for 90 minutes at 37 ºC and 20 minutes at 70 ºC, in preparation for sequencing. Sequencing PCR was carried out with big dye under the following cycle sequence: 5 minutes at 94 ºC, 10 s at 96 ºC, 5 s at 50 ºC, and 4 minutes at 60 ºC. The PCR products were then sequenced on an ABI Prism 310 Genetic Analyzer (Applied BioSystems, Foster City, CA) as per the instructions from manufacturer.

Table 7-1 Summary of patients and control subjects included in analysis

Tumor type	Treatment (s)	N	Ethnicity C: AA: others	Gender Male:Female	Information collected Survival	Toxicity
Cases						
mCRPC	Sorafenib	46	38 : 6 : 2	46 : 0	Yes	Yes
NSCLC	Sorafenib	22	16 : 2 : 4	13 : 9	Yes	Yes
CRC	Sorafenib + Cetuximab	18	13 : 1 : 4	9 : 9	Yes	Yes
KS	Sorafenib +/- Ritonavir	8	7 : 1 : 0	8 : 0	Yes	Yes
ST	Sorafenib + Bevacizumab	33	31 : 1 : 1	11 : 22	Yes	Yes
mCRPC	Bevacizuamb + Thalidomide + Docetaxel	60	50 : 8 : 2	60 : 0	Yes	Hypertension and HFSR
Survival controls						
mCRPC	Docetaxel	25	19 : 3 : 2	25 : 0	Yes	No
	Docetaxel + Ketoconazole	37	28 : 3 : 1	37 : 0	Yes	No
Risk controls						
No tumor	No cancer treatment received	292	143 :149	292 : 0	NA	NA

C: Caucasian, **AA**: African-American, **Others**: Hispanic or Asians, **mCRPC**: metastatic castrate resistant prostate cancer, **NSCLC**: non-small cell lung cancer, **CRC**: colorectal cancer, **KS**: Kaposi's sarcoma, **ST**: solid tumors, **HFSR**: hand-foot skin reaction syndrome, **NA**: not applicable

7-2.3 Statistical considerations

Hardy-Weinberg equilibrium was tested for only Caucasian patients and both Caucasian and African-American controls for both VEGFR2 SNPs using Chi-square test. The genotype and allele frequencies between Caucasian and African-American controls and patient and control groups were compared by Fisher's exact test or Chi-square test. Odds ratios and their 95% confidence intervals, estimated using logistic regression models, were used to compare the probability of genotypes between prostate cancer and control groups. Fisher's exact test was used to measure the strength of association between VEGFR2 genotypes and prostate cancer risk. The impact of genotypes on treatment-associated toxicities and association between toxicities were assessed by Fisher's exact test. Survival curves based on genotype or toxicity groups (grade $\leq$ 1/grade $\geq$ 2) were compared by the Kaplan-Meier method using a log-rank and stratified log-rank test. The latter test was used to adjust for trial-associated variation in PFS and frequency of toxicities, and from these tests only the less significant, more conservative, p-values were reported. All statistical analysis were two-tailed at a pre-specified significance level of <0.05. In view of the exploratory nature of analysis, p-values were not formally corrected for multiple testing.

7-3 Results

7-3.1 Genotyping

The genotype and allele frequencies of studied VEGFR2 SNPs in patients with solid tumor and male Caucasian and African-American controls are shown in **Table 7-2** and **7-3**. Both VEGFR2 SNPs were in Hardy-Weinberg equilibrium ($p<0.05$), when evaluated

individually for Caucasian patients, Caucasian controls and African-American controls. These frequencies are in close agreement with previous reports by Schneider et al (169, 170) and Försti et al (79). The genotype data were consistent with healthy Swedish Caucasians females ($p>0.14$), but did not match the data obtained in healthy Polish Caucasians females ($p\leq0.0204$) (79).

7-3.2 Are VEGFR2 H472Q and V297I genotype/allele frequencies different between Caucasian and African-American male controls?

As shown in **Table 7-3** the variant allele frequency for VEGFR2 H472Q was significantly greater in Caucasian male controls than African-Americans ($p=0.0137$), while for VEGFR2 V297I, the frequency of the variant allele was significantly higher for African-Americans ($p=0.003$) than Caucasian controls. Schneider *et al.* reported similar ethnicity-based differences in allele frequencies in patients with breast cancer with following variant allele frequencies respectively for Caucasian and African-American patients: H472Q, 0.25 and 0.10, and V297I 0.09 and 0.20 (169, 170).

7-3.3 Are VEGFR2 H472Q and V297I genotypes associated with risk of prostate cancer?

Genotype frequencies in the subgroup of Caucasian patients with prostate cancer and Caucasian male controls were compared to assess the impact of studied VEGFR2 SNPs on prostate cancer risk. Studied VEGFR2 SNPs had no significant association with the risk of prostate cancer (**Table 7-4**). Confidence intervals on odds ratios for heterozygous and variant genotypes compared to reference wild-type group included 1, suggesting that

the probability of observed genotype frequencies were not different between cancer patients and controls. However, these confidence intervals also included 2, suggesting that the true odds of disease in patients with variant alleles could be double the odds in other patients. This needs to be confirmed in a large prospective epidemiological study. The number of African-American prostate cancer patients on these trials was too low to assess the impact of VEGFR2 genotype on disease risk.

7-3.4 Are VEGFR2 H472Q and V297I genotypes associated with treatment associated toxicities for sorafenib and/or bevacizumab therapy?

All patients included in the current analyses were treated with either sorafenib and/or bevacizumab as one of the treatment modalities. There is some overlap in toxicity profiles of these drugs, for example both sorafenib and bevacizumab causes hypertension, diarrhea, gastrointestinal perforation etc (49, 120). However, dermatological toxicities such as skin rash and hand-foot skin reaction (HFSR) were only associated with sorafenib treatment. Combined therapy with bevacizumab and sorafenib has reported to result in increased incidences and severity of side-effects (60, 115).

Frequencies for most severe grades of five common sorafenib treatment associated toxicities, namely rash: desquamation, diarrhea, HFSR, hypertension and fatigue were compared between wild-type and variant allele groups for studied VEGFR2 SNPs. Toxicity data were available from all trials involving treatment with sorafenib, but only hypertension and HFSR toxicity data were available for patients treated with bevacizumab with thalidomide and docetaxel.

Only the associations of hypertension and HFSR with VEGFR2 H472Q SNP were significant ($p<0.016$; **Fig 7-1** and **Table 7-5**). The frequency of hypertension and HFSR was almost double for patients carrying the variant VEGFR2 H472Q polymorphism than for carriers of wild-type allele while on therapies against VEGF pathway (hypertension: variants, 39% vs. wild-type, 21%, p=0.0154; HFSR: 33% vs. 16%, p=0.0136). Similar results were obtained for following subgroups: patients treated with sorafenib monotherapy (hypertension: 37% vs. 18%, p=0.1051; HFSR: 40% vs. 16%, p=0.0302) and patients treated with sorafenib as at least one of the therapy (with or without bevacizumab; hypertension: 42% vs. 21%, p=0.0210; HFSR: 44% vs. 20%, p=0.0063). Analysis of the association between toxicities revealed that hypertension was associated with development of HFSR, with 19 of 126 patients (15.1%) with hypertension grades $\leq$ 1 developing HFSR (grades $\geq$ 2) compared to 19 of 52 (36.5%) who developed or worsened hypertension to grades $\geq$ 2 (p=0.0024). Earlier, an analysis based on a subgroup of patients receiving sorafenib and bevacizumab combination demonstrated association between hypertension and HFSR (60). Genotype-toxicity relationships for other toxicities and studied SNPs were non-significant (**Table 7-5**).

7-3.5 Are VEGFR2 H472Q and V297I genotypes associated with survival in patients treated with sorafenib and/or bevacizumab, with or without other agents?

The progression free survival (PFS) and overall survival (OS) was compared for the studied VEGFR2 SNPs across patients or patient subgroups using Kaplan survival analysis. The PFS was significantly different with respect to the VEGFR2 H472Q

polymorphism for patients with solid tumors receiving sorafenib as single agent or in combination therapy (5.7 months for heterozygotes, N=40, vs. 3.2 or 3.7 months for homozygous wild-type, N=76 or variants, N=6, p=0.044), with an apparent heterozygous advantage, as shown in **Fig 7-2**. Similar, but non-significant differences with tendency of heterozygous advantage was seen for following patient subgroups: patients treated with sorafenib monotherapy (p=0.25), patients treated with sorafenib and bevacizumab combination (p=0.48), patients treated with bevacizumab, docetaxel and thalidomide combination (p=0.57), and patients treated with bevacizumab with other agents (sorafenib/docetaxel and thalidomide, p=0.26. The observed heterozygous advantage was thought to be influenced by small sample size in homozygous variant group (N=6). Alternatively, it could be an outcome of overdominance or haplotype association of H472Q SNP with other functionally important SNPs conferring heterozygous advantage. It is important to note that patients with variant allele for VEGFR2 H472Q appeared to have longer PFS and were also more susceptible to hypertension and HFSR. The difference in OS based on VEGFR2 H472Q genotype was not statistically significant. The VEGFR2 V297I SNP was not related with either PFS or OS in studied patients. Earlier, a study in breast cancer patients reported no significant effect of these VEGFR2 SNPs on survival (170).

7-3.6 Are hypertension and HFSR phenotypic markers for effect of VEGFR2 H472Q SNP on PFS?

Because VEGFR2 H472Q SNP was related with both the PFS and toxicities (hypertension and HFSR), we evaluated whether these toxicities were also predictive of PFS (**Fig 7-3**).

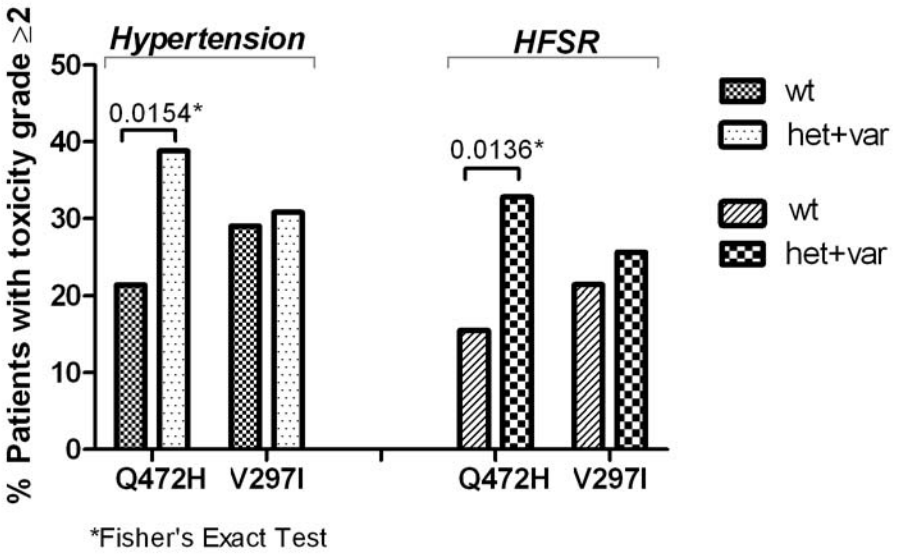

Fig 7-1 Comparison of incidence of hypertension and hand-foot skin reaction (HFSR) toxicities between VEGFR2 genotype groups

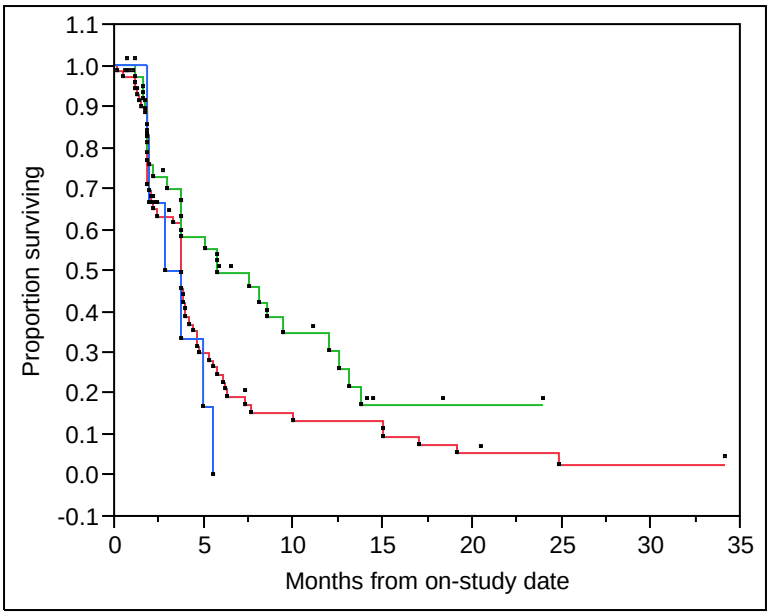

Fig 7-2 Kaplan-Meier survival curves following treatment with sorafenib (as a single agent or in combination therapy) versus VEGFR2 H472Q genotypes. Red: wild-type genotype (N=76), Green: heterozygous genotype (N=40) and Blue: variant genotype (N=6). *P*=0.0440 by a two-tailed log-rank test.

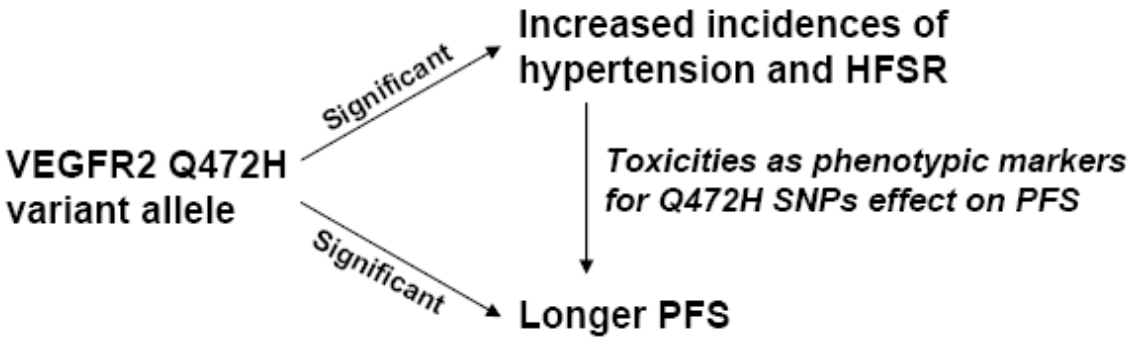

Fig 7-3 Diagram of possible association between VEGFR2 H472Q SNP, toxicities and PFS

The PFS and OS were compared between hypertension and HFSR toxicity groups (grades ≤ 1 and ≥ 2) using Kaplan Meier survival analysis. Hypertension (in patients receiving bevacizumab as one of the therapy) and HFSR (in patients receiving sorafenib as single

agent or in combination therapy) were predictive of longer PFS or slower disease progression. Patients who developed hypertension following treatment with bevacizumab in combination with sorafenib or docetaxel and thalidomide were also the patients who had relatively longer PFS or slower disease progression (p=0.0051; **Fig 7-4**). While patients who developed HFSR following treatment with sorafenib, either as single agent or in combination with ritonavir, bevacizumab or cetuximab, had longer PFS than patients without these toxicities (p=0.0011; **Fig 7-5**). Association of these toxicities with OS was not significant. These results suggest that treatment associated hypertension and HFSR act as phenotypic markers for effect of VEGFR2 H472Q on PFS in patients with solid tumor treated with therapies against VEGF pathway. Earlier, a study involving patients with breast cancer determined significantly longer OS for patients who developed hypertension on bevacizuamb and paclitaxel combination than patients without toxicity (170). Associations between other toxicities and PFS or OS were not significant.

7-3.7 The impact of VEGFR2 H472Q SNP in patients not treated with drugs against the VEGF pathway

To determine whether the effect of VEGFR2 Q472 SNP on PFS was restricted to use of drugs against the VEGF pathway or was common for other categories of drugs as well, we genotyped 62 patients who were on docetaxel therapy, as single agent (N=25) or in combination with ketoconazole (N=37). Kaplan-Meier curve of survival for these patients is shown in **Fig 7-6**; there was no significant difference in survival based on genotype (p=0.5703), and also no trend of survival advantage was observed for heterozygous

genotype. These results indicate that delay in disease progression (or longer PFS) based on VEGFR2 H472Q genotype was only limited to treatments with activity against VEGF pathway.

Table 7-2 Genotype and allele frequencies for SNP in VEGFR loci for solid tumor patients treated with sorafenib and/or bevacizumab, with or without other agents

Allelic variant	N	Gender (N)	Ethnicity (N)	Genotype frequencies, N (%)			Allelic freqencies	
		Male : Female	C : AA : Others	Wt	Het	Var	p	q
VEGFR2 H472Q	176	139:37	145:18:13	108 (61.4)	60 (34.1)	8 (4.5)	0.78	0.22
VEGFR2 V297I	176	138:38	145:18:13	135 (76.7)	38 (21.6)	3 (1.7)	0.87	0.13

C: Caucasians; **AA**: African-Americans; **Others**: Hispanic or Asians; **Wt**: wild-type genotype; **Het**: heterozygous genotype; **Var**: homozygous variant genotype; **p and q** are standard Hardy-Weinberg nomenclature for allele frequencies.

Table 7-3 Comparison of genotype and allele frequencies for two VEGFR2 SNPs between Caucasian and African-American male controls

Allelic variant	Ethnicity	N	Genotype frequencies, N (%)				Allelic frequencies		
			Wt	Het	Var	p-value†	p	q	p-value†
			TT	**TA**	**AA**		**T**	**A**	
VEGFR2 H472Q	Caucasian	138	93 (67.4)	36 (26.1)	9 (6.5)	0.0724	0.80	0.20	0.0137
	African-American	149	117 (78.5)	28 (18.8)	4 (2.7)		0.88	0.12	
			CC	**CT**	**TT**		**C**	**T**	
VEGFR2 V297I	Caucasian	143	117 (81.8)	22 (15.4)	4 (2.8)	0.0038	0.90	0.10	0.0030
	African-American	148	96 (64.9)	47 (31.8)	5 (3.4)		0.81	0.19	

†Chi-squares test was used to compare the genotype and allele frequencies between Caucasian and African-American controls

Table 7-4 Assessment of risk of prostate cancer based on VEGFR2 genotype

VEGFR2 SNP	Genotype frequency, N (%)		Odds ratio [95%CI]	p-value†
	Prostate Cancer Cases	Controls		
VEGFR2 H472Q				
TT	62 (62.6)	93 (67.4)	1	
TA	33 (33.3)	36 (26.1)	1.4 [0.8-2.4]	0.3066
AA	4 (4.0)	9 (6.5)	0.7 [0.2-2.3]	0.5705
(TA+AA) vs. TT	35 (37.4)	45 (32.6)	1.2 [0.7-2.1]	0.5798
VEGFR2 V297I				
CC	76 (77.6)	117 (81.8)	1	
CT	20 (20.4)	22 (15.4)	1.4 [0.7-2.7]	0.3870
TT	2 (2.0)	4 (2.8)	0.8 [0.1-4.3]	1.000
(CT+TT) vs. CC	22 (22.4)	26 (18.2)	1.3 [0.7-2.5]	0.4175

†p-values are based on Fisher's exact test

Table 7-5 Comparison of toxicities between wild type and variant allele groups for VEGFR2 SNPs

Toxicity grade ≥2 N (%*)	VEGFR2 H472Q			VEGFR2 V297I		
	wt allele	var allele	p-value†	wt allele	var allele	p-value†
Hypertension	22 (21.4)	26 (38.8)	**0.0154**	38 (29.0)	12 (30.8)	0.8431
HFSR	16 (15.5)	22 (32.8)	**0.0136**	28 (21.4)	10 (25.6)	0.6618
Rash:desquamation	17 (25.0)	13 (28.9)	0.6686	23 (27.7)	9 (30.0)	0.8165
Diarrhea	14 (20.6)	7 (15.6)	0.6236	19 (22.9)	3 (10.0)	0.1795
Fatigue	12 (17.7)	6 (13.3)	0.6080	14 (16.9)	4 (13.3)	0.7766

*% of total patients in that group, †p-values are based on Fisher's exact test. **wt**: wild-type, **var**: variant

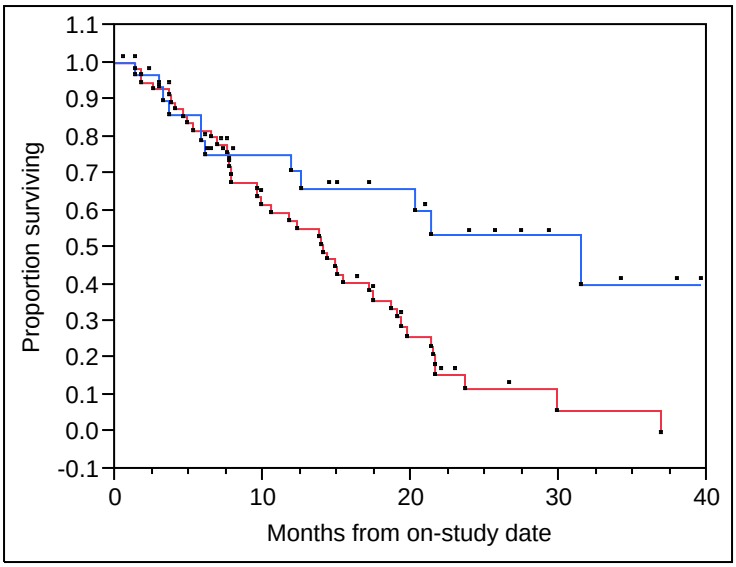

Fig 7-4 Kaplan-Meier survival curves following treatment with bevacizumab (in combination with sorafenib (N=27) or docetaxel and thalidomide (N=60)) versus hypertension grades (≤1 or ≥2). Red: hypertension grade ≤1 (N=57) and Blue: hypertension grade ≥2 (N=30). *P*=0.0051 by a two-tailed log-rank test.

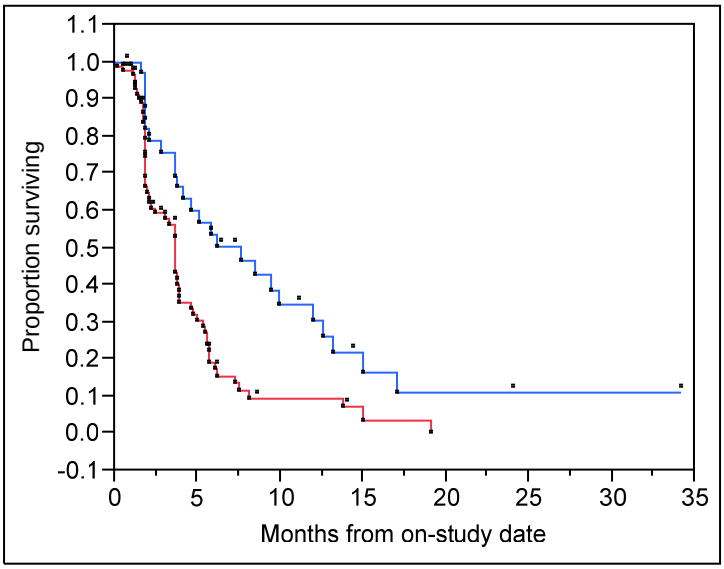

Fig 7-5 Kaplan-Meier survival curves following treatment with sorafenib (as single agent (N=76) or in combination with bevacizumab (N=27) or cetuximab (N=18)) versus HFSR grades (≤1 or ≥2). Red: HFSR grade ≤1 (N=87) and Blue: HFSR grade ≥2 (N=34). *P*=0.0011 by a two-tailed log-rank test.

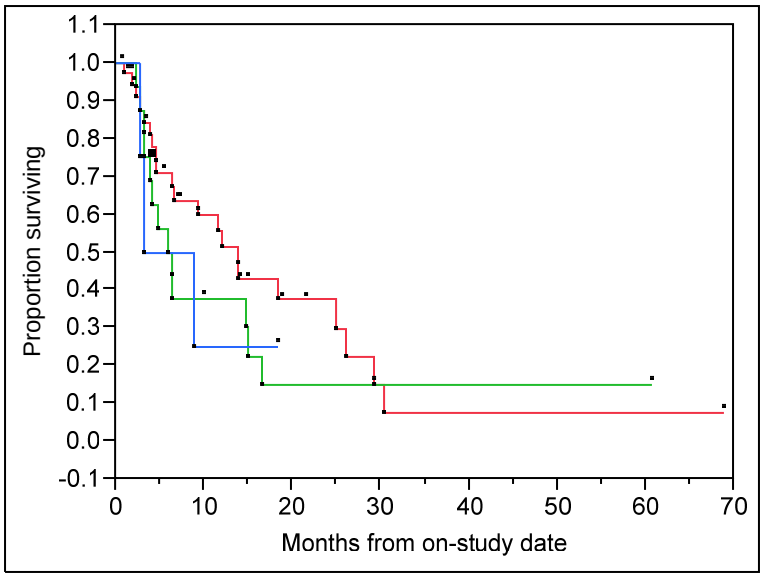

Fig 7-6 Kaplan-Meier survival curves following treatment with docetaxel (as a single agent (N=25) or in combination with ketoconazole (N=31)) versus VEGFR2 H472Q genotypes. Red: wild-type genotype (N=35), Green: heterozygous genotype (N=17) and Blue: variant genotype (N=4). *P*=0.5703 by a two-tailed log-rank test.

7-4 Discussion

Only a few studies have evaluated the role of VEGFR2 SNPs as a predictive or prognostic disease marker. Försti and colleagues assessed the impact of VEGF and VEGFR2 SNPs on the risk of breast cancer (79). Two studies by Schneider and colleagues investigated SNPs in VEGF and VEGFR2 gene as potential markers for breast cancer risk (169) and for the prediction of toxicity/treatment outcomes following treatment with paclitaxel with or without bevacizuamb (170). These studies were focused on a single tumor type. Additionally, two small studies evaluated the impact of VEGF/VEGFR2 SNPs on recurrence of colon cancer (171) and on the prediction of efficacy or toxicity in patients treated with anti-angiogenic therapy (172).

This is the first report evaluating the impact of two functionally important VEGFR2 SNPs on the risk of prostate cancer, and also investigating their role as prognostic and predictive markers in a diverse solid tumor patient population undergoing treatment with drugs having activity against VEGF pathway. For the first time, genotype and allele frequencies of VEGFR2 H472Q and V297I SNPs have been characterized and compared between Caucasian and African-American male subjects with no known diagnosis of cancer (i.e., controls) of U.S. origin.

The frequencies of these SNPs between male controls and patients with prostate cancer were not statistically different, suggesting that these SNPs would not act as predictive markers for risk of prostate cancer. Earlier, these polymorphisms were reported also not to be related with risk of breast cancer as well (79, 169).

The VEGFR2 H472Q SNP was related with better prognosis and risk of hypertension and HFSR. Few subjects carried the variant genotype; hence only joint toxicities in heterozygous and homozygous variant genotypes could be compared against wild-type carriers. Carriers of the variant allele for H472Q were more susceptible to both hypertension and HFSR, and these toxicities were associated with each other. These toxicities appeared to be the phenotypic markers for the effect of VEGFR2 H472Q SNP on disease progression in patients with solid tumor, treated with sorafenib and/or bevacizumab with or without other agents. Patients who developed these toxicities had longer PFS than others while on therapies against VEGF pathway. These findings suggest that patients who develop these toxicities are more likely to also achieve a therapeutic

benefit. Hence, these side effects should be effectively managed to avoid or delay the treatment disruption or discontinuation.

We observed a better prognosis for the heterozygous genotype compared to both wild-type or variant genotype. The difference in PFS for wild-type and variant genotypes appeared to be non-significant. The discrepant order of PFS for patients who carry two copies of the variant allele was thought to be biased by a small sample size in that group (N=6). The overdominance hypothesis may also explain the heterozygous allele superiority relative to homozygous alleles (173). The VEGFR2 H472Q (rs1870377; exon 11) SNP is linked with rs3816584 (intron 16), rs6838752 (intron 17), rs10016064 (intron 13), rs17085262 (intron 21), rs17085265 (intron 21), rs 2219471 (intron 20), rs13136007 (intron 13), rs1870378 (intron 15) and rs1870379 (intron15) based on CEU data from HapMap project. It is possible that H472Q acts as tag SNP for other functionally important SNPs. The VEGFR2 V297I (rs2305948; exon7) was not linked to any other SNPs; and was not related with progression free survival, overall survival or susceptibility to hypertension and HFSR. These results suggest a prognostic and predictive role for VEGFR2 H472Q SNP, but not for V297I SNP. The lack of impact on OS by these SNPs suggests that tumor biology was not altered based on their genotypes.

The exonic VEGFR2 V297I and H472Q SNPs are located in the third and fifth immunoglobulin like (Ig-like) domains of VEGFR2 receptor. The Ig-like domain 3 is critical for binding of VEGF (174), while domains 4-7 contain structural features that inhibit VEGFR2 signaling in the absence of VEGF (175). Wang et al studied the effect of

these SNPs on VEGF binding by transfecting the HEK293s cells with variant allele for one or both of these SNPs (176). As expected, transfects with variant VEGFR2 V297I SNP had significantly low VEGF binding efficiency regardless of VEGFR2 H472Q allele; while variant VEGFR2 H472Q allele had minimal effect on VEGF binding efficiency (176).

The non-synonymous amino acid change by VEGFR2 H472Q SNP may result in a loss of inhibition of VEGFR2 signaling in the absence of VEGF leading to a constitutively active VEGFR2 receptor. These patients with seemingly constitutive signaling appear to have a pronounced effect, following treatment with sorafenib and bevacizumab. Sorafenib acts intracellularly on VEGFR2 receptors to inhibit the auto-phosphorylation and receptor activation. Bevacizumab acts extracellularly to inhibit the binding of VEGF protein to VEGFR2 receptor. The site of VEGFR2 H472Q is downstream to the bevacizumab's target site in VEGF signaling pathway, even than it appears to be related with progression free survival and frequency of toxicities, suggesting that VEGFR2 H472Q receptor polymorphism may be important even in patients with reduced VEGF levels.

Hypertension is a common side effect associated with agents that block signaling through VEGF pathway, which is not unexpected given that VEGF receptors are present on endothelial cells on blood vessels. Hypertension has been reported in all studies involving bevacizumab (177). Azad and colleagues has presented several lines of evidence to

support the role of VEGF pathway in development of HFSR (115). These data also explain the effect of VEGFR2 SNP on susceptibility to hypertension and HFSR.

In conclusion, VEGFR2 H472Q SNP appears to play an important role in prediction of toxicities and treatment outcome following treatment with drugs having activity against the VEGF pathway. Treatment associated toxicities on these therapies should be aggressively treated, as opposed to taking patients off the trial after the first sign of toxicities, to achieve the optimal therapeutic benefit.

CHAPTER EIGHT

SUMMARY AND OVERALL CONCLUSIONS

A collaboration between Bayer and Onyx pharmaceuticals in the discovery of novel therapies targeting the Ras-Raf-MEK-ERK pathway using high-throughput screening and a combinatorial chemistry approach led to the identification of sorafenib as a potential anticancer agent (1). Sorafenib was found to be a potent inhibitor of wild-type b-raf, oncogenic *b-raf*V6600E serine/threonine kinases, c-raf, pro-angiogenic RTKs (VEGFR1, 2, 3, PDGFRβ, FGFR1) and other RTKs involved in tumorigenesis (c-Kit, Flt-3 and RET)(1). It has been tested as a potential treatment for patients with solid tumors in several clinical trials since year 2000 (1). In 2005, it was first approved by the FDA for the treatment of advanced renal cell carcinoma, and later in 2007, the original approval was extended to unresectable hepatocellular carcinoma (9). Currently, it is used in more than 70 countries worldwide for these indications (9). In general, sorafenib is well tolerated with a manageable side-effects profile (1). Therefore, it has also been (is being) evaluated in combination with other anticancer therapies, including the cytotoxic chemotherapies, immunological agents and anti-angiogenic agents (1).

Sorafenib's pharmacokinetics and toxicity profiles are well characterized in patients with solid tumors and normal organ functions (38-40, 63) and more recently, in special patient

populations, such as with hepatic or renal impairment (94). All published clinical studies reported high inter-patient variability in its systemic exposure, clinical efficacy and toxicities (**chapter 1**), suggesting that clinical outcomes are highly variable in patients treated with sorafenib. Hence, there was/is a critical need for identification of predictive markers for efficacy and toxicity to improve the clinical utility of sorafenib. To determine such markers, we designed several correlative studies for clinical trials being conducted at NCI involving administration of sorafenib. A total of five phase I/II clinical trials evaluated the safe dose or efficacy (response rate) of sorafenib in patients with mCRPC, CRC, NSCLC, KS and various ST following administration as a single agent or in combination with other chemotherapies. Sorafenib was orally administered at 200/400 mg BID dose levels. From patients enrolled into these trials, pharmacokinetic, pharmacodynamic and pharmacogenomic data were collected along with information about their demographic characteristics and organ functions. Analysis of pharmacokinetic characteristics, Pharmacokinetic-Pharmacodynamic-Pharmacogenomic correlative studies and *ex-vivo* cell line experiments were conducted to explore the potentially predictive markers based on available data.

For quantitation of sorafenib in plasma samples from patients enrolled in the above-mentioned trials, a LC-MS/MS bioanalytical method was required. Published bioanalytical methods were limited by complex extraction procedures, long run-times, poor sensitivity and requirement of large plasma volume. Hence, a simple, rapid, sensitive and efficient method was developed and validated. This method was based on a simple protein precipitation, required only 50 μL of plasma volume, and had short run

time of 4 minutes with a lower quantifiable limit of 5 ng/mL (152). Plasma samples from all patients enrolled in the above mentioned trials were analyzed using this method, and plasma concentration-time profiles were generated.

Exposure metrics and pharmacokinetic parameters were determined by non-compartmental analysis-general linear modeling (NCA-GLM; two-stage approach) and population pharmacokinetic modeling:

Sorafenib exposures after the first dose (AUC_{0-12}), maximum plasma concentration (C_{max}) and time to maximum plasma concentration (t_{max}) were estimated by non-compartmental analysis, using single-dose plasma concentration – time profiles over 12 hrs. The %CV on AUC_{0-12} and C_{max} for 400 mg BID dose ranged from 45 to 79% and 46 to 87%, respectively, and for the 200 mg BID dose %CV on both of these parameters were approximately 65%. To explain this variability, demographic (age, weight, height, BSA, gender, ethnicity), clinical (serum albumin, alkaline phosphatase, ALT, AST, bilirubin total, total protein, serum creatinine and estimated creatinine clearance) and pharmacogenetic (CYP3A4*1B, CYP3A5*3C, UGT1A9*3, UGT1A9*5, VEGFR2 H472Q and VEGFR2 V297I) factors were explored using general linear modeling of the ln-transformed exposure metrics. Body weight, BSA, serum albumin and UGT1A9*3 were statistically significant and mechanistically plausible covariates for both of these pharmacokinetic metrics. However, their contribution to the overall variability in systemic sorafenib exposure was small, making these effects clinically irrelevant and

would not justify any dose adjustments. Only one patient carried the UGT1A9*3*3 genotype; hence, its potential effects need to be evaluated in future studies.

The plasma concentration –time profiles from both single dose and steady-state were used together to perform the population pharmacokinetic modeling. A mechanism-based pharmacokinetic model was successfully developed; taking into account sorafenib's known pharmacokinetic properties. A one-compartmental body model with first-order absorption, discontinuous entero-hepatic recycling, serial GI transit absorption compartments (n=4) and first-order elimination best described the sorafenib pharmacokinetics. Only body weight was found to be a significant covariate for apparent volume of distribution (V/F), which reduced inter-patient variability in log-transformed plasma concentrations from 72% to 69%. Because the contribution of body weight to the variance on V/F was small, and a large proportion of the overall variability remains unexplained, this effect was clinically irrelevant and would not necessitate any dose adjustments. For a patient with a body weight of 81.5 kg, the typical population value for clearance (CL/F) was 8.0 L/h, V/F 217 L and GI absorption transit time 1.98 h. The model-predicted plasma concentrations were in reasonable agreement with observed concentrations, and the estimated typical population mean values were in accordance with sorafenib's known pharmacokinetic characteristics. Both NCA-GLM and population pharmacokinetic analysis appeared to agree on role of body weight as a statistically significant covariate; albeit, not clinically important.

In NCA-GLM analysis, serum albumin appeared to be an important covariate for C_{max}/D and AUC_{0-12}/D, but its contribution to overall variance in these exposure metrics was minimal. Serum albumin was also a significant covariate for V/F during stepwise-forward regression stages of covariate model building, but was not significant in the final population pharmacokinetic model. These effects were mechanistically plausible, but had minimal clinical relevance because of their small contribution to overall varianbility in pharmacokinetic/exposure parameters. Genetic variations in metabolic enzymes for sorafenib (i.e., CYP3A4 and CYP3A5) appeared to be unimportant in describing the variations in disposition of sorafenib. However, the UGT1A9*3 SNP appeared to be statistically significant covariate by NCA-GLM and during covariate model building stages of population pharmacokinetic analysis. Since only one patient carried the homozygous variant genotype (i.e., UGT1A9*3*3), its effect may have been biased by small (unbalanced) sample size in genotype subgroups. Nevertheless, these effects were mechanistically plausible, where UGT1A9*3 would reduce the metabolic activity of UGT1A9 enzyme resulting in higher plasma levels for carriers of this SNP. The effect of UGT1A9*3 on sorafenib exposure requires further prospective investigations with a larger sample sizes. None of the studied patients carried UGT1A9*5 SNP, hence, its effect on sorafenib disposition could not be evaluated.

The results of NCA-GLM and population pharmacokinetic analysis were in agreement with the results of published prospective clinical studies. In particular, a drug-interaction study investigated the effect of ketoconazole co-administration, a potent CYP3A4 inhibitor, on sorafenib pharmacokinetics (37). The CYP3A4 inhibition by ketoconazole

was reported to have no significant effect on sorafenib's systemic exposure, but reduced the levels of circulating N-oxide metabolites (37). Another study investigated the pharmacokinetics of sorafenib in patients with various degrees of liver and renal dysfunction (94). Sorafenib exposures were highly variable among these patients, but no association was apparent with extent of liver or kidney impairment. The collective conclusions from these studies support our findings that liver and kidney function parameters and genetic variation in CYP3A4 and CYP3A5 metabolic enzymes are not clinically important determinants of sorafenib exposure.

Following exploration for sources of variability in pharmacokinetics of sorafenib, we investigated possible associations between sorafenib exposure and clinical outcomes. The hypothesis was that higher exposures of sorafenib would be be associated with better efficacy and/or higher incidence or severity of treatment associated side-effects, assuming no major inter-patient differences in responsiveness to sorafenib.

Clinical efficacy and toxicities in patients treated with sorafenib were highly variable. Sorafenib appeared to have modest activity in patients with mCRPC. Co-administration with bevacizumab and cetuximab resulted in improved efficacy in patients with ST and CRC compared to historical response rates with single-agent therapies. Response evaluation in patients with NSCLC was limited by the small sample size. Up to 79% patients in combination therapy trials had partial response (PR) or stable disease (SD) compared to less than 50% patients in single agent trials. The combination of targeted therapies appears to improve on the modest activity of these drugs as single agents.

However, these combinations may also result in higher than expected toxicities; hence, they necessitate careful adjustments of doses and development of strategies for management of side-effects. We observed higher incidence and severity of treatment-associated side effects in patients treated with combination therapy than single agent alone. The incidence of treatment-associated toxicities, such as hypertension, hand-foot skin reaction (HFSR), rash: desquamation, fatigue and diarrhea, were normally less than 50% in single-agent sorafenib trials, which increased to 74% in trials involving combination therapies.

Exposure-efficacy relationship appeared to be non-significant for patients with mCRPC, CRC and ST based on sorafenib exposures alone. Clinical efficacy in patients with NSCLC appeared to be associated with systemic exposure of sorafenib; however, a lack of correlation between exposure (AUC_{0-12}) and PFS and small number of patients on this trial (N=18) suggests the need of further evaluation. The exposure-efficacy relationship was not evaluated for patients with KS because of limited enrollment of patients in that trial.

Assessment of exposure-toxicity relationships suggested an increase in the incidences of rash with increase in sorafenib exposure for single-agent sorafenib therapy. Following administration of sorafenib with bevacizumab, the incidence of HFSR appeared to be associated with sorafenib exposures, which was not significant for single-agent sorafenib studies. Other toxicities were not associated with sorafenib exposures, following

treatment as either single agent or in combination therapy. These results were also supported by published literature.

In addition to exposure-efficacy relationships, we evaluated prostate specific antigen (PSA) and *ex-vivo* anti-angiogenic activity as markers for clinical efficacy, respectively, in patients with mCRPC and ST.

PSA concentrations have long been used as an indicator of treatment efficacy and tumor progression (cancer staging) in patients with prostate cancer. Greater than 50% post-treatment declines in serum PSA concentrations were shown to be associated with survival advantage. Contrary to conventional chemotherapies, serum PSA concentrations increased following treatment with sorafenib, which declined after treatment discontinuation. Also, a few patients had improvement in bone scans despite of continuous rise in PSA. It was hypothesized that sorafenib may influence PSA concentrations independent of its effect on cellular-growth. To check this hypothesis we treated LNCaP human prostate cancer cells with increasing concentrations of sorafenib in *in-vitro* experiments. The concentrations of secreted PSA increased with increase in sorafenib concentrations, and as expected, cell counts declined. These results support the clinical observations and indicate that PSA is not a suitable surrogate marker of efficacy in prostate cancer patients treated with sorafenib. These changes in PSA secretion are thought to be in part due to drug-induced increase in PSA transcription activity.

We also investigated the association of *ex-vivo* anti-angiogenic activity for steady-state serum samples from patients on sorafenib and bevacizumab combination and their best clinical responses. The *ex-vivo* anti-angiogenic activity was assumed to act as a surrogate of combined plasma concentrations of these drugs and was measured by rat aortic ring assay using steady-state serum samples. The anti-angiogenic activity was not associated with clinical outcome, suggesting that it may not be used as a biomarker for clinical response; however, these results were limited by small sample size.

We also evaluated laboratory and pharmacogenetic markers for toxicities, which were selected based on mechanistic reasoning. HFSR, a sorafenib treatment associated side effect, mainly affects the palms of hands and soles of feet, causing erythema with swelling followed by blistering and desquamation. Eccrine sweat glands are abundant in these skin surfaces and are also adversely affected by HFSR, resulting in dilatation and dysmorphism of eccrine cells. Based on anatomical distribution of HFSR and effects on eccrine sweat glands, we hypothesized that its development might be associated with excretion of sorafenib in sweat. We collected sweat samples from patients with HFSR and determined sorafenib concentrations in them using a LC-MS/MS method with lower quantifiable limits of 5 ng/mL. Sorafenib was undetectable in these samples, suggesting that HFSR is not associated with leakage of sorafenib in sweat at concentrations measuring ≥5 ng/mL.

Development of HFSR has also been shown to be associated with inhibition of the VEGF pathway. Supporting evidence was offered by Azad and colleagues(60), (a) increase in

frequency and severity of HFSR following combination of sorafenib with bevacizumab, (b) predilection of HFSR for traumatic foci, suggesting that inhibition of VEGF may retard tissue repair from minor trauma, (c) direct association of cumulative bevacizumab dose with incidences of HFSR, and (d) the association of HFSR and development of hypertension, suggesting a role of vascular effects. Another side effect, hypertension, is a common side effect of drugs with anti-angiogenic activity (or activity against VEGF pathway) including sorafenib, which is not unexpected given that VEGF receptors are present on endothelial cells on blood vessels. Considering the role of the VEGF pathway in development of these toxicities, we evaluated the impact of genetic variation (SNPs) in VEGFR2 (i.e., H472Q and V297I), a receptor which mediates the majority of cellular responses of VEGF, on incidences of these toxicities. Patients with variant alleles for VEGFR2 H472Q SNP were more likely to develop hypertension and HFSR than carriers of the wild-type allele while on anti-angiogenic therapies. Patients who developed hypertension on anti-angiogenic therapies were also more likely to develop HFSR.

Because clinical effects of anti-angiogenic drugs used in current trials (i.e., sorafenib and bevacizumab) were also mediated by VEGFR2, the impact of genetic variation in VEGFR2 on overall and progression-free survival (OS and PFS) was also determined. Patients with VEGFR2 H472Q heterozygous genotype appeared to have longer PFS than carriers of homozygous wild-type or homozygous variant genotype while on anti-angiogenic therapy with sorafenib and/or bevacizumab, but OS was not associated with genotype. The exact mechanism of this apparent heterozygous advantage is not known, but possible explanations include the small sample size in the variant allele group (N=6),

and/or the phenomenon of overdominance or proxy role of H472Q SNP for other functionally important SNPs (i.e., haplotype association). It is important to note that variant allele for H472Q appears to be associated with both slower disease progression (or longer PFS) and higher incidence of HFSR and hypertension toxicities, suggesting that these patients are more responsive to anti-angiogenic therapies than wild-type carriers. Hypertension and HFSR appear to act as phenotypic markers for the effect of VEGFR2 H472Q SNP on PFS. The exact mechanism for this effect is not known, but based on the known functional roles of site where these SNPs are located, the variant H472Q allele appears to lead into constitutive activation of VEGFR2 receptors. Inhibition of constitutive signaling would result into prominent changes from baseline compared to inhibition of normal signaling, therefore, possibly resulting into pronounced effects on survival and toxicities. These findings also suggest that these side effects should be managed effectively to avoid or delay the discontinuation of treatment.

In addition to assessment of VEGFR2 SNPs as pharmacogenetic marker for efficacy and toxicity, we investigated their impact on risk of prostate cancer by conducting a case-control study. Both VEGFR2 H472Q and V297I were not associated with risk of prostate cancer.

Results of these all correlative studies are summarized in **Fig 8-1**.

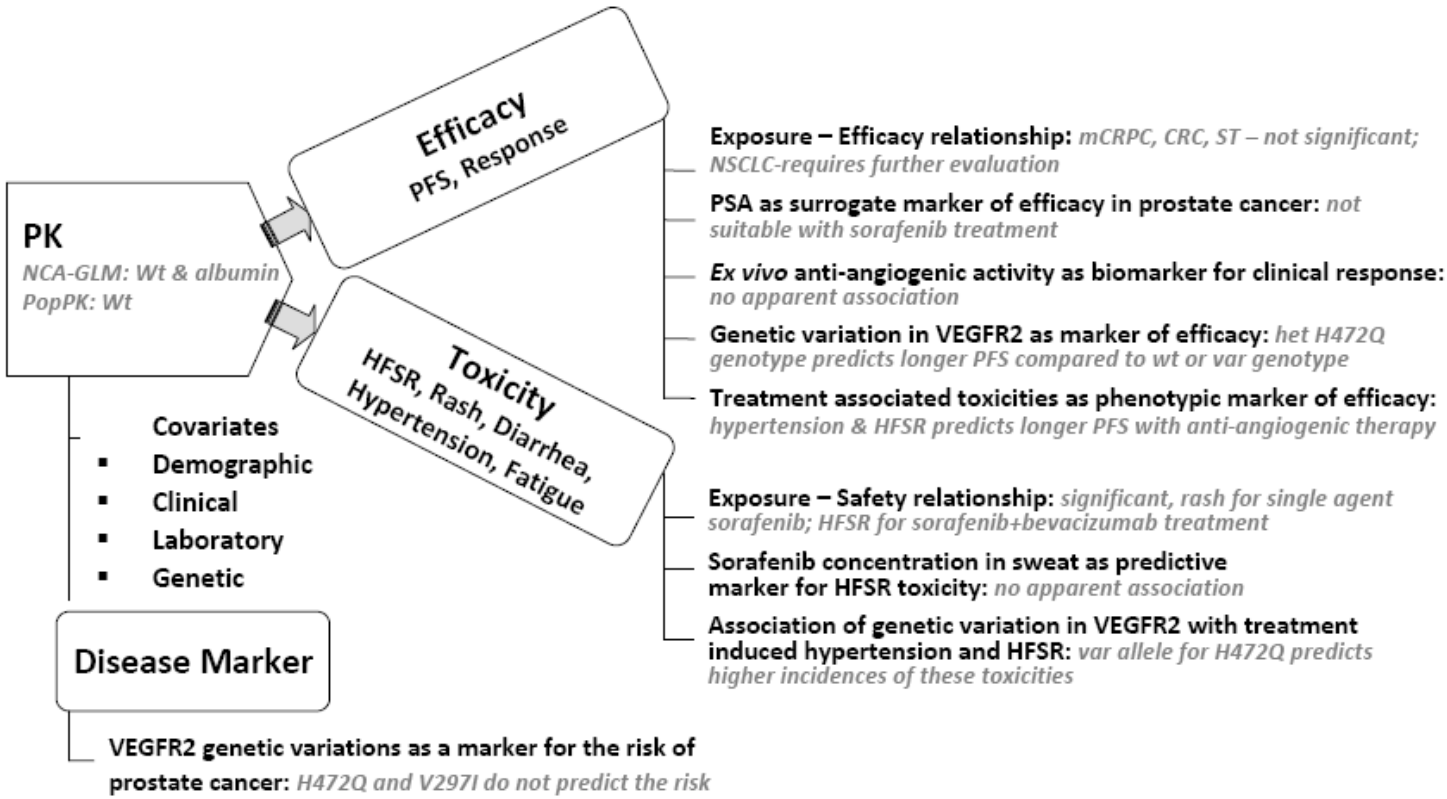

Fig 8-1 Schematic illustration of results from exploration of demographic, clinical, laboratory and pharmacogenetic markers for exposure, efficacy and toxicity in patients with solid tumors following treatment with sorafenib. Results from assessment of pharmacogenetic markers for risk of prostate cancer are also included.

Overall, in this research project, potential demographic, clinical, laboratory and pharmacogenetic factors contributing to variability in pharmacokinetics, clinical efficacy and toxicity for sorafenib treatment were explored. Pharmacogenetic markers for risk of prostate cancer were also investigated. There are several clinically important findings which are summarized below:

(a) No dose adjustments for sorafenib are necessary based on patient's demographic characteristics studied, namely their genotype for CYP3A4*1B, CYP3A5*3C and possibly UGT1A9*3 SNPs in metabolic enzymes, and liver and kidney function, at least based on the range of data available from the studies included in this analysis.

(b) Higher exposures of sorafenib may not translate into better clinical efficacy, but are likely to result in higher incidences of dermatological toxicities.

(c) For prostate cancer patients treated with sorafenib, markers other than PSA should be used to assess/predict the efficacy. The role of PSA as efficacy markers for other targeted therapies should also be examined before its clinical use, to avoid withdrawal of (clinically effective) therapies because of the possibility of a false indication of disease progression.

(d) Treatment with anti-angiogenic therapies should not be discontinued merely because of development of toxicities such as HFSR and hypertension. These side effects may actually be indicative of patient's favorable response to administered treatment. Hence, aggressive adjuvant therapies should be used to manage these side effects before discontinuation of treatment.

(e) Genetic variations in VEGFR2 predict the survival, and frequency of selected toxicities, indicating that activity of the VEGF pathway is indeed important for the

clinical effects of anti-angiogenic drugs. Combination of targeted drugs with activity against multiple (upstream and downstream) proteins in the VEGF pathway might result in better efficacy. However, the benefit-risk ratio in the context of each individual patient should be assessed, because treatment with drug combination may also increase the incidence of toxicities.

(f) Drugs decreasing the secretion of sweat might not be helpful in reducing the severity of HFSR associated with sorafenib treatment. This mechanism need to be evaluated further using methods with higher sensitivity, such as fluorescent labeling.

These studies are a step forward towards individualization of sorafenib treatment, with an ultimate aim to provide the right dose of sorafenib to right patient at right time. However, these results need to be confirmed in prospective clinical studies. Identification of markers for efficacy and toxicity are not only important to increase clinical utility, but also to avoid the false-negative conclusions about the inefficacy of sorafenib in certain tumor types. The later is critical to facilitate the availability of drugs with activity in a selected patient population.

References:

1. Wilhelm S, Carter C, Lynch M, et al. Discovery and development of sorafenib: a multikinase inhibitor for treating cancer. Nat Rev Drug Discov 2006; 5: 835-44.
2. Esteller M,Herman JG. Cancer as an epigenetic disease: DNA methylation and chromatin alterations in human tumours. J Pathol 2002; 196: 1-7.
3. Frost P,Kerbel RS. On a possible epigenetic mechanism(s) of tumor cell heterogeneity. The role of DNA methylation. Cancer Metastasis Rev 1983; 2: 375-8.
4. Kolch W. Meaningful relationships: the regulation of the Ras/Raf/MEK/ERK pathway by protein interactions. Biochem J 2000; 351 Pt 2: 289-305.
5. Mercer KE,Pritchard CA. Raf proteins and cancer: B-Raf is identified as a mutational target. Biochim Biophys Acta 2003; 1653: 25-40.
6. Saif MW,Shah M. K-ras mutations in colorectal cancer: a practice changing discovery. Clin Adv Hematol Oncol 2009; 7: 45-53, 64.
7. Deichmann M, Thome M, Benner A, Kirschner M, Hassanzadeh J,Kurzen H. Preponderance of the oncogenic V599E and V599K mutations in B-raf kinase domain is enhanced in melanoma cutaneous/subcutaneous metastases. BMC Cancer 2005; 5: 58.
8. Caraglia M, Tassone P, Marra M, Budillon A, Venuta S,Tagliaferri P. Targeting Raf-kinase: molecular rationales and translational issues. Ann Oncol 2006; 17: vii124-vii27.

9. Onyx Pharmaceuticals. Marketed Products: Sorafenib (Nexavar(R)).http://www.onyx-pharm.com/wt/page/marketed_products. Accessed on July 21, 2009

10. Wilhelm SM, Carter C, Tang L, et al. BAY 43-9006 exhibits broad spectrum oral antitumor activity and targets the RAF/MEK/ERK pathway and receptor tyrosine kinases involved in tumor progression and angiogenesis. Cancer Res 2004; 64: 7099-109.

11. Yu C, Bruzek LM, Meng XW, et al. The role of Mcl-1 downregulation in the proapoptotic activity of the multikinase inhibitor BAY 43-9006. Oncogene 2005; 24: 6861-9.

12. Ferrara N. VEGF and the quest for tumour angiogenesis factors. Nat Rev Cancer 2002; 2: 795-803.

13. National Cancer Institute: Prostate Cancer Home Page. http://www.onyx-pharm.com/wt/page/marketed_products. Accessed on July 21, 2009

14. Erlich S, Tal-Or P, Liebling R, et al. Ras inhibition results in growth arrest and death of androgen-dependent and androgen-independent prostate cancer cells. Biochem Pharmacol 2006; 72: 427-36.

15. Gioeli D. Signal transduction in prostate cancer progression. Clin Sci (Lond) 2005; 108: 293-308.

16. Brawer MK, Deering RE, Brown M, Preston SD,Bigler SA. Predictors of pathologic stage in prostatic carcinoma. The role of neovascularity. Cancer 1994; 73: 678-87.

17. Siegal JA, Yu E,Brawer MK. Topography of neovascularity in human prostate carcinoma. Cancer 1995; 75: 2545-51.

18. Melnyk O, Zimmerman M, Kim KJ,Shuman M. Neutralizing anti-vascular endothelial growth factor antibody inhibits further growth of established prostate cancer and metastases in a pre-clinical model. J Urol 1999; 161: 960-3.

19. Ryan CJ, Lin AM,Small EJ. Angiogenesis inhibition plus chemotherapy for metastatic hormone refractory prostate cancer: history and rationale. Urol Oncol 2006; 24: 250-3.

20. Ferrara N. VEGF as a therapeutic target in cancer. Oncology 2005; 69 Suppl 3: 11-6.

21. Richardson GE,Johnson BE. The biology of lung cancer. Semin Oncol 1993; 20: 105-27.

22. Johnson L, Mercer K, Greenbaum D, et al. Somatic activation of the K-ras oncogene causes early onset lung cancer in mice. Nature 2001; 410: 1111-6.

23. Ahrendt SA, Decker PA, Alawi EA, et al. Cigarette smoking is strongly associated with mutation of the K-ras gene in patients with primary adenocarcinoma of the lung. Cancer 2001; 92: 1525-30.

24. Kersting M, Friedl C, Kraus A, Behn M, Pankow W,Schuermann M. Differential frequencies of p16(INK4a) promoter hypermethylation, p53 mutation, and K-ras mutation in exfoliative material mark the development of lung cancer in symptomatic chronic smokers. J Clin Oncol 2000; 18: 3221-9.

25. Lee JT,McCubrey JA. BAY-43-9006 Bayer/Onyx. Curr Opin Investig Drugs 2003; 4: 757-63.

26. Reid A, Vidal L, Shaw H,de Bono J. Dual inhibition of ErbB1 (EGFR/HER1) and ErbB2 (HER2/neu). Eur J Cancer 2007; 43: 481-9.

27. Levin M. Advances in colon cancer. Drug News Perspect 2003; 16: 325-9.

28. Patiyil S,Alberts SR. Metastatic colorectal cancer: Therapeutic options. Curr Treat Options Oncol 2006; 7: 389-98.

29. Moosmann N, Laessig D, Michaely HJ, Schulz C,Heinemann V. Effective second-line treatment with cetuximab and bevacizumab in a patient with hepatic metastases of colorectal cancer and hyperbilirubinemia. Onkologie 2007; 30: 509-12.

30. Folpe AL, Veikkola T, Valtola R,Weiss SW. Vascular endothelial growth factor receptor-3 (VEGFR-3): a marker of vascular tumors with presumed lymphatic differentiation, including Kaposi's sarcoma, kaposiform and Dabska-type hemangioendotheliomas, and a subset of angiosarcomas. Mod Pathol 2000; 13: 180-5.

31. Skobe M, Brown LF, Tognazzi K, et al. Vascular endothelial growth factor-C (VEGF-C) and its receptors KDR and flt-4 are expressed in AIDS-associated Kaposi's sarcoma. J Invest Dermatol 1999; 113: 1047-53.

32. Flexner C. HIV-protease inhibitors. N Engl J Med 1998; 338: 1281-92.

33. EMEA Report on Sorafenib. http://www.emea.europa.eu/humandocs/PDFs/EPAR/nexavar/H-690-en6.pdf Accessed on July 21, 2009

34. Drug Bank. Drug card for Sorafenib (DB00398). http://www.drugbank.ca/drugs/DB00398 Accessed on May 10, 2009

35. Strumberg D, Richly H, Hilger RA, et al. Phase I clinical and pharmacokinetic study of the Novel Raf kinase and vascular endothelial growth factor receptor inhibitor BAY 43-9006 in patients with advanced refractory solid tumors. J Clin Oncol 2005; 23: 965-72.

36. Wu CY,Benet LZ. Predicting drug disposition via application of BCS: transport/absorption/ elimination interplay and development of a biopharmaceutics drug disposition classification system. Pharm Res 2005; 22: 11-23.

37. Lathia C, Lettieri J, Cihon F, Gallentine M, Radtke M,Sundaresan P. Lack of effect of ketoconazole-mediated CYP3A inhibition on sorafenib clinical pharmacokinetics. Cancer Chemother Pharmacol 2006; 57: 685-92.

38. Awada A, Hendlisz A, Gil T, et al. Phase I safety and pharmacokinetics of BAY 43-9006 administered for 21 days on/7 days off in patients with advanced, refractory solid tumours. Br J Cancer 2005; 92: 1855-61.

39. Clark JW, Eder JP, Ryan D, Lathia C,Lenz HJ. Safety and pharmacokinetics of the dual action Raf kinase and vascular endothelial growth factor receptor inhibitor, BAY 43-9006, in patients with advanced, refractory solid tumors. Clin Cancer Res 2005; 11: 5472-80.

40. Moore M, Hirte HW, Siu L, et al. Phase I study to determine the safety and pharmacokinetics of the novel Raf kinase and VEGFR inhibitor BAY 43-9006, administered for 28 days on/7 days off in patients with advanced, refractory solid tumors. Ann Oncol 2005; 16: 1688-94.

41. Yong WP, Ramirez J, Innocenti F,Ratain MJ. Effects of ketoconazole on glucuronidation by UDP-glucuronosyltransferase enzymes. Clin Cancer Res 2005; 11: 6699-704.

42. Adjei AA, Molina JR, Mandrekar SJ, et al. Phase I trial of sorafenib in combination with gefitinib in patients with refractory or recurrent non-small cell lung cancer. Clin Cancer Res 2007; 13: 2684-91.

43. Mross K, Steinbild S, Baas F, et al. Results from an in vitro and a clinical/pharmacological phase I study with the combination irinotecan and sorafenib. Eur J Cancer 2007; 43: 55-63.

44. Abou-Alfa GK, Schwartz L, Ricci S, et al. Phase II study of sorafenib in patients with advanced hepatocellular carcinoma. J Clin Oncol 2006; 24: 4293-300.

45. Huisman MT, Chhatta AA, van Tellingen O, Beijnen JH,Schinkel AH. MRP2 (ABCC2) transports taxanes and confers paclitaxel resistance and both processes are stimulated by probenecid. Int J Cancer 2005; 116: 824-9.

46. Shirakawa K, Takara K, Tanigawara Y, et al. Interaction of docetaxel ("Taxotere") with human P-glycoprotein. Jpn J Cancer Res 1999; 90: 1380-6.

47. van Asperen J, van Tellingen O,Beijnen JH. The role of mdr1a P-glycoprotein in the biliary and intestinal secretion of doxorubicin and vinblastine in mice. Drug Metab Dispos 2000; 28: 264-7.

48. Vlaming ML, Mohrmann K, Wagenaar E, et al. Carcinogen and anticancer drug transport by Mrp2 in vivo: studies using Mrp2 (Abcc2) knockout mice. J Pharmacol Exp Ther 2006; 318: 319-27.

49. Bayer Pharmaceuticals. Information brocheure for sorafenib (BAY 43-9006). 2005.
http://www.accessdata.fda.gov/drugsatfda_docs/label/2005/021923lbl.pdf
Accessed on July 21, 2009

50. Richly H, Kupsch P, Passage K, et al. Results of a phase I trial of BAY 43-9006 in combination with doxorubicin in patients with primary hepatic cancer. Int J Clin Pharmacol Ther 2004; 42: 650-1.

51. Rajagopalan P, Lathia C, Sundaresan P. Population pharmacokinetics of sorafenib in cancer patients. American Association of Pharmaceutical Sciences (AAPS), San Diego, CA, 2007.
http://www.aapsj.org/abstracts/AM_2007/AAPS2007-001221.PDF
Accessed on July 21, 2009

52. National Cancer Institute Clinical Trials: Imaging Response Criteria.
http://imaging.cancer.gov/clinicaltrials/imaging
Accessed on November 16, 2009

53. Escudier B, Eisen T, Stadler WM, et al. Sorafenib in advanced clear-cell renal-cell carcinoma. N Engl J Med 2007; 356: 125-34.

54. Llovet JM, Ricci S, Mazzaferro V, et al. Sorafenib in advanced hepatocellular carcinoma. N Engl J Med 2008; 359: 378-90.

55. Eisen T, Ahmad T, Flaherty KT, et al. Sorafenib in advanced melanoma: a Phase II randomised discontinuation trial analysis. Br J Cancer 2006; 95: 581-6.

56. Safarinejad MR. Safety and efficacy of sorafenib in patients with castrate resistant prostate cancer: A Phase II study. Urol Oncol 2008.

57. Elser C, Siu LL, Winquist E, et al. Phase II trial of sorafenib in patients with recurrent or metastatic squamous cell carcinoma of the head and neck or nasopharyngeal carcinoma. J Clin Oncol 2007; 25: 3766-73.

58. Takimoto CH,Awada A. Safety and anti-tumor activity of sorafenib (Nexavar((R))) in combination with other anti-cancer agents: a review of clinical trials. Cancer Chemother Pharmacol 2007.

59. Porta C, Paglino C, Imarisio I,Bonomi L. Uncovering Pandora's vase: the growing problem of new toxicities from novel anticancer agents. The case of sorafenib and sunitinib. Clin Exp Med 2007; 7: 127-34.

60. Azad NS, Aragon-Ching JB, Dahut WL, et al. Hand-foot skin reaction increases with cumulative sorafenib dose and with combination anti-vascular endothelial growth factor therapy. Clin Cancer Res 2009; 15: 1411-6.

61. Vernoese M. Mechanism of hypertension associated with BAY 43-9006. Journal of clinical oncology; 22: 2035.

62. Morrow GR, Andrews PL, Hickok JT, Roscoe JA,Matteson S. Fatigue associated with cancer and its treatment. Support Care Cancer 2002; 10: 389-98.

63. Strumberg D, Clark JW, Awada A, et al. Safety, pharmacokinetics, and preliminary antitumor activity of sorafenib: a review of four phase I trials in patients with advanced refractory solid tumors. Oncologist 2007; 12: 426-37.

64. Ulrich CM, Robien K,McLeod HL. Cancer pharmacogenetics: polymorphisms, pathways and beyond. Nat Rev Cancer 2003; 3: 912-20.

65. Undevia SD, Gomez-Abuin G,Ratain MJ. Pharmacokinetic variability of anticancer agents. Nat Rev Cancer 2005; 5: 447-58.

66. Scripture CD, Sparreboom A,Figg WD. Modulation of cytochrome P450 activity: implications for cancer therapy. Lancet Oncol 2005; 6: 780-9.

67. Ozdemir V, Kalow W, Tang BK, et al. Evaluation of the genetic component of variability in CYP3A4 activity: a repeated drug administration method. Pharmacogenetics 2000; 10: 373-88.

68. Ingelman-Sundberg M, Sim SC, Gomez A,Rodriguez-Antona C. Influence of cytochrome P450 polymorphisms on drug therapies: Pharmacogenetic, pharmacoepigenetic and clinical aspects. Pharmacol Ther 2007; 116: 496-526.

69. He P, Court MH, Greenblatt DJ,Von Moltke LL. Genotype-phenotype associations of cytochrome P450 3A4 and 3A5 polymorphism with midazolam clearance in vivo. Clin Pharmacol Ther 2005; 77: 373-87.

70. Bosch TM, Meijerman I, Beijnen JH,Schellens JH. Genetic polymorphisms of drug-metabolising enzymes and drug transporters in the chemotherapeutic treatment of cancer. Clin Pharmacokinet 2006; 45: 253-85.

71. Shimada T, Yamazaki H, Mimura M, Inui Y,Guengerich FP. Interindividual variations in human liver cytochrome P-450 enzymes involved in the oxidation of drugs, carcinogens and toxic chemicals: studies with liver microsomes of 30 Japanese and 30 Caucasians. J Pharmacol Exp Ther 1994; 270: 414-23.

72. Chowbay B, Zhou S,Lee EJ. An interethnic comparison of polymorphisms of the genes encoding drug-metabolizing enzymes and drug transporters: experience in Singapore. Drug Metab Rev 2005; 37: 327-78.

73. Strassburg CP, Nguyen N, Manns MP,Tukey RH. UDP-glucuronosyltransferase activity in human liver and colon. Gastroenterology 1999; 116: 149-60.

74. Girard H, Court MH, Bernard O, et al. Identification of common polymorphisms in the promoter of the UGT1A9 gene: evidence that UGT1A9 protein and activity levels are strongly genetically controlled in the liver. Pharmacogenetics 2004; 14: 501-15.

75. Villeneuve L, Girard H, Fortier LC, Gagne JF,Guillemette C. Novel functional polymorphisms in the UGT1A7 and UGT1A9 glucuronidating enzymes in Caucasian and African-American subjects and their impact on the metabolism of 7-ethyl-10-hydroxycamptothecin and flavopiridol anticancer drugs. J Pharmacol Exp Ther 2003; 307: 117-28.

76. Jinno H, Saeki M, Saito Y, et al. Functional characterization of human UDP-glucuronosyltransferase 1A9 variant, D256N, found in Japanese cancer patients. J Pharmacol Exp Ther 2003; 306: 688-93.

77. Girard H, Villeneuve L, Court MH, et al. The novel UGT1A9 intronic I399 polymorphism appears as a predictor of 7-ethyl-10-hydroxycamptothecin glucuronidation levels in the liver. Drug Metab Dispos 2006; 34: 1220-8.

78. Sandanaraj E, Jada SR, Shu X, et al. Influence of UGT1A9 intronic I399C>T polymorphism on SN-38 glucuronidation in Asian cancer patients. Pharmacogenomics J 2007.

79. Forsti A, Jin Q, Altieri A, et al. Polymorphisms in the KDR and POSTN genes: association with breast cancer susceptibility and prognosis. Breast Cancer Res Treat 2007; 101: 83-93.

80. Afify S, Rapp UR,Hogger P. Validation of a liquid chromatography assay for the quantification of the Raf kinase inhibitor BAY 43-9006 in small volumes of

mouse serum. J Chromatogr B Analyt Technol Biomed Life Sci 2004; 809: 99-103.

81. Blanchet B, Billemont B, Cramard J, et al. Validation of an HPLC-UV method for sorafenib determination in human plasma and application to cancer patients in routine clinical practice. J Pharm Biomed Anal 2009; 49: 1109-14.

82. Zhao M, Rudek MA, He P, et al. A rapid and sensitive method for determination of sorafenib in human plasma using a liquid chromatography/tandem mass spectrometry assay. J Chromatogr B Analyt Technol Biomed Life Sci 2007; 846: 1-7.

83. Dahut WL, Scripture C, Posadas E, et al. A phase II clinical trial of sorafenib in androgen-independent prostate cancer. Clin Cancer Res 2008; 14: 209-14.

84. ACD/ChemSketch Freeware, version 9.0, Advanced Chemistry Development, Inc., Toronto, ON, Canada. www.acdlabs.com 2006.

85. Calvert AH,Egorin MJ. Carboplatin dosing formulae: gender bias and the use of creatinine-based methodologies. Eur J Cancer 2002; 38: 11-6.

86. Relling MV, Hancock ML, Boyett JM, Pui CH,Evans WE. Prognostic importance of 6-mercaptopurine dose intensity in acute lymphoblastic leukemia. Blood 1999; 93: 2817-23.

87. Stewart CF, Baker SD, Heideman RL, Jones D, Crom WR,Pratt CB. Clinical pharmacodynamics of continuous infusion topotecan in children: systemic exposure predicts hematologic toxicity. J Clin Oncol 1994; 12: 1946-54.

88. Strother RM, Jones DR, Skaar T, Huh WS, Porter J, Foster A and Sweeney C. Erlotinib-associated rash correlates with plasma levels at steady state.ASCO

Annual Meeting 2006. J Clin Oncol (Post-Meeting Edition, June 20 supplement) 2006; 24. Abstract no. 13008

89. Aventis Pharmaceutical, Inc. Docetaxel prescribing information. http://www.ff.up.pt/toxicologia/monografias/ano0708/g46_docetaxel/Docetaxel%20-%20fda.pdf Accessed on July 21, 2009

90. Williams PJ,Ette EI. The role of population pharmacokinetics in drug development in light of the Food and Drug Administration's 'Guidance for Industry: population pharmacokinetics'. Clin Pharmacokinet 2000; 39: 385-95.

91. Strumberg D, Awada A, Hirte H, et al. Pooled safety analysis of BAY 43-9006 (sorafenib) monotherapy in patients with advanced solid tumours: Is rash associated with treatment outcome? Eur J Cancer 2006; 42: 548-56.

92. Medicine Plus (National Library of Medicine). ALT and AST. http://www.nlm.nih.gov/medlineplus/ency/article/003473.htm Accessed on July 21, 2009

93. Domanski TL, Finta C, Halpert JR,Zaphiropoulos PG. cDNA cloning and initial characterization of CYP3A43, a novel human cytochrome P450. Mol Pharmacol 2001; 59: 386-92.

94. Miller AA, Murry DJ, Owzar K, et al. Phase I and pharmacokinetic study of sorafenib in patients with hepatic or renal dysfunction: CALGB 60301. J Clin Oncol 2009; 27: 1800-5.

95. Ette EI,Williams PJ. Population pharmacokinetics II: estimation methods. Ann Pharmacother 2004; 38: 1907-15.

96. US FDA Guidance for Industry Population Pharmacokinetics. 1999.

http://www.fda.gov/downloads/Drugs/GuidanceComplianceRegulatoryInformation/Guidances/UCM072137.pdf Accessed on July 21, 2009

97. Boeckmann A.J. Beal S., Sheiner L.B. NONMEM User's guide, part v. 1994.

98. Grasela TH, Jr., Antal EJ, Townsend RJ, Smith RB. An evaluation of population pharmacokinetics in therapeutic trials. Part I. Comparison of methodologies. Clin Pharmacol Ther 1986; 39: 605-12.

99. Wang Y. Derivation of various NONMEM estimation methods. J Pharmacokinet Pharmacodyn 2007; 34: 575-93.

100. Holford NH. A size standard for pharmacokinetics. Clin Pharmacokinet 1996; 30: 329-32.

101. West GB, Brown JH,Enquist BJ. A general model for the origin of allometric scaling laws in biology. Science 1997; 276: 122-6.

102. Wilkins J.J., Mats K.O., Niclas J.E. Patterns and power for the visual predictive check. PAGE 2006 meeting, Brugge/Bruges, Belgium. Abstract no. 1029 http://www.page-meeting.org/?abstract=1029

103. Jadhav PR, Gobburu JV. A new equivalence based metric for predictive check to qualify mixed-effects models. AAPS J 2005; 7: E523-31.

104. Jain L, Woo S, Dahut WL, Kohn EC, Kummar S, Gutierrez M, Yarchoan R, Giaccone G, Azad NS, Venitz J, Figg WD. Population Pharmacokinetics Of Sorafenib In Cancer Patients. ASCPT annula meeting 2009, Vol. 85, pp. S43. Washington D.C.: Clinical pharmacology & Therapeutics, 2009.

105. Savic RM, Jonker DM, Kerbusch T,Karlsson MO. Implementation of a transit compartment model for describing drug absorption in pharmacokinetic studies. J Pharmacokinet Pharmacodyn 2007; 34: 711-26.

106. Jiao Z SJ, Ding JJ, Zhong LJ, Shi XJ. Modified population pharmacokinetic model for enterohepatic circulation of mycophenolic acid and its application in a bioequivalence study. Asian Journal of Pharmacodynamics and Pharmacokinetics 2007; 7: 153-60.

107. Moon YJ, Wang L, DiCenzo R,Morris ME. Quercetin pharmacokinetics in humans. Biopharm Drug Dispos 2008; 29: 205-17.

108. NMusers. Adaptation of multiple-dose enterohepatic circulation model suggested by Luann Phillips (after Stuart Beal). (11 June 2002).

109. Roberts MS, Magnusson BM, Burczynski FJ,Weiss M. Enterohepatic circulation: physiological, pharmacokinetic and clinical implications. Clin Pharmacokinet 2002; 41: 751-90.

110. Aragon-Ching JB, Jain L, Gulley JL, et al. Final analysis of a phase II trial using sorafenib for metastatic castration-resistant prostate cancer. BJU Int 2009; 103: 1636-40.

111. Lesko LJ,Atkinson AJ, Jr. Use of biomarkers and surrogate endpoints in drug development and regulatory decision making: criteria, validation, strategies. Annu Rev Pharmacol Toxicol 2001; 41: 347-66.

112. Robert J, Illiadis A, Hoerni B, Cano JP, Durand M,Lagarde C. Pharmacokinetics of adriamycin in patients with breast cancer: correlation between pharmacokinetic

parameters and clinical short-term response. Eur J Cancer Clin Oncol 1982; 18: 739-45.

113. Santini J, Milano G, Thyss A, et al. 5-FU therapeutic monitoring with dose adjustment leads to an improved therapeutic index in head and neck cancer. Br J Cancer 1989; 59: 287-90.

114. Wilson PM, Ladner RD,Lenz HJ. Predictive and prognostic markers in colorectal cancer. Gastrointest Cancer Res 2007; 1: 237-46.

115. Azad NS, Posadas EM, Kwitkowski VE, et al. Combination targeted therapy with sorafenib and bevacizumab results in enhanced toxicity and antitumor activity. J Clin Oncol 2008; 26: 3709-14.

116. Nicosia RF,Ottinetti A. Growth of microvessels in serum-free matrix culture of rat aorta. A quantitative assay of angiogenesis in vitro. Lab Invest 1990; 63: 115-22.

117. Zhu WH,Nicosia RF. The thin prep rat aortic ring assay: a modified method for the characterization of angiogenesis in whole mounts. Angiogenesis 2002; 5: 81-6.

118. Go RS,Owen WG. The rat aortic ring assay for in vitro study of angiogenesis. Methods Mol Med 2003; 85: 59-64.

119. Kruger EA,Figg WD. Protein binding alters the activity of suramin, carboxyamidotriazole, and UCN-01 in an ex vivo rat aortic ring angiogenesis assay. Clin Cancer Res 2001; 7: 1867-72.

120. Genentech Inc. Bevacizumab prescribing information. http://www.gene.com/gene/products/information/pdf/avastin-prescribing.pdf

Accessed on July 21, 2009

121. Anderson J. Treatment of Prostate Cancer - The role of primary hormonal therapy. EAU-EBU update series 2003; 1: 32-39.

122. Schneider BP, Sledge GW, Jr. Drug insight: VEGF as a therapeutic target for breast cancer. Nat Clin Pract Oncol 2007; 4: 181-9.

123. Heist RS, Zhai R, Liu G, et al. VEGF polymorphisms and survival in early-stage non-small-cell lung cancer. J Clin Oncol 2008; 26: 856-62.

124. Yamaguchi T, Bando H, Mori T, et al. Overexpression of soluble vascular endothelial growth factor receptor 1 in colorectal cancer: Association with progression and prognosis. Cancer Sci 2007; 98: 405-10.

125. Ferrer FA, Miller LJ, Andrawis RI, et al. Angiogenesis and prostate cancer: in vivo and in vitro expression of angiogenesis factors by prostate cancer cells. Urology 1998; 51: 161-7.

126. Chi KN, Ellard SL, Hotte SJ, et al. A phase II study of sorafenib in patients with chemo-naive castration-resistant prostate cancer. Ann Oncol 2008; 19: 746-51.

127. Steinbild S, Mross K, Frost A, et al. A clinical phase II study with sorafenib in patients with progressive hormone-refractory prostate cancer: a study of the CESAR Central European Society for Anticancer Drug Research-EWIV. Br J Cancer 2007; 97: 1480-5.

128. Kelly WK, Scher HI, Mazumdar M, Vlamis V, Schwartz M,Fossa SD. Prostate-specific antigen as a measure of disease outcome in metastatic hormone-refractory prostate cancer. J Clin Oncol 1993; 11: 607-15.

129. Bubley GJ, Carducci M, Dahut W, et al. Eligibility and response guidelines for phase II clinical trials in androgen-independent prostate cancer: recommendations from the Prostate-Specific Antigen Working Group. J Clin Oncol 1999; 17: 3461-7.

130. Kato RB, Srougi V, Salvadori FA, Ayres PP, Leite KM,Srougi M. Pretreatment tumor volume estimation based on total serum psa in patients with localized prostate cancer. Clinics (Sao Paulo) 2008; 63: 759-62.

131. Alpha Diagnostic International. Human prostate specific antigen (Catalog no. 1500).
https://www.4adi.com/objects/catalog/product/extras/catalog2009.pdf?czuid=1258355403454
Accessed on July 19th, 2009.

132. Dojindo Molecular Technologies, Inc. Cell Counting Kit # 8 (Catalog no. CK04-11).
http://www.dojindo.com/home/index.php?page=shop.product_details&flypage=flypage.tpl&product_id=23&category_id=29&option=com_virtuemart&Itemid=58
Accessed on July 19th, 2009.

133. Ferro MA, Gillatt D, Symes MO,Smith PJ. High-dose intravenous estrogen therapy in advanced prostatic carcinoma. Use of serum prostate-specific antigen to monitor response. Urology 1989; 34: 134-8.

134. Dixon SC, Knopf KB,Figg WD. The control of prostate-specific antigen expression and gene regulation by pharmacological agents. Pharmacol Rev 2001; 53: 73-91.

135. Stoller RG, Hande KR, Jacobs SA, Rosenberg SA,Chabner BA. Use of plasma pharmacokinetics to predict and prevent methotrexate toxicity. N Engl J Med 1977; 297: 630-4.

136. Evans WE, Schentag JJ, Jusko WJ (ed.) Applied Pharmacokinetics: Principles of therapeutic drug monitoring 3 edition: Lippincott Williams & Wilkins, 1992.

137. Fanucchi MP, Walsh TD, Fleisher M, et al. Phase I and clinical pharmacology study of trimetrexate administered weekly for three weeks. Cancer Res 1987; 47: 3303-8.

138. Grochow LB, Noe DA, Dole GB, et al. Phase I trial of trimetrexate glucuronate on a five-day bolus schedule: clinical pharmacology and pharmacodynamics. J Natl Cancer Inst 1989; 81: 124-30.

139. Grochow LB, Noe DA, Ettinger DS,Donehower RC. A phase I trial of trimetrexate glucuronate (NSC 352122) given every 3 weeks: clinical pharmacology and pharmacodynamics. Cancer Chemother Pharmacol 1989; 24: 314-20.

140. Ratain MJ, Mick R, Schilsky RL, Vogelzang NJ,Berezin F. Pharmacologically based dosing of etoposide: a means of safely increasing dose intensity. J Clin Oncol 1991; 9: 1480-6.

141. Egorin MJ, Van Echo DA, Tipping SJ, et al. Pharmacokinetics and dosage reduction of cis-diammine(1,1-cyclobutanedicarboxylato)platinum in patients with impaired renal function. Cancer Res 1984; 44: 5432-8.

142. Egorin MJ, Van Echo DA, Olman EA, Whitacre MY, Forrest A,Aisner J. Prospective validation of a pharmacologically based dosing scheme for the cis-

diamminedichloroplatinum(II) analogue diamminecyclobutanedicarboxylatoplatinum. Cancer Res 1985; 45: 6502-6.

143. Evans WE, Hon YY, Bomgaars L, et al. Preponderance of thiopurine S-methyltransferase deficiency and heterozygosity among patients intolerant to mercaptopurine or azathioprine. J Clin Oncol 2001; 19: 2293-301.

144. Wasserman E, Myara A, Lokiec F, et al. Severe CPT-11 toxicity in patients with Gilbert's syndrome: two case reports. Ann Oncol 1997; 8: 1049-51.

145. Huang RS,Ratain MJ. Pharmacogenetics and pharmacogenomics of anticancer agents. CA Cancer J Clin 2009; 59: 42-55.

146. Jacobi U, Waibler E, Schulze P, et al. Release of doxorubicin in sweat: first step to induce the palmar-plantar erythrodysesthesia syndrome? Ann Oncol 2005; 16: 1210-1.

147. Bristol-Myers Squibb. Cetuximab (Erbitux) prescribing information. http://www.gene.com/gene/products/information/pdf/avastin-prescribing.pdf Accessed on July 21, 2009.

148. Rudin CM, Liu W, Desai A, et al. Pharmacogenomic and pharmacokinetic determinants of erlotinib toxicity. J Clin Oncol 2008; 26: 1119-27.

149. Ratain MJ, Eisen T, Stadler WM, et al. Phase II placebo-controlled randomized discontinuation trial of sorafenib in patients with metastatic renal cell carcinoma. J Clin Oncol 2006; 24: 2505-12.

150. Blum JL, Jones SE, Buzdar AU, et al. Multicenter phase II study of capecitabine in paclitaxel-refractory metastatic breast cancer. J Clin Oncol 1999; 17: 485-93.

151. Chiara S, Nobile MT, Barzacchi C, et al. Hand-foot syndrome induced by high-dose, short-term, continuous 5-fluorouracil infusion. Eur J Cancer 1997; 33: 967-9.

152. Jain L, Gardner ER, Venitz J, Dahut W,Figg WD. Development of a rapid and sensitive LC-MS/MS assay for the determination of sorafenib in human plasma. J Pharm Biomed Anal 2008; 46: 362-7.

153. Drug Bank. Drug cards for sorafenib (DB00398), sunitinib (DB01268), doxorubicin (DB00997), fluorouracil (DB00544), cytarabine (DB00987), hydroxyurea (DB01005) and capecitabine (DB01101).
http://www.drugbank.ca/
Accessed on July 19th, 2009.

154. Lacouture ME, Reilly LM, Gerami P,Guitart J. Hand foot skin reaction in cancer patients treated with the multikinase inhibitors sorafenib and sunitinib. Ann Oncol 2008; 19: 1955-61.

155. Yang CH, Lin WC, Chuang CK, et al. Hand-foot skin reaction in patients treated with sorafenib: a clinicopathological study of cutaneous manifestations due to multitargeted kinase inhibitor therapy. Br J Dermatol 2008; 158: 592-6.

156. Griffioen AW,Molema G. Angiogenesis: potentials for pharmacologic intervention in the treatment of cancer, cardiovascular diseases, and chronic inflammation. Pharmacol Rev 2000; 52: 237-68.

157. Park HW, Lee JE, Shin ES, et al. Association between genetic variations of vascular endothelial growth factor receptor 2 and atopy in the Korean population. J Allergy Clin Immunol 2006; 117: 774-9.

158. Hicklin DJ,Ellis LM. Role of the vascular endothelial growth factor pathway in tumor growth and angiogenesis. J Clin Oncol 2005; 23: 1011-27.

159. Koukourakis MI, Giatromanolaki A, Thorpe PE, et al. Vascular endothelial growth factor/KDR activated microvessel density versus CD31 standard microvessel density in non-small cell lung cancer. Cancer Res 2000; 60: 3088-95.

160. Giatromanolaki A, Sivridis E, Brekken R, et al. The angiogenic "vascular endothelial growth factor/flk-1(KDR) receptor" pathway in patients with endometrial carcinoma: prognostic and therapeutic implications. Cancer 2001; 92: 2569-77.

161. Duque JL, Loughlin KR, Adam RM, Kantoff P, Mazzucchi E,Freeman MR. Measurement of plasma levels of vascular endothelial growth factor in prostate cancer patients: relationship with clinical stage, Gleason score, prostate volume, and serum prostate-specific antigen. Clinics (Sao Paulo) 2006; 61: 401-8.

162. Peyromaure M, Badoual C, Camparo P, et al. Plasma levels and expression of vascular endothelial growth factor-A in human localized prostate cancer. Oncol Rep 2007; 18: 145-9.

163. Shariat SF, Anwuri VA, Lamb DJ, Shah NV, Wheeler TM,Slawin KM. Association of preoperative plasma levels of vascular endothelial growth factor and soluble vascular cell adhesion molecule-1 with lymph node status and biochemical progression after radical prostatectomy. J Clin Oncol 2004; 22: 1655-63.

164. Miyake H, Muramaki M, Kurahashi T, Yamanaka K,Hara I. Urinary levels of vascular endothelial growth factor in patients with prostate cancer as a predictor of disease progression. Anticancer Res 2005; 25: 3645-9.

165. Peyromaure M, Camparo P, Badoual C, Descazeaud A,Dinh-Xuan AT. The expression of vascular endothelial growth factor is associated with the risk of cancer progression after radical prostatectomy. BJU Int 2007; 99: 1150-3.

166. Ellis LM,Fidler IJ. Angiogenesis and metastasis. Eur J Cancer 1996; 32A: 2451-60.

167. Pallares J, Rojo F, Iriarte J, Morote J, Armadans LI,de Torres I. Study of microvessel density and the expression of the angiogenic factors VEGF, bFGF and the receptors Flt-1 and FLK-1 in benign, premalignant and malignant prostate tissues. Histol Histopathol 2006; 21: 857-65.

168. Launay-Vacher V,Deray G. Hypertension and proteinuria: a class-effect of antiangiogenic therapies. Anticancer Drugs 2009; 20: 81-2.

169. Schneider BP, Radovich M, Sledge GW, et al. Association of polymorphisms of angiogenesis genes with breast cancer. Breast Cancer Res Treat 2008; 111: 157-63.

170. Schneider BP, Wang M, Radovich M, et al. Association of vascular endothelial growth factor and vascular endothelial growth factor receptor-2 genetic polymorphisms with outcome in a trial of paclitaxel compared with paclitaxel plus bevacizumab in advanced breast cancer: ECOG 2100. J Clin Oncol 2008; 26: 4672-8.

171. Lurje G, Schultheis AM, Hendifar AE, Ashouri S, Zhang W, Gordon MA, Nagashima F, Chang HM, Yang D, Lenz HJ. VEGF and VEGF receptor-2 (VEGFR2) gene polymorphisms predict tumor recurrence in stage II and III colon cancer. ASCO Annual Meeting-2007 Proceedings Part I. J Clin Oncol; 25. Abstract no. 4004.

172. Jurado J, Ortega JA, Iglesias P, García-Puche JL, Belon J. Vascular endothelial growth factor receptor-2 (VEGFr-2) genetic polymorphisms as predictors to antiangiogenic therapy. ASCO Annual Meeting 2009. J Clin Oncol; 27 (suppl) abstract no. e14561.

173. Deng HW, Fu YX,Lynch M. Inferring the major genomic mode of dominance and overdominance. Genetica 1998; 102-103: 559-67.

174. Fuh G, Li B, Crowley C, Cunningham B,Wells JA. Requirements for binding and signaling of the kinase domain receptor for vascular endothelial growth factor. J Biol Chem 1998; 273: 11197-204.

175. Tao Q, Backer MV, Backer JM,Terman BI. Kinase insert domain receptor (KDR) extracellular immunoglobulin-like domains 4-7 contain structural features that block receptor dimerization and vascular endothelial growth factor-induced signaling. J Biol Chem 2001; 276: 21916-23.

176. Wang Y, Zheng Y, Zhang W, et al. Polymorphisms of KDR gene are associated with coronary heart disease. J Am Coll Cardiol 2007; 50: 760-7.

177. Bergsland E,Dickler MN. Maximizing the potential of bevacizumab in cancer treatment. Oncologist 2004; 9 Suppl 1: 36-42.

Appendix 1-1

Phase I single agent or combination studies of sorafenib

Type of clinical trial	Patient population	Sorafenib Dose (mg)	Dosing schedule	MTD	Response rate	AE	Remarks	Ref
Phase I, dose exploratory	Advanced refractory solid tumors	50 q5d, 50 q2d, (100, 200, 300, 400, 600, 800) bid	21 days on/7days off	400 mg bid	50 % SD	HFS, Diarrhea, rash, desquamation, fatigue	Sorafenib is well tolerated.	Awada et al, British J Cancer, 2005
Phase I, dose exploratory	Advanced refractory solid tumors	100, 200, 400, 600, 800 bid	7 days on / 7 days off	600 mg bid	26 % SD	Rash, desquamation, hypertension	Sorafenib is well tolerated.	Clark et al, Clin Cancer Res, 2005
Phase I, dose exploratory	Advanced refractory solid tumors	50 q4d, (50,100) qd, (100,200,400,600) bid	28 days on/7days off	400 mg bid	22% SD	HFS, Fatigue	Sorafenib is well tolerated.	Moore et al, Annals of oncology 2005
Phase I, dose exploratory	Advanced refractory solid tumors	(50-800) qd, bid	varying weekly schedule	400 mg bi d	18% SD	diarrhea, nausea	Sorafenib is well tolerated.	Strumberg et al, JCO, 2005
Phase I, safety, efficacy	Japanese HCC	200, 400 bid	28 days continuous cycle	400 mg bid	4% PR 83% SD	HFS, desquamation, rash, hypertension, elevated amylase and lipase	Sorafenib is well tolerated.	Furuse et al, Cancer Sci, 2007
Phase I, sorafenib (S)+ **Erlotinib**(Erl)	Advanced refractory solid tumors	1. 200 bid S + 100 qd Erl 2. 200 bid S + 150 qd Erl 3. 400 bid S + 150 qd Erl	S for 1 week followed by both S and E	400 mg bid S + 150 mg qd E ; may require modification on longer	20% PR, 60% SD	Fatigue, Diarrhea, Acneiform rash, hypophospthatemia	Combination well tolerated and has promising activity. No PK interaction.	Duran et al, Clin Cancer Res, 2007

				administration				
Phase I S+ **Gefitinib** (Gef)	Refractory or recurrent NSCLC	S (200-400) bid + Gef 250 qd	(21 days on one agent, 7 days off), (crossover to second agent for 21 days on, 7 days off), followed by 28 days cycles	400 mg bid S + 250 mg qd Gef	1 PR, 65% SD, Median PFS 133 days	Diarrhea, elevated ALT, rash, fatigue,	Decreases Gef plasma levels, activation of CYP3A4 by S resulting in increased biotransformation of Gef	Adjei et al, Clin Cancer Res, 2007
Drug interaction with **Ketoconazole** (ket)	Healthy subjects	S 50, Ket 400	S, 10 days washout, followed by 3 days Ket and 4th day S	-		Nausea , tremor, hypertension	-No clinically significant increase in sorafenib exposure. -Level of sorafenib N-oxide went down	Lathia et al, Cancer Chemother Pharmacol, 2006
Safety, efficacy and PK in combination with **irinotecan** (Irc)	Advanced refractory solid tumors	Cohort 1-3 (100, 200, 400) bid S+ 125 mg/m^2 Irc Cohort 4 400 bid S + 140 mg Irc	6 wk cycles of S combined with wkly i.v. Irc for 4 wks followed by 2 wks without Irc	MTD was not reached	1 PR, 60% SD in cohort 1-3, 77% SD in cohort 4	Diarrhea, decreased ANC/AGC, decreased leukocytes ***-Increased exposure of Irc and SN-38 following concomitant S 400 administration didn't increase the toxicity***	**-O**nly in S 400 bid + Irc 125 mg/m^2 group; S mean AUC_{0-10} went up by 68% and C_{max} went up by 78%. **-C**ohort 3, Irc $AUC_{0-\infty}$ and C_{max} increased by 26 & 36% respectively. **-C**ohort 4, Irc $AUC_{0-\infty}$ and C_{max}	Mross et al, European J of Cancer, 2007

							increased by 42 & 73% respectively. -**M**ean AUC_{0-48} and C_{max} for SN-38 increased by 120% with Irc 125 mg/m^2 and by 70% with Irc 140 mg.	
Phase I, S + **Doxorubicin** (Dox)	Refractory solid tumors	Dox 60 mg/m^2 + S (100, 200, 400) bid cohort 1-3	Administer Dox (21 days cycle) 1st day, from 4th day continuous S. S free period 48 hr before and 24 hr after 2nd dose of Dox	MTD was not reached	48% SD	HFS, Neutropenia, Diarrhea, stomatitis	-**S** partly increased AUC_{0-8} or C_{max} but no effect on steady state S PK. -**D**ox PK no effect with 100, 200 mg bid S. -**C**ontradictory findings for cohort 3 based on dose denominations (50 mg tablet vs. 200 mg tablet). -**D**ox exposure may increase with S. S may reverse the resistance to Dox	Richy et al, Annals of oncology, 2006
Phase I, S+ **Gemcitabine** (Gem)	Refractory solid tumors and	Gem 1000 mg/m^2 + S (100, 200,	Escalating doses of S bid	S 400 bid + Gem 1000	10.5% PR, 63% SD. Pancreatic	HFS, rash, diarrhea, hypertension,	-**N**o clinically relevant PK	Siu et al, Clin Cancer Res, 2006

	extended cohort of Advanced pancreatic cancer	400 w/ 50 mg tab, 400 w/ 200 mg tab) bid	continuous administration schedule + Gem 1000 mg/m^2 wkly (initially 7 consecutive wk, 1 wk rest, followed by 3 wk for every 4 wks)	mg/m^2 wkly (initially 7 consecutive wk, 1 wk rest, followed by 3 wk for every 4 wks)	cohort 53% SD	elevated hepatic transaminases and bilirubin, elevated pancreatic enzymes	interaction between S + Gem. -**S** may reverse resistance to Gem	
Phase I, S + **IFNα-2a**	Unreseceta ble and/or metastatic RCC or malignant melanoma	Cohort 1, S 200 bid + s.c. IFN 6 MIU Cohort 2, S 400 bid + s.c. IFN 6 MIU Cohort 3, S 400 bid + s.c. IFN 9 MIU	S continuously, IFN thrice wkly ***DCE-US****-to measure dynamic changes in tumor volume and/or tumor vasculature* ***Biomarker****, pERK levels in circulating PBLs*	MTD not reached	1 PR RCC, 61.5% SD (7 RCC + 1 melanoma)	HFS, Diarrhea, fatigue, weight loss, nausea,	-**N**o effect of S PK -**T**rend toward reduction in absolute value of lymphocytes. -**N**o significant dose dependent inhibition of ERK phosphorylation	Escudier et al, Clin Cancer Res, 2007
Phase I, S+ **Oxaliplatin** (Oxl)	Refractory solid tumor including colorectal cancer	Oxl 130 mg/m^2 on day 1 of a 3 wk cycle + S from 4th day 200 bid (cohort 1), 400 bid (cohort 2A, 2B &	Oxl day 1 of 3 wk cycle + S from 4th day bid continuous	MTD not reached (Recommended 400 mg bid S + Oxl 130 mg/m^2)	78% SD	Diarrhea, sensory neuropathy, other dermatological toxicities	-**N**o PK interaction	Kupsch et al, Clin Colorectal Cancer, 2005

		3)						
Phase I , S+ **Dox**	Primary Liver cancer				1 PR, 1 unconfirmed PR, 61% SD			Richly et al, Int J Clin Pharmacol Ther, 2004
Phase I	AML/MLD patients	NR	NR ***Biomarker-*** *pERK in PBLs using PMA activation or SCF activation*	NR	NR	NR	-**N**o evidence of decrease in ERK activation	Tong et al, Clinical cytometry
Phase I, S + Carboplatin +Paclitaxel (Melanoma pts were analyzed for B-raf mutation)	solid tumors	S 100,200,400 mg bid Paclitaxel 225 mg/m^2 day 1 Carbolplatin, corresponding to area under the curve (AUC) of 6	S, oral, days 2-19 of 21 day cycle Paclitaxel and Carboplatin, i.v., day 1	S, 400 mg bid Paclitaxel 225 mg/^{2} Carboplatin AUC equal to 6	(3% CR, 23% PR) in pts of melanoma	Hematologic, Rash:desquamation , HFSR	-**P**ts with melanoma respond favorably to this combination -**E**xposure to Paclitaxel was not altered by co-administration of sorafenib	Flaherty KT, CCR 2009

S: sorafenib, CR: complete response, PR: partial response, SD: stable disease, Gef: Gefitinib, Erl: erlotinib, ALT: Alanine amino transferase, Gem: Gemcitabine, Ket: Ketoconazole, Irc: Irinotecan, ANC: absolute neutrophil count, AGC: absolute granulocyte count, Dox: doxorubicin, DCE-US: dynamic contrast enhanced ultra sonography, Oxl: Oxaliplatin, AML: Acute myeloid leukemia, MLD: myelodysplastic syndrome, PBL: peripheral blood lymphocytes, PMA: phorbol myristate acetate, NR: Not reported, qd: Once-a-day, bid: Twice-a-day, i.v.: Intra-venous

Appendix 1-2

Phase II single agent or combination studies of sorafenib

Type of clinical trial	Patient population	Sorafenib Dose (mg)	Dosing schedule	Response rate	Toxicities	Remarks	Ref
Phase II RDT ***Biomarker-*** *B-raf, N-ras, K-ras status*	Advanced melanoma	400 bid	a). 12 wk run-in phase, b). Assigned to S or placebo or withdrawn from study based on response	19% SD 62% PD 19% unevaluable Overall median PFS 11 wks	Rash, desquamation, HFSR, diarrhea, fatigue	No relation between b-raf$_{V599E}$ and disease stability **No antitumor activity as a single agent**	Eisen T et al, BJCancer 2006
Phase II RDT	RCC	400 bid	a). 12 wk run-in phase, b). Assigned to S or placebo or withdrawn from study based on response	Overall median PFS 29 wks, 50% SD	Rash, desquamation, HFSR, pain, diarrhea, hypertension	S has antitumor activity against RCC	Ratain et al, JCO, 2006
Phase II ***Biomarker-*** *pERK levels in PreRx biopsies & blood cell RNA expression*	Patients with inoperable HCC	400 bid	4 week continuous cycles	Overall median survival 9.2 months, 34% SD, 8% PR or MR	Fatigue, diarrhea, HFSR	Modest efficacy as single agent **PreRx pERK levels correlated with TTP. Identified panel of 18 genes whose expression distinguished progressors from non-progressors**	Abou-alfa et al, JCO, 2006
Phase II ***Biomarkers***	Pts with recurrent or	400 bid	4 week continuous cycles	Halted after 1st stage.	Fatigue, lymphopenia, HFS,	Modest anticancer efficacy.	Elser et al, JCO, 2007

pERK-Signal transduction; Ki67-proliferation; Mcl-1-apoptosis; CD31 & SMA –angiogenesis	metastatic squamous cell carcinoma of the head and neck or nasopharyngeal carcinoma			1 PR (total 21 pts) Overall median survival 4.2 months	hypertenision, anemia, mucositis		
Phase II	Japanese RCC pts, received nephrectomy and failed at least one cytokine therapy	400 bid	Continuous dosing schedule	12.4% PR, 72% SD, Disease control rate 73.6% Median PFS 224 days	HFSR, hypertension, elevated lipase, increased amylase, diarrhea, rash/desquamation	S has antitumor efficacy	Akaza et al, Jpn J Clin Oncol 2007
Phase II, S+ IFNα-2b VHL gene mutation analysis	Advanced RCC	S 400 bid + INFα-2b 10 MU on 3 nonconsecutive days weekly	28 days cycles	19% PR, 50% SD, Median PFS 7 months OS 17 months	Fatigue, rigors, chills, fever leukopenia, hypertension, diarrhea	RR is greater than expected with either S or INF alone. VHL mutations may be associated with longer PFS among patients receiving VEGF targeted therapy	Ryan et al, JCO 2007
Phase II, S+ IFNα-2b	Metastatic RCC	S 400 bid + INFα-2b 10 MU on 3 nonconsecutive days weekly	8 wks cycle, followed by 2 cycle break	5%CR, 28% PR, 45% SD Median PFS 10 months	Fatigue, anorexia, anemia, diarrhea, rash, nausea, hypophophatemia, HFSR	Combination has substantial activity in treatment naive and IL-2 treated patients with RCC	Gollob et al, JCO, 2007

Phase II, S+Gem or S+Erl	Advanced NSCLS in elderly pts or pts with performance status 2	Gem 1200 mg/m^2 + S 800 mg/m^2 OR Erl 150 mg/m^2 + S 800 mg/m^2	Gem days 1 & 8 every 3 wks for max 6 cycles. S and Erl daily	Currently ongoing			Gridelli et al, Clinical lung cancer, 2007
Phase II, S	Pts with progressive hormone-refractory prostate cancer	S 400 mg bid	Continuously	27% SD by PSA and RECIST criteria. Median PFS 8 weeks	Fatigue, Pain, Skin, Diarrhea, Hypertension	S has activity in HRPCP when evaluated for RECIST and PSA based response	Steinbild S et al, Br J Can, 2007
Phase II, S	Metastatic castrate resistant prostate cancer	S 400 mg bid	28 days continuous cycle	4% PR, 42% SD Median PFS 3.7 months, Median OS 18 months	HFSR, Rash, liver function abnormalities, fatigue	S has moderate activity as second line treatment for mCRPC	Aragon-Ching JB et al, BJUI, 2008
Phase II, S + Dacarbazine	Advanced melanoma	S 400 mg bid	21 days continuous cycle	24% PR, 47% SD, 29% PD Median PFS 21.1 weeks, Median OS 51.3 weeks	Hematologic side effects, hypertension, nausea, fatigue	S was well tolerated, had encouraging improvement in PFS but not in OS	McDermott DF et al, JCO, 2008
Phase II, S	Advanced thyroid cancer	S 400 mg bid	28 days continuous cycle	23% PR, 53% SD Median PFS 79 weeks	Rash, HFSR, fatigue, weight loss, diarrhea, nausea	S has clinical activity in pts with metastatic, iodine-refractory thyroid carcinoma	Gupta-Abramson V et al, JCO, 2008

Phase II, S	Chemo-naïve castration-resistant prostate cancer	S 400 mg bid	Continuous cycles	Median PFS 2.3 months	HFSR, Increased AST, Fatigue, Lymphopenia, Anemia	S has limited activity. Limitations of using PSA as an indicator of progression and response	Chi KN et al, Annals of Oncology, 2008
Phase II, S	Metastatic breast cancer, had received prior treatment	S 400 mg bid	28 days continuous cycle	No CR or PR	No grade 4 and few grade 3 toxicities. Fatigue, anorexia, diarrhea, nausea, skin reaction etc.	Trial was stopped after first stage because of lack of efficacy	Moreno-Aspitia S et al, JCO 2009
Phase II, S or INF-α-2a	untreated advanced renal cancer	S 400 mg bid or 9 million U INF-α-2a, s.c.	S continuously, INF-α-2a 3 times	5% PR, 74% SD, 10% PD Median PFS 5.3 months	Fatigue, Diarrhea, Pain, Alopecia, HFSR, Rash:desquamation	S resulted in better tumor size reduction, better QOL, and better tolerability	Escudier B et al, JCO, 2009
Phase II, S	Metastatic thyroid cancer	S 400 mg bid	21 days continuous cycle	15% PR, 56% SD Median PFS 15 months	Hand-foot skin reaction, musculoskeletal pain, fatigue	S is reasonably well tolerated and has biological activity in metastatic PTC	Kloos RT et al, JCO 2009
Phase II, S	Advanced HCC in a Hepatitis B-endemic Asian population	S 400 mg bid	28 days continuous cycle	8% PR, 18% SD. Median OS 5 months	Diarrhea, malaise, HFSR	S demonstrated good efficacy and acceptable tolerability	Yau T et al, Cancer, 2009

S : Sorafenib, HFSR: Hand-foot skin reaction, Gem: Gemcitabine, Erl: Erlotinib, RCC: Renal cell carcinoma, HCC: Hepato-cellular carcinoma, mCRPC: metastatic castrate resistant prostate cancer, PTC: Papillary thyroide cancer, SD: Stable disease, PR: Partial response, CR: Complete response, PD: Progressive disease, PFS: Progression free survival, OS: Overall survival.

Appendix 1-3

Phase III trials for sorafenib as a single agent or in combination with chemotherapy

Type of clinical trial	Patient population	Sorafenib Dose (mg)	Dosing schedule	Response rate	AE	Remarks	Ref
Phase III placebo controlled **TARGET trial**	Advanced clear-cell RCC	400 bid	Continuous	Median PFS 5.5 months, PR 10% pts	Diarrhea, rash, fatigue, HFSR, hypertension	S prolongs PFS	Escudier et al, NEJM, 2007
Phase III placebo controlled **SHARP trial**	Unresectable HCC	400 bid	Continuous	PR 2% Median overall survival 10.7 months Median (radiologic) PFS 5.5 months	Hypertension, Fatigue, HFSR, rash/ desquamation	S improved overall survival by 44 % in HCC patients **S levels are low in patients with hepatic impairment compared to clinical trials for other indications**	Llovet JM et al, NEJM, 2008
Phase III randomized double blind placebo controlled trial	Advanced HCC patients from Asia – Pacific region	400 bid	Continuous in 6 weeks cycles	PR 3.3%, SD 54% Median overall survival 6.5 months Median PFS 2.8 months	HFSR, Diarrhea, Fatigue, Rash :desquamation, Hypertension	S is effective for treatment of advanced HCC, and it is well tolerated.	Cheng AL, Lancet Oncol 2009
Phase III S+/-(Carboplatin+ Paclitaxel)	Melanoma	S, 400 bid Paclitaxel 225 mg/m^2 Carboplatin dose equal to area under the curve of 6	S, days 2-19 Paclitaxel and Carboplatin on day 1	Response rate 12% S vs. 11% Placebo PFS, 17.4 weeks S vs. 17.9 weeks placebo	Dermatological events, thrombocytopenia, diarrhea, fatigue	S can not be recommended in the second-line setting for pts with advanced melanoma	Hauschild A, JCO, 2009

Phase III S+/-(Carboplatin+ Paclitaxel)	NSCLC	400 bid	Trial ongoing				
Phase III S+Cisplatin+ Gemcitabine	NSCLC						

S : Sorafenib, HFSR: Hand-foot skin reaction, RCC: Renal cell carcinoma, HCC: Hepato-cellular carcinoma,NSCLC: Non small cell lung cancer, SD: Stable disease, PR: Partial response, CR: Complete response, PD: Progressive disease, PFS: Progression free survival, OS: Overall survival.

Appendix 1-4

Drug interaction studies with sorafenib

Study	Interacting drug	Patient population	Findings	Conclusion
Lathia C et al, Cancer Chemo Pharmaco (2005)	***Ketoconazole***	Healthy volunteers	**N**o increase in exposure of sorafenib	**S**afe to co-administer with CYP3A4 inhibitors/substrates
Kupsch P et al, Clin Colorectal Cancer (2005)	***Oxaliplatin***	Advanced solid tumors	**N**o detectable drug interaction	**S**afe to administer in combination
Richly et al, Int J Clin Pharmacol Ther (2004)	***Doxorubicin***	Primary hepatic cancer	**2**1% increase in AUC of doxorubicin. **N**o apparent increase in toxicity.	**N**o apparent increase in the toxicity of these agents
Richly et al, Annals of Oncology (2006)	***Doxorubicin***	Refractory solid tumors	**A**AUC_{0-8} and C_{max} of sorafenib partly increased. **S**orafenib may increase the levels of doxorubicin	**S**orafenib may reverse the resistance to sorafenib
Mross K et al, Int J Clin Pharmacol Ther (2003)	***Irinotecan***	(CPT-11) Solid tumors	**6**7-120 % increase in AUC of SN-38; 26-42 % increase in AUC of irinotecan	**C**aution recommended. No apparent increase in the toxicity of these agents
Siu et al, CCR, 2006	***Gemcitabine***	Refractory solid tumor; extended cohort of advanced pancreatic cancer	**N**o clinically relevant PK interaction **S**lightly decreased, but not significant gemcitabine exposure observed in pancreatic extension	**S**orafenib may reverse the resistance to gemcitabine
Falherty et al, J	***Carboplatin/Paclitaxel***	Metastatic	**N**o change in PK values of	**C**ombination well tolerated,

Clin Oncol 22: 7507 (Abstract)		melanoma	paclitaxel, 6-OH paclitaxel, total or free platinum	without any unexpected adverse events and PK interaction.
Sorafenib prescribing information, revised 11/2007	***Docetaxel*** Sorafenib administration after 3 day break around Docetaxel dosing		**3**6-80 % increase in Docetaxel AUC; 16-32 % increase in Docetaxel C_{max}	**C**aution recommended.
Figer et al, Ann Oncol 15:iii87 (Abstract 327)	***Fluorouracil***		**B**oth increase (21-47 %) and decrease (10 %) in AUC of fluorouracil was observed	**C**aution recommended upon sorafenib co-administration with fluorouracil or leucovorin
Sorafenib prescribing information, revised 11/2007	Rifampicin & other ***CYP3A4 inducers***		**3**7 % reduction in sorafenib AUC with rifampicin	**O**ther CYP3A4 inducers (e.g., St. John's wort, phenytoin, carbamazepine, phenobarbital and dexamethasone) might increase sorafenib metabolism
In-vitro				
Sorafenib prescribing information, revised 11/2007	***CYP2B6 & CYP2C8 substrate***		***I****n-vitro* Ki values are 6 and 1-2 μM respectively.	**S**ystemic exposure of CYP2B6 and CYP2C8 substrates is expected to increase upon co-administration with sorafenib
Sorafenib prescribing information, revised 11/2007	*In-vitro* studies indicate sorafenib is a competitive inhibitor of ***CYP2C19*** (Ki=17 μM), ***CYP2D6*** (Ki=22μM) and ***CYP3A4*** (Ki= 29 μM)		**C**oncomitant administration of sorafenib didn't alter the exposure of midazolam (CYP3A4 substrate), dextromethorphan (CYP2D6 substrate) and omeprazole (CYP2C19 substrate)	**U**nlikely to have *in-vivo* interaction with substrates of these enzymes

Appendix 4-1

Details of population pharmacokinetic model presented at ASCPT-2009 annual meeting

Table A Number of patients and sample collection time

Cancer Type	Phase	Course	No. of patients		Sample collection time (hr)
			SD	SS	
mCRPC	Phase II	C1D1	46	-	0, 0.25, 0.5, 1, 2, 4, 6, 8, 12 & 24
NSCLC	Phase II	C1D1 & C1D15	17	16	0, 0.25, 0.5, 1, 2, 4, 6, 8, 12 & 24
ST	Phase I	C1D1 & C2D1	28	12	0, 0.25, 0.5, 1, 2, 4, 6, 8, 12 & 24
CR	Phase II	C1D1	15	-	0, 1, 2, 4, 8, 12, 16 & 24
KS	Phase I	C1D7	-	8	0, 1, 2, 4, 8, 12, 16 & 24

SD: Single Dose; SS: Steady-state; mCRPC: metastatic castrate-resistant prostate cancer; NSCLC: Non-small cell lung cancer; ST: refractory solid tumors; CR: Colorectal cancer; KS: Kaposi's sarcoma

Table B Patient baseline characteristics

Characteristic	Value
Number of patients	109
Demographics	Median (Range) or n(%)
Age, years	63.9 (30-85)
BSA, m2	1.9 (1.2-2.5)
Weight, kg	81.3 (35-133)
Gender (F/M)	33 (30%) / 76 (70%)
Race (Caucasian/African-American/Hispanic/Asian)	89 (81%) / 13(12%) / 2(2%) / 5(5%)
Clinical	Median (Range)
Albumin, g/dL	3.6 (2.2-4.4)
Total protein, g/dL	6.6 (4.6-8.0)
Alakaline phosphatase, U/L	81 (34-414)
Bilirubin total, mg/dL	0.6 (0.1-1.7)
SGOT, U/L	26 (13-90)
SGPT, U/L	21 (8-75)
Creatinine clearance, mL/min	96.5 (26-150)
Genetic	(wt/het/var) – n(%)
CYP3A4*1B	67(86%) / 5(6.4%) / 6(7.6%)
CYP3A5*3C	7(8%) / 15(16%) / 69(76%)
UGT1A9*3	87(97%) / 2(2%) / 1(1%)
UGT1A9*5	89(100%) / 0(0%) / 0(0%)
VEGFR2 Val297Ile	61(70%) / 24(28%) / 2(2%)
VEGFR2 Gln472His	60(69%) / 24(28%) / 3 (3%)

Final Model:

$CL/F_i = \theta_{CL/F} \cdot \exp(\eta_{CL/Fi})$

$V/F_i = \theta_v \cdot (weight/70) \cdot \exp(\eta_{V/Fi})$

$Ka_i = \theta_{Ka} \cdot \exp(\eta_{Kai})$

$TK_{0i} = \theta_{TK0} \cdot \exp(\eta_{TK0i})$

$ALAG1_i = (\theta_{ALAG1} + Ethnicity*\theta_{ALAG1\sim African\text{-}American}) \cdot \exp(\eta_{ALAG1i})$

Method = HYBRID, ZERO = (2,3,5)

θ: Population estimates or fixed effect parameters

η: Random inter-individual variability

Covariate Model:

- **First**, Body weight was identified as covariate for apparent volume of distribution (V/F).
- **Second**, Ethnicity was included as covariate for tlag. African American subjects had relatively higher ALAG1 as compared to other subjects [which included Caucasians, Asians and Hispanics].

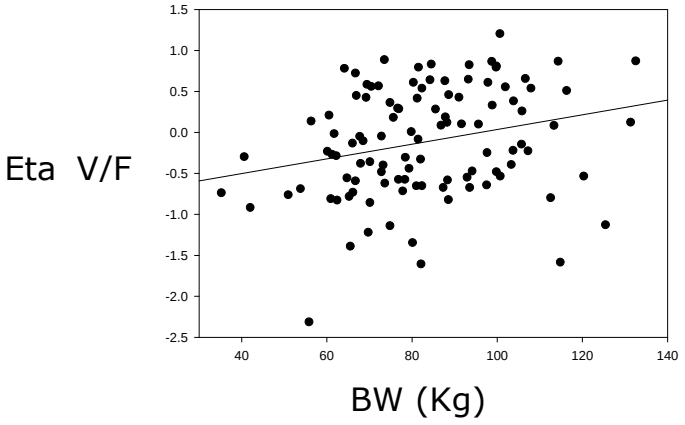

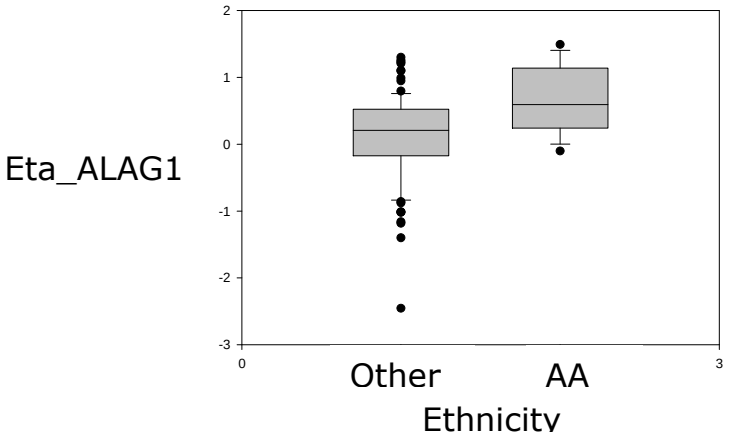

Table C Parameter estimates from the earlier developed population pharmacokinetic model

Parameter	Population mean	%RSE	95%CI
Population estimates (typical values)			
$\theta_{CL/F}$, L/h	4.74	11.6	[3.7, 5.8]
$\theta_{V/F}$, L	156	9.8	[126, 186]
θ_{Ka}, 1/h	1.04	17	[0.7, 1.4]
θ_{TK0}, h	1.92	16.5	[1.3, 2.5]
θ_{ALAG1}, h	0.196	11.5	[0.15, 0.24]
θ ALAG1~African American	0.696	5.9	[0.62, 0.78]
Between subject variability			
CL/F (%CV)	45%	27.9	[34%, 56%]
V/F (%CV)	80%	20.9	[54%, 106%]
k_a (%CV)	136%	35.6	[7%, 266%]
T_{K0} (%CV)	30%	39.4	[23%, 37%]
t_{lag} (%CV)	145%	55.9	[-88%, 378%]
Residual error			
Additive (ng/mL)	68.3	44	[-3989, 4125]
Proportional (%CV)	48%	12	[42%, 53%]

Diagnostic plots

Fig 2. Diagnostic plot of population predicted concentration (black) and individual predicted concentration (Red) vs. Observed concentration

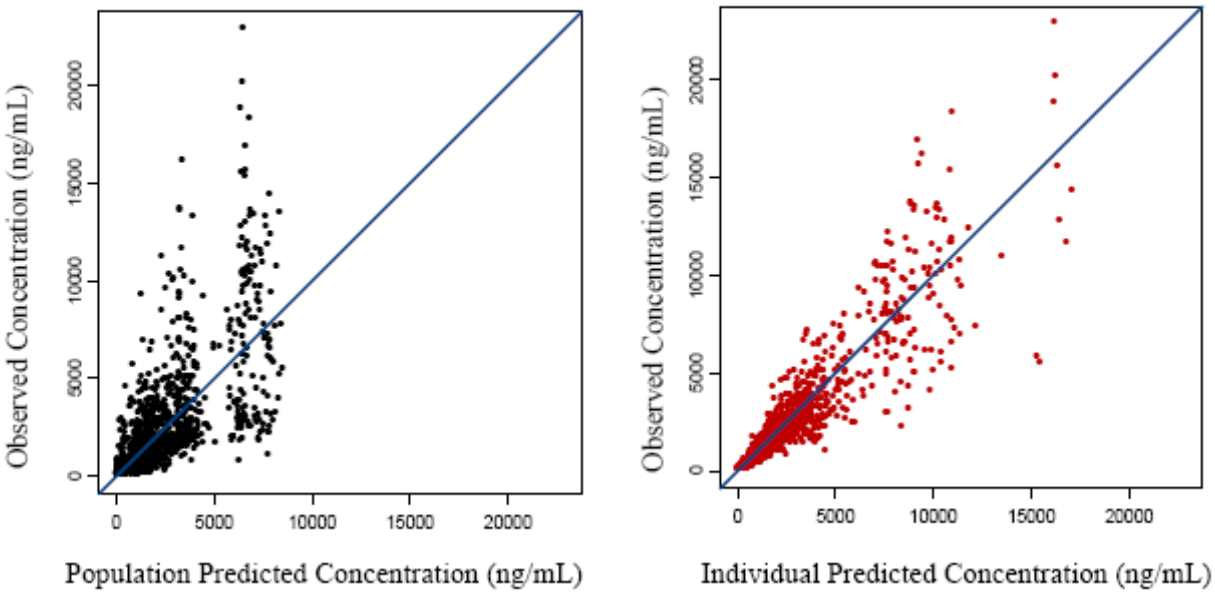

Conclusions

- A population pharmacokinetic model for sorafenib in a diverse oncology population was developed successfully.
- The sequential zero- and first-order absorption adequately described the sorafenib's GI solubility-limited absorption, as reported in published phase I dose escalation studies.
- Body weight and ethnicity were found to be statistically significant covariates for volume of distribution and absorption lag time; however, their contribution to BSV was minor. Their ultimate clinical importance needs to be further evaluated by simulations.
- The causes of the apparent ethnicity-related differences in absorption lag time are unclear but differences in expression of influx/efflux transporters (e.g., P-gp, sorafenib is a weak substrate of P-gp) between ethnic groups may be one of the reasons.
- The genetic variation in selected metabolic enzymes did not explain the variability in sorafenib disposition, in studied population.

Vita

Lokesh Jain was born on March 20, 1980, in Ajmer, India and is an Indian citizen. Lokesh received his bachelor of pharmacy (B. Pharm.) degree in 2002 from L. M. College of Science and Technology, Jodhpur affiliated with Rajasthan University, India. He received his master of pharmacy (M. Pharm.) degree in 2005 from Birla Institute of Technology and Science, Pilani, India. In the same year, he joined the Virginia Commonwealth University/National Cancer Institute joint track clinical pharmacology Ph.D. program and has conducted his graduate research under supervision of Drs. Jürgen Venitz, M.D., Ph.D. and William D. Figg, Pharm. D., M.B.A.

During his graduate research, he has worked on drug development aspects related to bioanalysis, pharmacokinetic and pharmacogenetic analysis, exposure-genotype-response studies as well as translational studies for anti-cancer drugs. His research work has been published in peer-reviewed journals. He is a member of American College of Clinical Pharmacology (ACCP) and the American Association of Pharmaceutical Scientists (AAPS). He has received several awards during his graduate career, including the AAPS-2009 CPTR graduate symposium award, ACCP-2009 student/trainee abstract award, VCU School of Pharmacy Dean's award-2009, VCU Department of Pharmaceutics John Wood award-2009 and Thacker award-2007.